Rhodium and Palladium Catalysed Unusual Regioselective Hydroformylation and Rhodium Catalysed Reductive Carbonylation

Benedetta Palucci

UNIVERSITAT ROVIRA i VIRGILI

Rhodium and Palladium Catalysed Unusual Regioselective Hydroformylation and Rhodium Catalysed Reductive Carbonylation

Benedetta Palucci

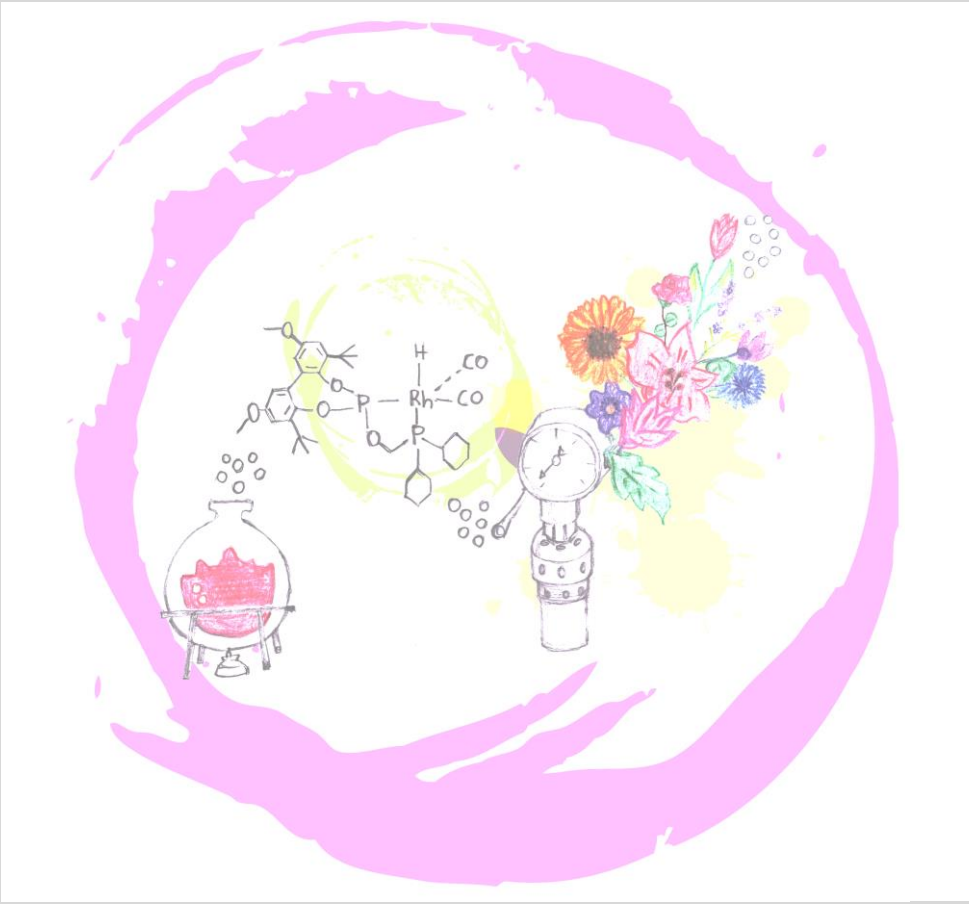

DOCTORAL THESIS
2020

Rhodium and Palladium Catalysed Unusual Regioselective Hydroformylation and Rhodium Catalysed Reductive Carbonylation

Benedetta Palucci

Rhodium and Palladium Catalysed Unusual Regioselective Hydroformylation and Rhodium Catalysed Reductive Carbonylation

Benedetta Palucci

Benedetta Palucci

Rhodium and Palladium Catalysed Unusual Regioselective Hydroformylation and Rhodium Catalysed Reductive Carbonylation

DOCTORAL THESIS

Supervised by
Prof. Dr. Cyril Godard, Prof. Dr. Carmen Claver and Dr. Jorge Sánchez Quesada

Departament de Química Física i Inorgànica

UNIVERSITAT ROVIRA I VIRGILI

Tarragona 2020

Rhodium and Palladium Catalysed Unusual Regioselective Hydroformylation and Rhodium Catalysed Reductive Carbonylation

Benedetta Palucci

UNIVERSITAT ROVIRA I VIRGILI

Departament de Química i Física i Inorgànica
C/ Marcel.lí Domingo s/n, Edifici N4
Campus Sescelades, 43007 Tarragona
Tel. 977 55 80 46

Prof. Dr. Cyril Godard and Prof. Dr. Carmen Claver from the Department of Physical and Inorganic Chemistry at Universitat Rovira i Virgili, and Dr. Jorge Sánchez Quesada from International Flavors & Fragrances, Research and Development department at Benicarló.

I STATE that the present study, entitled "*Rhodium and Palladium Catalysed Unusual Regioselective Hydroformylation and Rhodium Catalysed Reductive Carbonylation*", presented by Benedetta Palucci for the award of the degree of Doctor, has been carried out under our supervision at the UTQ (Unitat de Tecnologies Químiques) of Eurecat, Centre Tecnològic de Catalunya, and the Department of Physical and Inorganic Chemistry at Universitat Rovira I Virgili.

Tarragona, November 22th 2020
Doctoral Thesis Supervisors

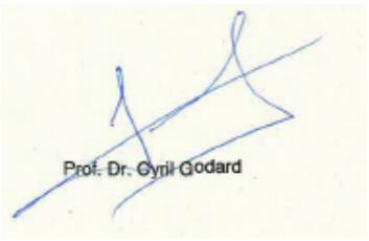

Prof. Dr. Carmen Claver

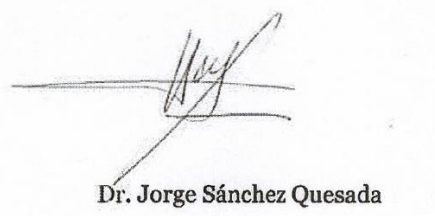

The present Doctoral Thesis has been carried out thanks to the “a Martí Franquès scholarship (2017-PMF-PIPF-5).

The work developed in this doctoral thesis has been possible thanks to the financial support from the following research projects:

- El Ministerio de Economia y Competividad through the project MINECO CTQ2016-75016-R.
- IFF International Flavors & Fragrances, Inc.

Rhodium and Palladium Catalysed Unusual Regioselective Hydroformylation and Rhodium Catalysed Reductive Carbonylation

Benedetta Palucci

Rhodium and Palladium Catalysed Unusual Regioselective Hydroformylation and Rhodium Catalysed Reductive Carbonylation

Benedetta Palucci

Acknowledgments

I would like to express my sincere gratitude to Prof. Carmen Claver for giving me the opportunity to be part of her research group, as well as for her support and encouragement over these four years. I would like to thank Prof. Cyril Godard for his honesty and straightforwardness, that helped me in the process of self-growth as a scientist and as a person. I am thankful to Dr. Jorge Sánchez Quesada for giving me the opportunity to collaborate with the IFF for my doctoral studies, which allowed me to gain a new perspective on the world of industrial research. I would like to thank Prof. Sergio Castillón for the help and tips about organic synthesis throughout these years. Moreover, I would like to thank Dr. Benjamin Amorelli for the interesting and stimulating scientific discussion during the IFF meetings.

I am thankful to all the former and current members of the group for all the scientific and non-scientific moments shared together. Olivia, Myriam, and Raquel, for the coffee break, for our chemistry discussion, for the support over the years in the lab and outside. Roger, Laia and Emma, for all the laugh, the good advice, the positivity and the inspirations, but mainly for the Spanish and Italian lessons. Toni, Jorge, Aitor, Isa, Montse, Miriam, for sharing happy moments in the CTQC, for our chat at the nitrogen, for sharing your positivity in the post-lockdown. I am grateful to Ramon, with his patience and peacefulness he made possible all the NMR experiments. Sara and Itziar, thanks for making me feel part of the family since day one, and for your passion for science. Mimmo and Rita, the Italian crew, thanks for the chat, the laugh, the support, the friendship, and all the dancing moments under the red lights of your lab.

I would like to thank all the people that I have met outside the lab. Grazie Serena, per la calma e il caos, per i pranzi della domenica, per il pacco da giù. Grazie Giandomenico, per la sincerità della nostra amicizia, e anche per le partite a tresette. Grazie Marco, per i biscotti con il caffè, per il divano, per quegli abbracci, pochi ma con il cuore. Grazie Carolina e Laura, per il vostro

supporto e affetto. Grazie a Giulio e Giacomo per le lezioni di cucina. Grazie a Riccardo, Giulia, Stefano, Jesus, per i momenti spensierati passati insieme. Grazie alle mie amiche di sempre, Giulia, Martina e Rosa, un pezzo di cuore, abbiamo vissuto tutto insieme, non solo piccole cose, ma grandi momenti. Avanti con la prossima avventura, sempre insieme!

Vorrei fare un ringraziamento al Prof. Pier Giorgio Cozzi, per i consigli, per il coraggio trasmesso e per l'umanità, per essere stato una guida e un mentore.

Grazie a Giuseppe, Giovanni e Giorgia per l'accoglienza e la fiducia.

C'è però una persona che più di altri ha contribuito in questo percorso, sei stato casa, famiglia, supervisor, guida, ispirazione, motivazione. Grazie Daniele per esserci, per la pazienza, per il tuo amore, per aver creduto in me, più di ogni altro, più di me stessa. Ad Maiora!

Infine, voglio ringraziare la mia famiglia, che da sempre ha sostenuto ogni mia scelta, con non pochi sacrifici. Grazie mamma e papà, per essere fonte di ispirazione nella vita e nel lavoro, per la forza, la determinazione, l'impegno, la gentilezza e l'onestà. Grazie mamma, per la bellissima copertina. Grazie nonna per avermi insegnato che nella vita bisogna vivere il mondo con curiosità, coraggio, e grande forza, come hai fatto tu.

Rhodium and Palladium Catalysed Unusual Regioselective Hydroformylation and Rhodium Catalysed Reductive Carbonylation

Benedetta Palucci

Rhodium and Palladium Catalysed Unusual Regioselective Hydroformylation and Rhodium Catalysed Reductive Carbonylation

Benedetta Palucci

A Nonna e alla nostra tappa in Spagna

Rhodium and Palladium Catalysed Unusual Regioselective Hydroformylation and Rhodium Catalysed Reductive Carbonylation

Benedetta Palucci

Table of Contents

Rhodium and Palladium Catalysed Unusual Regioselective Hydroformylation and Rhodium Catalysed Reductive Carbonylation

Benedetta Palucci

Rhodium and Palladium Catalysed Unusual Regioselective Hydroformylation and Rhodium Catalysed Reductive Carbonylation

Benedetta Palucci

Summary

The global flavours and fragrances market historically was inspired by the aroma derived from natural products. Therefore, for hundreds of years, the fragrances employed in the perfumes were extracted from plants and flowers. Only at the end of the 19th century, the production of such compounds was implemented with the use of organic synthesis and organometallic chemistry. This demand was urged by the high cost of the natural products (including extraction and purification) and the large amounts required in the cosmetic and food goods. The progress of the synthetic chemistry in this field allowed the large-scale production of these compounds at lower price. As numerous scented natural substances contain an aldehyde group, hydroformylation processes have become invaluable tools for the fragrance companies to produce these derivatives. As an example, depicted in Scheme 1, the hydroformylation of terminal olefins produces linear or branched aldehydes, as shown in Scheme 1.

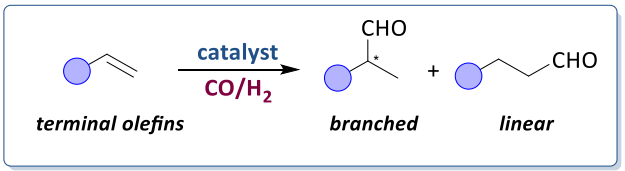

Scheme 1. Hydroformylation of terminal olefins.

In the last decades, one of the main targets in this process was the achievement of high selectivity towards one of the two possible aldehydes. The regioselectivity of the hydroformylation of alkenes determining the production of linear or branched aldehyde is function of many factors. These include inherent substrate preferences, directing effects exerted by functional groups as part of the substrate, as well as metal and ligand effects. As a general trend, alkylic olefins such as 1-octene and 1-hexene react to yield linear aldehydes while styrene derivatives afford the corresponding branched product.

The objectives of this Thesis are the development of homogenous catalytic systems employing both newly synthesised and commercially available ligands to deliver the desired aldehydes with unconventional selectivity, namely branched and linear aldehydes from terminal olefins and styrene, respectively. For this purpose, we focused our attention on the synthesis of several phosphorus based ligands for Rh-catalysed hydroformylation and on the use of an alternative metal, namely palladium. During the course of this work, investigations into the reductive carbonylation of cinnamyl allylic acetate were also conducted.

In this manuscript, the current state-of-the-art of rhodium catalysts providing unconventional selectivities in the hydroformylation of olefins is presented in Chapter I while the general objectives are described in Chapter II. Chapter III describes the synthesis and the application of bidentate phosphorus-nitrogen-centred ligands and their application in the rhodium catalysed branched hydroformylation of 1-hexene (Scheme 2).

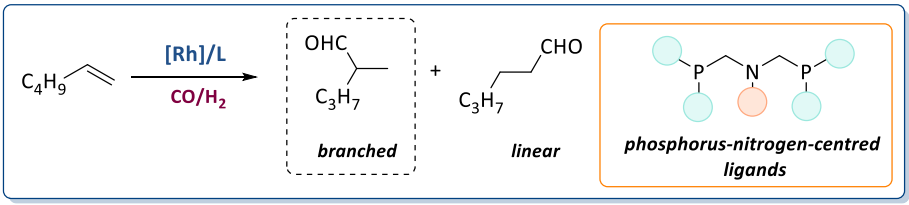

Scheme 2. Bidentate phosphorus-nitrogen-centred ligands applied in the Rh-catalysed branched hydroformylation of 1-hexene Chapter III.

As reported by Nozaki *et al.*, bidentate phosphorus-nitrogen-centred ligands, provide moderate selectivity for the production of branched aldehydes in the rhodium catalysed hydroformylation of terminal alkenes. Motivated by these findings, one of the objectives of this Thesis was the synthesis of a library of bidentate ligands to compare the activity and selectivity of the corresponding Rh catalytic systems in the hydroformylation of 1-hexene to extract information over the effect on the regioselectivity. *In situ* HP-NMR experiments were conducted to determine the coordination modes of two of these ligands exhibiting distinct electronic and steric properties ligands in

rhodium hydride dicarbonyl species to evaluate the potential relationship between coordination mode and the regioselectivities observed in catalysis (Figure 1).

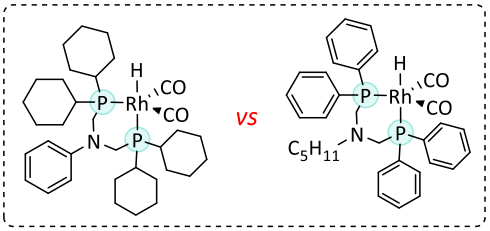

Figure 1.Chapter III: Rhodium hydride dicarbonyl species.

Chapter IV describes the synthesis of a new family of phosphine-phosphite and phosphine-phosphoramidite ligands and their use in the hydroformylation of 1-octene catalysed by rhodium, to obtain the selective formation of the branched aldehyde (Scheme 3). The potential correlation between the nature of the substituents and the selectivity towards the formation of the branched aldehyde was particularly looked at.

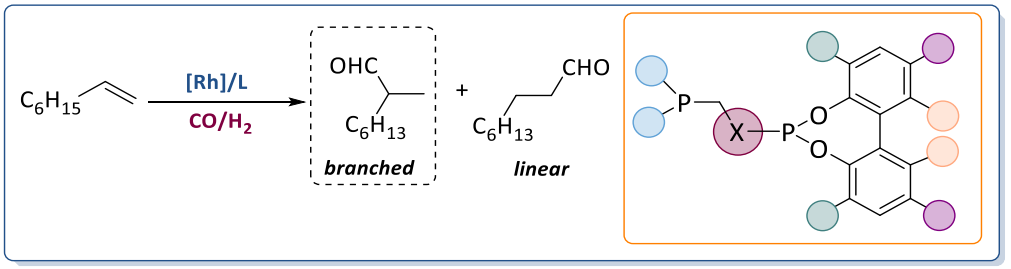

Scheme 3. Chapter IV: phopshine-phosphite and phosphine-phosphoramidite ligands in Rh-catalysed hydroformylation of 1-octene.

After a brief optimization, the best performing catalytic system in terms of branched to linear ratio was studied by HP-NMR to determine the coordination mode in the corresponding rhodium hydride dicarbonyl species (Scheme 4).

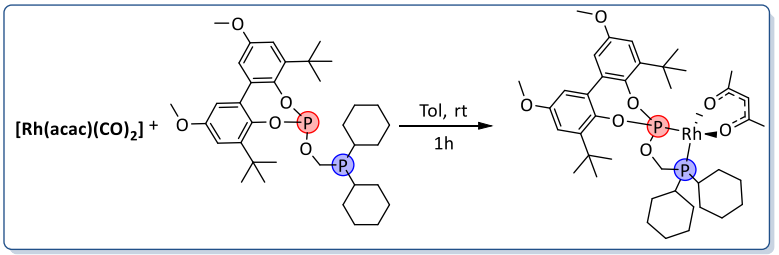

Scheme 4. Chapter IV: Rhodium hydride dicarbonyl species.

The investigation carried out in Chapter V focuses on the development of a novel family of bis(dipyrrolyl-phosphorodiamidite) ligands for their application in the rhodium catalysed linear hydroformylation of styrene (Scheme 5). Various reaction parameters (such as temperature, Rh to ligand ratio, Rh loading and CO:H_2 pressure) were varied to understand their effect over the linear selectivity in this process (Scheme 5).

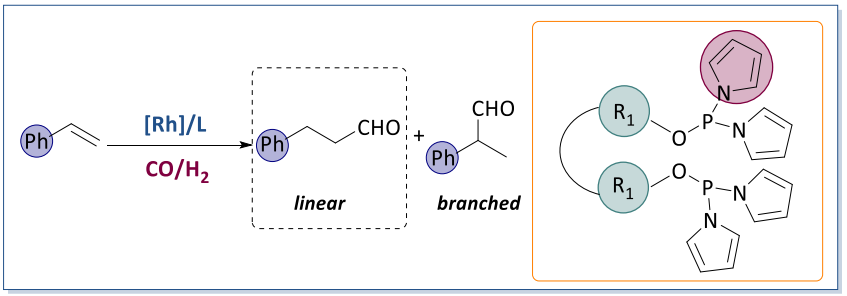

Scheme 5. Chapter V: bis(dipyrrolyl-phosphorodiamidite) ligands in Rh-catalysed hydroformylation of styrene.

Chapter VI describes the use of a Pd catalytic system and formaldehyde as an alternative syngas source to promote the selective formation of the linear aldehyde from styrene (Scheme 6).

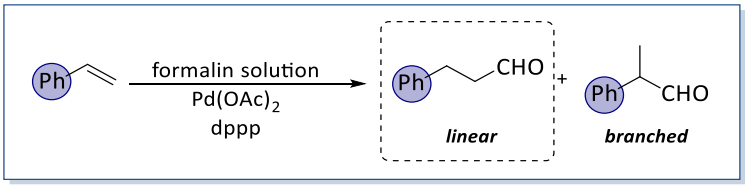

Scheme 6.Chapter VI: Palladium catalysed linear hydroformylation of styrene using formaldehyde as syngas surrogate.

The selective formation of the linear aldehyde was achieved by careful optimization of the reaction parameters. To get insights into the reaction mechanism, NMR monitoring, isotopic labelling experiments and kinetic studies were also performed.

Chapter VII describes the rhodium catalysed reductive carbonylation of cinnamyl acetate for the production of aldehydes (Scheme 7).

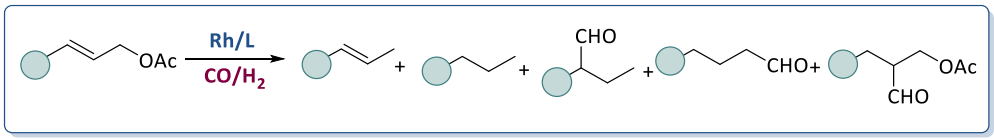

Scheme 7.Chapter VII: Rh-catalysed reductive carbonylation of cinnamyl acetate.

In situ HP-NMR experiment were conducted to study of the reactivity of cinnamyl acetate and two Rh systems towards CO, and H_2/CO pressure. A catalytic cycle for this process was proposed based on the results obtained experimentally.

Rhodium and Palladium Catalysed Unusual Regioselective Hydroformylation and Rhodium Catalysed Reductive Carbonylation

Benedetta Palucci

Chapter I

General introduction

Rhodium and Palladium Catalysed Unusual Regioselective Hydroformylation and Rhodium Catalysed Reductive Carbonylation

Benedetta Palucci

1.1 Introduction

1.1.1 Hydroformylation process

The hydroformylation of alkenes is nowadays one of the most important industrial application of homogeneous catalysis (Scheme 1).[1, 2] Today, more than 10 million metric tons of aliphatic aldehydes of different chain lengths are produced annually in plants across the globe: up to 100.000 t/y by the giants of the chemical industry, and much smaller quantities by small companies producing fine chemicals. Moreover, a study of patent activities and academic publications between 2010 and 2015 offers clear evidence that hydroformylation is still an important focus of industrial research.[3] The majority of these oxo-products are obtained from the hydroformylation of propene **1.2**, which is a fraction of the steam-cracking process. The resulting products *iso*-butyraldehyde **1.2** and *n*-butanal **1.3** are important intermediates for the production of esters, acrylates and 2-ethylhexanol (Scheme **1.1**).[1, 2]

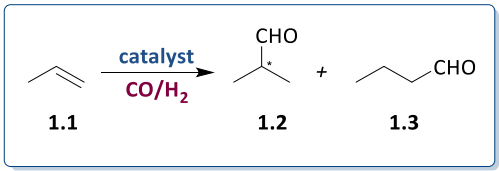

Scheme 1.1. Hydroformylation of propene.

From a synthetic point of view, the reaction is a one-carbon chain elongation caused by the addition of carbon monoxide and hydrogen across the π system of a C=C double bond.[3, 4] As a pure addition reaction, the hydroformylation reaction meets all requirements of an atom economic process.[5] Furthermore, the synthetically valuable aldehydic function is introduced, which allows subsequent skeleton expansion that may even be achieved in one-pot sequential transformations.[6, 7] Apart from aldehydes, the versatility of this reaction allows the one-step production under special hydroformylation conditions of many other functional groups, such as alcohols, acetals,

carboxylic acids, esters, amines and amides.[8] Among the metals that can catalyse hydroformylation reactions, rhodium has been largely studied due to its intrinsic properties that provide high activity, and selectivity for this type of reaction.[9, 10] As such, rhodium is nowadays the metal of choice in hydroformylation process due to its high activity, and selectivity.[11] In terms of sustainability, the production of aldehydes from inexpensive feedstock (alkenes, syngas) in a single step under essentially neutral reaction conditions is the most suitable route. However, several issues are still to overcome.[3, 4] Among the most significant there are (a) the low reaction rates at low temperature where high selectivity is usually observed, (b) the difficulty to control simultaneously the chemo-, regio- and, when required, the enantioselectivity and (c) the limited substrate scope for any single catalytic system.

1.1.2 Rhodium catalysed hydroformylation mechanism

The hydroformylation (HF) reaction was discovered in 1938 by Otto Roelen while he was working on the Fischer-Tropsch process, and named it "oxo process".[12] Heck and Breslow proposed a mechanism using a cobalt catalyst that remains accepted for the rhodium catalysed hydroformylation.[13] Here, this mechanism is described for a bidentate ligand, and consists in the Wilkinson's dissociative mechanism (Scheme 1.2). The determination and structural characterization of the resting state [RhH(L-L)$(CO)_2$] **1.4** by *in situ* spectroscopic techniques such as High Pressure-Infrared (HP-IR) and High Pressure-Nuclear Magnetic Resonance (HP-NMR), provided great understanding of the mechanism. In the case of bidentate ligands, the species **1.5** can be observed as two different isomers where the ligand is coordinated in equatorial-axial (eq-ax) or equatorial-equatorial (eq-eq) mode.

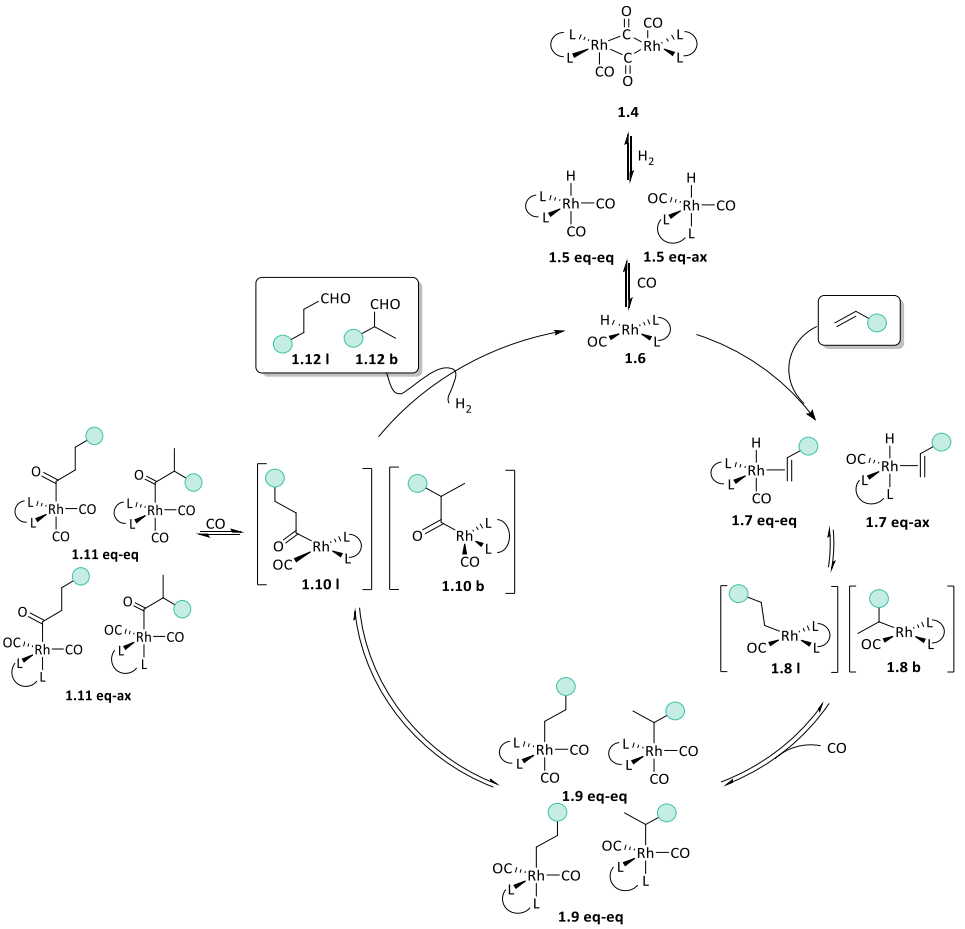

Scheme 1.2. Rhodium catalysed hydroformylation mechanism in the presence of bidentate ligand (L-L).

First, fast dissociation of equatorial CO from **1.5** takes place to form the square planar intermediate **1.6** which upon coordination of the alkene in the equatorial plane, provides the complexes **1.7**. In this intermediate, the bidentate ligand can once more be coordinated in the eq-eq and/or eq-ax mode, while the hydride lies in the apical position. In this step, the enantioface discrimination takes place.[14-17] Although it has not been completely established whether the coordination of the alkenes is reversible or not, all the steps in Scheme 1.2 are described as reversible except from the final hydrogenolysis. From **1.7**, migratory insertion of the alkene generates

the square-planar alkyl complexes **1.8.** Experiments using deuterated substrates suggest that alkene coordination and insertion into the Rh-H bond can be reversible, certainly when the pressures are low. This species can undergo β-hydride elimination, thus leading to isomerization, or can react with CO to form the trigonal bipyramid (TBP) complexes **1.9**. Thus, under low pressure of CO more isomerization may be expected.[18] At low temperatures (< 70 °C) and at sufficiently high pressure of CO (> 10 bar) the insertion reaction is usually irreversible and thus the regioselectivity and the enantioselectivity in the hydroformylation of alkenes is determined at this point. It is between species **1.7** and **1.8** where the regioselectivity is determined. The acyl square planar species **1.10** are generated by CO insertion, which finally undergo irreversible hydrogenolysis to provide the aldehyde products (**1.12l** and **1.12b**) and regenerate the hydride species **1.6**. The reaction with H_2 involves presumably oxidative addition and reductive elimination, but for rhodium no trivalent intermediates have been observed.[19] The species **1.10** can also undergo CO coordination and provide acyl pentacoordinated species **1.11**. Such species have been recently observed by HP-IR and HP-NMR studies using bidentate ligands.[15, 17] Depending on the reaction conditions and characteristics of the system, the rate determining step can switch between the equilibriums from species **1.5** to **1.9**. The regioselectivity of the hydroformylation of alkenes is function of many factors. These include inherent substrate preferences, directing effects exerted by functional groups as part of the substrate, as well as catalyst effects.[3, 4] In order to appreciate substrate inherent regioselectivity trends, alkenes have to be classified according to the number and nature of their substituents (Scheme 1.3).[6, 7]

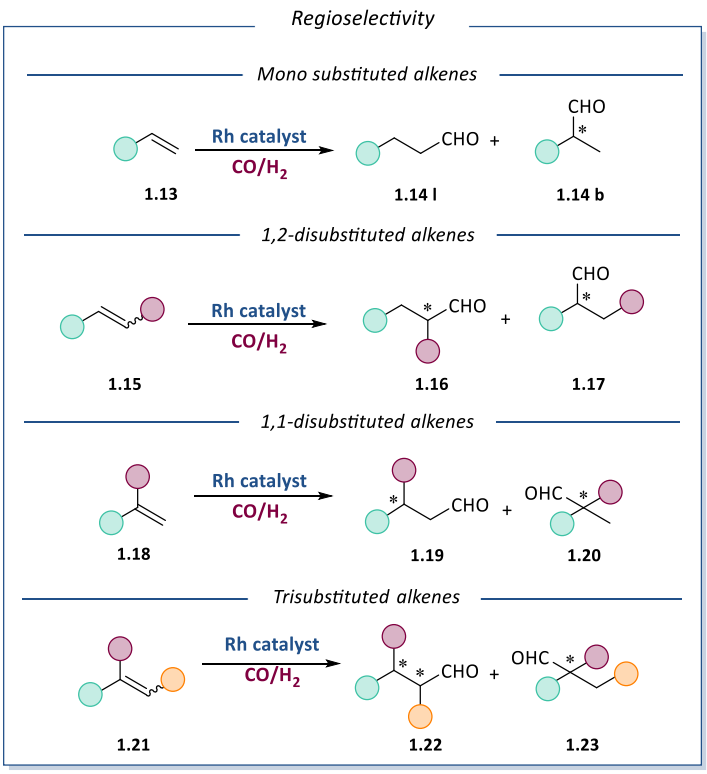

Scheme 1.3. Regioselectivity trends in rhodium catalysed hydroformylation of various alkenes.

For instance, the exponential drop of alkene reactivity when increasing the number of substituents on the double bond causes many problems in the control of chemoselectivity and regioselectivity in the low-pressure hydroformylation of alkenes. Until very recently, there are only few catalytic systems able to efficiently catalyse the hydroformylation of complex alkenes under low-pressure conditions. These catalytic systems were composed by organometallic complexes of rhodium with strong π-acceptor ligands, such as bulky phosphites[20,21] and phosphobenzene systems.[22] Nonetheless, these systems produced mixtures of aldehydes since the high activity of the corresponding rhodium catalysts is always associated with a high tendency towards alkene isomerization and renders a position-selective hydroformylation of an internal alkene so far impossible. The regioselectivity

issue usually arises for terminal and 1,2-disubstituted alkenes. For alkyl-substituted terminal alkenes **1.13**, there is a slight preference for the linear product **1.14l**. For terminal alkenes **1.13** containing electron-withdrawing substituent the formation of the branched product **1.14b** is favored and is sometimes the exclusive product. These preferences usually also apply for the regioselectivity of 1,2-disubstituted alkenes **1.15**. Both 1,1'-disubstituted **1.18** and trisubstituted **1.21** alkenes generally provide only one regioisomer (**1.19** and **1.22**, respectively) based on Keuleman's rule, which states that the formyl group is usually added in order to avoid the formation of a quaternary carbon centre.[23] Over the last years, several reports have demonstrated that these commonly accepted trends in regioselectivity can be overcome through the utilization of the appropriate ligands and/or modification of the substrates, as it will be detailed in the next paragraphs.

1.1.3 Rhodium catalysed hydroformylation: regioselectivity issues

As previously mentioned, the regioselectivity of the hydroformylation of terminal alkenes is mainly determined by the electronic properties of the substituents attached to the substrate. The presence of electron-withdrawing groups strongly favours the formation of the branched aldehydes while the linear product is usually favored when an electron donating substituent such as an alkyl group is present. However, several catalytic systems have recently emerged providing the opposite regioselectivity. In the following sections, the most relevant results in this area will be described.

1.1.3.1 Linear hydroformylation of terminal alkenes bearing electron-withdrawing substituents: Vinyl arenes

In the case of vinyl arenes, the rhodium catalysed hydroformylation of styrene into the corresponding aldehydes has been largely reported[24-26] and its

mechanism has been studied in depth.[27] The proposed catalytic cycle is depicted in Scheme 1.4.

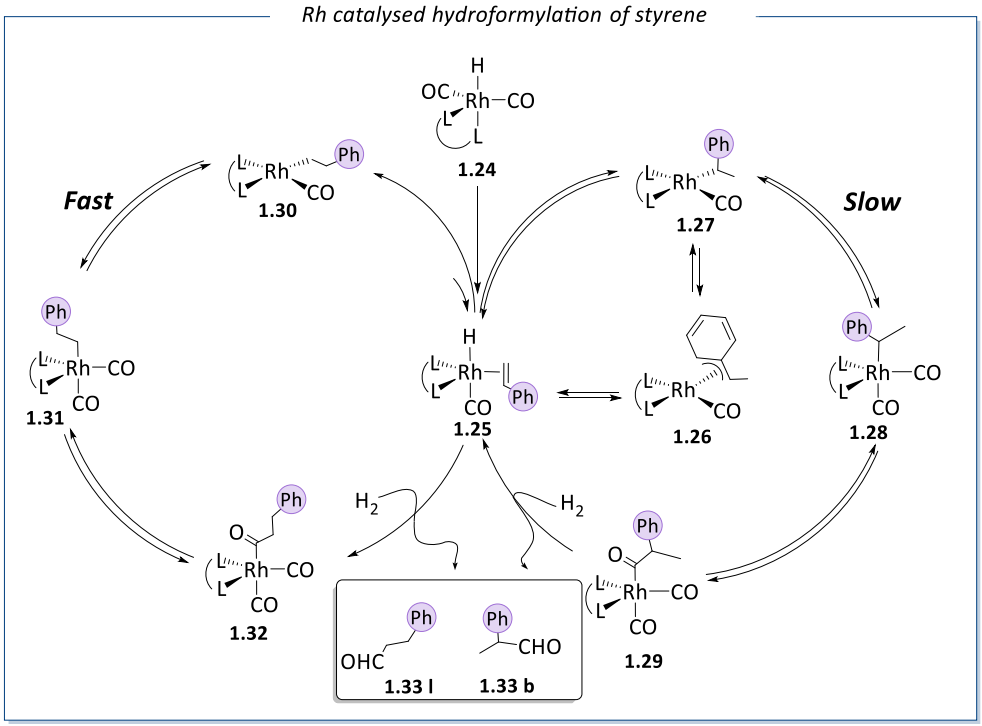

Scheme 1.4. Proposed mechanism for the rhodium catalysed hydroformylation of styrene.

In this mechanism, the formation of the rhodium alkyl intermediates **1.28** and **1.31** from the rhodium hydride species **1.25** is the key step controlling the regioselectivity. Lazzaroni and co-workers showed that in this reaction, the kinetic product is the branched aldehyde and is therefore favored when the reaction is conducted at low temperature. The formation of this product is also favored by the formation of the stable Rh (η^3-allyl) species **1.26**, which is in equilibrium with the branched Rh-alkyl species **1.27** that is at the origin of the production of the branched aldehyde. The presence of these species tends to shift the equilibrium towards the catalytic cycle affording the branched product. In these studies, the effect of temperature was shown to affect the regioselectivity of the overall process and isotopic labeling experiments demonstrated that the formation of both linear and branched

Rh-alkyl species is irreversible at low temperature but becomes reversible at high temperature.[27] Brown and Kent reported that the coordination mode of the phosphine ligands could also influence the regioselectivity of the reaction: the steric hindrance provided by the ee coordination favours the formation of the linear alkyl complex while the eq-ax coordination of the ligand favours the formation of the branched product.[28] There are only a few examples in the literature concerning the selective formation of the linear aldehyde in the Rh-catalysed hydroformylation of styrene.[29-32]

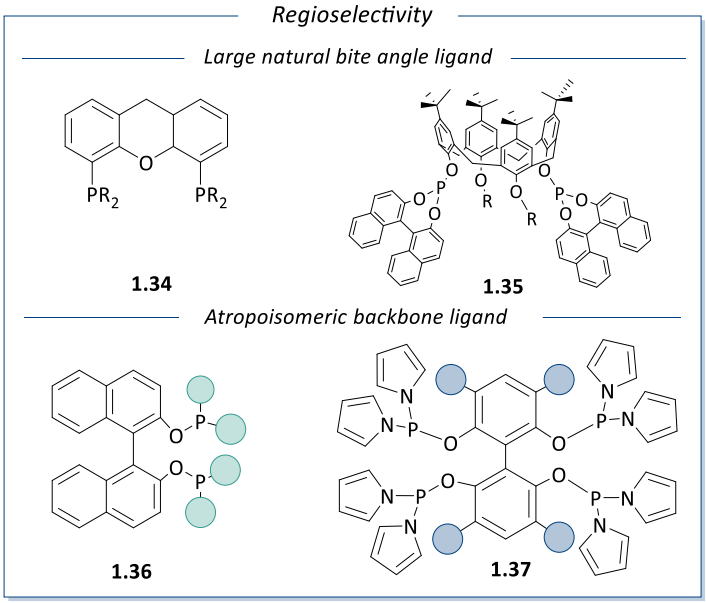

Figure 1.1. Ligands reported to provide high linear regioselectivity in the Rh-catalysed hydroformylation of styrene.

In the following sections, the most relevant systems providing the regioselective linear hydroformylation of styrene will be described according to the types of ligands used: those presenting a large natural bite angle and those presenting an atropoisomeric backbone (Figure 1.1).

Large natural bite angle ligands:

Xantphos-type ligands

In 1998, van Leeuwen and co-workers reported a study on the electronic effect in the rhodium catalysed hydroformylation of alkene using a series of thixantphos ligands **1.40** (Scheme 1.6) bearing several electron donating and electron withdrawing groups in *para* position of the phenyl substituents on the phosphorus.[14] In the hydroformylation of styrene, an increase in l/b ratio and activity was observed with decreasing phosphine basicity (Scheme 1.5).

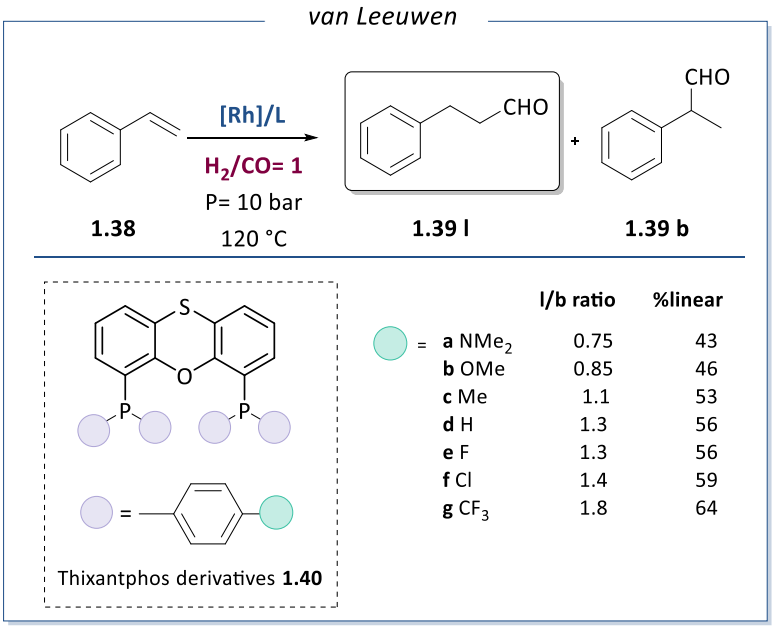

Scheme 1.5. Electronic effect in the Rh-catalysed hydroformylation of styrene using thixantphos ligands.

In contrast, for 1-octene, the selectivity for linear aldehyde formation was between 92% and 93% for all ligands and it was concluded that the overall selectivity for linear aldehyde is not influenced by phosphine basicity for this substrate. A pronounced effect of phosphine basicity was also observed on the chelation mode of the ligands in the RhH(diphosphine)$(CO)_2$complexes. The eq-eq / eq-ax isomer ratio, observed in the *in situ* IR and NMR spectra,

showed a regular increase with decreasing phosphine basicity. The electronic ligand effect on catalysis is reflected in both hydroformylation and β-hydrogen elimination rates. However, the regiochemistry in the hydroformylation reaction could not be clearly correlated with the chelation mode in the $RhH(CO)_2$(diphosphine) complexes and a better correlation was observed between the linear selectivity and the calculated natural bite angle of the ligands. These results indicated that the effect of the bite angle on the regioselectivity of the rhodium diphosphine catalysed hydroformylation is not clear if the structure of the five-coordinate $RhH(CO)_2$(diphosphine) complexes is considered, but could perhaps be explained by its role at the tetra-coordinate $RhH(CO)_2$(diphosphine) intermediates. To investigate the exact correlation between the selectivity and the natural bite angle of diphosphine ligands in the rhodium catalysed hydroformylation of styrene, the same group developed a new family of ligand based on xanthene backbone and hypothesized an increase in selectivity to linear aldehyde with the increase of the natural bite angle.[31] In this study, the styrene hydroformylation process was carried out at 120 °C and 10 bar of 1:1 CO/H_2 using a 0.5 mM solution of rhodium precatalyst and 10 equivalents of ligand. These reaction conditions were previously reported to enhance the l/b ratio in this reaction. The results of this work are summarized in Scheme 1.6 In this study, the authors concluded that the natural bite angle of the ligands correlates well with the selectivity for linear aldehyde in the hydroformylation of styrene due to a higher congestion around the metal center. However, no clear correlation between the natural bite angle and the ratio of eq-eq/eq-ax $[RhH(CO)_2(PP)]$ isomers was observed.

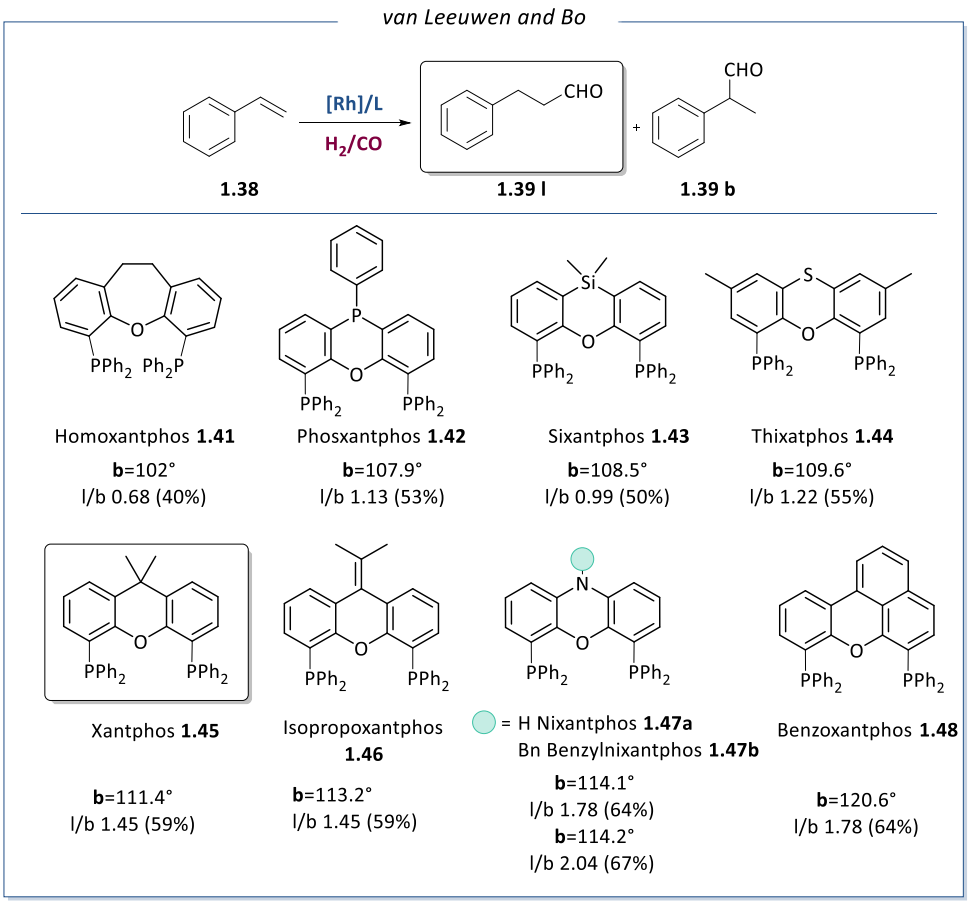

Scheme 1.6. Rh-catalysed hydroformylation of styrene using Xantphos derivatives.

Later, van Leeuwen and Bo reported a theoretical study to unravel the origin of selectivity in hydroformylation for this type of catalytic system using 1-octene as substrate.[33] They concluded that the regioselectivity is governed by the nonbonding interactions between the diphenylphosphino substituents of the Xantphos ligands and the substrate, whereas the effects directly associated to the bite angle seem to have a smaller influence. When the bite angle was increased from 102° to 114°, an increase in linear to branched ratio was clearly observed. However, when ligand **1.48**, which exhibits a natural bite angle of 120°, was used, the selectivity slightly decreased. Within this series, the highest selectivity was obtained with ligand **1.47b** (67%). The same

research group later analyzed the effect of the structure of the ligand backbone on the selectivity of the Rh-catalysed hydroformylation and demonstrated that the rigidity of the ligand backbone is also an important factor.[29] Indeed, comparing results obtained with a series of bidentate ligands presenting large natural bite angles (Scheme 1.7), they showed that a rigid backbone such as that of Xantphos (**1.45**) provides the highest l/b ratio in this process.

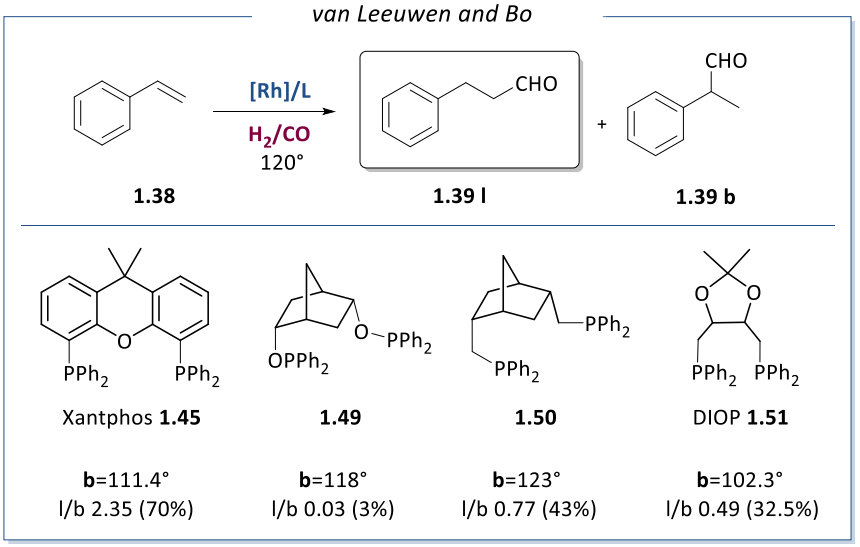

Scheme 1.7. Rh-catalysed regioselective styrene hydroformylation.

In summary, the works developed by the group of van Leeuwen showed that large bite angle diphosphine ligands provide high regioselectivity in the Rh-catalysed hydroformylation of alkenes to the linear aldehyde products. However, the effect of the natural bite angle remains unclear since the electronic properties and rigidity of the backbone were also shown to affect the regioselectivity of this process.

Calixarene-based diphosphites ligands

Calix[4]arenes diphosphite ligands were first applied in the rhodium-catalysed hydroformylation of 1-alkene by BASF.[34] In 2010, Semeril and co-

workers studied the use of calixarene-based diphosphites ligands in the Rh-catalysed hydroformylation of styrene and 1-octene, mainly focusing on the regioselectivity of this reaction (Scheme 1.8).[35]

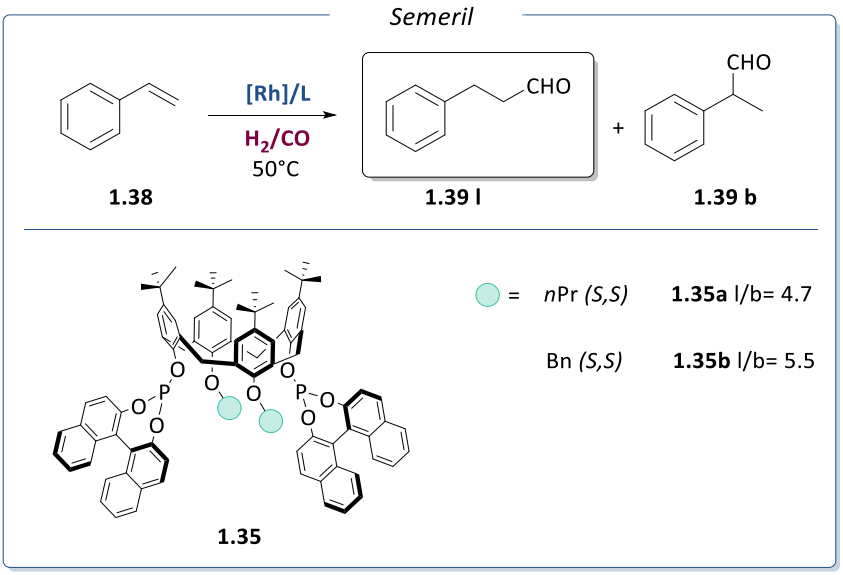

Scheme 1.8. Calixarene-based diphosphites reported by Semeril and co-workers.

Two of these large bite angle calixarene based diphosphite ligands (**1.35a** and **1.35b**) were tested in the rhodium catalysed hydroformylation of styrene at 50 °C and 10 bar of 1:2 CO/H_2. Although the $[RhH(CO)_2(LL)]$ species containing these ligands exhibited similar structures with eq-eq coordination of the ligands, these two systems provided very distinct selectivity: a linear to branched ratio of 4.7 was achieved using ligand **1.35a** while a value of 5.5 was obtained when **1.35b** was used. The authors attributed the high selectivity for linear aldehydes to the ability of the hemispherical ligands to embrace the catalytic center.

Atropoisomeric bidentate ligands

The two other families of ligands reported to provide high linear selectivity in the Rh-catalysed hydroformylation of styrene present an atropoisomeric backbone and are based on either bis(hydroxy)phenol or binaphthol

structures. The results reported for these ligands will be described in the following sections.

Tetraphosphorus binol-based Ligands

The family of ligands based on bis(hydroxy)phenol contain four phosphorus atoms (Scheme 1.9) and was developed by Zhang and co-workers.[32]

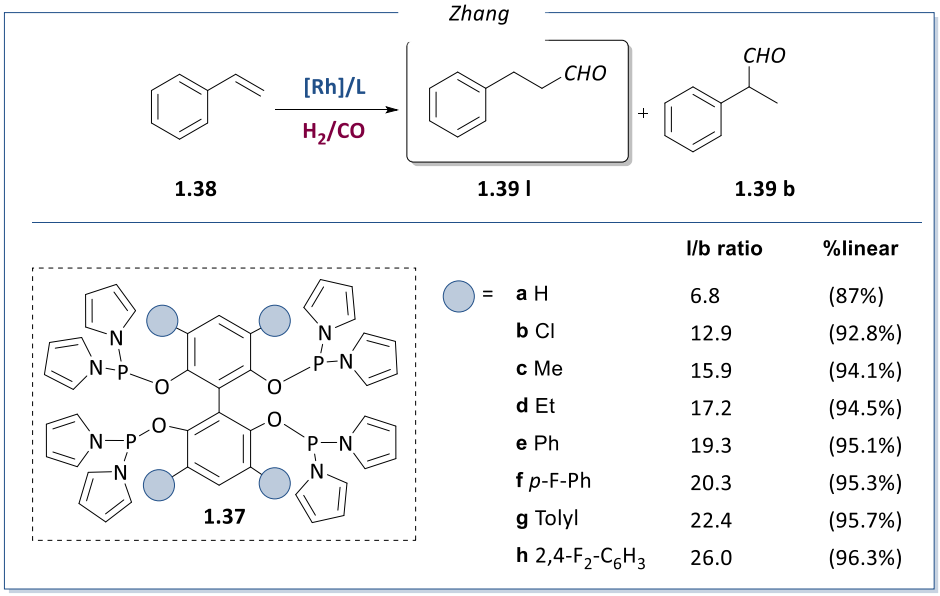

	l/b ratio	%linear
a H	6.8	(87%)
b Cl	12.9	(92.8%)
c Me	15.9	(94.1%)
d Et	17.2	(94.5%)
e Ph	19.3	(95.1%)
f *p*-F-Ph	20.3	(95.3%)
g Tolyl	22.4	(95.7%)
h 2,4-F_2-C_6H_3	26.0	(96.3%)

Scheme 1.9. Styrene hydroformylation with tetraphosphorus derivatives reported by Zhang.

Using these ligands, the styrene hydroformylation process was carried out at 80 °C and 10 bar of 1:1 CO/H_2 using a 1.0 mM solution of rhodium precatalyst and 3 equivalents of ligand. These results clearly indicated that an increase in steric bulk in 3,3'-5,5' positions of the biphenyl moiety favour the regioselectivity of the reaction towards the linear aldehyde while the electronic properties of the ligand mainly affect the catalytic activity. Indeed, the use of ligand **1.37b** bearing a chloride substituent increased the linear to branched ratio from 6.8 to 12.9 when compared to the unsubstituted ligand. Similar regioselectivity was obtained using the alkyl substituted ligands **1.37c** and **1.37d** although in these latter cases, the conversion dropped

significantly. Further increase in steric hindrance of the ligands by introduction of aryl substituents provided l/b ratios up to 26. The difference observed between the catalytic performance of **1.37g** and **1.37h** was attributed to an electronic effect since similar steric hindrance is expected for both ligands. They concluded that for two ligands exhibiting similar steric hindrance, the presence of electron withdrawing groups like in **1.37h** favours the formation of the linear aldehyde. To explain these excellent results, the authors postulated that the high steric hindrance at the ortho position could inhibit the formation of the η^3-benzylic rhodium coordination that favours the formation of the branched aldehyde, and therefore results in a higher linear regioselectivity. Furthermore, the steric hindrance at the ortho position could facilitate the reductive elimination, which could explain the high activity observed. To better understand these results, the Hammett constants for *para* substituent on phenyl group of ligands **1.37a** to **1.37h** were analysed. The Hammett equation that explain the influence of the aromatic substituents can be simply expressed through the use of two different kinetic constants (one for the formation of linear aldehyde and one branched aldehyde). Their results clearly showed that an electron-withdrawing group had a positive effect on the linear selectivity. The highest linear selectivity was afforded by ligand **1.37h** (Scheme 1.10 l/b ratio of 26), which bears 2 strong electron-withdrawing CF_3- groups on the phenyl ring (Hammet constant σ_p = 0.4).

Bidentate binaphthol based ligands

The second family of atropoisomeric ligands that provided high selectivity to the linear aldehyde is constituted by binaphthol based ligands, which had been previously applied in several other catalytic reactions.[36, 37] In 2013, Vogt et al. compared the catalytic performance of a series of rhodium catalysts bearing various bidentate ligands: four binaphthol based ligands, one Xantphos derivative and a tetraphosphorus ligand (Scheme 1.10). [38]

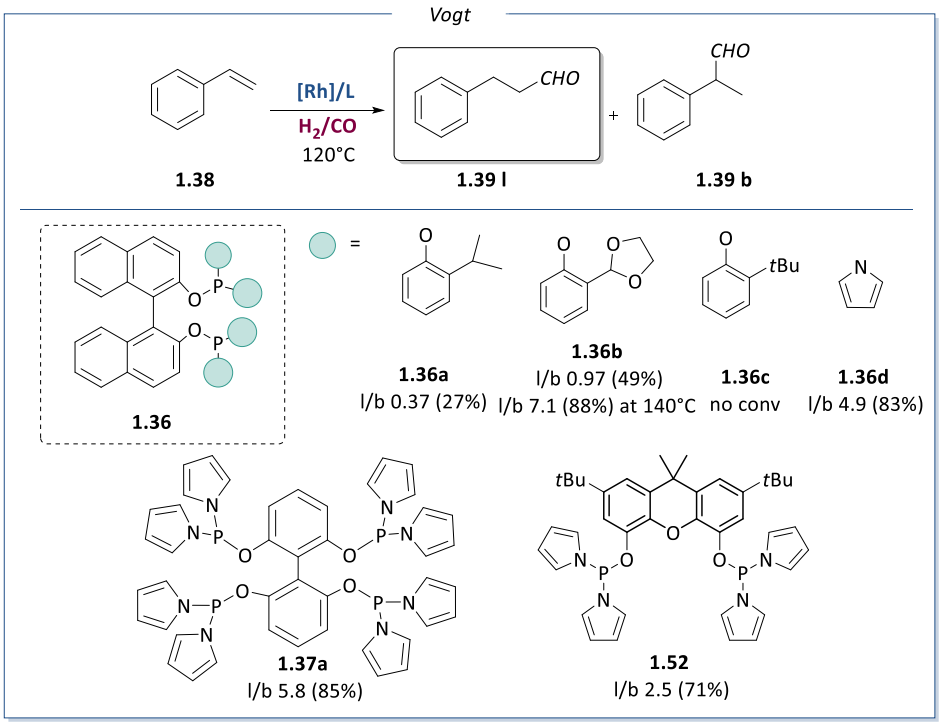

Scheme 1.10. Rh-catalysed hydroformylation of styrene using binaphthol derivatives and phosphorodiamidite based ligands.

The binaphthol based ligands **1.36a**, **1.36b** and **1.36d** showed good activity, while **1.36c** did not provide any conversion. The absence of activity in the latter case was attributed to the high steric hindrance induced by the *tert*-butyl groups in the *ortho* position of the phenoxy moiety on the ligand. When the reaction was performed with ligand **1.36b** at 140°C an increase in linear to branched ratio up to 7.1 was observed, although a higher amount of the hydrogenation product was also detected. The highest regioselectivities at 80 °C were obtained with the pyrrole substituted ligands **1.36d**, **1.37a** and **1.51,** indicating that ligands with more pronounced π-accepting properties favor the linear product under these conditions. In 2013, Zheng and co-workers compared a series of ligands based on various types of backbones.[39] Eight different ligand backbones were tested under the same conditions and the

ligands that contain the pyrrole moiety showed better performance in terms of regioselectivity to linear aldehyde (Scheme 1.11).

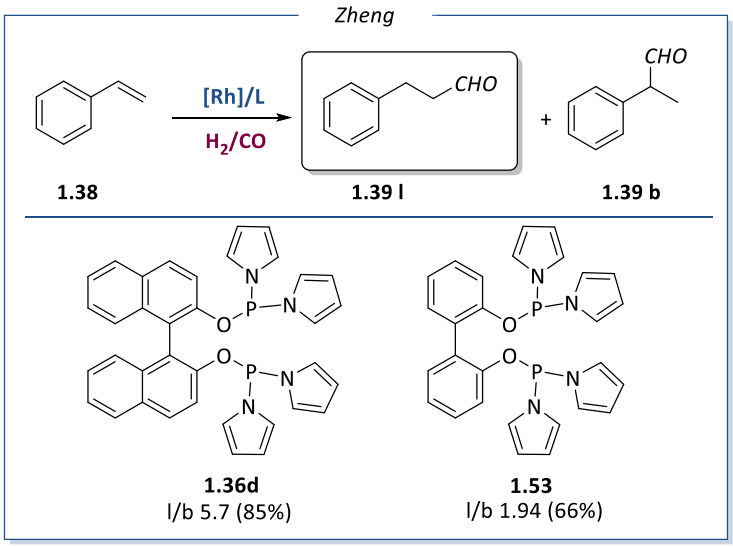

Scheme 1.11. Comparison of the results reported by Zheng on the Rh-catalysed hydroformylation of styrene using binaphthol and binol-based ligands.

The binaphthol based ligand **1.36d** provided the highest regioselectivity with 85% of linear aldehyde. Interestingly, the ligand **1.53**, which presents structural properties related to those of **1.36d**, provided much lower selectivity to the linear aldehyde under the same conditions, indicating that the atropoisomeric backbone is key to reach high selectivity in this reaction.

1.1.3.2 Branched hydroformylation of terminal alkenes bearing electron-donating substituents

In the Rh-catalysed hydroformylation of 1-alkenes bearing electron-donating substituents, the linear product is usually preferentially obtained and selective systems have been developed.[40] However, some efforts have also focused on obtaining the branched aldehydes, although mainly in the context of enantioselective hydroformylation since these products contain a chiral carbon center. In this reaction, the regioselectivity is determined by steric

and electronic properties of the alkenes, but also by the metal catalyst, the ligand and the reaction conditions (mainly temperature, pressure and *syngas* ratio). Terminal olefins are selectively hydroformylated to linear aldehydes by using diphosphite ligands such as BiphePhos[41-43] or diphosphine ligand such as BISBI[44] or Xantphos.[45] Instead, activated alkenes such as dienes,[46] vinyl acetates and amides,[47, 48] bearing electron poor moieties, give the branched aldehydes as major products. One of the first examples of asymmetric hydroformylation of 1-alkene was reported by Takaya and Nozaki in 1997 using *(R,S)*-BINAPHOS.[49] High enantioselectivity was obtained (82% *ee*) using 1-hexene as substrate but with low regioselectivity for the branched aldehyde (24%). In this context, Morken and co-workers reported the regioselective hydroformylation of 1-alkene using commercial (*S,S*)-Ph-BPE ligand, with good regioselectivities and enantioselectivities towards the branched aldehyde (Scheme 1.12).[50] 1-dodecene was selected as model substrate and was hydroformylated under 10 bar of syngas ($CO:H_2$ = 1:1). Both ligand Me-DuPhos **1.55b** and Me-BPE **1.56a** promote the hydroformylation reaction with respectively 0.5 and 0.9 of branched to linear ratio. Changing from methyl groups to larger isopropyl (*i*-DuPhos **1.55a**) and phenyl (Ph-BPE **1.56b**) groups provided higher enantioselectivity and slightly higher regioselectivity toward the branched product (1.2 b/l, 95% *ee*).

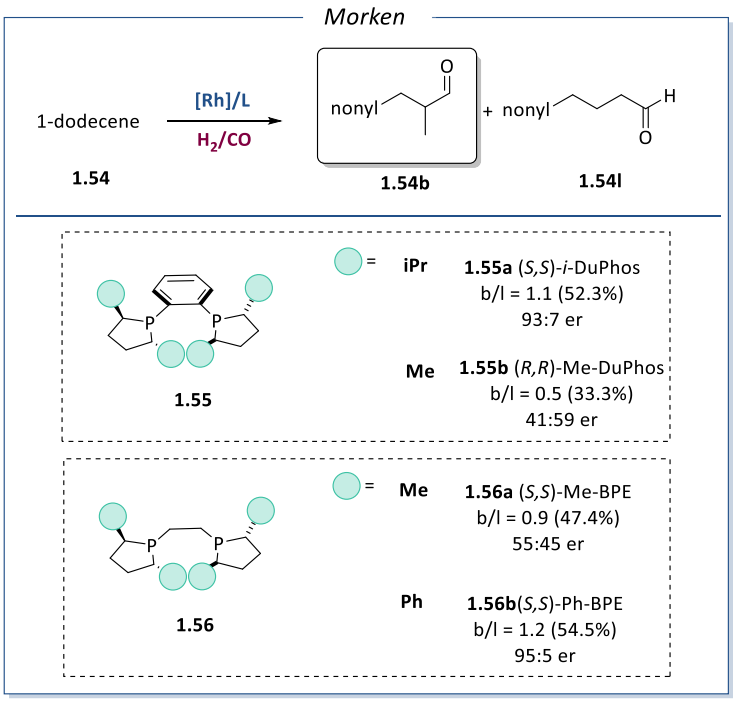

Scheme 1.12. Comparison of the results reported by Morken on the Rh-catalysed hydroformylation of 1-dodecene using bis phospholane-derivatives ligands.

In 2012, Clarke and co-workers described the synthesis and the application of BOBPHOS ligand **1.59** in the asymmetric hydroformylation of alkyl alkenes (Scheme 1.13).[51] Remarkably, ligand **1.59** which combine the structural properties of Ph-BPE **1.56b** and Kelliphite ligands, provided much higher selectivity to the branched aldehyde and enantioselectivity than the parent ligands. Low temperature (15 °C) and 5 bar of 1:1 CO/H_2 are required to obtain 3.0 branched to linear selectivity and 93% of enantioselectivity, using 1-hexene as model substrate.

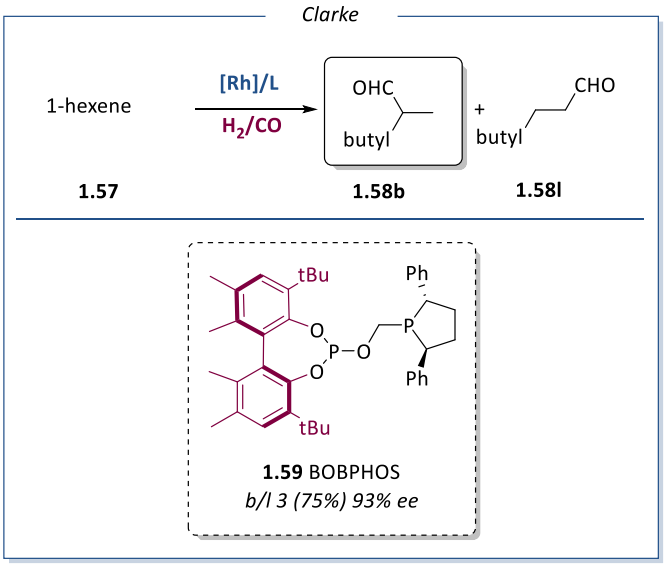

Scheme 1.13. Rh-catalysed hydroformylation of 1-hexene using BOBPHOS ligand **1.59**.

The same research group later analyzed the effect of the structure of the ligand backbone on the selectivity of the Rh-catalysed hydroformylation. They concluded that the combinations of the rigid structure of Rh/BOBPHOS catalyst, that leaves an open space for the branched alkyl formation, and of the attractive interactions during an early stage in C–H bond formation, forbids the formation of a linear Rh-alkyl species, thus favoring the formation of the branched product.[15] In 2018, Clarke and co-workers, faced the unsolved problem of the *iso*-selective hydroformylation of propene as substrate. Inspired by the BOBPHOS **1.59** ligand the authors reported the use of *tropos,rac*-ligand/Rh catalyst with good branched selectivity. It is noteworthy that the reaction was performed in hexafluorobenzene as solvent, which was key to obtain high *iso/n* selectivity (Scheme 1.14).[52]

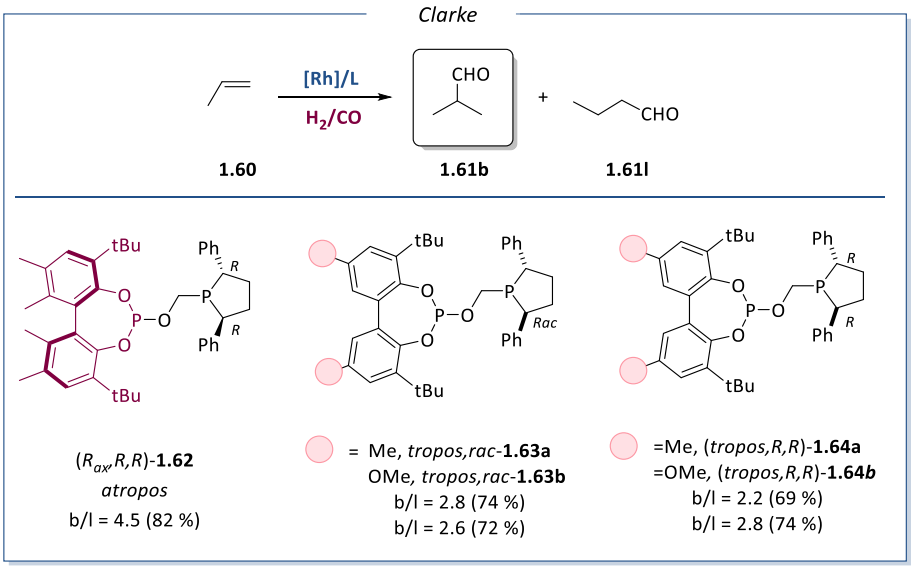

Scheme 1.14. Rh-catalysed hydroformylation of propene using *tropos* ligand.

The results obtained using the *tropos-rac* ligands **1.63a**, **1.63b** and the two (*tropos,R,R)* **1.64a** and **1.64b** were comparable in terms of regioselectivity and activity to the enantiopure (R_{ax},*R*,*R*)-BOBPHOS ligand **1.59** (82% *iso*). The authors demonstrated that the *tropos* ligand performs like a single enantiomer during catalysis, when is coordinated to the rhodium complex, providing a preferred conformation. In 2004, Reek *at al.*, established a new supramolecular strategy using Rh-complexes based on pyridine-substituted phosphines as template where the pyridine coordinates to zinc(II) or ruthenium(II) porphyrin moieties (Scheme 1.15).[53] These closed structure that encapsulated the active metal with three porphyrins on tris-3-pyridylphosphine **1.67a** and **1.67b** gave a good selectivity over the branched aldehyde (62%, 67%) in the rhodium hydroformylation of 1-octene. The authors proposed that this selectivity raises from the steric restriction imposed on the metal-substrate complex inside the capsule.

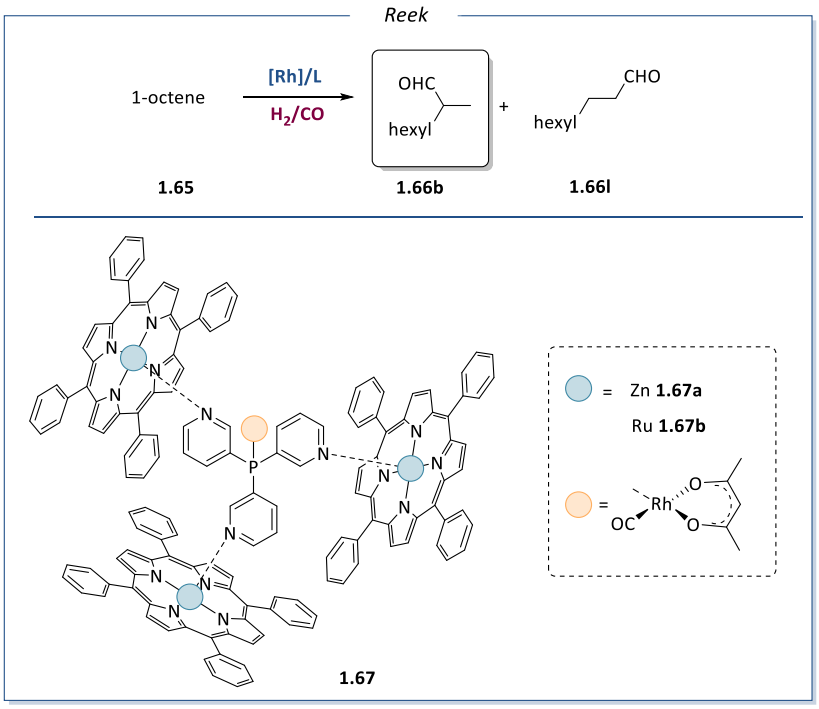

Scheme 1.15. Rh-catalysed hydroformylation of 1-octene using zinc(II) or ruthenium(II) porphyrins in transition metal complexes based on pyridine-substituted phosphine ligands.

Dabbawala *et al.* demonstrated that rhodium complexes with PNp_3 **1.68** and $P(ONp)_3$ **1.69** provide good results in terms of branched 2-aldehydes formation (Scheme 1.16) due to the steric hindrance induced by these two ligands at 110 °C and 40 bar of syngas pressure up to 54-58%.[54] The chemo- and regioselectivity were increased by the use of the phosphite $P(ONp)_3$ as auxiliary ligand in the Rh/ PNp_3 catalysed hydroformylation of 1-hexene.

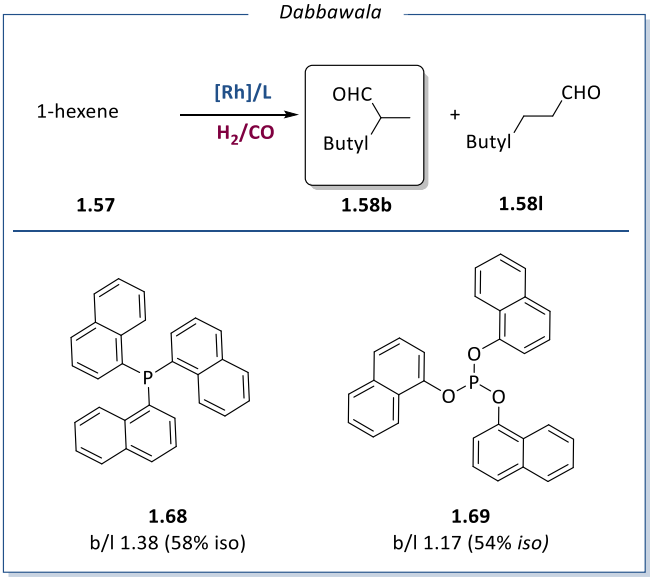

Scheme 1.16. Rh-catalysed hydroformylation of 1-hexene using PNp_3 and $P(ONp)_3$ ligands.

Recently Nozaki and co-workers reported the use of nitrogen centred di- or tri-phosphine ligands in the rhodium hydroformylation of terminal olefin. The comparison of the two ligands shows that the incorporation of a nitrogen in the ligand backbone improves the selectivity towards the branched product (Scheme 1.17).[55]

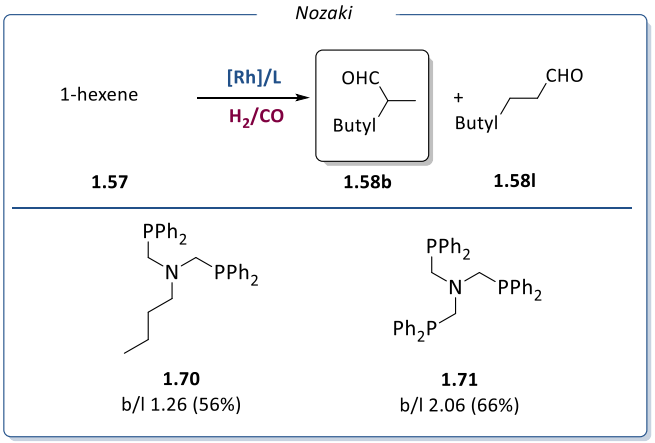

Scheme 1.17. Rh-catalysed hydroformylation of 1-hexene using nitrogen centred di- or tri-phosphine ligands.

The diphosphine ligand **1.70** provided a b/l ratio of 1.26 at 50 °C under 10 bar of syngas (CO/H_2 1:4), when 1-hexene was used as substrate, whereas the aza triphos ligand **1.71** provided higher selectivity at lower temperature (b/l= 2.06 at 25 °C). The difference observed between the catalytic performance using ligands **1.70** and **1.71** was attributed to an electronic effect since similar steric hindrance is expected for both ligands. The authors, trough mechanistic and labelling studies, proposed that the regioselectivity arises from the irreversible trapping of the branched Rh-alkyl species, with respect to the reversible trapping of the linear analogue.

1.1.4 Alternative syngas surrogates

The functionalisation of substrates using CO as the carbonyl source comes in as one of the most important industrial process for the manufacture of bulk and fine chemicals.[56] The most common CO and H_2 source for hydroformylation until now has been the synthesis gas (syngas). The synthesis gas is a mixture of CO and H_2 that can be derived from almost every carbon source, such as natural gas, naphta or coal.[57] The use of CO surrogates serves as a convenient and safe approach for the synthesis of carbonyl derivatives avoiding the need to use gaseous CO. In 2004, Morimoto and Kakiuchi[58] and Beller[59] summarized several developments in the carbonylation area without the use of gaseous CO including some hydroformylation examples.
Scheme 1.18 summarises different ways to obtain this mixture, in which the different oxidation state that the carbon atom adopts is the main difference.

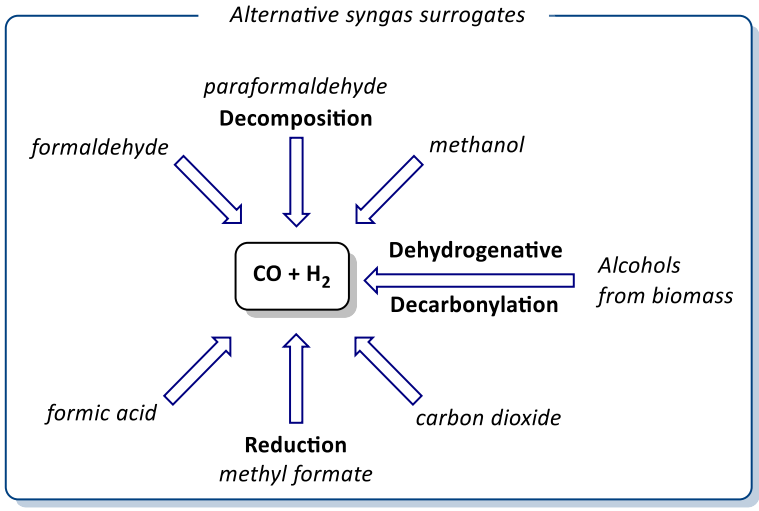

Scheme 1.18. Syngas surrogates.

Typically, industrial hydroformylation processes are performed at medium or high pressure (20–100 bar) of syngas at temperatures between 100–140°C in the presence of rhodium. Despite the significant industrial interest in hydroformylation reactions, little work has been performed with catalysts based on other metals. Palladium-catalysed hydroformylation has been studied for 1-octene by Beller *et al*[60] using syngas as CO and H_2 source. By using dppp as ligand, and under 40 bar of pressure they reported a 95% of conversion and a chemoselectivity towards the aldehyde of a 13% with a l:b ratio of 6:4. As indicated in Scheme 1.19, formaldehyde is a possible syngas surrogate that could be utilized in the hydroformylation of olefins.[61,62] Formaldehyde has been used as CO and H_2 source for the hydroformylation of olefins using various metals such as rhodium[63,64,65,66] or ruthenium[67] but there is no information about palladium catalysed hydroformylation using formaldehyde as syngas surrogate. Formaldehyde can be found in different forms, and the most common ones are in aqueous solution and in the solid state (as a polymer). Formalin (or formol) is the name for the commercial solution of formaldehyde in water that contains *ca*. 37% weight, while paraformaldehyde (PFA) is a solid polymer with an average degree of

polymerization of 8-100 units.[68] By dry heating, PFA can depolymerize to formaldehyde and then subsequently, CO and H_2 are released.[69] There are two pathways to obtain the aldehyde product in the hydroformylation process using formaldehyde (Scheme 1.19). The first one is by decomposition into CO and H_2, which generally depends strongly on reactant concentration, via a chain mechanism,[70] and on the temperature.[71] In this case, the classical hydroformylation mechanism operates.

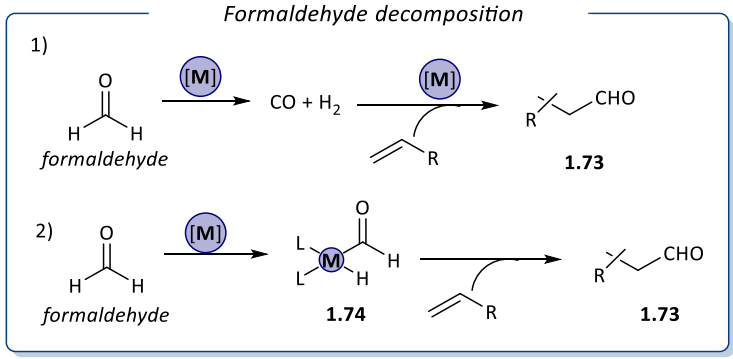

Scheme 1.19. Formaldehyde pathways to obtain CO and H_2.

On the other hand, the oxidative addition of formaldehyde to a metal centre to form a metal hydride formyl unit **1.74** was also proposed.[72] In this case, the formyl group can be transferred to the olefin into the coordination sphere of the transient metal-acyl complex, providing the aldehyde product. Baricelli et al reported experimental results and theoretical DFT-calculations which allowed them to propose a catalytic cycle, in which the insertion of the olefin into the rhodium species (generated by oxidative addition of formaldehyde) was considered as the rate determining state.[72]

1.1.5 Palladium catalyst for hydroformylation process

In contrast to rhodium catalysis, palladium has not played a significant role in the area of hydroformylation of olefins[10] since catalysts based on this metal originally targeted the formation of alternating polyketones from olefins with carbon monoxide,[73] or esters/carboxylic acids in the presence of methanol or

water as nucleophiles.[74] The palladium catalysed hydroformylation was first discovered by Shell,[75] and very little is known. To have an idea about the mechanism, it's necessary to understand the background of other carbonylation reactions with palladium catalyst such as methoxycarbonylation of olefins or copolymerization.[73,76,77,78,79,80] The mechanism of the palladium catalysed hydroformylation has been investigated by Drent and Budzelaar[81] where upon hydrogenolysis of the palladium acyl bond, an aldehyde is released. But because of the high hydrogenation activity of palladium complexes, the aldehydes can be quickly converted into the corresponding alcohols. There is also a competition between hydroacylation and copolymerization owing to the possible insertion of a second olefin (Scheme 1.20).[68]

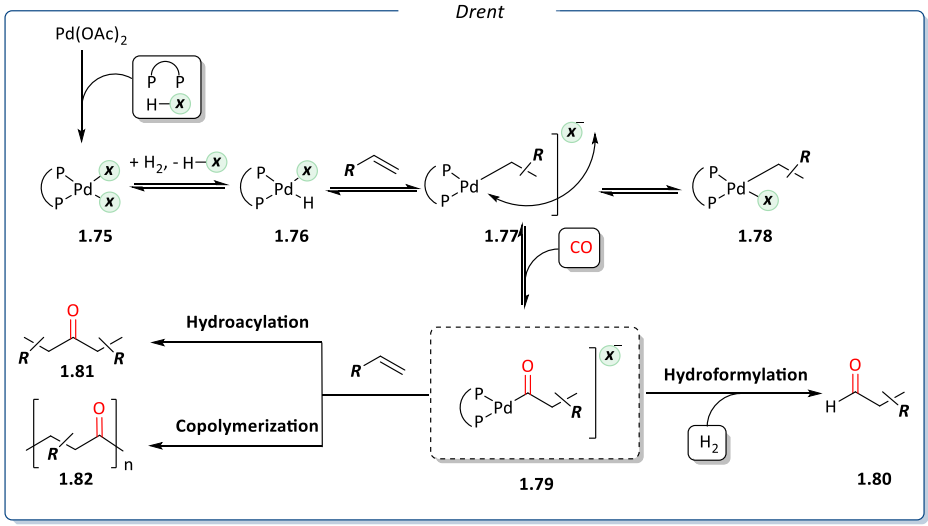

Scheme 1.20. Mechanism of the palladium catalysed hydroformylation and alternative reaction routes proposed by Drent and coworkers.

In 2016, the group of Shi reported how, employing formic acid and acetic anhydride as syngas surrogates, extremely high regioselectivity toward the linear product could be achieved for a range of alkene substrate (Scheme 1.21).[82] In this study, the nature of the ligand and solvent, as well as the presence of additive, were key parameters to obtain high selectivity.

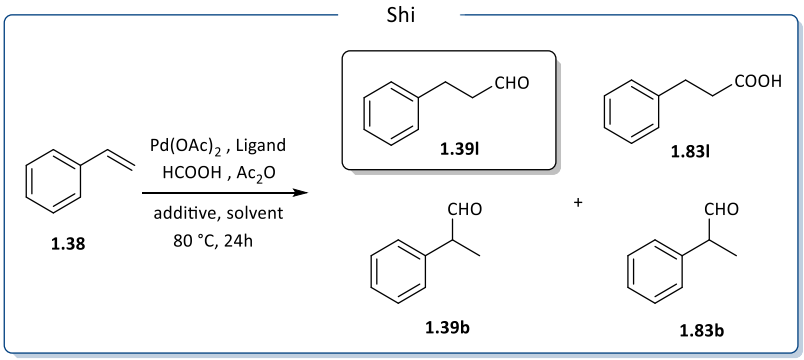

Scheme 1.21. Palladium catalysed hydroformylation of styrene reported by Shi.

It should be noted that formic acid had previously been used as hydrogen source in rhodium hydroformylation processes but the addition of CO gas was required.[83,84] In the palladium catalysed reaction reported by Shi and co-workers, CO was generated from the formic acid and the acetic anhydride. The authors proposed a catalytic cycle, shown in Scheme 1.22.

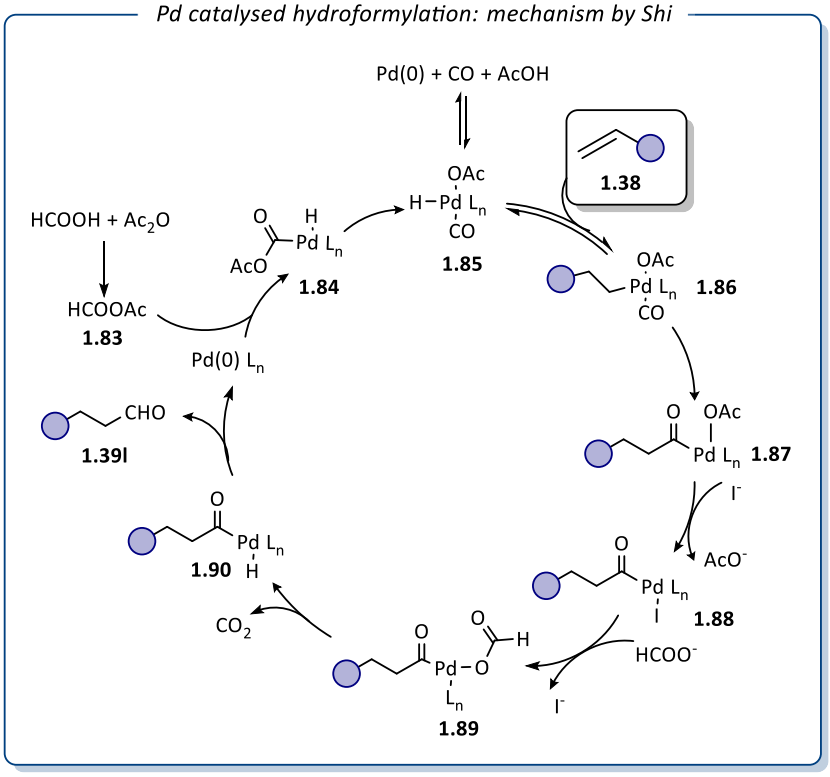

Scheme 1.22. Palladium hydroformylation mechanism reported by Shi.

Palladium (0) complex may be oxidatively inserted into HCOOAc **1.83** to give palladium hydride complex **1.84,** which would rearrange to complex **1.85**. Olefin **1.38** would be hydropalladated by **1.85** to generate alkylpalladium complex **1.86**, which would undergo migratory insertion to give acylpalladium complex **1.87.** The acetate group of **1.87** would subsequently be replaced by the iodide to give Pd–I complex **1.88**, which would react with formate to deliver complex **1.89**. The palladium hydride complex **1.90** would be formed from complex **1.89** via extrusion of CO_2. Reductive elimination of **1.90** would then lead to aldehyde **1.39l** and regenerate the Pd(0) catalyst. This study evidenced that high selectivity can be achieved in the transformation of styrene into 3-phenyl propanal without syngas using a palladium catalyst bearing dppp as ligand under mild reaction conditions.

1.2 References

1. K. Weissermel and H. Arpe, in *Industrial Organic Chemistry*, eds. K. Weissermel and H. Arpe, Wiley, Weinheim, 5th edn., **2008**, Ch. 6.

2. R. Franke, D. Selent and A. Börner, *Chem. Rev.*, **2012**, *112*, 5675-5732.

3. A. Börner and R. Franke, *Hydroformylation: Fundamentals, Processes, and Applications in Organic Synthesis*, Wiley-VCH Verlag GmbH & Company, **2016**.

4. M. Taddei and A. Mann, *Hydroformylation for Organic Synthesis*, Springer Berlin Heidelberg, **2014**.

5. P. T. Anastas and A. Lapkin, *Green Chemical Engineering*, Wiley, **2018**.

6. P. W. N. M. van Leeuwen, *Homogeneous Catalysis: Understanding the Art*, Springer, **2004**.

7. P. W. N. M. Van Leeuwen, C. Claver and Editors, *Rhodium Catalyzed Hydroformylation. [In: Catal. Met. Complexes,* **2000***; 22]*, Kluwer, **2000**.

8. E. V. Gusevskaya, J. Jiménez-Pinto and A. Börner, *ChemCatChem*, **2014**, *6*, 382-411.

9. *Rhodium Catalysis*, Springer Nature, C. Claver Editor, Switzerland, **2018**.

10. J. Pospech, I.Fleischer, R. Franke, S. Buchholz, and M. Beller, *Angew. Chem. Int. Ed.,* **2013**, *52*, 2852-2872.

11. *C-1 Building Blocks in Organic Synthesis 1. Additions to Alkenes, Alkynes, and Carbonyl Compounds*, Thieme, Stuttgart, Germany, **2013**.

12. R. Franke, D. Selent and A. Börner, *Chem. Rev.*, **2012**, *112*, 5675-5732.

13. R. F. Heck, *Acc. Chem. Res.*, **1969**, *2*, 10-16.

14. L. A. van der Veen, M. D. K. Boele, F. R. Bregman, P. C. J. Kamer, P. W. N. M. van Leeuwen, K. Goubitz, J. Fraanje, H. Schenk and C. Bo, *J. Am. Chem. Soc.,* **1998**, *120*, 11616-11626.

15. P. Dingwall, J. A. Fuentes, L. Crawford, A. M. Z. Slawin, M. Bühl and M. L. Clarke, *J. Am. Chem. Soc.*, **2017**, *139*, 15921-15932.

16. K. Nozaki, T. Matsuo, F. Shibahara and T. Hiyama, *Organometallics*, **2003**, *22*, 594-600.

17. E. R. Nelsen, A. C. Brezny and C. R. Landis, *J. Am. Chem. Soc.,* **2015**, *137*, 14208-14219.

18. A. Castellanos-Páez, S. Castillón, C. Claver, P. W. N. M. van Leeuwen and W. G. J. de Lange, *Organometallics*, **1998**, *17*, 2543-2552.

19. P. P. Deutsch and R. Eisenberg, *Organometallics*, **1990**, *9*, 709-718.

20. T. Jongsma, G. Challa and P. W. N. M. van Leeuwen, *J. Organomet. Chem.*, **1991**, *421*, 121-128.

21. A. van Rooy, E. N. Orij, P. C. J. Kamer and P. W. N. M. van Leeuwen, *Organometallics*, **1995**, *14*, 34-43.

22. B. Breit, R. Winde, T. Mackewitz, R. Paciello and K. Harms, *Chem. Eur. J.*, **2001**, *7*, 3106-3121.

23. A. I. M. Keulemans, A. Kwantes and T. van Bavel, *Recl. Trav. Chim. Pays-Bas Belg.*, **1948**, *67*, 298-308.

24. A. T. Axtell, C. J. Cobley, J. Klosin, G. T. Whiteker, A. Zanotti-Gerosa and K. A. Abboud, *Angew. Chem.*, **2005**, *44*, 5834-5838.

25. T. P. Clark, C. R. Landis, S. L. Freed, J. Klosin and K. A. Abboud, *J. Am. Chem. Soc.*, **2005**, *127*, 5040-5042.

26. M. Diéguez, O. Pàmies, A. Ruiz, S. Castillón and C. Claver, *Chem. - Eur. J.*, **2001**, *7*, 3086-3094.

27. R. Lazzaroni, A. Raffaelli, R. Settambolo, S. Bertozzi and G. Vitulli, *J. Mol. Catal.*, **1989**, *50*, 1-9.

28. J. M. Brown and A. G. Kent, *J. Chem. Soc., Perkin Trans. 2*, **1987**, 1597-1607.

29. M. Kranenburg, Y. E. M. van der Burgt, P. C. J. Kamer, P. W. N. M. van Leeuwen, K. Goubitz and J. Fraanje, *Organometallics*, **1995**, *14*, 3081-3089.

30. L. A. van der Veen, M. D. K. Boele, F. R. Bregman, P. C. J. Kamer, P. W. N. M. van Leeuwen, K. Goubitz, J. Fraanje, H. Schenk and C. Bo, *J. Am. Chem. Soc.*, **1998**, *120*, 11616-11626.

31. L. A. van der Veen, P. H. Keeven, G. C. Schoemaker, J. N. H. Reek, P. C. J. Kamer, P. W. N. M. van Leeuwen, M. Lutz and A. L. Spek, *Organometallics*, **2000**, *19*, 872-883.

32. S. Yu, Y. M. Chie, Z. H. Guan, Y. Zou, W. Li and X. Zhang, *Org. Lett.*, **2009**, *11*, 241-244.

33. J. J. Carbó, F. Maseras, C. Bo and P. W. N. M. van Leeuwen, *J. Am. Chem. Soc.*, **2001**, *123*, 7630-7637.

34. *Germany Pat.,* DE 4321194, **1995**.

35. L. Monnereau, D. Sémeril and D. Matt, *Eur. J. Org. Chem*, **2010**, *16,* 3068-3073.

36. Y. Chen, S. Yekta and A. K. Yudin, *Chem. Rev.* , **2003**, *103*, 3155-3212.

37. P. C. J. Kamer and P. W. N. M. van Leeuwen, *Phosphorus(III) Ligands in Homogeneous Catalysis: Design and Synthesis*, John Wiley & Sons, Ltd, Chichester, **2012**.

38. E. Boymans, M. Janssen, C. Müller, M. Lutz and D. Vogt, *Dalton Trans.*, **2013**, *42*, 137-142.

39. C.-y. Zheng, M. Mo, H.-r. Liang, X.-l. Zheng, H.-y. Fu, M.-l. Yuan, R.-x. Li and H. Chen, *Appl. Organomet. Chem.*, **2013**, *27*, 474-478.

40. R. P. J. Bronger, P.C.J. Kamer, D. Vogt *C1-Building Blocks in Organic Synthesis 1*, Thieme, **2013**.

41. *US Pat.,* US4769498 (A), **1988**.

42. G. D. Cuny and S. L. Buchwald, *J. Am. Chem. Soc.*, **1993,** *115*, 2066-2068.

43. G. D. Cuny and S. L. Buchwald, *Synlett*, **1995**, 519-522.

44. *US Pat.,* US4694109 (A), **1987**.

45. M. Kranenburg, P. C. J. Kamer and P. W. N. M. van Leeuwen, *Eur. J. Inorg. Chem.*, **1998**, 155-157.

46. A. L. Watkins and C. R. Landis, *Org. Lett.*, **2011**, *13*, 164-167.

47. K. Nozaki, T. Matsuo, F. Shibahara and T. Hiyama, *Adv. Synth. Catal.*, **2001**, *343*, 61-63.

48. F. Shibahara, K. Nozaki and T. Hiyama, *J. Am. Chem. Soc.*, **2003**, *125*, 8555-8560.

49. K. Nozaki, N. Sakai, T. Nanno, T. Higashijima, S. Mano, T. Horiuchi and H. Takaya, *J. Am. Chem. Soc.*, **1997**, *119*, 4413-4423.

50. Z. Yu, M. S. Eno, A. H. Annis and J. P. Morken, *Org. Lett.*, **2015**, ***17***, 3264-3267.

51. G. M. Noonan, J. A. Fuentes, C. J. Cobley and M. L. Clarke, *Angew. Chem. Int. Ed.,* **2012**, *51*, 2477-2480.

52. L. Iu, J. A. Fuentes, M. E. Janka, K. J. Fontenot and M. L. Clarke, *Angew. Chem. Int. Ed.*, **2019**, *58*, 2120-2124.

53. V. F. Slagt, M. Roeder, P. C. J. Kamer, P. W. N. M. Van Leeuwen and J. N. H. Reek, *J. Am. Chem. Soc.*, **2004**, *126*, 4056-4057.

54. A. A. Dabbawala, R. V. Jasra and H. C. Bajaj, *Catal. Commun.*, **2011**, *12*, 403-407.

55. A. Phanopoulos and K. Nozaki, *ACS Catal.*, **2018**, *8*, 5799-5809.

56. P. Gautam and B. M. Bhanage, *Catal. Sci. Technol.*, **2015**, *5*, 4663–4702.

57. L. J. C. Jens Rostrup-Nielsen, *Concepts in Syngas Manufacture*, Imperial College Press, London, **2011**.

58. T. Morimoto and K. Kakiuchi, *Angew. Chem. Int. Ed.*, **2004**, *43*, 5580-5588.

59. L. Wu, Liu, Q., Jackstell, R., and Beller, M., *Angew. Chem. Int. Ed.*, **2014**, *53*, 6310-6320.

60. R. P. Jennerjahn, I.; Jackstell, R., Franke, R.; Wiese, K.D.; Beller, M., *Chem. Eur. J.*, **2009**, *15*, 6383-6388.

61. J. A. P. Fuentes, R.; Clarke, M, *Chem. Eur. J.*, **2015**, *21*, 10645-10649.

62. G. M. Makado, T; Sugimoto, Y; Tsutsumi, K; Kagawa, N; Kakiuchi, K;, *Adv. Synth. Catal.*, **2010**, *352*, 299-304.

63. A. S. C. Chan, W. E. Carrol and D. E. Willis, *J. Mol. Catal.*, **1983**, *19*, 377-391.

64. H. Ren and W. D. Wulff, *Org. Lett.*, **2012**, *15*, 242-245.

65. M. Uhlemann, S. Doerfelt and A. Börner, *Tetrahedron Lett.*, **2013**, *54*, 2209-2211.

66. H.-S. Ahn, S.-H. Han, S.-J. Uhm, W.-K. Seok, H.-N. Lee and G.A. Korneeva, *J. Mol. Catal.,* **1999**, *144*, 295-306.

67. G. Jemier, E. M. Nahmed and S. Libs-Konrath, *J. Mol. Catal.*, **1991**, *64,* 337-347.

68. A. F. R. Börner, *Hydroformylation: Fundamentals, Processes and Applications in Organic Synthesis*, **2016**.

69. J. M. Yates, T,E; Dresser, M, *J. Catal.*, **1973**, *30*, 260-275.

70. E. Irdam and J. Kiefer, *Int. J. Chem. Kinet.*, **1993**, *25*, 285-303.

71. K. Saito, T. Kakumoto, Y. Nakanishi and A. Imamura, *J. Phys. Chem*, **1985**, *89*, 3109-3113.

72. M. Rosales, H. Pérez, F. Arrieta, R. Izquierdo, C. Morationos and P. J. Baricelli, *J. Mol. Catal. A Chem.,* **2016**, *421*, 122-130.

73. B. H. M. Drent E., *Chem. Rev.*, **1996**, *96*, 663-681.

74. I. del Río, C. Claver and P. W. N. M. van Leeuwen, *Eur. J. Inorg. Chem*, **2001**, 2719-2738.

75. *US Pat.,* US5763497 (A), **1986**.

76. S.G. Davies, *Organotransition Metal Chemistry: Application of organic Synthesis*, Pergamon, Oxford, UK, **1982**.

77. R. Van Asselt, E. E. C. G. Gielens, R. E. Rulke, K. Vrieze, and C. J. Elsevier., *J. Am. Chem. Soc.*, **1994**, *116*, 977-985.

78. G. P. C. M. Dekker, C. J. Elsevier, K. Vrieze , P. W. N. M. Van Leeuwen, C. F. Roobeek, *J. Organomet. Chem.*, **1992**, *430*, 357-372.

79. B. A. Markies, D. Kruis, M. H. P. Rietveld, K. A. N. Verkerk, J. Boersma, H. Kooiman, M. T. Lakin, A. L. Spek, G. Van Koten, *J. Am. Chem. Soc.*, **1995**, *117*, 5263-5274.

80. P. M. Maitlis, *The Organic Chemistry of Palladium*, Academic Press, London, UK, **1971**.

81. E. Drend and P. H. M. Budzelaar, *J. Organomet. Chem.*, **2000**, *593-594*, 211-225.

82. W. Ren, W. Chang, J. Dai, Y. Shi, J. Li, and Y. Shi , *J. Am. Chem. Soc.*, **2016**,*138*, 14864-14867.

83. A. Somasunderam and H. Alper, *J. Mol. Catal.*, **1994**, *92*, 35-40.

84. B. El Ali, G. Vasapollo, H. Alper, *J. Mol. Catal. A Chem.*, **1996**, *112*, 195-201.

Rhodium and Palladium Catalysed Unusual Regioselective Hydroformylation and Rhodium Catalysed Reductive Carbonylation

Benedetta Palucci

Chapter II

Objectives

Rhodium and Palladium Catalysed Unusual Regioselective Hydroformylation and Rhodium Catalysed Reductive Carbonylation

Benedetta Palucci

The main objective of this Ph.D. thesis deals with the development of efficient systems able to provide unusual regioselectivity in the Rh catalysed hydroformylation of terminal olefins. For this purpose, the present work includes various strategies: the synthesis of bidentate ligands for the application in the rhodium catalysed hydroformylation of 1-hexene, 1-octene and styrene, and the use of a palladium catalyst and formaldehyde as syngas surrogate in the hydroformylation of styrene.

Specifically, the work detailed in Chapter III aims at the application of the newly synthetised bidentate phosphorus-nitrogen-centred ligands in the rhodium catalysed hydroformylation of 1-hexene, toward the formation of the branched aldehyde. The specific objectives of this chapter are:

- The development of a protocol for the synthesis of the bidentate phosphorus-nitrogen-centred ligands.
- The study of the effect of the substituents on the bidentate phosphorus-nitrogen-centred ligands in the selective production of the branched aldehyde in the hydroformylation of 1-hexene.
- The study of the reactivity towards H_2/CO of the rhodium precursors in the presence of bidentate phosphorus-nitrogen-centred ligands, using HP NMR spectroscopy.

The work described in Chapter IV deals with the development of a family of phosphine-phosphite and phosphine-phosphoramidite ligands and their application in the rhodium catalysed hydroformylation of 1-octene, toward the branched aldehyde. The specific objectives of this chapter are:

- The development of a protocol for the synthesis of the phosphine-phosphite and phosphine-phosphoroamidite ligands.
- The study of the effect of the substituents on the phosphine-phosphite and phosphine-phosphoroamidite ligands on the regioselectivity of the Rh-catalysed hydroformylation of 1-octene.

- The study of the reactivity towards H_2/CO of the rhodium precursors in the presence of phosphine-phosphite ligand, using HP NMR spectroscopy.

The research described in Chapter V deals with the development of a novel family of bis(dipyrrolyl-phosphorodiamidite) and bis(dipyrazolyl-phosphorodiamidite) ligands and their application in the rhodium catalysed hydroformylation of styrene for the production of linear aldehyde. The specific objectives of this chapter are:

- The synthesis of bis(dipyrrolyl-phosphorodiamidite) ligands using commercially available diols and amine.
- The synthesis of bis(dipyrazolyl-phosphorodiamidite) ligands using commercially available pyrazole and derivatives.
- The study of the effect of rhodium to ligand ratio, rhodium loading, total pressure, and temperature on the reaction outcome.
- The study of the performance of the newly synthesised ligands in the selective production of the branched aldehyde in the hydroformylation of styrene.

The work described in Chapter VI deals with the development of a palladium catalyst for the linear hydroformylation of styrene using formaldehyde as syngas surrogate. The specific objectives of this chapter are:

- The study of the effect of the acid, ligand and palladium precursors in the palladium catalysed hydroformylation reaction of styrene.
- The study of the effect of temperature and the formaldehyde source in the palladium catalysed hydroformylation reaction of styrene.
- The study of the reactivity towards H_2/CO and CO pressures in the outcome of the palladium catalysed hydroformylation of styrene.

- To perform mechanistic studies by evaluating deuterium-incorporation, kinetic isotopic effect (KIE), and NMR analysis of the catalytic system.

The main objective of Chapter VII is the development of the rhodium catalysed reductive carbonylation of cinnamyl acetate process for the production of aldehyde, into the investigation of the catalytic mechanism. The specific objectives of this chapter are:

- The study of the effect of the ligand on the reductive carbonylation process.
- The study of the reactivity towards CO, and H_2/CO pressure of the rhodium precursors $RhH(CO)(PPh_3)_3$ in the presence of cinnamyl acetate, using HP NMR spectroscopy.
- The study of the reactivity towards CO, and H_2/CO pressure of the rhodium precursor $Rh(acac)(CO)_2$ in the presence of cinnamyl acetate, using HP NMR spectroscopy.

Rhodium and Palladium Catalysed Unusual Regioselective Hydroformylation and Rhodium Catalysed Reductive Carbonylation

Benedetta Palucci

Chapter III

Rhodium catalysed hydroformylation of 1-hexene with bidentate phosphorus-nitrogen-centred ligands

Rhodium and Palladium Catalysed Unusual Regioselective Hydroformylation and Rhodium Catalysed Reductive Carbonylation

Benedetta Palucci

3.1 Introduction

3.1.1 Bidentate phosphorus-nitrogen-centred ligands

Transition metal complexes are indispensable tools in synthetic chemistry and ideally, the metal catalysed processes should be clean, efficient (and fast), and selective. The definition of a pincer ligand is a chelating ligand that binds to three adjacent coplanar sites on the metal centre.[1] There are many pincer ligands, and the most common type is the η^3-"ECE" type design (Scheme 3.1, **3.2**). In these ECE type pincer ligands, E represents a neutral two-electron donor such as PR_2, SR or NR_2 and these lead to pincer like PCP, SCS, or NCN type systems. In recent times, coordination modes have been extended beyond the "ECE" systems to include, but not limited to, ONS, CNS, NNN, NNS, NNO, PNP, CNC, SNS, SeNSe, and these ligands have been employed as chelates to numerous categories of metal centres.[2,3,4,5,6,7,8,9,10]

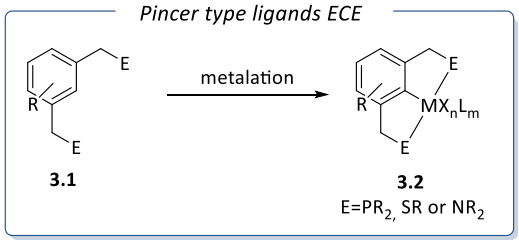

Scheme 3.1.pincer type ligands ECE.

The PNP and PCP pincer type ligands containing phosphorus at coordination sites, have found many applications in catalysis.[2,11,12,13,14,15,16]

These ligands can stabilize metal centres with high and low oxidation states. It was reported that even changes in the PNP or PCP ligand backbone can have dramatic effects on the reactivity of the metal complexes.[14] The use of pincer ligands was described in a range of metal catalysed process and, for instance, platinum PNP and PCP complexes were used as precatalysts for Heck-Mizoroki,[16,17] Suzuki-Miyaura,[12,16] and Sonogashira cross-coupling[16]

reactions, aliphatic dehydrogenations[18], olefination[19], C-H bond activation[20,21], α-arylation of ketone enolates[22], with good activity and selectivity. Moreover, the use of pincer ligands in metal-catalysed processes revealed useful to activate CO_2 and CO.[23]

3.1.2 Diphosphine ligands

Diphosphine ligands were extensively applied in the rhodium catalysed hydroformylation of olefins.[24] One of the first successful example of the use of a diphosphine ligand was reported by Devon *et al.* in 1987, where the ligand BISBI **3.3** (Figure 3.1) shows a very high regioselectivity for the formation of linear aldehydes from propene.[25] An important study by Casey and co-workers showed that the bite angle of bidentate diphosphines can have a dramatic influence on the regioselectivity of the rhodium-catalysed hydroformylation of 1-alkenes. For example, the equatorial:equatorial coordinated BISBI **3.3** ligand (bite angle 113°) shows l/b aldehyde ratio of 66:1, while the equatorially-axially coordinating dppe ligand (bite angle 90°) gave a linear to branched ratio of only 2.1.[26]

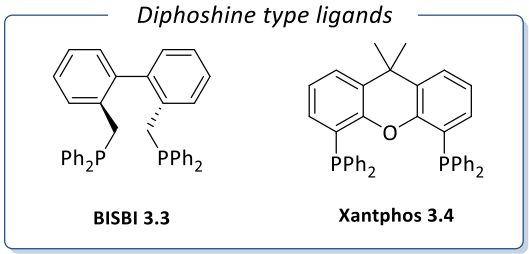

Figure 3.1. Diphosphine type ligands.

In 1995, van Leeuwen and co-workers reported the preparation of a broad set of ligands with a larger bite angle than the common range of 75 to 99°, which led to the discovery of the well-established Xantphos ligand **3.4**, and his derivatives (Figure 3.2).[27] Comparison with BISBI **3.3** showed that the rigidity of the ligand backbone is essential for obtaining high selectivity in the hydroformylation reaction. The Xantphos ligand **3.4** provided high

selectivity towards the formation of linear aldehydes (l/b of 97.7%) in the rhodium-catalysed hydroformylation of 1-octene.[27]

3.1.3 Rh-catalysed hydroformylation of 1-hexene with bidentate phosphorus-nitrogen-centred ligands towards branched selectivity

The rhodium catalysed hydroformylation of terminal olefin has been extensively studied, mainly with the aim of producing the linear regioisomer. Only recently, a few catalytic systems able to efficiently catalyse the hydroformylation of terminal alkenes, providing branched aldehydes, were reported.[28,29,30] In 2004, Reek *et al.*, established a new supramolecular strategy using Rh-complexes based on pyridine-substituted phosphines as template where the pyridines coordinate to zinc (II) porphyrins moieties **3.7** (Scheme 3.2).[30] This closed structure gave a good selectivity to the branched aldehyde (62%) in the Rh hydroformylation of 1-octene. Here the selectivity originates from the steric restriction imposed to the metal-substrate complex inside the capsule.

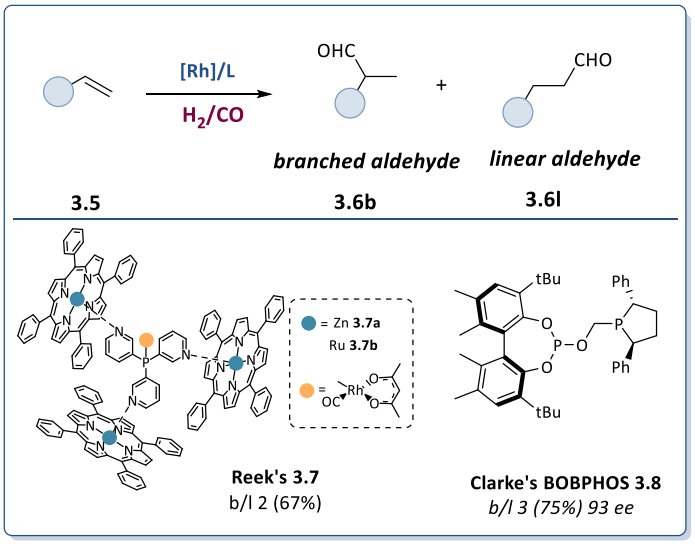

Scheme 3.2. Branched-Selective Rh-catalysed hydroformylation of olefins, and the ligands reported in previous studies.

In 2012, Clarke and co-workers described the synthesis and application of the BOBPHOS ligand **3.8** in the asymmetric hydroformylation of alkyl alkenes.[28] The BOBPHOS ligand **3.8**, delivered the branched aldehydes with good selectivity and excellent enantioselectivity. Low temperature (15 °C) and 5 bar of 1:1 CO/H_2 are required to obtain, in the case of 1-hexene, 75% selectivity to the branched aldehyde together with 93% enantioselectivity.Recently, Nozaki and co-workers reported the use of either nitrogen-centred di- or tri-phosphine ligands in the rhodium hydroformylation of terminal olefins (Scheme 3.3).[29]

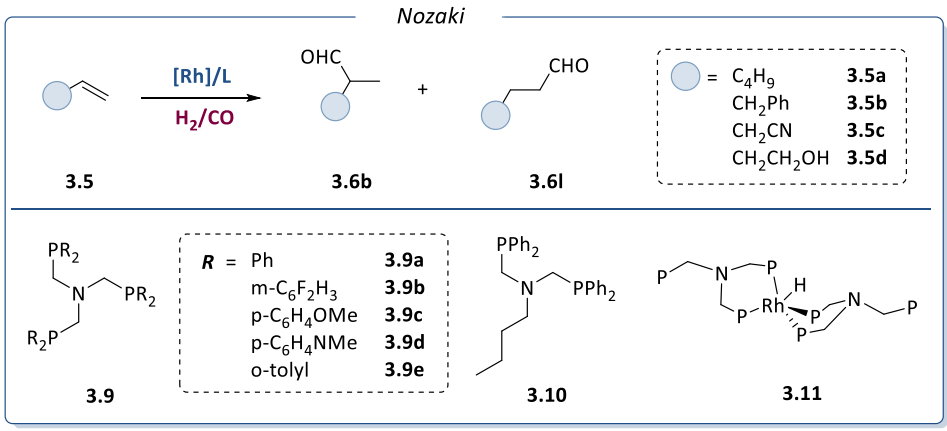

Scheme 3.3. Rh-catalysed hydroformylation of terminal olefins reported by Nozaki *et al.*, using ligand **3.8**, **3.10**, and complex **3.11**

Nozaki *et al.* reported a series of triphosphine derivatives, bearing different substituents on the phosphorus atoms (Scheme 3.3). As a starting point of the catalytic tests, tris(diphenylphosphinomethyl)amine **3.9a** was used with $[Rh(acac)(CO)_2]$ in the hydroformylation of 1-hexene at 100 °C, obtaining a linear to branched ratio of 1.1 (Table 3.1, Entry 1). When using a more electron-withdrawing substituent at the phosphorus atom, such as the *meta*-difluorophenyl in ligand **3.9b**, the conversion was not affected but the selectivity was shifted towards the linear aldehyde (Table 3.1, Entry 2).[31] On the other hand, when using a more electron-donating substituent at the phosphorus atom, such as *p*-methoxyphenyl (**3.9c**) or *p*-*N*,*N*-

dimethylaminophenyl (**3.9d**) ones, a slight improvement towards the branched selectivity (Table 3.1, Entries 3 and 4) was observed with a decrease in the activity. This suggests that there is a slight electronic preference for the formation of the branched aldehyde when increasing the electron-donating properties of these ligands.

Table 3.1. Rh-catalysed hydroformylation of 1-hexene using nitrogen centred diphosphine ligands

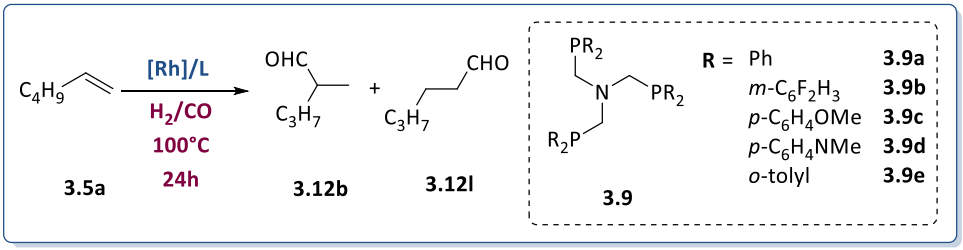

Entry [a]	ligand	TOF(h^{-1})	Chemo%	b/l
1	**3.9a**	26	89.4	1.10
2	**3.9b**	28	97.7	0.92
3	**3.9c**	23	79.2	1.11
4	**3.9d**	17	57.8	1.16
5	**3.9e**	20	70.9	0.43

Reaction conditions: toluene (3.75 mL), 1-hexene (250 µL, 500 mM),[Rh]=[$Rh(acac)(CO)_2$] (1.0 mol %, 5 mM), 1 (2.0 mol %, 10 mM), CO (10 bar), H_2 (10 bar), 3.5 h;

Variation of the electronic properties of phosphorus based ligands in previously reported systems indicated that the use of less basic ligands such as (di)phosphites (rather than phosphines) afford aldehydes with greater linear selectivity.[32,33] This behaviour was explained by the increased tendency to undergo β-hydride elimination from the branched Rh-alkyl species when decreasing basicity of the ligands, yielding 2-octene rather than the branched aldehyde.[32a] In contrast, Nozaki and co-workers postulated that in the system with triphosphine ligands, the formation of the branched Rh–alkyl complex is irreversible, so that the β-hydride elimination is not favoured.

Alternatively, the influence of the electronic parameters of the ligand on the regioselectivity could be originated from a perturbation of the equatorial-equatorial:equatorial-axial (ee:ea) isomers ratio. As the authors proposed, in the case of bidentate ligands, higher the electron donating behaviour, higher the proportion of the ee (equatorial:equatorial) isomer, compared to the ea (equatorial:axial) one. This is reflected into an higher percentage of linear aldehyde.[34,35,36] In the system described by Nozaki *et al.*, the more basic ligand could have caused the higher "hydricity" of the Rh–H species to increase the proportion of branched Rh–alkyl species present since the terminal olefinic carbon possess a partial positive charge, compared to the internal one.[37, 38] As for the reaction rate, electron donating ligands generally lower the hydroformylation rate due to a strengthening of the Rh–CO bonds, retarding CO dissociation and the formation of the required unsaturated species for olefin coordination.[33] As may be expected, the use of an electron-donating but sterically encumbering substituent, ortho-tolyl (**3.9e**), resulted in an increased linearity (Table 3.1, Entry 5), presumably due to a localized steric hindrance around the metal centre. Within the same study, the authors found out that lowering the temperature of the process from 100 to 50 °C improved the selectivity of the reaction, from 1.10 to 1.66 using ligand **3.9a**, although at the cost of the activity.

Table 3.2. Comparing aza-diphosphine **3.9a** with aza-triphosphine **3.10** ligands

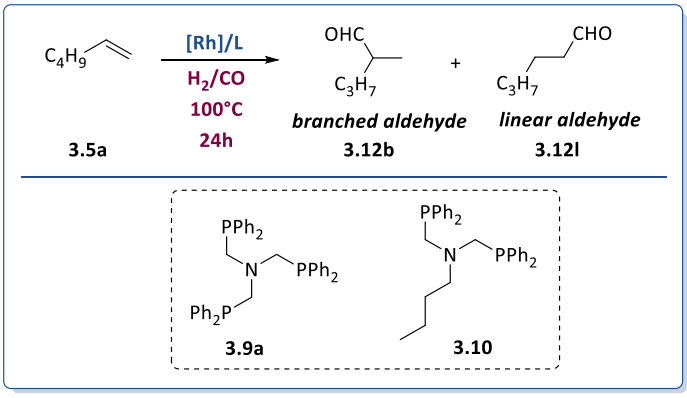

Entry (a)	Ligand	Rh/L	T (°C)	CO (bar)	H2 (bar)	TOF (h-1)	Chemo%	b/l
1	**3.8a**	1:2	100	10	10	28	99.4	1.10
2	**3.8a**	1:1	100	10	10	26	90	0.99
3(b)	**3.8a**	1:1	50	2	8	2.8	66	1.30
4(b)	**3.8a**	1:1	25	2	8	0.2	3.7	2.06
5	**3.9**	1:2	100	10	10	27	93.1	1.10
6	**3.9**	1:1	100	10	10	29	>99	1.07
7(b)	**3.9**	1:1	50	2	8	4.1	99.4	1.26
8(b)	**3.9**	1:1	25	2	8	1.5	35.4	0.54

Reaction conditions: a) toluene (3.75 mL), 1-hexene (250 µL, 500mM),[Rh]=[Rh(acac)$(CO)_2$] (1.0 mol %, 5 mM), 1 (2.0 mol %, 10 mM), CO (10 bar), H_2 (10 bar), 3.5 h. b) 24 h.

The authors also performed a comparative analysis between tri- and di-phospine ligands, using ligands **3.9a** and **3.10**. The main differences between the two ligands arise from their coordination to the Rh centre. In the trisphosphine ligands **3.8a,** the third phosphine group is free, "hanging" without being coordinated to the metal. The activity and the selectivity of both systems were evaluated, Under the same catalytic conditions (Rh:L 1:2, 100 °C, CO/H_2 (1:1), 20 bar, Table 2.2, Entries 1 and 5), they showed similar activity and selectivity. However, lowering the rhodium to ligand ratio, at 1:4 CO:H_2 (1:1), ratio and at low temperatures (25–50 °C), the triphosphine **3.8a** is more selective toward the formation of the branched product (2.06), while the diphosphine **3.10** provided the branched isomer with poor selectivity (0.54) (Table 3.2, Entry 4 and 8, respectively). Next, in order to investigate the mechanism involved when the system **3.9a**/Rh was employed in the hydroformylation process, they performed a mechanistic investigation. The deuterioformylation, (reaction using D_2 instead of H_2), shows that the formation of the linear Rh–alkyl intermediate is somewhat reversible while formation of the analogous branched Rh–alkyl intermediate is not. Afterward, extensive NMR analyses were performed in the absence and in the presence of the alkene. In the absence of the olefin, the main species observed

was the rhodium bis-ligated monohydride complex [RhH(**3.9a**)$_2$] (**3.11**) (Scheme 3.4), obtained under the catalytic conditions described in Table 3.2, Entry 1 (Rh:L 1:2, CO/ H_2 (1:1) = 20 bar, 100 °C, 0.5 h). This species was detected by $^{31}P\{^1H\}$ NMR as a set of signals δ_P: 15.4 ppm (d, $J_{P\text{-}Rh}$ = 141.0 Hz), −30.9 (s) corresponding to the coordinated and uncoordinated P moieties, respectively.

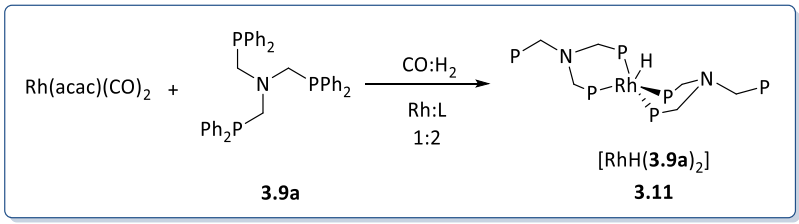

Scheme 3.4. Formation of rhodium complex with ligand **3.8a** described by Nozaki *et al.*

In solution, the complex has a fluxional behaviour, with the hydride moving from face to face of the complex. After treatment of the rhodium hydride species **3.11** with 5 bar of CO, three main species have been observed and assigned as [RhH(CO)(**3.9a**)] (**A**), [Rh(CO)(μ-CO)(**3.9a**)]$_2$ (**B**), and [RhH(CO)$_2$(**3.9a**)] (**C**) (Scheme 3.5).

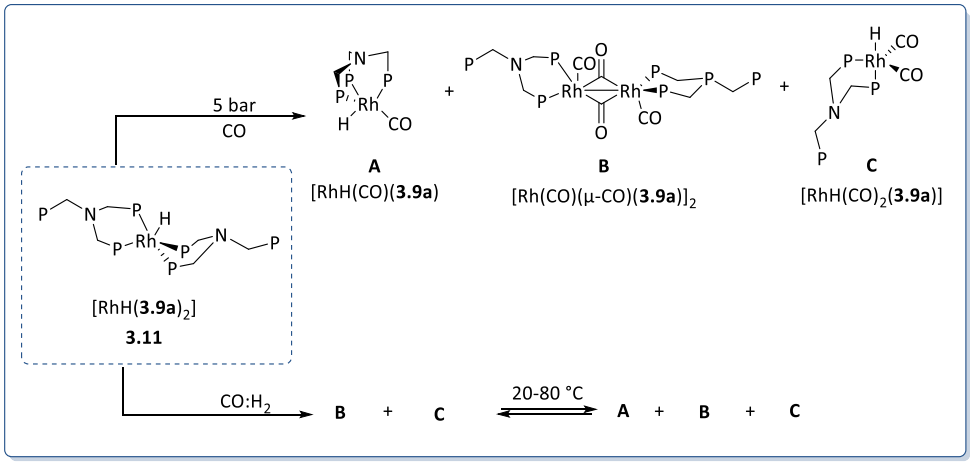

Scheme 3.5. Rhodium complex with ligand **3.9a** described by Nozaki *et al.* under 5 bar CO (left top) and CO/H2 (left bottom); stacked ^1H NMR spectra of hydride region of complex **3.11** under 5 bar CO (middle top) and CO/H_2 (middle bottom); and stacked $^{31}P\{^1H\}$ spectra of

complex **3.11** under 5 bar CO (right top) and CO/H_2 (right bottom): showing equilibrium mixture of species **A–C**.

These three species were observed in the ratio A:B:C = 1.0:9.0:6.4 at room temperature. When the complex [RhH(**3.9a**)$_2$] (**3.11**) was treated with $CO:H_2$ (1:1, 5 bar) at room temperature, the two species **B** and **C** were detected in a ratio 1.0:2.4 (Scheme 3.5 bottom). Increasing the temperature of the system, the appearance of species **A**, along with **B** and **C**, was detected.

Nozaki and co-workers investigated the activity of complex **3.11** in the presence of 1-hexene and either CO or CO/H_2, and noticed that in the absence of CO or H_2, complex **3.11** is unreactive toward 20 equivalents of 1-hexene. When to the system of rhodium complex **3.11** and 1-hexene were added 5 bar of CO, the same mixture of species observed in the absence of the olefin were detected (**A:B:C** = 1.0:8.0:6.2). Next, H_2 was introduced in the reaction mixture and the aldehydes were detected. The authors concluded that these species (**A**, **B** and **C**) were non actively involved in the catalytic cycle, but act as rhodium species that likely exist in a dynamic equilibrium as the catalytic resting state.

In view of the promising results reported using the ligand **3.10**, a systematic study involving the preparation of a series of symmetric nitrogen-centred ligands and the evaluation of their performance in the Rh catalysed hydroformylation of 1-hexene was carried out. This study aimed at determining the influence of the substituents at both the phosphorus and nitrogen atoms on the catalytic output of the reaction and on the coordination mode of these ligands to the rhodium centre.

3.2 Objectives

The main objective of this chapter is the development of a novel family of bidentate phosphorus-nitrogen-centred ligands, for the rhodium catalysed hydroformylation of 1-hexene to selectively provide the formation of the branched aldehyde.

The specific objectives of this chapter are:

- The development of a protocol for the synthesis of the new bidentate phosphorus-nitrogen-centred ligands.
- The study of the effect of the substituents on the bidentate phosphorus-nitrogen-centred ligands in the selective production of the branched aldehyde in the hydroformylation of 1-hexene.
- The study of the reactivity towards H_2/CO of the rhodium precursors in the presence of bidentate phosphorus-nitrogen-centred ligands, using HP NMR spectroscopy.

3.3 Results and discussion

3.3.1 Synthesis of bidentate phosphorus-nitrogen-centred ligands 3.16a-k

At the beginning of the project, we combined two synthetic routes reported in literature to obtain an efficient and direct method to synthesise the desired bidentate phosphorus-nitrogen-centred ligands.

This two-step procedure (Scheme 3.6) consists of:

- A first step where the hydroxyphosphine fragment **3.15** is obtained by condensation between phosphine **3.13** and paraformaldehyde **3.14** under neat conditions.[39]
- A second step consisting of a nucleophilic substitution with the selected amine **3.16**, delivering symmetric bidentate phosphine ligands **3.17**.[40]

This protocol affords the bidentate phosphorus-nitrogen-centred ligands **3.17a-k** in excellent yields, regardless of the substitution pattern, employing commercially available precursors.

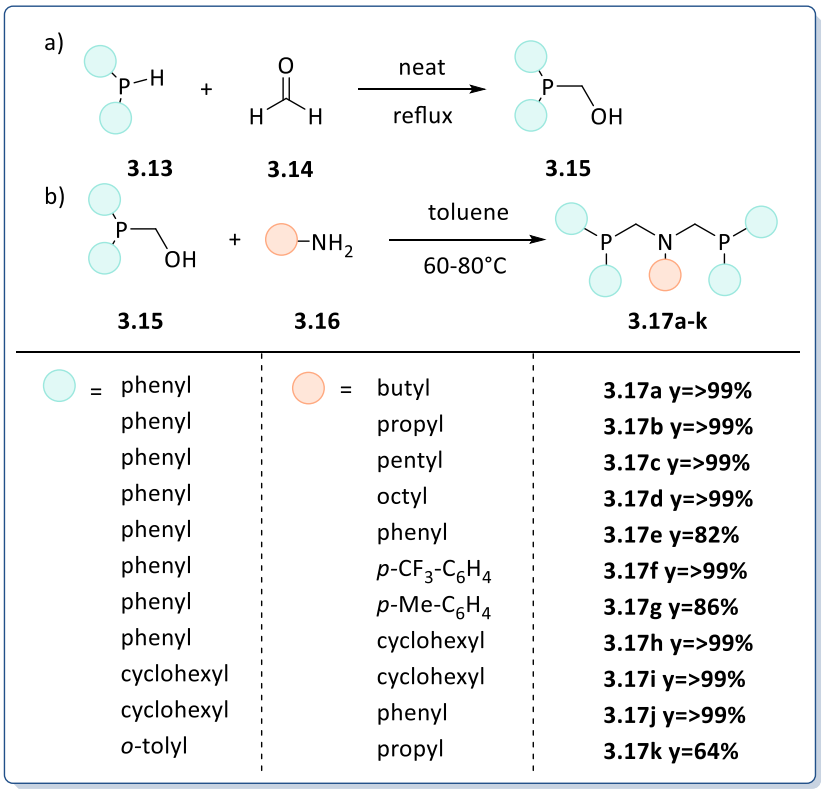

Scheme 3.6. Synthetic procedure for the generation of ligands **3.17a–k**

The two-step procedure was followed by ^{1}H NMR and ^{31}P NMR spectroscopy. As an example of the reaction monitoring, the synthesis of bidentate phosphorus-nitrogen-centred ligand **3.17c** will be detailed in the following section. In the ^{1}H NMR spectrum of the reaction crude of the first step, the formation of a doublet was observed at 4.15 ppm with a J_{P-H} couplings of 8.3 Hz. This was diagnostic for the formation of the CH_2 of the hydroxyphosphine fragments **3.15a**. Subsequently, **3.15a** was reacted with the selected amine **3.16** to yield the desired compound **3.17c**. The ^{1}H NMR spectrum shows the appearance of several peaks (Figure 3.3, a): a doublet at 3.56 ppm with a J_{P-H} couplings of 3.56 Hz, attributed to the new methylene bridge between the phosphorus and nitrogen atoms, and other signals that were attributed to the alkyl chains of **3.17c**.

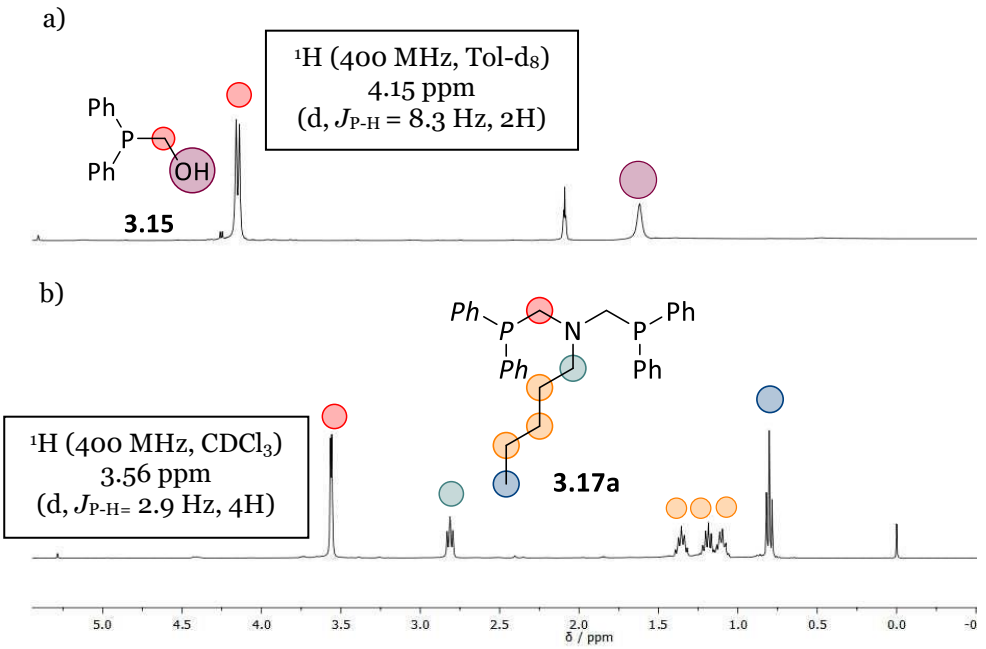

Figure 3.3. Selected ^{1}H NMR spectra for two-step procedure in the synthesis of ligand **3.17c**: a) ^{1}H NMR spectrum in of the hydroxyphosphine fragments **3.15a**. b) ^{1}H NMR spectrum in of the ligand **3.17c**.

In the ^{31}P{^{1}H} NMR spectrum, the hydroxyphosphine fragments **3.15a** displays one signal at -10.74 ppm (Figure 3.4, a). When fragment was reacted with the desired amine **3.16**, the formation of a new singlet was detected by ^{31}P{^{1}H} NMR spectroscopy at -28.47 ppm (Figure 3.4, b). This change in the ^{31}P{^{1}H} NMR spectrum is in agreement with the selective formation of the desired bidentate phosphorus-nitrogen-centred ligand **3.17c.**

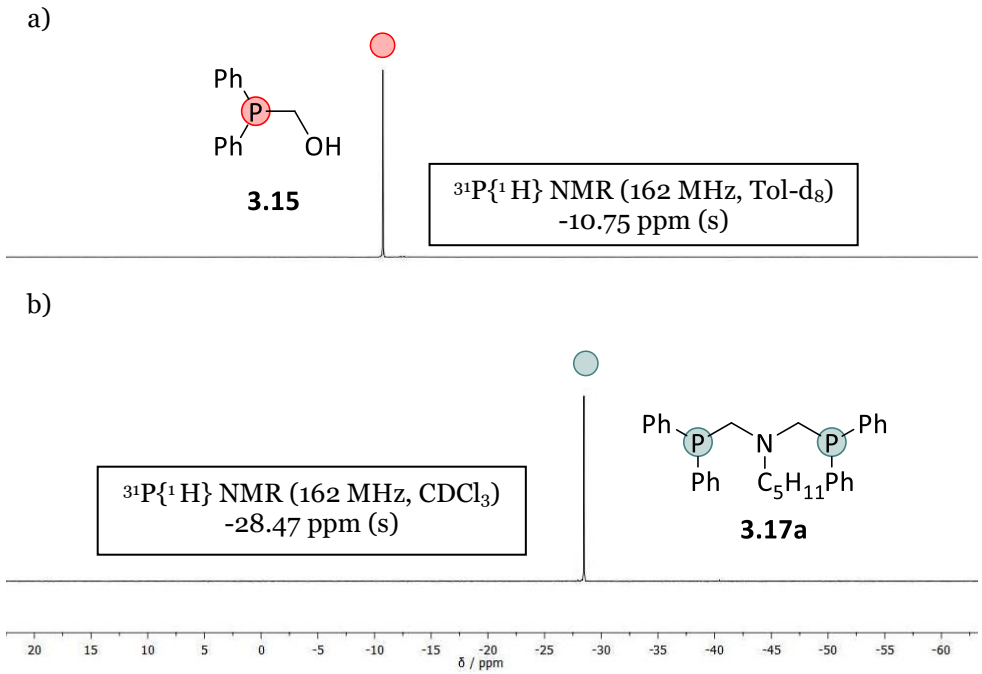

Figure 3.4. Selected $^{31}P\{^{1}H\}$ spectra for two-step procedure in the synthesis of ligand **3.17c**: a) $^{31}P\{^{1}H\}$ NMR spectrum in of the hydroxyphosphine fragments **3.15a**. b) $^{31}P\{^{1}H\}$ NMR spectrum in of the ligand **3.17c**.

The newly bidentate phosphorus-nitrogen-centred ligands **3.17a-k** were characterised by ^{1}H NMR, ^{31}P NMR and ^{13}C NMR spectroscopy and MS spectrometry. With this new family of ligands in hand, we investigated their activity and selectivity towards the hydroformylation of 1-hexene.

3.3.2 Total pressure optimization

First, the bidentate phosphorus-nitrogen-centred ligand **3.17b** was selected to perform the optimization of the total pressure in the rhodium catalysed hydroformylation of 1-hexene. Thus, $[Rh(acac)(CO)_2]$ was used as metal precursor in the presence of 1.1 equivalent of ligand **3.17b**, at 50 °C, for 24 hours (Table 3.3). When 5 bar of syngas were used (Entry 1), full conversion and 81% of chemoselectivity, with b/l ratio of 0.8 was observed (Table 3.3).

When the pressure was increased up to 10 bar (Entry 2), the conversion was not affected but both chemo- and regioselectivity increased.

Table 3.3. Optimization of the reaction conditions with diphosphine ligands **3.17b**

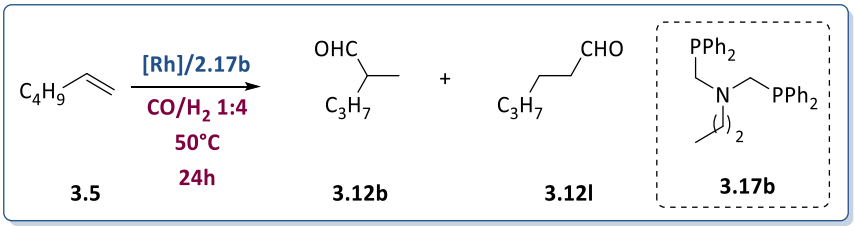

Entry [a]	Tot P (bar)	Conv%	Chemo%	b/l
1	**5**	>99	81	0.8
2	**10**	>99	94	1.0
3	**20**	64	68	0.7

Reaction conditions:[a] 1-hexene **3.5** (2 mmol), $[Rh(acac)(CO)]_2$ (1 mol%), Ligand **3.17b** (1.1 mol), $CO:H_2$ 1:4, 50 °C for 24 h. Conversion, chemoselectivity and regioselectivity determined by GC-FID and NMR using bicyclohexyl as internal standard.

Surprisingly, when the pressure was increased up to 20 bar (Entry 3), a similar effect was observed and conversion, chemo- and regioselectivity dramatically decreased. This could be explained in base of the requirement of a minimum of CO for the hydroformylation (2 bar of Entry 2, 1:4 $CO:H_2$), while employing a large excess (4 bar of Entry 3) of CO can lead to the deactivation of the active rhodium species. Then, under the selected reaction conditions (Table 3.3, Entry 2) for the rhodium hydroformylation of 1-hexene, several ligands (**3.17a-k**) were tested in order to study the effect under the same catalytic system. Thus, $[Rh(acac)(CO)_2]$ (1 mol%) was used as metal catalyst, 1-hexene was used as the model substrate, at 50 °C and 10 bar of 1:4 CO/H_2 for 24 hours. We screened all the previously synthetized ligands **3.17a-k** (1.1 mol%) described in Scheme 3.6, as depicted in Table 3.4.

Table 3.4. Phosphorus-nitrogen-centred ligands **2.17a-k** screening

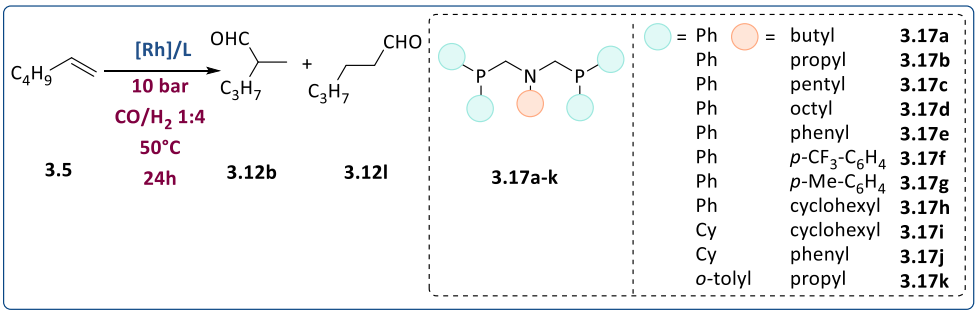

Entry[a]	Ligand	**Conv%**	**Chemo%**	b/l
1	**3.17a**	80	95	1.3
2	**3.17b**	>99	94	1.0
3	**3.17c**	95	99	1.4
4	**3.17d**	83	99	1.3
5	**3.17e**	>99	99	0.4
6	**3.17f**	96	96	0.4
7	**3.17g**	>99	46	0.6
8	**3.17h**	62	75	0.5
9	**3.17i**	>99	99	0.5
10	**3.17j**	>99	99	0.6
11	**3.17k**	96	64	0.3
12	Dppp **3.18**	60	99	0.9
13	Dppe **3.19**	>99	99	1.0
14	2,6-$(PPh2)_2$ pyridine **3.20**	>99	99	1.0
15	-	96	49	0.5

Reaction conditions:[a] 1-hexene **3.5** (2 mmol), $[Rh(acac)(CO)]_2$ (1 mol%), Ligand (1.1 mol), 10 bar $CO:H_2$ 1:4, 50 °C for 24 h. Conversion, chemoselectivity and regioselectivity determined by GC-FID and NMR using bicyclohexyl as internal standard.

At first, we reproduced the catalytic conditions described by Nozaki and co-workers using ligand **3.17a** (Table 3.4, Entry 1). In this case, the hydroformylation product was obtained with slightly reduced efficiency

(80%) but similar chemoselectivity (95%) and regioselectivity (1.3). On the other hand, when employing ligand **3.17b** (Entry 2), the reaction provided full conversion (99%) together with a good chemoselectivity (94%) but lower b/l ratio (b/l 1). When ligand **3.17c**, that contains a *n*-pentyl substituent on the nitrogen atom, was tested in the reaction, slightly higher regioselectivity was observed (1.4), while conversion and chemoselectivity remained unchanged (Entry 3). Using ligand **3.17d** (Entry 4), that bears *n*-octyl on the amine chains, the b/l ratio obtained was 1.3. When the aniline was incorporated, **3.17e** in Entry 5, 0.4 of b/l ratio and full conversion and chemoselectivity were observed. When ligand **3.17f**, incorporating a *p*-trifluoromethylaniline group at nitrogen centre, was used (Entry 6), both conversion and chemoselectivity were high although the regioselectivity was low (b/l=0.4). The use of ligand **3.17g**, incorporating a *p*-methylaniline (Entry 7), delivered the target compound with complete conversion but with low chemoselectivity (43%) and branched to linear ratio (0.6). When the ligand **3.17h**, bearing a basic and bulky cyclohexylamine, was employed, low activity (62%) and chemoselectivity (75%) together with a b/l ratio of 0.6 were obtained (Entry 8). The use of ligand **3.17i**, that contains two dicyclohexyl phosphine fragments and a cyclohexyl amine moiety (Entry 9), gave high conversion (94%) and chemoselectivity (99%), but a b/l ratio of 0.7. When ligand **3.17j**, that incorporates a simple phenyl group on the nitrogen atom and the two cyclohexyl phosphine, was used (Entry 10), both conversion and chemoselectivity were very high although the regioselectivity was again low (b/l=0.6). Using the ligand **3.17k**, which bears ortho-tolyl groups, the reaction was completed with high conversion but with 64% chemoselectivity and a branched to linear ratio of 0.3 (Entry 11).

The results described in Entries 6-11 therefore indicate that an increase in steric hindrance, either at the nitrogen or at the phosphorus centres, severely affects the regioselectivity of the reaction in favour of the linear product. Using the commercial dppp **3.18** ligand to investigate the effect of the

presence of an amine fragment in the structure of these ligands (Entry 12), low activity (60%) and intermediate regioselectivity (0.9) were observed. In Entry 13, dppe **3.19,** that contains a 3 carbon chain in between the two phosphorus atoms, yielded a b/l ratio of 1.0 , and full conversion and chemoselectivity. As a further reference, the commercial 2,6-$(PPh2)_2$ pyridine **3.20**, that contain a nitrogen atom in the skeleton, produced a b/l of 1.0. (Entry 14). As expected, the hydroformylation of 1-hexene with the unmodified rhodium pre-catalyst, led to a b/l of 0.5 (Entry 15). It was therefore concluded that the presence of *N*-*n*-alkyl fragment has a beneficial effect on the regioselectivity of the reaction while larger groups at the nitrogen atom or the replacement of the *n*-alkyl moiety by a methylene group both favour the formation of linear product. An increase of the length of the alkyl chain substituent on the amine slightly improved the branched to linear ratio when going from propyl to butyl and pentyl (Entries 1-4). However, when the chain at nitrogen contained 8 carbons, the regioselectivity in branched aldehyde decreased.

3.3.3 HP-NMR studies

In order to gain understanding into the reactivity of the Rh species present during the catalysis, HP-NMR experiments were conducted under different reaction conditions. These studies were performed using 0.01 mmol of $[Rh(acac)(CO)_2]$ as metal precursor, 0.011 of ligand, toluene-d_8 as solvent in a total volume of 0.4 mL. Systems bearing the ligands **3.17j** and **3.17c** were thus investigated using a 5 mm HP-NMR tube and analysing the reaction mixtures by ^{1}H, ^{31}P and ^{13}C NMR spectroscopies. These HP-NMR *in situ* experiments were motivated to determine the coordination mode in the resting state of the rhodium hydride dicarbonyl species, as it is commonly performed. Moreover, the use of two ligands with different electronic and steric properties, as the ligand **3.17c** and **3.17j**, could provide further

information on the relationship between the nature of the ligand and the coordination mode.

3.3.3.1 Determination of the coordination mode of [Rh H(3.17j)(CO)$_2$] in the resting state

The system [Rh(acac)(CO)$_2$]/**3.17j** was submitted to 10 bar of syngas (H_2/CO, 4:1) at 50°C for 1 hour (Scheme 2.8). Under these conditions, the rhodium hydride dicarbonyl species [RhH(**3.17j**)(CO)$_2$] **3.22** was readily detected by NMR spectroscopy. In the ^{1}H NMR spectrum, the formation of a doublet of triplets was observed at -9.47 ppm with a J_{Rh-H} of 11 Hz and a J_{P-H} of 52 Hz (Scheme 3.7, a).

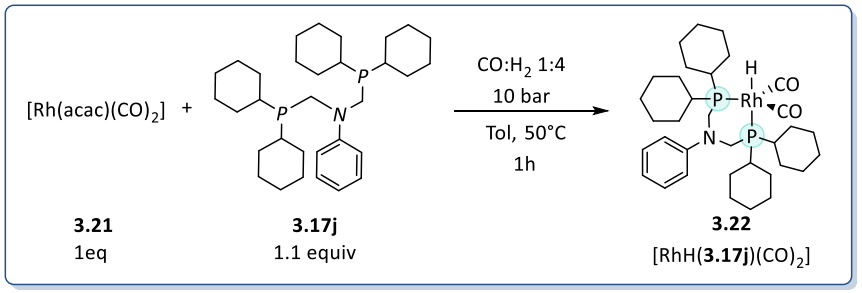

a)

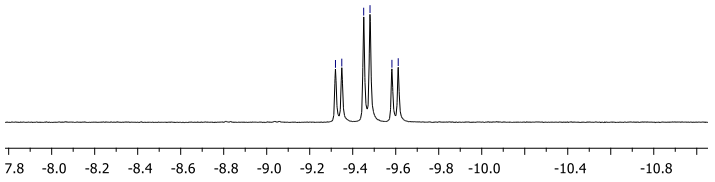

Scheme 3.7. [RhH(**2.17j**)(CO)$_2$] structure in tol-d^8 (10 bar CO/H_2, 50 °C, 1h); (a) ^{1}H NMR (400 MHz, RT) of the hydride of the [RhH(**3.17j**)(CO)$_2$].

It is a general assumption that (di)phosphine and (di)phosphite ligands, when coordinated with a rhodium pre-catalyst, form a trigonal bipyramidal hydride dicarbonyl rhodium complex, known to be the resting state in the hydroformylation reaction.[41] Depending of the length and the flexibility of the

bridging chain between the two phosphorus atoms, two structures are proposed based on their stability. The equatorial:axial complex or the equatorial:equatorial complex (Figure 3.5).

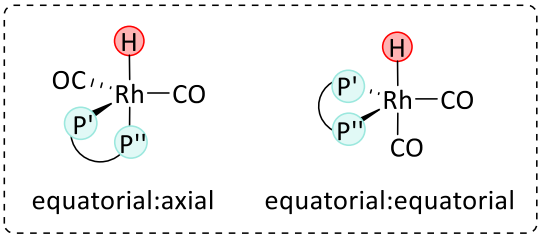

Figure 3.5. [RhH(**L-L**)$(CO)_2$] complexes, equatorial:axial and equatorial:equatorial complexes.

As described by Van Leeuwen *et al.*, short-bridged diphosphites forming up to seven membered rings coordinate in an equatorial-axial fashion to rhodium, generating a bite angle close to 90° (equatorial:axial). In contrast, diphosphites forming flexible eight- or nine-membered chelate rings coordinate in equatorial:equatorial mode, since the bite angle may reach values close to 120°.[48] The larger bidentate ligand usually show a preferential bis-equatorial coordination due to the less steric congestion in the equatorial plane of the trigonal bipyramidal (TBP) rhodium complex, as reported by Brown and Kent.[41]

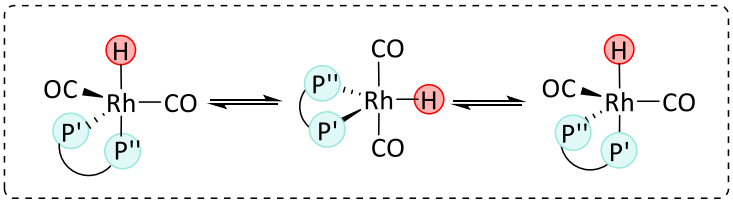

Scheme 3.8. Berry type rearrangements.

The equatorial-axial ligand exchange in TBP complexes has been explained by the so called Berry-type and turnstile rotations.[42] In both mechanisms, two axial nuclei exchange positions with two of the equatorial nuclei in one step. As described by Meakin for monophosphites, such a rearrangement in RhH(**L-L**)$(CO)_2$ bidentate ligand complexes for equatorial-axial phosphorus

exchange seems very unlikely because it requires two successive Berry-type interconversions (Scheme 3.8) *via* a high energy intermediate containing an equatorially coordinated hydride ligand.[42,43] Furthermore, this Berry-type mechanism requires relatively flexible diphosphine ligands because the bite angle varies between 90° and 120°. By contrast, Meakin proposed a low-energy rearrangement mechanism, where a simple hydride motion interconverts the equatorial (P') and the axial (P") phosphorus atoms (Scheme 3.9).[43] This rearrangement has been proposed by Meakin for monophosphites, and it was extended towards the fluxional behaviour observed in complexes containing flexible diphosphite.

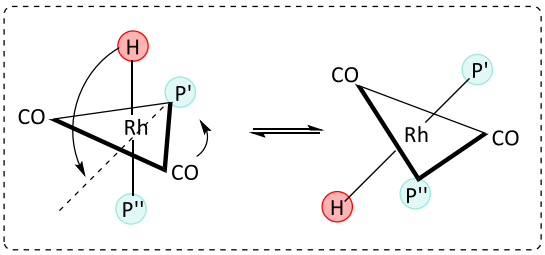

Scheme 3.9: Equatorial axial phosphorus exchange of the [RhH(**3.17j**)$(CO)_2$].

A simultaneous bending motion of the hydride and the carbon monoxide ligands now places the hydrogen axially to P', thus exchanging both phosphorus nuclei. As a result, in the $^{31}P\{^1H\}$ NMR a doublet is detected, which means that either the chemical shifts of both phosphorus atoms accidentally coincide or that they exchange rapidly on the NMR time scale. In our study, the ^1H NMR spectrum shows a doublet of triplets (dt) structure in the hydride region. This set of signals is caused by the coupling with two degenerate phosphorus atoms and the coupling with rhodium metal centre (Scheme 3.9). Usually a small *cis* coupling constant for the phosphorus-hydrogen coupling (up to 3 Hz) has been described for equatorial:equatorial diphosphine and diphosphite hydride dicarbonyl rhodium complexes RhH(**L-L**)$(CO)_2$.[35,44,45] In contrast, a *trans* relationship is responsible for a large coupling constant between the phosphorus and the hydrogen atoms in

the hydride species (150-220 Hz).[46] In order to resolve this time-averaged phosphorus-hydride coupling constant (J_{P-H} 52 Hz) observed in Scheme 3.8 with the system [Rh(acac)$(CO)_2$]/**3.17j**, the temperature was lowered down to -75 °C. The sequence is described in figure 3.6.

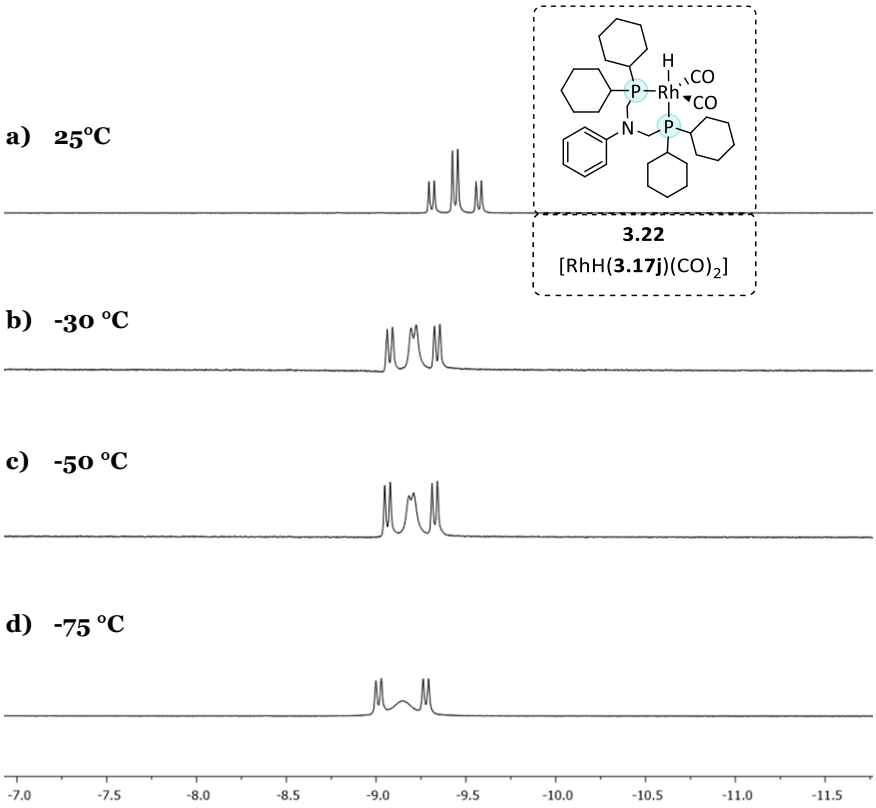

Figure 3.6. ^{1}H NMR (400 MHz, RT) of the hydride species [RhH(**3.17j**)$(CO)_2$], recorded at variable temperature.

At room temperature (Figure 3.6, a), a doublet of triplet at -9.47 ppm with a J_{Rh-H} couplings of 11 and J_{P-H} 52 Hz, respectively, was observed. Nonetheless, when the temperature was progressively decreased up to -75 °C, the multiplicity changed from a clear doublet of triplets to a pseudo doublet of doublets at -9.15 ppm in the ^{1}H NMR spectrum (Figure 3.6, d). The large coupling constants of the phosphorus in *trans* (J_{P-H} 105 Hz) to the hydride can be observed, while the small coupling constants of the phosphorus in *cis*

to the hydride cannot be detected.[47] According to the reported data, the bidentate phosphorus-nitrogen-centred ligand **3.17j** provides the hydride dicarbonyl rhodium intermediate with an equatorial:axial structure, thus confirmed by the variable-temperature NMR study performed. This behaviour suggests a time-averaged *cis-trans* relationship between the phosphorus and the hydrogen atoms bonded to the rhodium, postulated By Meakin (Scheme 3.9)and described by van Leeuwen and co-workers.[48,43]

The non-coordinated phosphine ligand **3.17j** displays in the $^{31}P\{^{1}H\}$ NMR spectrum one signal at -15.53 ppm (Scheme 3.7, a). When the precursor [Rh(acac)$(CO)_2$] was mixed with ligand **3.17j** under syngas pressure, the formation of a doublet was detected by $^{31}P\{^{1}H\}$ NMR spectroscopy at 26.53 ppm ($J_{Rh\text{-}P}$ = 111.3 Hz) (Figure 3.12 bottom).

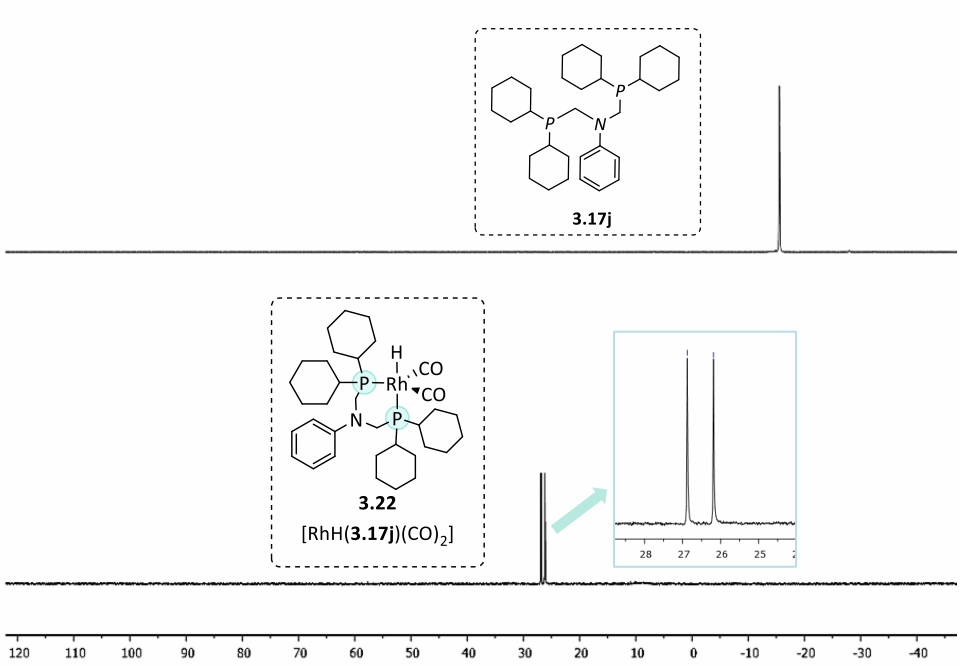

Figure 3.7. Top: $^{31}P\{^{1}H\}$ NMR spectrum (162 MHz, RT) of the **3.17j** ligand. Bottom: $^{31}P\{^{1}H\}$ NMR spectrum (162 MHz, RT) of the [RhH(**3.17j**)$(CO)_2$].

Additionally, terminal carbonyls coordinated to rhodium were also detected by ^{13}C NMR spectroscopy as two triplets at 201.21 ($J_{P\text{-}C}$ = 10.1 Hz, $J_{Rh\text{-}C}$ = 69.8

Hz) and 200.53 ppm (J_{P-C} = 10.1 Hz, J_{Rh-C} = 69.2 Hz). ^{1}H-^{31}P Heteronuclear Multiple Bond Correlation NMR (HMBC) exhibited correlation between the hydride signal at -9.47 ppm in ^{1}H NMR spectrum of the [RhH(**3.17j**)$(CO)_2$], and the corresponding phosphorus signal at 26.53 ppm in $^{31}P\{^{1}H\}$ NMR spectrum. The CH_2 bridge between the nitrogen and the phosphorus atoms, a singlet at 3.19 ppm ^{1}H NMR, exhibited a correlation with the hydride signal at -9.47 ppm in $^{31}P\{^{1}H\}$ NMR spectrum. Two signals at 1.83 and 1.58 ppm in the ^{1}H NMR spectrum, part of the cyclohexyl structure of the ligand, also exhibited a correlation with the doublet at 26.53 ppm in $^{31}P\{^{1}H\}$ NMR spectrum and the hydride signal at -9.47 ppm.

Furthermore, selective decoupling experiments allowed us to attribute that the P,H coupling constant (J_{P-H} = 52 Hz) of the hydride signal at -9.47 ppm in ^{1}H NMR spectrum, is due to the phosphorus signal at 26.53 ppm. 1D and 2D NMR spectroscopy experiments were also carried out. The data obtained are summarized in Figure 3.8 and Table 3.5.

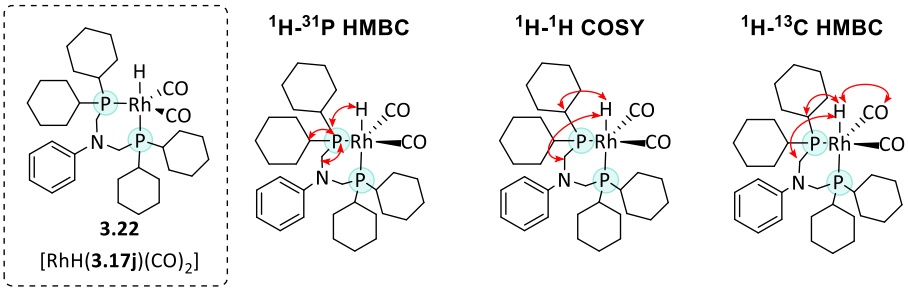

Figure 3.8 : Correlations observed via 2D NMR experiments for the characterization of the coordination sphere of the [RhH(**3.17j**)$(CO)_2$] complex.

δ ^{31}P ppm	δ ^{1}H ppm	δ ^{13}CO ppm
26.53 (d, J_{Rh-P} = 111.3 Hz)	-9.47 (td, J_{Rh-H} = 11 Hz, J_{P-H} = 52 Hz)	200.53 (dt, J_{P-C} = 10.1 Hz, J_{Rh-C} = 69.8 Hz) 201.21 (dt, J_{P-C} = 10.1 Hz, J_{Rh-C} = 69.2 Hz)

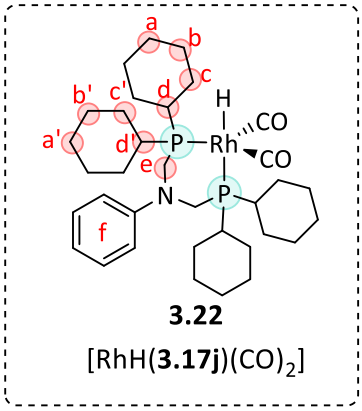

3.22

[RhH(**3.17j**)$(CO)_2$]

Table 3.5. Selected spectroscopic data of the rhodium coordination sphere from rhodium complex **3.22**.

δ ^{1}H ppm	δ ^{13}C ppm	Assignment
1.17 (m, C$\underline{H}_2$)	23.8 (s, $\underline{C}H_2$)	**A**
	27.0 (t, $J_{P,C}$ = 5 Hz, $\underline{C}H_2$)	**C**
	28.6 (s, $\underline{C}H_2$)	**B**
1.76 (m, C$\underline{H}_2$)	25.9 (s, $\underline{C}H_2$)	**A'**
	27.3 (t, $J_{P,C}$ = 5 Hz, $\underline{C}H_2$)	**C'**
	29.3 (s, $\underline{C}H_2$)	**B'**
	36.7 (t, J_{P-C} = 11 Hz, $\underline{C}H$)	**D**
3.19 (s, C$\underline{H}_2$)	52.26 (t, J_{P-C} = 17 Hz, $\underline{C}H_2$)	**E**
6.9 (m, C$\underline{H}$)	119.7 (s, $\underline{C}H$)	**F**
	121.1 (s, $\underline{C}H$)	
	129.1 (s, $\underline{C}H$)	
	155.0 (m, C)	

It was therefore concluded that under these conditions, the bidentate hydride dicarbonyl rhodium intermediate [RhH(**3.17j**)$(CO)_2$] **3.22** is formed and is coordinated in an equatorial:axial mode.

3.3.3.2 Determination of the coordination mode of [Rh H(3.17c)(CO)$_2$] in the resting state

The system [Rh(acac)(CO)$_2$]/**3.17c** was submitted to 10 bar (H_2/CO, 4:1) of syngas at 50 °C for 24 hours. Under these conditions, the rhodium hydride dicarbonyl species [RhH(**3.17c**)(CO)$_2$] was detected by NMR spectroscopy. The ^{1}H NMR spectrum revealed the formation of a doublet of triplets, at -8.64 ppm with a J_{Rh-H} of 10 and a J_{P-H} of 52 Hz. As previously reported, this behaviour indicated a time-averaged *cis-trans* relationship between the phosphorus and the hydrogen atoms bonded to the rhodium (Scheme 3.10).[48]

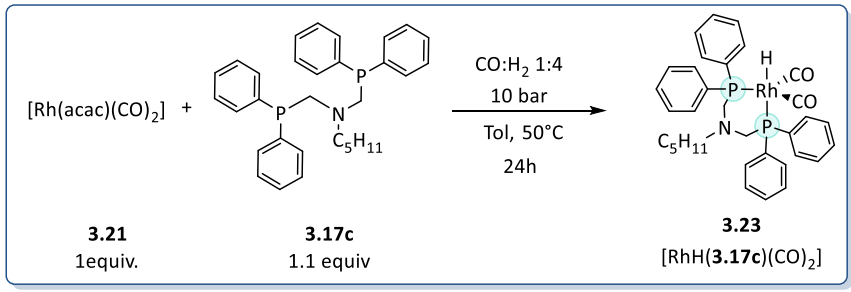

a)

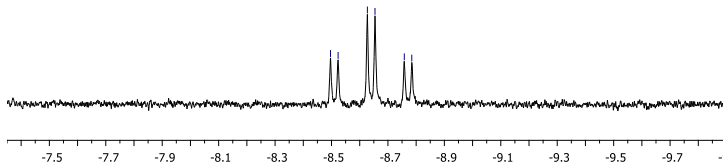

Scheme 3.10 : [RhH(**3.17c**)(CO)$_2$] structure in tol-d^8 (10 bar CO/H_2, 50 °C, 1h); (a) ^{1}H NMR (400 MHz, RT) of the hydride of the [RhH(**3.17c**)(CO)$_2$].

According to the reported data, the bidentate phosphorus-nitrogen-centred ligand **3.17c** provides the hydride dicarbonyl rhodium intermediate [RhH(**3.17c**)(CO)$_2$] **3.23** with an equatorial: axial structure, as explained in section **3.3.3.1** in the case of ligand **3.17j**. Under these conditions, two

doublets were detected by $^{31}P\{^{1}H\}$ NMR spectroscopy at 4.35 ppm (J_{Rh-P} = 151 Hz) and at 11.03 ppm (J_{Rh-P} = 114.4 Hz) (Figure 3.4 bottom). ^{1}H-^{31}P HMBC exhibited a correlation between the signal corresponding to the phosphorus resonance at 4.35 ppm in $^{31}P\{^{1}H\}$ NMR spectrum and the signals corresponding to the hydride (-8.64 ppm), the CH_2 bridge between nitrogen and phosphorus atoms (3.39 ppm), and the first CH_2 of the alkyl chain of the nitrogen atom (2.23 ppm), in ^{1}H NMR spectrum.

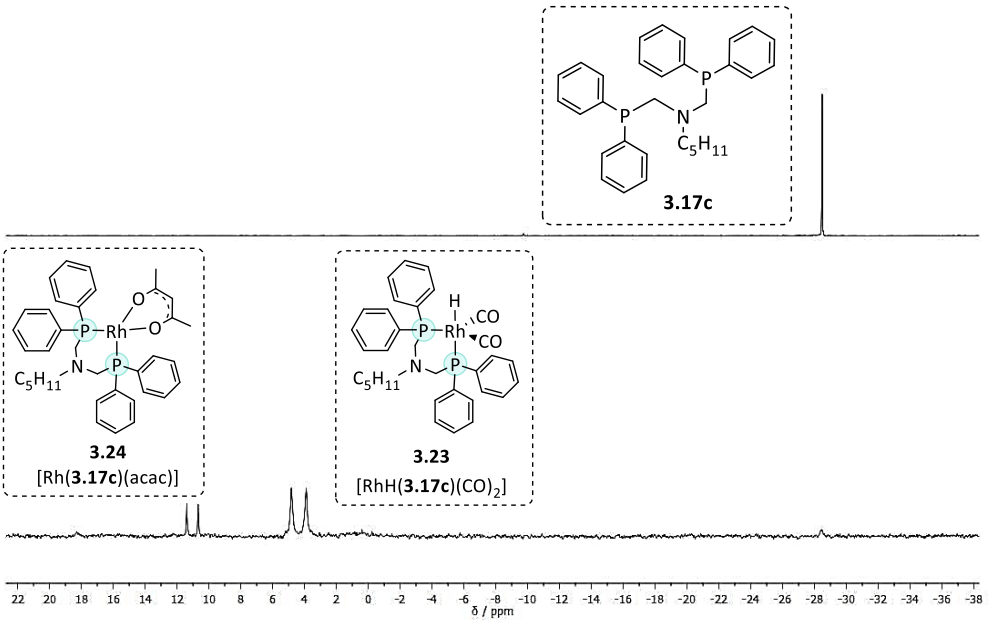

Figure 3.9: Top: $^{31}P\{^{1}H\}$ NMR spectrum (162 MHz, RT) of the **3.17c** ligand. Bottom: $^{31}P\{^{1}H\}$ NMR spectrum (162 MHz, RT) of the [RhH(**3.17c**)$(CO)_2$] and [Rh(**3.17c**)(acac)].

Furthermore, selective decoupling experiments allowed us to attribute that the P,H coupling constant (J_{P-H} = 52 Hz) observed in the hydride signal, is due to the phosphorus signal at 4.35 ppm. The doublet at 11.03 ppm detected in the $^{31}P\{^{1}H\}$ NMR spectrum suggests the formation of a Rh complex identified as the square planar complex [Rh(**3.17j**)(acac)] **3.24**. The signal exhibited a J_{Rh-P} coupling of 114.4 Hz and this data is in agreement with similar complexes previously described in the literature for other chelate

ligands.[28] 1D and 2D NMR spectroscopy experiments were also carried out. The data obtained are summarized in Figure 3.10 and Table 3.6.

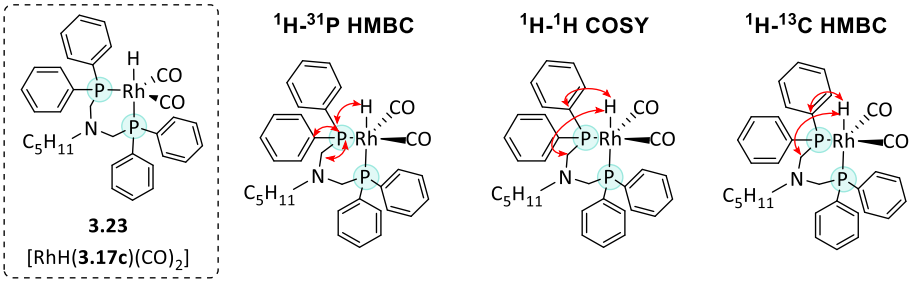

δ ^{31}P ppm	δ ^{1}H ppm
4.35 (d, J_{Rh-P} = 114.4 Hz)	-8.46 (td, J_{Rh-H} = 10 Hz, J_{P-H} = 52 Hz)

Figure 3.10. Correlations observed via 2D NMR experiments for the characterization of the [RhH(**3.17c**)$(CO)_2$] complex.

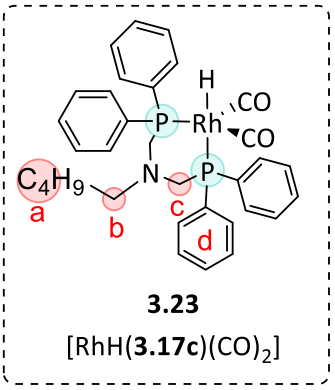

3.23

[RhH(**3.17c**)$(CO)_2$]

Table 3.6: Selected spectroscopic data of the rhodium coordination sphere from rhodium complex **3.23**.

δ ^{1}H ppm	δ ^{13}C ppm	Assignment
	14.1 (s, $\underline{C}H_3$)	
1.26-1-10 (m, $C\underline{H}_3$)	22.7 (s, $\underline{C}H_2$)	**A**
1.09-0.97 (m, $C\underline{H}_2$)	23.9 (s, $\underline{C}H_2$)	
0.90-0.68 (m, $C\underline{H}_2$)	27.0 (s, $\underline{C}H_2$)	
2.23 (bs, $C\underline{H}_2$)	44.4 (d, $J_{P\text{-}C}$ = 6.5 Hz, $\underline{C}H_2$)	**B**
3.39 (bs, $C\underline{H}_2$)	58.5 (s, $\underline{C}H_2$)	**C**
7.06 (m, C$\underline{H}$)	131.2 (d, $J_{P\text{-}C}$ = 2.7 Hz, $\underline{C}H_2$)	
7.80 (m, C$\underline{H}$)	133.4 (d, $J_{P\text{-}C}$ = 11.6 Hz, $\underline{C}$H)	**D**
7.86 (m, C$\underline{H}$)	131.6 (d, $J_{P\text{-}C}$ = 8.6 Hz, $\underline{C}$H)	
-	137 (s, $\underline{C}$)	

It was therefore concluded that under these conditions, the bidentate phosphorus-nitrogen-centred ligand **3.17c** provides the hydride dicarbonyl rhodium intermediate [RhH(**3.17c**)$(CO)_2$] with an equatorial:axial structure. In conclusion, the rhodium hydride dicarbonyl resting states **3.22** and **3.23**, presented the same coordination mode, as equatorial:axial coordination mode. Therefore, it can be concluded that the difference in selectivity observed for these ligands in the Rh-catalysed hydroformylation of 1-hexene

cannot be attributed to a distinct coordination mode, and might be due in the difference of electronic properties between these two ligands.

3.4 Conclusions

From the study described in this chapter, the following conclusions can be extracted:

I. The development of a protocol for the synthesis of new bidentate phosphorus-nitrogen-centred ligands **3.17a-k** was achieved *via* a two-step procedure.
II. The optimized conditions for catalytic hydroformylation included the use of [Rh(acac)$(CO)_2$] (1 mol%) as rhodium precursor, 1.1 mol% of ligand **3.17a-k**, at 50 °C, 10 bar of total pressure with 1:4 CO/H_2 for 24 hours.
III. The screening of the ligands **3.17a-k** in the rhodium catalysed hydroformylation of 1-hexene under the optimized conditions, indicated that an increase in steric hindrance at the nitrogen or at the phosphorus centres, severely affects the regioselectivity of the reaction in favour of the linear product.
IV. When the **3.17a-c** ligands, that contain a *N*-*n*-alkyl fragment, are used in the Rh catalysed hydroformylation of 1-hexene, the branched to linear ratio increased up to 1.4 b/l.
V. When the ligands **3.17i-k,** that contain a bulky phosphine fragment, are used in the Rh catalysed hydroformylation of 1-hexene, a negative effect on the branched selectivity of the reaction (b/l=0.5, 0.6, 0.3) is observed.
VI. When the ligands **3.17e-h,** that contain a larger group at nitrogen atom, are used in the Rh catalysed hydroformylation of 1-hexene, the formation of the linear aldehyde (b/l=0.5, 0.4) is favoured.

VII. The length of the alkyl chain on the nitrogen atom improved slightly the branched to linear ratio when going from propyl to butyl and pentyl (ligand **3.17a, 3.17b** and **3.17c**). However, in the case of ligand **3.17d**, where the nitrogen atom is bearing an octyl chain, the regioselectivity in branched aldehyde decreased.

VIII. When the ligand **3.17c** was employed under the optimized conditions, the system delivered the highest value of branched to linear ratio in hydroformylation of 1-hexene (b/l= 1.4).

IX. When the system [Rh(acac)$(CO)_2$]/**3.17c** was submitted to 10 bar (H_2/CO, 4:1) of syngas at 50 °C for 24 hours, the rhodium hydride dicarbonyl species [RhH(**3.17c**)$(CO)_2$] was detected by NMR spectroscopy, revealing an eq:ax coordination mode.

X. When the system [Rh(acac)$(CO)_2$]/**3.17j** was submitted to 10 bar (H_2/CO, 4:1) of syngas at 50 °C for 1 hour, the rhodium hydride dicarbonyl species [RhH(**3.17j**)$(CO)_2$] was detected by NMR spectroscopy, also revealing an eq:ax coordination mode for this ligand.

XI. The ligands **3.17c** and **3.17j** therefore both present the same coordination mode in the corresponding rhodium hydride dicarbonyl [RhH(**3.17c**)$(CO)_2$] **3.22** and [RhH(**3.17j**)$(CO)_2$] **3.23**, thus suggesting that the coordination mode of these ligands cannot be hold responsible for the difference in performance in the Rh-catalysed hydroformylation of 1-hexene.

3.5 Experimental Part

3.5.1 General information

All the reactions were carried out using Schlenk-line inert atmosphere techniques or glovebox techniques. Anhydrous solvents were collected from

the system Braun MB SPS-800. Commercially available reagents and solvents were purchased at the highest commercial quality from Sigma-Aldrich, Fluka, Alfa Aesar, Fluorochem, Strem and were used as received, without further purification, unless otherwise stated. ^{1}H, $^{13}C\{^{1}H\}$ and $^{31}P\{^{1}H\}$ NMR spectra were recorded using a Varian Mercury VX 400 (400, 100.6, and 161.97 MHz respectively). Chemical shift values (δ) are reported in ppm relative to TMS (^{1}H and $^{13}C\{^{1}H\}$) or H_3PO_4 ($^{31}P\{^{1}H\}$), and coupling constants are reported in Hertz. The following abbreviations are used to indicate the multiplicity: s, singlet; d, doublet; t, triplet; q, quartet; m, multiplet; bs, broad signal. High-resolution mass spectra (HRMS) were recorded on an Agilent Time-of-Flight 6210 using ESI-TOF (electrospray ionization-time of flight). Samples were introduced to the mass spectrometer ion source by direct injection using a syringe pump and were externally calibrated using sodium formate. The instrument was operating in the positive ion mode. Reactions were monitored by TLC carried out on 0.25 mm E. Merck silica gel 60 F_{254} glass or aluminium plates. Developed TLC plates were visualized under a short-wave UV lamp (254 nm) and by heating plates that were dipped in potassium permanganate. The Rh-catalysed hydroformylation reaction were set up in a 7 tube autoclave from HEL Inc. and single tube autoclave from HEL Inc and were stirred with a teflon-coated magnetic stir bar.

3.5.2 General procedure for hydroformylation of 1-hexene reaction

A 10 mL glassware reactor tube was charged with 1-hexane **3.5** (2 mmol), Dicarbonyl(acetylacetonato)rhodium(I) (1 mol%) in toluene (3.75 mL) and ligand (1.1 mmol%), the autoclave was closed in the glove-box. The reaction tube was placed in the reactor which was pressurized at the desired pressure, heated to 50 °C and left stirring at 900 rpm. The reaction was stopped after 24 hours by cooling the reactor in an ice bath for 20 minutes followed by venting of the system. After completion of the reaction, the crude mixture was

analysed by GC-MS, GC-FID and ^{1}H NMR and the results compared to those previously reported in literature.

3.5.3 Synthesis of bidentate phosphorus-nitrogen-centred ligands 3.17a-k

General Procedure A:

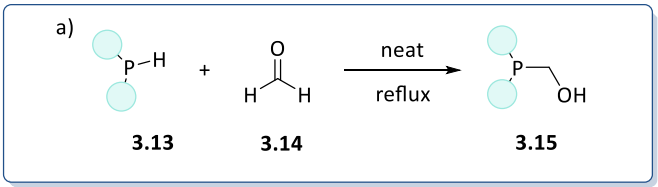

Figure 3.17: synthesis of hydroxyphosphine fragments **3.15**

The reaction was carried out in an oven dried, argon purged, Schlenk fitted with a argon inlet and a septum, following a reported procedure.[39,40] Neat mixture of phosphine **3.13** (10 mmol) and paraformaldehyde **3.14** (10 mmol) was stirred and heated to 110 °C from 30 minutes to 1 hour, until the paraformaldehyde was completely converted, highlighted by the appearance of a clear solution. The liquid was then allowed to cool to room temperature to afford the desired compound **3.15** in quantitative yield.

Synthesis of (hydroxymethyl)diphenyl phosphine 3.15a

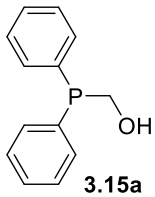

General procedure A was followed employing diphenyl phosphine (10 mmol) and paraformaldehyde (10 mmol). Compound **3.15a** was obtained as a clear liquid. Yield of **3.15a**: 2.46 g (100%); **^{1}H NMR** (400 MHz, Tol-d_8): δ 7.46–7.37 (m, 5H), 7.13–7.02 (m, 5H), 4.15 (d, $J_{P\text{-}H}$= 8.3 Hz, 2H), 1.36 (bs). **^{31}P{^{1}H} NMR** (162 MHz, Tol-d_8): δ –10.5 ppm. **^{13}C NMR** (101 MHz, $CDCl_3$): δ 138.5 (d, $J_{P\text{-}C}$ = 13.0 Hz), 133.2 (d, $J_{P\text{-}C}$ = 18.2 Hz), 128.4 (dd, $J_{P\text{-}C}$ = 9.3, 5.9 Hz), 59.0 (dd, $J_{P\text{-}C}$ = 9.2, 5.2 Hz). These signals are in agreement with those reported in the literature. [49]

Synthesis of (hydroxymethyl)dicyclohexyl phosphine 3.15b

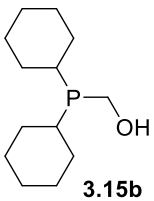

3.15b

General procedure A was followed employing dicyclohexyl phosphine (10 mmol) and paraformaldehyde (10 mmol). Compound **3.15b** was obtained as a clear liquid. Yield of **3.15b**: 2.28 g (100%); **^{1}H NMR** (400 MHz, $CDCl_3$): δ 4.01 (d, J_{H-P} = 6.5 Hz, 4H), 2.91 (bs, 1H), 1.99 – 1.52 (m, 11 H), 1.49 – 0.97 (m, 11 H). **^{31}P{^{1}H} NMR** (162 MHz, $CDCl_3$): δ -1.27.

General Procedure B:

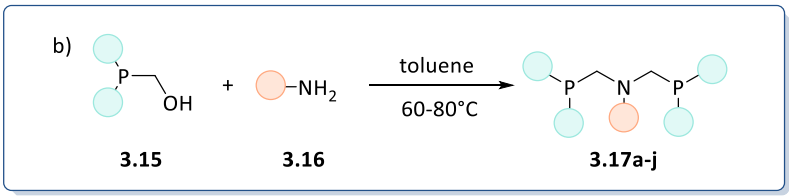

To an oven dried, argon purged, Schlenk tube containing the desired amine (1 equiv.) **3.16** in toluene (1 M), the previously synthesised compound **3.15** (2 equiv.) was added. The resulting mixture was stirred and heated from 60 °C to 80 °C for 24 hours. The mixture was then allowed to cool to room temperature, filtered over dried and neutralized silica, and then concentrated *in vacuo* to afford the desired phosphine nitrogen centred ligand **3.17a-j.**

Bidentate nitrogen centred phosphorus ligand (3.17a)

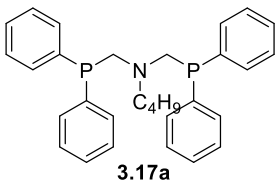

3.17a

General procedure B was followed employing *n*-butylamine (73 mg, 1 mmol) and (hydroxymethyl)diphenylphosphine (432 mg, 2 mmol). The reaction was heated at 60 °C. Compound **3.17a** (464 mg, 99%) was obtained as a colorless oil. Yield **3.17a**: 464 mg (99%). **^{1}H NMR** (400 MHz, $CDCl_3$): δ 7.44 – 7.38 (m, 8H), 7.29 – 7.24 (m, 12H), 3.56 (d, J_{H-P} = 2.9 Hz, 4H), 2.80 (dd, J_{H-H} = 22.8, 15.5 Hz, 2H), 1.39 – 1.30 (m, 2H), 1.20 – 1.10 (m, 2H), 0.80 (dt, J_{H-H} = 7.2 Hz, 3H). **^{31}P{^{1}H} NMR** (162 MHz, $CDCl_3$): δ –28.45. **^{13}C NMR** (101 MHz,

$CDCl_3$) δ 138.52 (d, J_{C-P} = 13.0 Hz), 133.24 (d, J_{C-P} = 18.2 Hz), 128.45 (m), 58.98 (dd, J_{C-P} = 9.2, 5.2 Hz), 56.26 (t, J_{C-P} = 9.1 Hz), 28.76 (s), 20.45 (s), 14.14 (s). **ESI-HRMS:** Calculated for $C_{30}H_{33}NP_2$. Exact: (M: 469.2088, M+H: 470.2167); Experimental: (M+H: 470.2171).

Bidentate nitrogen centred phosphorus ligand (3.17b)

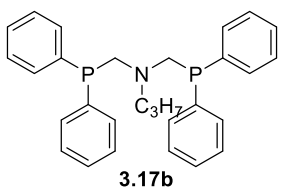

3.17b

General procedure B was followed employing propylamine (59 mg, 1 mmol) was added on a solution of (hydroxymethyl)diphenylphosphine (432 mg, 2 mmol). The reaction was heated at 60 °C. Compound **3.17b** (450 mg, 99%) was isolated as a colorless oil. Yield **3.17b**: 450 mg (99%);**^{1}H NMR** (400 MHz, $CDCl_3$): δ 7.44 – 7.38 (m, 8H), 7.29 – 7.24 (m, 12H), 3.56 (d, J_{H-P} = 2.9 Hz, 4H), 2.80 (dd, J_{H-H}= 22.8, 15.5 Hz, 2H), 1.47 – 1.35 (m, 2H), 0.80 (dt, J_{H-H} = 7.2 Hz, 3H). **^{31}P {^{1}H} NMR** (162 MHz, $CDCl_3$): δ –28.37. **^{13}C NMR** (101 MHz, $CDCl_3$): δ 138.39 (d, J_{C-P} = 13.0 Hz), 133.13 (d, J_{C-P} = 18.2 Hz), 128.35 (m), 58.84 (dd, J_{C-P} = 9.2, 5.1 Hz), 58.30 (t, J_{C-P} = 9.1 Hz), 19.72 (s), 11.62 (s). **ESI-HRMS:** Calculated for $C_{29}H_{31}NP_2$. Exact: (M: 455.1932, M+H: 456.2004); Experimental: (M+H: 456.2015).

Bidentate nitrogen centred phosphorus ligand (3.17c)

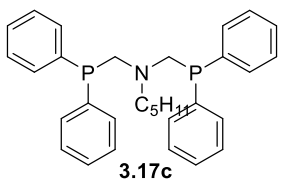

3.17c

General procedure B was followed employing amylamine (87 mg, 1 mmol) was added on a solution of (hydroxymethyl)diphenylphosphine (432 mg, 2 mmol). The reaction was heated at 60 °C. Compound **3.17c** (478 mg, 99%) was obtained as a colorless oil. Yield **3.17c**: 478 mg (99%). **^{1}H NMR** (400 MHz, $CDCl_3$): δ 7.44 – 7.38 (m, 8H), 7.29 – 7.24 (m, 12H), 3.56 (d, J_{H-P} = 2.9 Hz, 4H), 2.80 (dd, J_{H-H} = 22.8, 15.5 Hz, 2H), 1.36 (dt, J_{H-H} = 14.7, 7.4 Hz, 2H), 1.23 – 1.16 (m, 2H), 1.14 – 1.05 (m, 2H), 0.80 (dt, J_{H-H} = 7.2 Hz, 3H). **^{31}P{^{1} H} NMR** (162 MHz, $CDCl_3$): δ

−28.47. **^{13}C NMR** (101 MHz, $CDCl_3$): δ 138.52 (d, J_{C-P} = 13.0 Hz), 133.24 (d, J_{C-P} = 18.2 Hz), 128.45 (dd, J_{C-P} = 9.3, 5.9 Hz), 58.98 (dd, J_{C-P} = 9.2, 5.2 Hz), 56.26 (t, J_{C-P} = 9.1 Hz), 29.51 (s), 26.32 (s), 22.72 (s), 14.21 (s). **ESI-HRMS:** Calculated for $C_{31}H_{35}NP_2$. Exact: (M: 483.2245, M+H: 484.2317); Experimental: (M+H: 484.2312).

Bidentate nitrogen centred phosphorus ligand (3.17d)

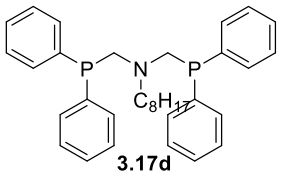

3.17d

General procedure B was followed employing octylamine (129 mg, 1 mmol) was added on a solution of (hydroxymethyl)diphenylphosphine (432 mg, 2 mmol). The reaction was heated at 60 °C. Compound **3.17d** (519 mg, 99%) was isolated as a colorless oil. Yield **3.17d**: 519 mg (99%); **^{1}H NMR** (400 MHz, $CDCl_3$): δ 7.44 – 7.38 (m, 8H), 7.29 – 7.24 (m, 12H), 3.56 (d, J_{H-P} = 2.9 Hz, 4H), 2.80 (dd, J_{H-H} = 22.8, 15.5 Hz, 2H), 1.40-1.07 (m, 12H), 0.80 (dt, J_{H-H} = 7.2 Hz, 3H). **^{31}P{^{1}H} NMR** (162 MHz, $CDCl_3$): δ −28.46. **^{13}C NMR** (101 MHz, $CDCl_3$) δ 138.4 (d, J_{C-P} = 13.1 Hz), 133.1 (d, J_{C-P} = 18.2 Hz), 128.5 – 128.2 (m), 58.8 (dd, J_{C-P} = 9.3, 5.2 Hz), 56.4 (t, J_{C-P} = 9.2 Hz), 31.8 (s), 29.5 (s, J_{C-P} = 20.2 Hz), 29.3 (s), 27.2 (s), 26.5 (s), 22.70 (s), 14.15 (s).**ESI-HRMS:** Calculated for $C_{34}H_{41}NP_2$. Exact: (M: 525.2714, M+H: 526.2787); Experimental: (M+H:526.2786).

Bidentate nitrogen centred phosphorus ligand (3.17e)

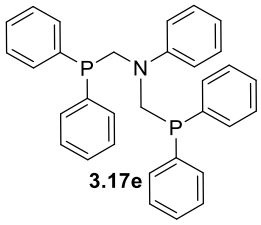

3.17e

General procedure B was followed employing aniline (93 mg, 1 mmol) was added on a solution of (hydroxymethyl)diphenylphosphine (432 mg, 2 mmol). The reaction was heated at 60 °C. Compound **3.17e** (400 mg, 82%) was obtained as a colorless oil. Yield **3.17e**: 400 mg (82%).**^{1}H NMR** (400 MHz, $CDCl_3$): δ 7.38 – 7.25 (m, 20H), 7.20 – 7.12 (m, 2H), 6.83 – 6.77 (m, 2H), 6.76 – 6.68 (m, 1H), 3.95 (d, J_{H-P} = 4.5 Hz, 4H). **^{31}P{^{1}H} NMR** (162 MHz, $CDCl_3$): δ -27.58 (s). **^{13}C NMR**

(101 MHz, $CDCl_3$): δ 148.02 (s), 137.45 (dt, J_{C-P} = 8.1, 3.4 Hz), 133.26 (dt, J_{C-P} = 11.0, 4.1 Hz), 117.54 (s), 114.64 (t, J_{C-P} = 2.9 Hz), 54.02 (q, J_{C-P} = 7.5 Hz). **ESI-HRMS:** Calculated for $C_{32}H_{29}NP_2$. Exact: (M: 489.1775, M+H: 490.1858); Experimental: (M+H:490.1854).

Bidentate nitrogen centred phosphorus ligand (3.17f)

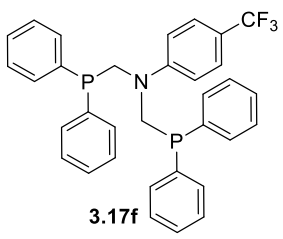

3.17f

General procedure B was followed employing *p*-CF_3-aniline (161 mg, 1 mmol) was added on a solution of (hydroxymethyl)diphenylphosphine (432 mg, 2 mmol). The reaction was heated at 80 °C. Compound **3.17f** (557 mg, 99%) was obtained as a colorless oil. Yield **3.17f**: 557 mg (99%). **^{1}H NMR** (400 MHz, CDCl3): δ 7.49 – 7.23 (m, 22H), 6.74 (d, J_{H-H} = 8.8 Hz, 2H), 3.88 (d, J_{H-P} = 4.8 Hz, 4H). **^{19}F NMR** (377 MHz, CDCl3) δ -61.01 (s). **^{31}P{^{1}H} NMR** (162 MHz, CDCl3): δ -27.90 (s). **^{13}C NMR** (101 MHz, $CDCl_3$): δ 149.93 (s), 136.92 (dt, J_{C-P} = 7.5, $J_{C-F=}$ 3.2 Hz), 133.54 – 133.21 (m), 129.27 (s), 128.88 – 128.72 (m), 126.35 (dd, J_{C-P} = 7.8, 3.8 Hz), 113.06 (t, J_{C-P} = 3.2 Hz), 53.56 (q, J_{C-P} = 6.4 Hz). **ESI-HRMS:** Calculated for $C_{33}H_{28}F_3NP_2$. Exact: (M: 557,1649, M+H: 558.1727); Experimental: (M+H: 558.1715).

Bidentate nitrogen centred phosphorus ligand (3.17g)

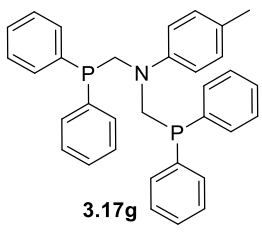

3.17g

General procedure B was followed employing *p*-me-aniline (107 mg, 1 mmol) was added on a solution of (hydroxymethyl)diphenylphosphine (432 mg, 2 mmol). The reaction was heated at 80 °C. Compound **3.17g** (432 mg, 86%) was obtained as a colorless oil. Yield **3.17g**: 432 mg (86%); **^{1}H NMR** (400 MHz, $CDCl_3$): δ 7.44 – 7.38 (m, 20H), 6.99 (d, J_{H-H}= 8.4 Hz, 2H), 6.74 (d, J_{H-H}= 8.4 Hz, 2H) 3.94 (d, J_{H-P} = 2.9 Hz, 4H), 2.24 (s, CH_3), **^{31}P{^{1}H} NMR** (162 MHz, $CDCl_3$): δ –27.27. **^{13}C NMR** (101 MHz, $CDCl_3$): δ 146.13 (s), 137.64 (dt, J_{C-P} = 7.6, 3.2 Hz), 133.73 –

132.69 (m), 129.58 (s), 128.75 (s), 128.60 – 128.31 (m), 115.48 (s), 54.66 (q, J_{C-P} = 7.6 Hz), 20.39 (s). **ESI-HRMS:** Calculated for $C_{32}H_{35}NP_2$. Exact: (M: 503.1923, M+H: 504.2004); Experimental: (M+H: 504.2015).

Bidentate nitrogen centred phosphorus ligand (3.17h)

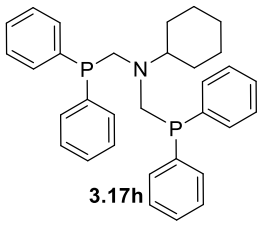

3.17h

General procedure B was followed employing cyclohexylamine (99 mg, 1 mmol) was added on a solution of (hydroxymethyl)diphenylphosphine (432 mg, 2 mmol). The reaction was heated at 60 °C. Compound **3.17h** (459 mg, 99%) was obtained as a white solid. Yield **3.17h**: 449 mg (99%). **^{1}H NMR** (401 MHz, $CDCl_3$): δ 7.47 – 7.35 (m, 8H), 7.33 – 7.20 (m, 12H), 3.56 (d, J_{H-P} = 3.3 Hz, 4H), 3.03 (s, 1H), 1.65-1.46 (m, 5H) 1.21 – 0.87 (m, 5H). **^{31}P{^{1}H} NMR** (162 MHz, $CDCl_3$): δ −26.43. **^{13}C NMR** (101 MHz, $CDCl_3$): δ 138.41 (d, J_{C-P} = 13.2 Hz), 133.26 (d, J_{C-P} = 18.8 Hz), 128.40 (s), 128.32 – 128.12 (m), 60.77 (t, J_{C-P} = 7.9 Hz), 54.69 (d, *J* = 6.1 Hz), 28.61 (s), 26.28 (s), 25.95 (s). **ESI-HRMS:** Calculated for $C_{32}H_{35}NP_2$. Exact: (M: 495.2245, M+H: 496.2323); Experimental: (M+H: 496.2325).

Bidentate nitrogen centred phosphorus ligand (3.17i)

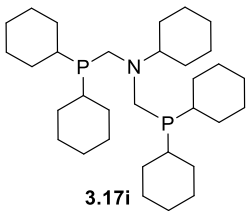

3.17i

General procedure B was followed employing cyclohexylamine (99 mg, 1 mmol) was added on a solution of (hydroxymethyl)dicyclohexylphosphine (507 mg, 2 mmol). The reaction was heated at 60 °C. Compound **3.17i** (518 mg, 99%) was obtained as a white solid. Yield **3.17i**: 518 mg (99%);**^{1}H NMR** (401 MHz, $CDCl_3$): δ 3.26 (m, 1H), 2.79 (s), 1.72 (m, 33H), 1.23 (m, 37H). **^{31}P{^{1}H} NMR** (162 MHz, $CDCl_3$): δ -17.55 (s). **^{13}C NMR** (101 MHz, $CDCl_3$): δ 58.66 (t, *J* = 9.7 Hz), 47.83 – 47.69 (m), 32.72 (d, J_{C-P} = 12.9 Hz), 29.77 (dd, J_{C-P} = 10.9, 9.2 Hz), 27.63 – 27.24

(m), 27.09 (s), 26.63 (s), 26.07 (s). **ESI-HRMS:** Calculated for $C_{32}H_{59}NP_2$. Exact: (M: 519.4123, M+H: 520.4196); Experimental: (M+H: 520.4187).

Bidentate nitrogen centred phosphorus ligand (3.17j)

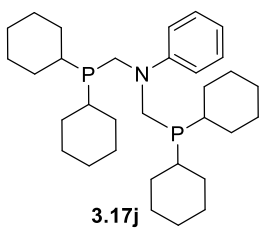

3.17j

General procedure B was followed employing aniline (93 mg, 1 mmol) was added on a solution of (hydroxymethyl)dicyclohexylphosphine (507 mg, 2 mmol). The reaction was heated at 60 °C. Compound **3.17j** (513 mg, 99%) was obtained as a white solid. Yield **3.17j**: 513 mg (99%). **^{1}H NMR** (400 MHz, $CDCl_3$): δ 7.22 – 7.16 (m, 2H), 6.89 (d, J_{H-H} = 7.9 Hz, 2H), 6.72 (t, J_{H-H} = 7.3 Hz, 1H), 3.72 (d, J_{H-P} = 1.5 Hz, 4H), 1.70 (d, J_{H-H} = 31.4 Hz, 21H), 1.26 – 1.14 (m, 23H). **^{31}P{^{1}H} NMR** (162 MHz, $CDCl_3$): δ –15.53. **^{13}C NMR** (101 MHz, $CDCl_3$): δ 150.29 (s), 128.72 (s), 117.42 (s), 112.69 (s), 47.79 (dd, J_{C-P} = 14.0, 8.9 Hz), 32.89 (d, J_{C-P} = 14.5 Hz), 29.84 (dd, J_{C-P} = 10.8, 8.8 Hz), 27.37 (d, J_{C-P} = 8.9 Hz), 26.50 (s). **ESI-HRMS:** Calculated for $C_{32}H_{53}NP_2$. Exact: (M: 513,3657, M+H: 513,3653); Experimental: (M+H: 514.3730).

Bidentate nitrogen centred phosphorus ligand (3.17k)

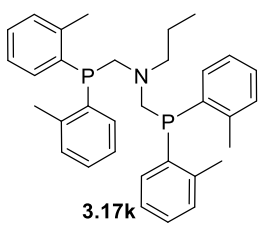

3.17k

General procedure B was followed employing aniline (93 mg, 1 mmol) was added on a solution of (hydroxymethyl)di-*o*-tolylphosphine (507 mg, 2 mmol). The reaction was heated at 80°C. Compound **3.17k** (327 mg, 99%) was isolated as a white solid. Yield **2.17k**: 327 mg (99%). **^{1}H NMR** (400 MHz, $CDCl_3$): δ 7.30 – 6.96 (m, 16H), 3.38 (t, J_{H-P} = 5.2 Hz, 4H), 2.87 – 2.81 (m, 2H), 2.36 (d, J_{H-H} = 5.6 Hz, 12H), 1.58 – 1.41 (m, 2H), 0.84 – 0.74 (m, 3H). **^{31}P{^{1}H} NMR** (162 MHz, $CDCl_3$): δ –47.39. **^{13}C NMR** (101 MHz, $CDCl_3$): δ 142.31 (s), 142.06 (s), 136.52 (d, J_{C-P} = 13.2 Hz), 132.11 (s), 129.95 (d, J_{C-P} = 4.8 Hz), 129.18 (s), 128.38 (s), 125.98 (s), 58.29 (t, J_{C-P} = 9.0 Hz), 56.55 (dd, J_{C-P} = 9.1, 3.2 Hz), 21.46 (d, J_{C-}

$_P$ = 20.8 Hz), 18.99 – 18.95 (m), 11.84 – 11.82 (m). **ESI-HRMS:** Calculated for C_{33} H_{39} N P_2. Exact: (M: 511,2558, [M+H^+]: 512,2630); Experimental: (M+H^+:512,2629).

3.5.3 In situ HP-NMR experiments

In a typical experiment, a sapphire tube (Ø = 5 mm) was filled under nitrogen atmosphere with a solution of the rhodium precursor Rh(acac)$(CO)_2$ and the ligand **3.17** in a ratio Rh/L = 1:1.1 in a total volume of 0.4 mL. The HP-NMR tube was purged CO, pressurized to the appropriate pressure of H_2/CO, heated if required, and left shaking. After that, the solution was analysed by NMR spectroscopy.

3.6 References

[1] G. Bauer and X. Hu, *Inorg. Chem. Front.*, **2016**, *3*, 741-765.

[2] Z. Lu, C. White, A.L. Rheingold and R.H. Crabtree, *Inorg. Chem.*, **1993**, *32*, 3991-3994.

[3] J.M. Vila, M. Teresa Pereira, J.M. Ortigueira, M. Grana, D. Lata, A. Suarez, J.J. Fernandez, A. Fernandez, M. Lopez-Torres and H. Adams, *J. Chem. Soc., Dalton Trans.,* **1999**, 4193-4201.

[4] L. Wang, H.-R. Pan, Q. Yang, H.-Y. Fu, H. Chen and R.-X. Li, *Inorg. Chem. Comm.*,**2011**, *14*, 1422-1427.

[5] M.A.W. Lawrence, Y.A. Jackson, W.H. Mulder, P.M. Björemark and M. Håkansson, *Aust. J. Chem.,* **2015**, *68*, 731-741.

[6] M. Bakir, M.A.W. Lawrence and M. Singh-Wilmot, *J. Coord. Chem.*, **2007**, *60*, 2385-2399.

[7] K. Arashiba, Y. Miyake and Y. Nishibayashi, *Nat. Chem.*, **2011**, *3*, 120-125.

[8] E. Peris, J.A. Loch, J. Mata and R.H. Crabtree, *Chem. Commun.*, **2001**, 201-202.

[9] T. Teratani, T.-A. Koizumi, T. Yamamoto, K. Tanakab and T. Kanbara, *Dalton Trans.*, **2011**, *40*, 8879-8886.

[10] B.J. Charette and J.S. Ritch, *Inorg. Chem.*, **2016**, *55*, 6344-6350.

[11] D. Benito-Garagorri and K. Kirchner, *Acc. Chem. Res.*, **2008**, *41*, 201-213.

[12] C.M. Jensen, *Chem. Commun.*, **1999**, 2443-2449.

[13] R.B. Bedford, S.M. Draper, P. Noelle Scully and S.L. Welch, *New J. Chem.*, **2000**, *24*, 745-747.

[14] W. Leis, H.A. Mayer and W.C. Kaska, *Coord. Chem. Rev.*, **2008**, *252*, 1787–1797.

[15] M.R. Eberhard, *Org. Lett.*, **2004**, *6*, 2125-2128.

[16] I. Moreno, R. SanMartin, B. Inés, F. Churruca and E. Domínguez, *Inorg. Chim. Acta*, **2010**, *363*, 1903-1911.

[17] D. Morales-Morales, C. Grause, K. Kasaoka, R.O. Redón, R.E. Cramer and C.M. Jensen, *Inorg. Chim. Acta*, **2000**, *300-302*, 958-963.

[18] D. Morales-Morales, R.O. Redón, C. Yung and C.M. Jensen, *Inorg. Chim. Acta*, **2004**, *357*, 2953-2956.

[19] D. Morales-Morales, R. Redon, C. Yung and C.M. Jensen, *Chem. Commun.*, **2000**, 1619-1620.

[20] M. Albrecht and G. van Koten, *Angew. Chem., Int. Ed.*, **2001**, *40*, 3750-3781.

[21] A. Sundermann, O. Uzan, D. Milstein and J.M.L. Martin, *J. Am. Chem. Soc.*, **2000**, *122*, 7095-7104.

[22] F. Churruca, R. SanMartin, I. Tellitu, E. Domínguez, *Tetrahedron Lett.*, **2006**, *47*, 3233-3237.

[23] a) D.W. Lee, C.M. Jensen and D. Morales-Morales, *Organometallics*, **2003**, *22*, 4744-4749, b) R. Tanaka, M. Yamashita and K. Nozaki, J. *Am. Chem. Soc.,* **2009**, *131*, 14168-14169.

[24] P. W. N. M. Van Leeuwen, C. Claver and Editors*, Rhodium Catalyzed Hydroformylation*. [In: Catal. Met. Complexes, **2000**; 22], Kluwer, **2000**.

[25] T. J. Devon, G. W. Phillips, T. A. Puckette, J. L. Stavinoha and J. J. Vanderbilt, *U.S. Patent*, 694, 109, **1987**.

[26] C. P. Casey, G. T. Whiteker, M. G. Melville, L. M. Petrovich, J. Gamey and D. R. Powell, *J. Am. Chem. Soc.,* **1992**, *114*, 5535-5543.

[27] M. Kranenburg, Y. E. M. van der Burgt, P. C. J. Kamer, P. W. N. M. Van Leeuwen, K. Goubitz, and J. Fraanje, *Organometallics*, **1995**, *14*, 3081-3089.

[28] G. M. Noonan, J. A. Fuentes, C. J. Cobley and M. L. Clarke*, Angew. Chem. Int. Ed.,* **2012**, *51*, 2477-2480.

[29] A. Phanopoulos and K. Nozaki, *ACS Catal.* **2018**, *8*, 579-5809.

[30] V. F. Slagt, M. Roeder, P. C. J. Kamer, P. W. N. M. Van Leeuwen and J. N. H. Reek, J. *Am. Chem. Soc.,* **2004**, *126*, 4056-4057.

[31] A. Phanopoulos, A. J. P. White, N. J. Long and P. W. Miller, *Dalton Trans.* **2016**, *45*, 5536-5548.

[32] (a) J. D. Unruh and J. R. A, Christenson, *J. Mol. Catal.,* **1982**, *14*, 19-34. (b) W. R. Moser, C. J. Papile, D. A. Brannon, R. A. Duwell and S. J. Weininger, *J. Mol. Catal.*, **1987**, *41*, 271-292.

[33] L. A. Van der Veen, M. D. K. Boele, F. R. Bregman, P. C. J. Kamer, P. W. N. M. van Leeuwen, K. Goubitz, J. Fraanje, H. Schenk and C. Bo, *J. Am. Chem. Soc.* **1998**, *120*, 11616-11626.

[34] C. P. Casey, E. L. Paulsen, E. W. Beuttenmueller, B. R. Proft, L. M. Petrovich, B. A. Matter, D. R. Powell, *J. Am. Chem. Soc.,* **1997**, *119*, 11817-11825.

[35] M. Kranenburg, Y. E. M. van der Burgt, P. C. J. Kamer and P. W. N. M. van Leeuwen, *Organometallics*, **1995**, *14*, 3081-3089.

[36] Z. Freixa and P. W. N. M. van Leeuwen, *Dalton Trans.*, **2003**, 1890–1901.

[37] E. S. Wiedner, M. B. Chambers, C. L. Pitman, R. M. Bullock, A. J. M. Miller and A. M. Appel, *Chem. Rev.* **2016**, *116*, 8655-8692.

[38] M. R. Axet, S. Castillon and C. Claver, *Inorg. Chim. Acta*, **2006**, *359*, 2973-2979.

[39] F. Kuhl, S. Blaurock, J. Sieler and E. Hey-Hawkins, *Polyhedron*, **2001**, *20*, 2171-2177.

[40] C. Klemps, E. Payet, L. Magna, L. Saussine, L. X. Le Goff and P. Le Floch *Chem Eur. J.*, **2009**, *15*, 8259-8268.

[41] a) J. M. Brown and A. G. Kent, *J. Chem. Soc., Perkin Trans. II,* **1987**, 1597. b) C. P. Casey, G. T. Whiteker, M. G. Melville, L. M. Petrovich, J. A. Jr. Gavney and D. R. Powell, *J. Am. Chem. Soc.,* **1992**, *114*, 5535-5543.

[42] a) R. S. Berry, *J. Chem. Phys.*, **1960**, *32*, 933. b) P. Meakin and E. L. Muetterties, *J. Am. Chem. Soc.*, **1972**, *94*, 5271-5285.

[43] P. Meakin, J. P. Jesson, F. N. Tebbe and E. L. Muetterties, *J. Am. Chem. Soc.*, **1971**, *93*, 1797-1799.

[44] b) M. Kranenburg, *New diphosphine ligands with large natural bite angles. Ph.D. Thesis*, Van't Hoff Research Institute, University of Amsterdam, The Netherlands, **1996**.

[45] a) G. J. H. Buisman, *Asymmetric hydroformylation with chiral diphosphite ligands. Ph.D. Thesis*, Van't Hoff Research Institute, University of Amsterdam, The Netherlands, **1995**. b) A. van Rooy, *Rhodium catalysed hydroformylation with bulky phosphites as modifying ligands. Ph.D. Thesis,* Van't Hoff Research Institute, University of Amsterdam, The Netherlands, **1995**.

[46]A) P. Meakin, E. L. Muetterties, J. P. Jesson, *J. Am. Chem. Soc.* **1972**, 94, 5271. (b) E. M. Hyde, J. R. Swain, J. G. Verkade, P. Meakin, *J. Chem. Soc., Dalton Trans.* **1976**, 1169-1175.

[47] B. Heaton, *Mechanisms in Homogeneous Catalysis*, Eds. Wiley-VCH, Darmstadt, Germany, **2005**.

[48] G. J. H. Buisman, L. A. van der Veen, P. C. J. Kamer and P. W. N. M. van Leeuwen, *Organometallics*, **1997**, *16*, 5681-5687.

[49] O. Kuhl, S. Blaurock , J. Sieler and E. Hey-Hawkins, *Polyhedron*, **2001**, *17*, 2171-2177.

Chapter IV

Rhodium catalysed hydroformylation of 1-octene with phosphine-phosphite and phosphine-phosphoramidite ligands

Rhodium and Palladium Catalysed Unusual Regioselective Hydroformylation and Rhodium Catalysed Reductive Carbonylation

Benedetta Palucci

4.1 Introduction

4.1.1 Phosphine-phosphite ligands and phosphine-phosphoramidite ligands

While bidentate diphosphine and diphosphite ligands have been widely employed in the rhodium catalysed hydroformylation of alkenes, the use of combined phosphine-phosphite ligand was developed more recently.[1] In 1993, Takaya *et al.* reported that the combination of phosphite and phosphine moieties leads to a higher stability and selectivity in the hydroformylation of styrene derivatives.[2] In particular, the chiral phosphine-phosphite ligands BINAPHOS (structures **4.4a-d**, Scheme 4.1), constituted a breakthrough in the field of rhodium catalysed asymmetric hydroformylation.[2] The Rh(I) complex of C_1-symmetric (R,S)-BINAPHOS **4.4a** provided much higher enantioselectivity than either C_2 symmetric diphosphine ligands or diphosphite ligands, for a wide variety of both functionalized and internal alkenes.[2]

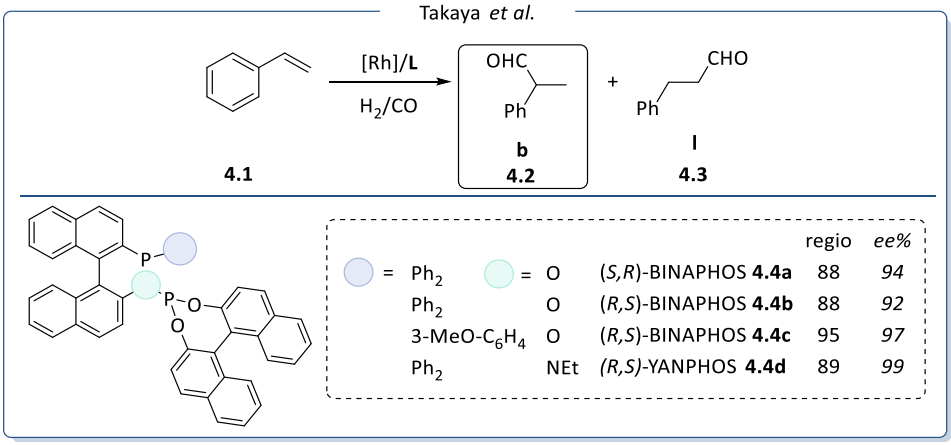

Scheme 4.1. BINAPHOS family of ligands **4.4a, 4.4b, 4.4c** and **4.4d**.

The BINAPHOS derivative ligand **4.4c**, with a variation on the aryl group of the phosphine moiety, provided excellent selectivity for various vinyl arenes

(up to 97% ee)[3] while the (*R*,*S*)-YANPHOS ligand **4.4d**, containing a phosphoramidite moiety instead of a phosphite, afforded good regioselectivities (up to 89%) and excellent *ee* (up to 99%).[4] Moreover, the ligand **4.4d**, was used in the asymmetric hydroformylation of *N*-allylamides (up to 96% ee).[5] Albeit the excellent results for substrates such as styrene derivatives and *N*-allylamides, the intrinsic issue in the regioselective hydroformylation of terminal alkyl olefins limits the pool of suitable substrates for this reaction. Indeed, in the case of terminal alkyl olefins, a marked preference for the formation of the linear product over the branched one has been observed, albeit with good control over the enantioselectivity, when BINAPHOS ligand **4.4b** was employed (Scheme 4.2).[6]

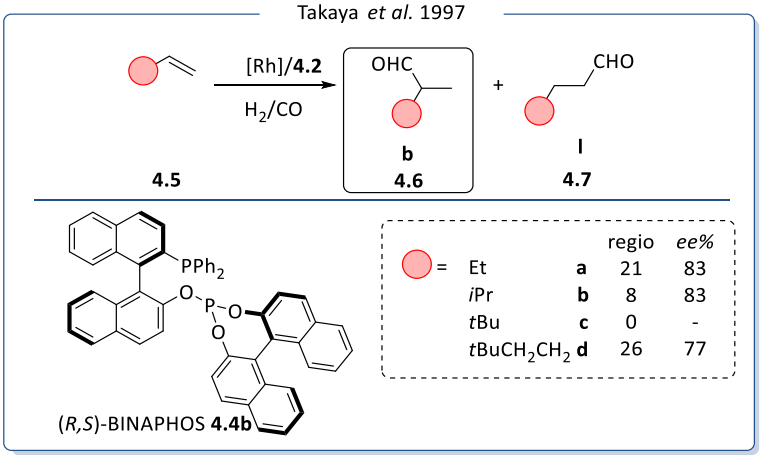

Scheme 4.2. BINAPHOS **4.4b** in hydroformylation of family of terminal alkyl olefins.

Despite this issue, methods able to selectively obtain the branched hydroformylated products have been reported and will be detailed in the next section.

4.1.2 Rh-catalysed hydroformylation of 1-alkenes with phosphine-phosphite ligands towards branched selectivity

Until very recently, only a few catalytic systems able to efficiently catalyse the hydroformylation of nonactivated terminal alkenes towards the branched aldehyde were reported.[7,8,9] All these examples involve the use of rhodium as the metal catalyst. Branched aldehyde products are increasingly desired due to their use in the fragrance, flavour, and life-sciences industries. However, to achieve branched-selective hydroformylation is challenging. Originally, the best selectivity could only be obtained at low temperatures (*e.g.* 19 °C).[10] It is worth to mention that Reek *et al.* achieved the hydroformylation of propene with good levels of branched selectivity (ca. 50%) at 70 °C employing a rhodium encapsulation complex.[10,11] Recently Nozaki and co-workers reported the use of nitrogen centred tri-phosphine ligands in the Rh hydroformylation of terminal olefins. The aza-triphos ligand provided a b/l ratio of 2.06 at 25 °C under 10 bar of syngas (CO/H_2, 1:4), when 1-hexene was used as substrate.[9] Clarke *et al.* have reported excellent branched selectivity in the hydroformylation of a range of olefins using a catalyst derived from the phosphite-phospholane bidentate ligand, BOBPHOS (**4.11**, Scheme 4.1).[7] This pioneering work was the first example of enantioselective hydroformylation of unfunctionalized olefins. Low temperature (15 °C) and 5 bar of 1:1 CO/H_2 are required to obtain, in the case of 1-hexene, 75% branched selectivity and 93% of enantioselectivity. In addition, Clarke *et al.* have applied this system in the hydroformylation of allylglycine derivatives which give chiral intermediates of industrial importance for new antibiotics.[12] The origin of the branched selectivity produced from the Rh/BOBPHOS system **4.11** has been investigated in details.[13,14] It was concluded that the combinations of the rigid structure of Rh/BOBPHOS catalyst **4.11**, and the attractive interactions during an early stage in C–H bond formation, forbid

the formation of a linear Rh-alkyl species, favouring the formation of the branched product.

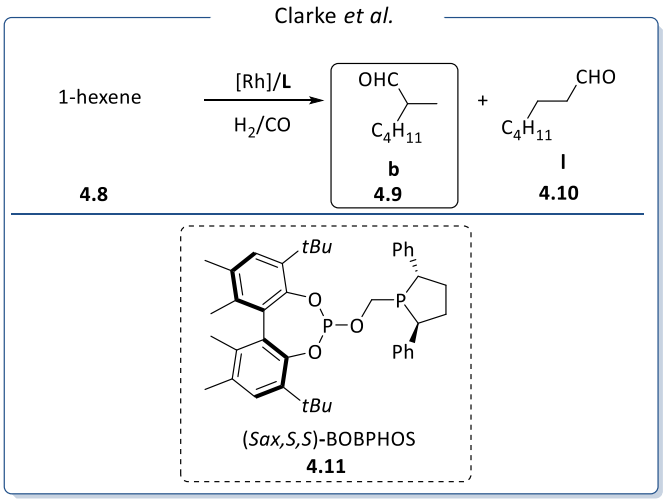

Scheme 4.3. Rhodium catalysed hydroformylation of 1-hexene using (*Sax,S,S*)-BOBPHOS ligand **4.11**. Reaction condition: [Rh(acac)(CO)2] (0.4 mol%), Ligand (0.5 mol%), Ligand/Rh (1.1), 1-hexene (1 mmol), 1-hexene/Rh (250), CO/H_2 (1:1, 5 bar), Solvent (2 ml).

In 2019, unprecedent high branched selectivity (82%) in the hydroformylation of propene was obtained using the *tropos,rac*-ligand/Rh catalyst (Scheme 4.4, **4.18** and **4.19**). The authors demonstrated that the *tropos* ligand, when coordinated to the Rh complex, performs like a single enantiomer during catalysis. The use of an unusual solvent such as octafluorotoluene, was also crucial to the selectivity observed and relatively high temperatures were used to achieve fast conversion.[15,16,17]

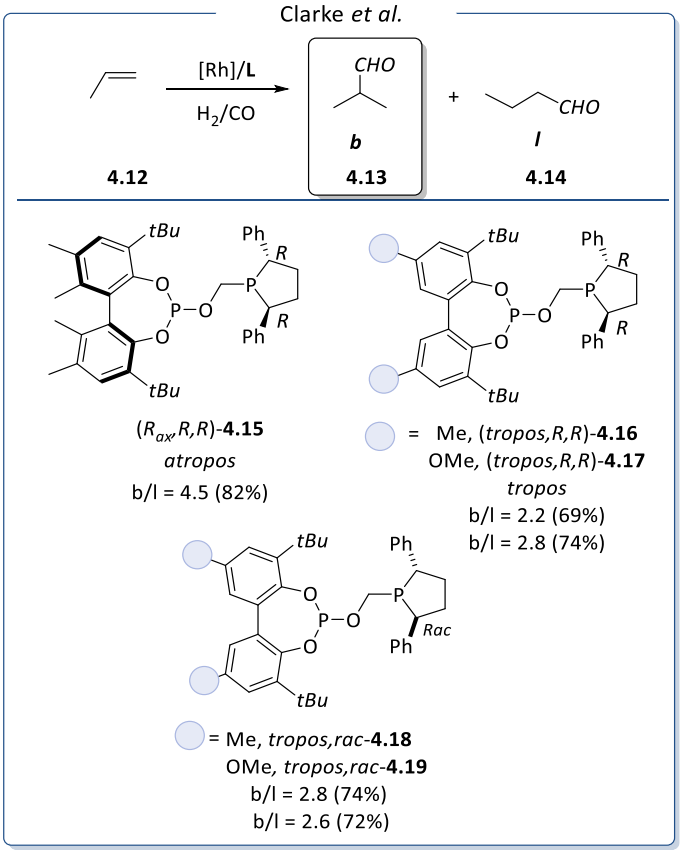

Scheme 4.4. Rh-catalysed hydroformylation of propene using *tropos* ligand. Reaction conditions: [Rh(acac)(CO)2] (5.12 x $^{10-3}$ mmol), Ligand (6.40 and 10.24 μmol), Ligand/Rh (1.2 and 2.0), propene/CO/H_2 in 1:4.5:4.5 ratio (20 bar initial pressure), CO/H_2 (1:1, 20 bar), Solvent (19.35 mL).

However, for the authors, there is not enough data to make any correlation between axial:equatorial coordination mode and selectivity.

This prompted us to study a family of ligands and investigate their coordination modes. Our objective was to understand how ligand structure could control the selectivity for bis-equatorial *vs*. axial:equatorial isomers and whether the isomer formed has any implication on rate, selectivity, stability or activation times in hydroformylation catalysis.

4.2 Objectives

The main objective of this chapter is the development of a family of phosphine-phosphite and phosphine-phosphoramidite ligands and their application in the rhodium catalysed hydroformylation of 1-octene, aiming at the selective formation of the branched aldehyde.

The specific objectives of this chapter are:

- The development of a protocol for the synthesis of phosphine-phosphite and phosphine-phosphoramidite ligands.
- The application of the new phosphine-phosphite and phosphine-phosphoramidite ligands in the hydroformylation of 1-octene.
- The study of the reactivity towards H_2/CO of the rhodium precursors in the presence of phosphine-phosphite ligand using HP-NMR spectroscopy.

4.3 Results and discussion

4.3.1 Synthesis of phosphine-phosphite and phosphine-phosphoramidite ligands

Inspired by the ligand structure of the BOBPHOS ligand **4.11**, it was thought that variations over the backbone structure (Figure 4.1) could provide interesting results in the hydroformylation reaction. We also aimed at determining a correlation between the nature of the substituents and the selectivity to the branched aldehyde in the Rh-catalysed hydroformylation of 1-octene.[7]

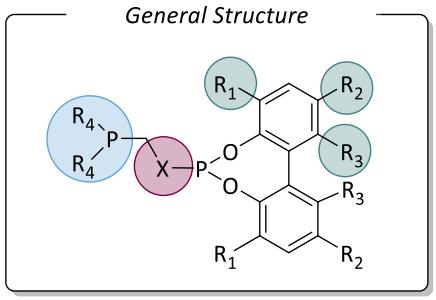

Figure 4.1. General structure of the ligands to be prepared in this chapter.

The novel phosphine-phosphite ligands proposed were readily accessed in three steps (Scheme 4.5):

- A first step where the hydroxyphosphine fragment **4.22** is obtained by condensation between phosphine **4.20** and paraformaldehyde **4.21** under neat conditions.[18]
- In parallel, reaction between biphenol **4.23** and PCl_3 in the presence of triethylamine affords phosphochloridite **4.24**.
- Finally, a nucleophilic substitution between **4.24** with the desired hydroxymethylphosphine fragment **4.22**, delivered the desired ligand.[19]

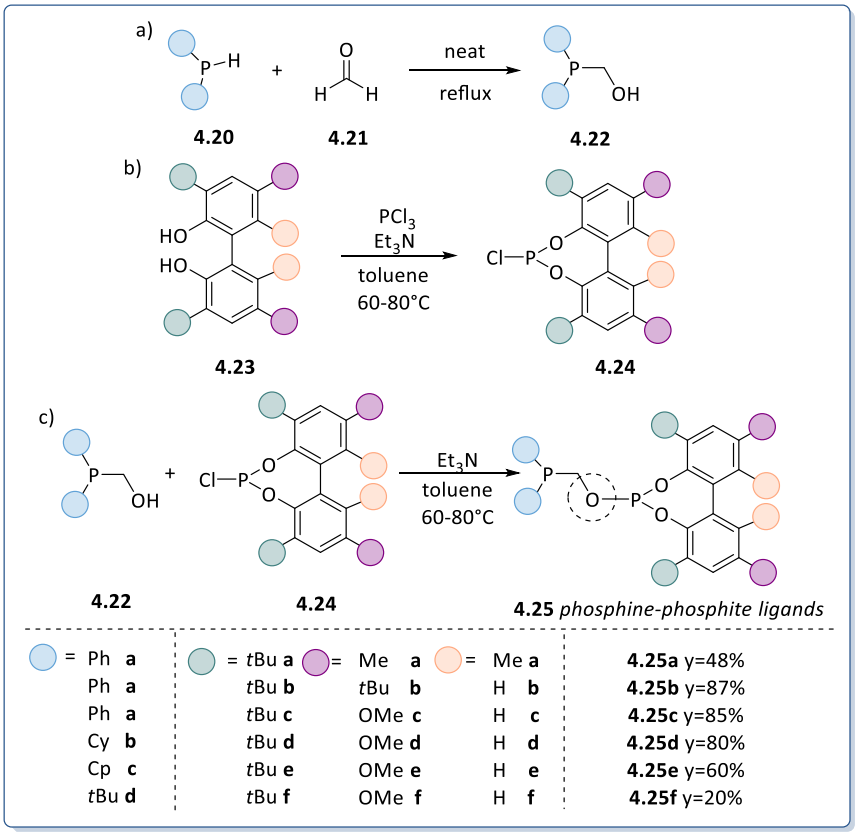

Scheme 4.5. Synthesis of phosphine-phosphite ligands **4.31a-f.**

The procedures were monitored by ^{31}P NMR spectroscopy. As an example, the synthesis of phosphine-phosphite ligand **4.25d** will be detailed in the following section. In the $^{31}P\{^{1}H\}$ NMR spectrum, the hydroxymethylphosphine fragments **4.22b** displayed one singlet at -1.27 ppm (Figure 4.2, a). At the same time, the diagnostic peak for the phosphochloridite **4.24d** in the $^{31}P\{^{1}H\}$ NMR spectrum consisted of a singlet centred at 172.30 ppm (Figure 4.2, b). When the hydroxymethylphosphine fragments **4.22a** was reacted with phosphochloridite **4.24d,** the phosphine-phosphite **4.25d** is formed. The ^{31}P NMR spectrum of the latter showed two characteristic singlets for both the phosphine (-2.91 ppm) and phosphite (135.93 ppm) part (Figure 4.2, c). This change in the $^{31}P\{^{1}H\}$ NMR spectrum

is in agreement with the selective formation of the desired phosphine-phosphite ligand **4.25d**.

This protocol afforded the phosphine-phosphite ligands **4.25a-f** in excellent yields employing commercially available precursors and following a simple procedure. The newly synthesised ligands **4.25a-f** were characterised by ^{1}H NMR, ^{31}P NMR and ^{13}C NMR spectroscopy and MS spectrometry.

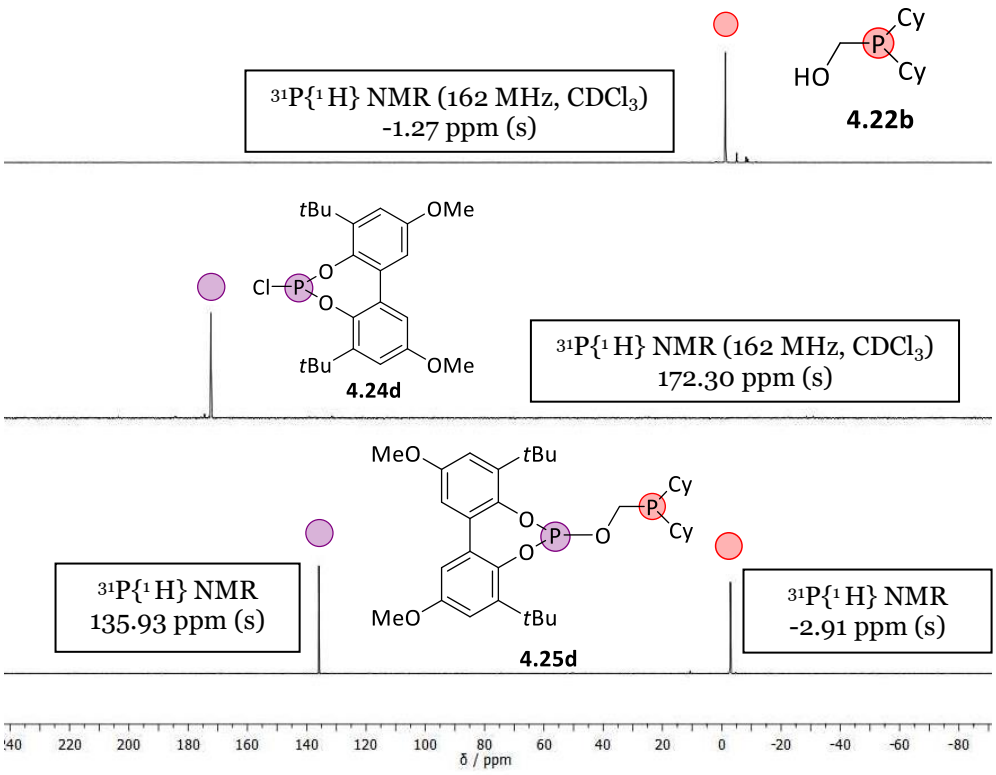

Figure 4.2. Selected ^{31}P{^{1}H} spectra for the synthesis of ligand **4.25d**: a) ^{31}P{^{1}H} NMR spectrum of the hydroxyphosphine fragments **4.22b**. b) ^{31}P{^{1}H} NMR spectrum of phosphochloridite **4.24d**. b) ^{31}P{^{1}H} NMR spectrum of the ligand **4.25d**.

In the same manner, the new phosphine-phosphoramidite compounds **4.27** were readily synthesized with a two-step synthesis (Scheme 4.6). A nucleophilic substitution between phosphochloridite intermediate **4.24d** with the desired commercial amine **4.26**, delivered the desired ligands. [19]

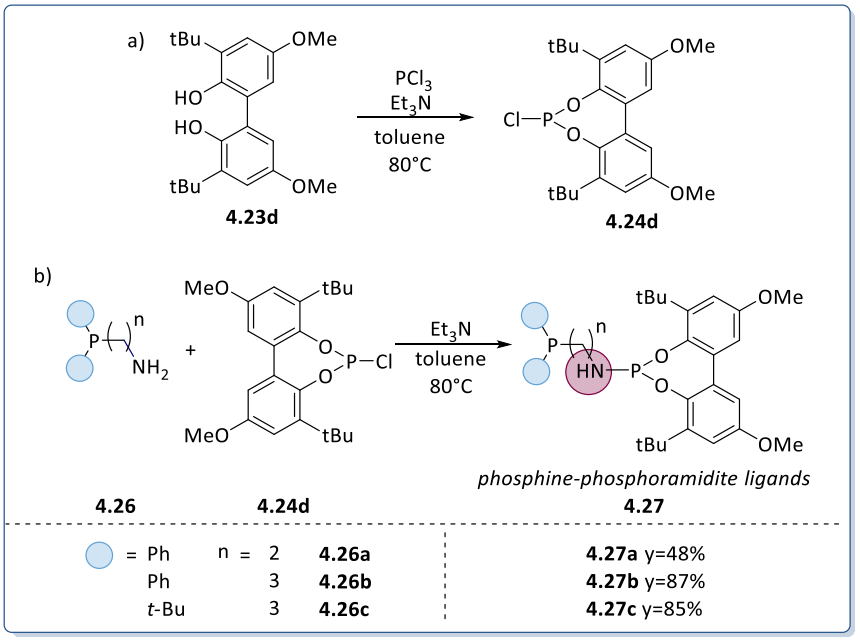

Scheme 4.6. Synthesis of phosphine-phosphoramidite ligands **4.27a-c.**

The two-step procedure was monitored by ^{31}P NMR spectroscopy. When the phosphochloridite **4.24d** was reacted with the selected commercial amine **4.26c**, two signals were detected by ^{31}P NMR (Figure 4.3, c). These signals were attributed to the phosphine moiety, at 19.90 ppm, and the phosphoramidite fragment, at 145.45 ppm. These signals, shown in the $^{31}P\{^{1}H\}$ NMR spectrum, are in agreement with the selective formation of the desired phosphine-phosphoramidite ligand **4.27d**.

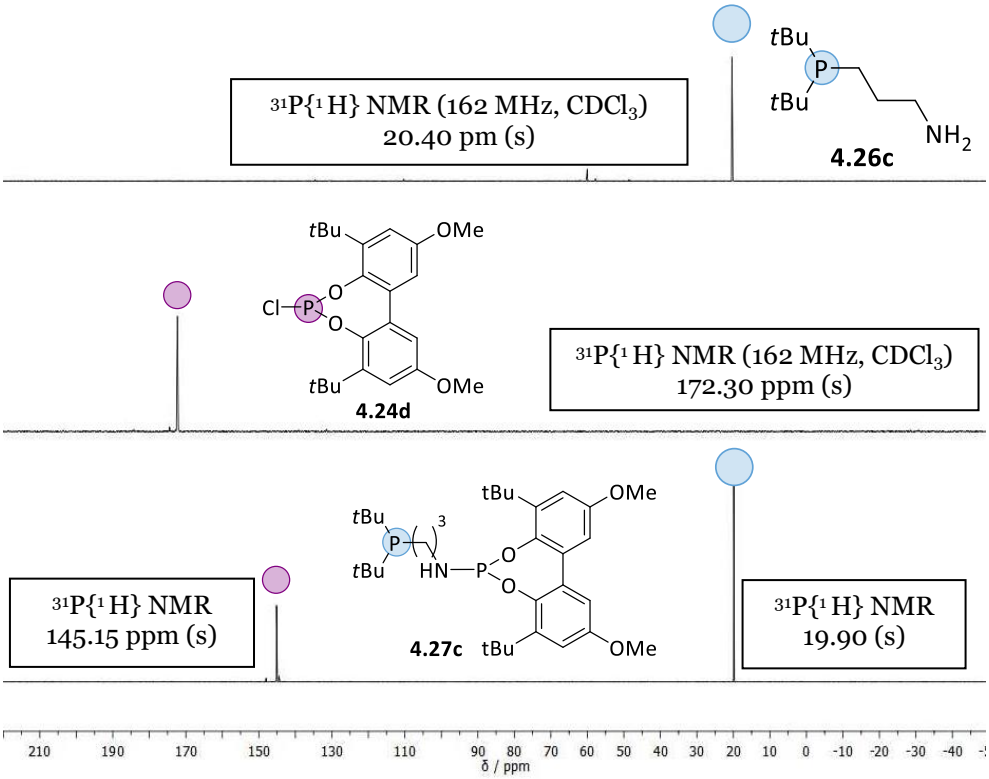

Figure 4.3. Selected $^{31}P\{^{1}H\}$ spectra for the synthesis of ligand **4.27c**: a) $^{31}P\{^{1}H\}$ NMR spectrum of the commercial **4.26c**. b) $^{31}P\{^{1}H\}$ NMR spectrum of the phosphochloridite **4.24d**. b) $^{31}P\{^{1}H\}$ NMR spectrum of ligand **4.27c.**

For these derivatives, the synthesis proceeded smoothly to afford the phosphine-phosphoramidite ligands **4.27a-c** in good yields employing commercially available precursors (Scheme 4.6). The newly synthesised ligands **4.27a-c** were characterised by ^{1}H NMR, ^{31}P NMR and ^{13}C NMR spectroscopy and MS spectrometry.

We also attempted in the synthesis of phosphine-phosphoramidite ligands with a spacer between the phosphorus and the nitrogen atoms, consisting of a simple methylene bridge following a reported procedure (**4.29**, Scheme 4.7), as proposed in the general structure of the ligand (Figure 4.1), inspired by BOBPHOS **4.11**. [20]

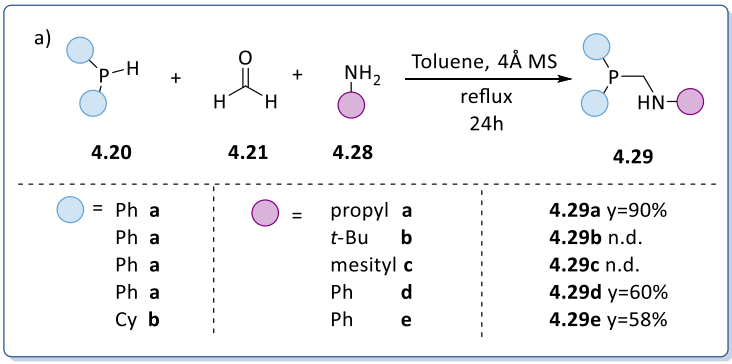

Scheme 4.7. Synthesis of aminophosphine fragments **4.29a-e.**

For this one-step procedure, some limitations were observed in the case of sterically hindered amines as starting materials, indeed when *tert*-butyl and mesityl amines were used, the reaction product was not detected.[20]

Next, the amino-phosphine compounds previously synthesized were used in the synthesis of the phosphine-phosphoroamidite ligand **4.30**. The first attempts were performed using fragment **4.29a** (Scheme 4.8).

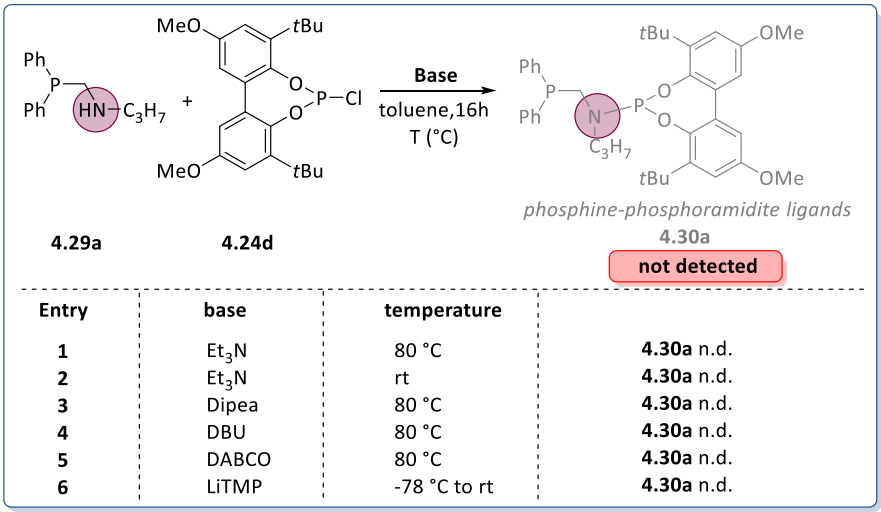

Scheme 4.8. Synthesis attempts of phosphine-phosphoramidite ligands **4.38a.**

Initially, the reaction between fragments **4.29a** and **4.24d** was conducted in the presence of Et_3N, based on conditions reported for other phosphoramidite ligands.[19] When the reaction was carried out at 80 °C (Entry

1), the formation of several by-products was observed by ^{31}P NMR analysis. The main by-product was readily identified as the bidentate phosphorus-nitrogen-centred ligand **4.31**, which was also isolated (Scheme 4.9).

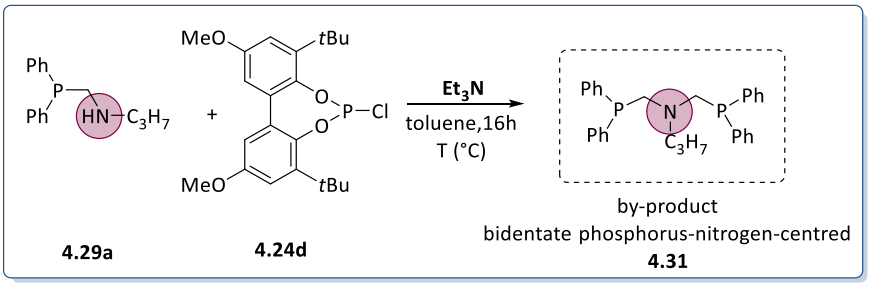

Scheme 4.9. By-product from the attempt of synthesis of the phosphine-phosphoramidite ligand.

However, through ^{31}P NMR analysis, we observed the formation of the desired product in traces amount. In order to obtain **4.30** selectively, a screening of reaction conditions was performed in order to avoid the formation of the disphosphine nitrogen centred ligand **4.31**. When the reaction temperature was lowered to room temperature (Scheme 4.8, Entry 2), lower conversion was obtained (10%) and the formation of **4.31** was once more detected along with other by-products. In this case, the traces of product formed in the previous experiments which presents the expected NMR features, was not observed. Next, the screening of various bases was performed. When DIPEA, DBU or DABCO were employed (Scheme 4.8, Entries 3-5), a complex mixture of products was detected mainly due to degradation of the aminophosphine starting material. In all the aforementioned cases, the formation of **4.31** was detected, indicating that under these reaction conditions, **4.29a** degrades to form **4.31.** The use of LiTMP at -78 °C to room temperature (Scheme 4.8, Entry 6) generated a complex mixture of products but the desired product was not formed. To explain these results, the following mechanism is proposed and depicted in Scheme 4.10.

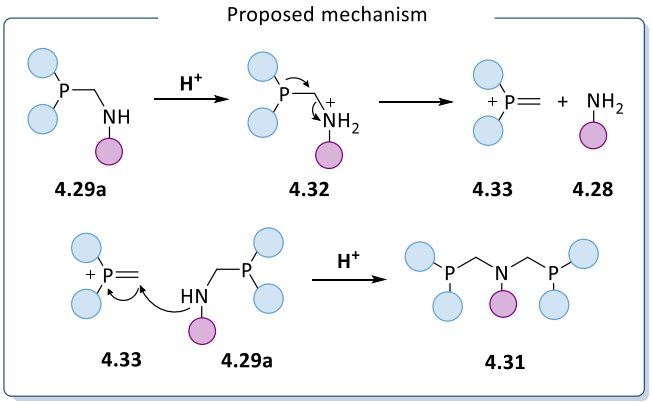

Scheme 4.10. Proposed mechanism for the formation of the by-product **4.31**

After the protonation of the amine moiety of the compound **4.29a**, a very reactive ammonium intermediate (**4.32**) is formed that undergoes elimination of the amine **4.28** to generate a phosphonium ion **4.33**. The latter is very prone to nucleophilic addition by another molecule of **4.29a** to deliver compound **4.31**. A careful analysis of the literature concerning the formation of ligands containing the fragment $R_2P\text{-}CH_2\text{-}N\text{-}P$ **4.30a** revealed that for this type of compounds, the selection of the substituents at phosphorus and at nitrogen atoms is critical for the stability of the reaction intermediates.[21]

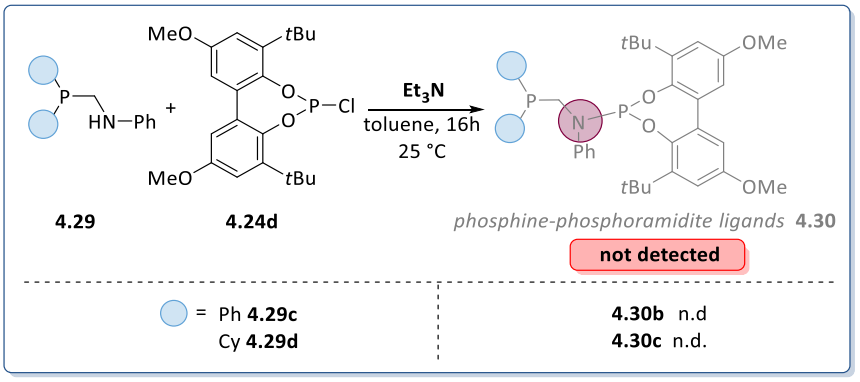

Scheme 4.11. Attempts in the synthesis of phosphine-phosphoramidite ligands **4.30b-c**.

It was therefore planned to change these substituents to use more basic phosphine units and less basic amine moieties (Scheme 4.11).In this case, the reaction of **4.29c** and **4.24d** provided the desired compound **4.30c** in 15% NMR yield. It rapidly decomposes to unknown compounds. When the reaction was conducted between **4.29c** and **4.24,** no product was observed. The conclusion from this experiment and the ones previously reported is that the aminophosphine fragment is very labile.

In summary, phosphine-phosphite ligands **4.25a-f** and phosphine-phosphoramidite ligands **4.27a-c** were synthetised by a simple procedure. Next, their activity and selectivity was tested in the rhodium catalysed hydroformylation of 1-octene.

4.3.2 Optimization of the hydroformylation conditions

An optimization of the reaction conditions was carried out for the rhodium hydroformylation of 1-octene. For this purpose, [Rh(acac)$(CO)_2$] was selected as the rhodium precursor and the phosphine-phosphite **4.25a-f** or phosphine-phosphoramidite **4.27a-c** as ligands (1.1 equiv./Rh). The reaction was run in toluene for 4h. Initially, the effect of the total syngas pressure, the partial CO and H_2 pressure and the Rh loading was looked at employing ligand **4.25b** (Table 4.1).

We used as initial reaction conditions: [Rh(acac)$(CO)_2$] (1 mol%), 1.1 mol% of ligand **4.25b**, at 50 °C, 1:4 CO:H_2 for 4 hours. Using 5 bar of syngas total pressure, a considerable amount of isomerization product (2-octene) was obtained (Entry 1). It was concluded that with low amount of CO in the system (1 bar), the carbonylation step is disfavoured and thus isomerization via β-hydride elimination is favoured. Under 10 bar of syngas pressure (Entry 2), isomerization was suppressed and the branched aldehyde was observed as major product, (b/l ratio =1.22).

Table 4.1. Optimization of the reaction conditions with ligands **4.25b**

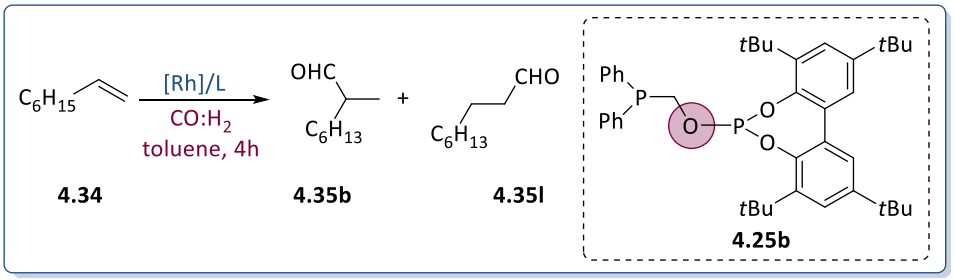

4.34 4.35b 4.35l 4.25b

Entry (a)	CO:H_2 ratio	Tot P	Rh mol %	Conv%	Chemo%	b/l
1	**1:4**	5	1	>99	49	**0.67**
2	**1:4**	10	1	>99	95	**1.23**
3	**1:4**	20	1	>99	99	**1.38**
4	1:1	**5**	1	90	92	**1.22**
5	1:1	**10**	1	>99	99	**1.38**
6	1:1	**20**	1	90	99	**1.0**
7	1:1	10	**0.5**	>99	99	**1.38**
8	1:1	10	**0.1**	54	75	**0.80**

Reaction conditions:[a] 1-octene **4.34** (2 mmol) 50 °C, [Rh(acac)$(CO)_2$] (1 mol%), ligand (1.1 mol%), 4 hours in toluene. Conversion, chemoselectivity and regioselectivity determined by GC-FID and NMR using bicyclohexyl as internal standard.

Using 20 bar of syngas total pressure, the branched hydroformylation product is further favoured and consequently, the regioselectivity improved up to 1.38 (Entry 3). These results could indicate that a minimum limit of 2.5 bar of CO partial syngas pressure is required to favour the hydroformylation reaction (Entries 2, 3). Next, the syngas ratio was changed from 1:4 to 1:1 to analyse the effect of the partial CO pressure on the regioselectivity. Using a CO:H_2 ratio of 1:1, the branched aldehyde was obtained in 45% (b/l=1.22) using 5 bar of total syngas pressure (Entry 4). Only 8% isomerization was observed in comparison to 51% when the CO:H_2 ratio was 1:4 under the same total pressure (Entry 1). When the total pressure was increased to 10 bar (Entry 5), the b/l ratio increased to 1.38. However, when the pressure was

further increased to 20 bar, the conversion decreased and the branched regioselectivity was lower (Entry 6, b/l=1.0), possibly due to the saturation of the coordination sites of the Rh centre. When 1 and 0.5 mol% of Rh pre-catalyst were used (Entries 5 and 7), identical results were obtained. Nevertheless, when the Rh loading was decreased to 0.1 mol% (Entry 8), the conversion, chemo- and regioselectivity were severely affected. In view of these results, the conditions described in Entry 5 were selected to test the phosphine-phosphite **4.25a-f** and phosphine-phosphoramidite **4.27a-c** ligands previously synthetized. The catalytic conditions selected were 50 °C and 10 bar of 1:1 CO/H_2 using 1 mol% of $[Rh(acac)(CO)_2]$ pre-catalyst and 1.1 mol% of ligand for 4 hours (Table 4.2). When ligand **4.25a** was employed, a branched to linear ratio of 1.14 was observed, in combination with full conversion and selectivity towards aldehydes (Table 4.2, Entry 1). With ligand **4.25b** (Entry 2), full conversion was obtained with a b/l ratio 1.38, as reported in Table 2, Entry 5. When the phopsphine-phosphite ligand **4.25c**, differing from **4.25b** by the replacement of *t*Bu group in 4-position of the biphenol moiety by OMe group, was used, the branched to linear ratio was slightly lower (b/l=1.22). The ligand **4.25d**, containing a dicyclohexylphosphine fragment, provided a b/l ratio of 1.44, with full conversion (Entry 4). When the equivalent ligand **4.25e** containing a cyclopentyl moiety on the phosphorus atom (Entry 5) was employed, the regioselectivity dropped to a b/l ratio of 0.66. When the analogous ligand **4.25f,** containing a bis(*tert*-butyl)phosphine moiety, was used (Entry 6), the regioselectivity towards the b/l ratio was 0.81.

Table 4.2. Optimization of the reaction conditions with ligands **4.25a-f** and **4.27a-d.**

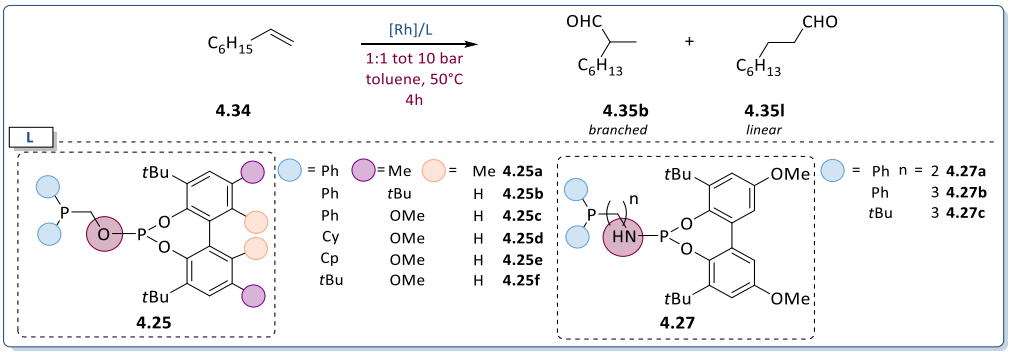

Entry [a]	ligand	Conv%	Chemo%	b/l
1	**4.25a**	>99	>99	**1.14**
2	**4.25b**	>99	>99	**1.38**
3	**4.25c**	>99	>99	**1.22**
4	**4.25d**	>99	>99	**1.44**
5	**4.25e**	>99	>99	**0.66**
6	**4.25f**	>99	>99	**0.81**
7	**4.27a**	>99	>99	**0.72**
8	**4.27b**	>99	>99	**0.81**
9	**4.27c**	44	>99	**0.72**
10	**BOBPHOS 4.11**	>99	>99	**1.44**

Reaction conditions:[a] 1-octene **4.34** (2 mmol) 50 °C, 10 bar, 1:1 $CO:H_2$, 1 mol% of [Rh(acac)(CO)2], 1.1 mol% of ligand for 4 hours in toluene. Conversion, chemoselectivity and regioselectivity determined by GC-FID and NMR using bicyclohexyl as internal standard.

When the phosphine-phosphoramidite ligands **4.35a** and **4.35b**, that differs by one and two CH_2 between the nitrogen and phosphorus atoms, respectively, were used, the branched to linear ratio was affected in favour of the linear product (Table 4.2, Entries 7 and 8). The phosphine-phosphoramidite ligand **4.35c** was tested provided low conversion, and

regioselectivity towards the branched aldehyde (b/l= 0.72) (Entry 9). The phosphine moieties also affected the outcome of the reaction conversion, since ligands bearing diphenyl phosphine fragments provided higher values in terms of conversion than the ligand that contained the bis(*tert*-butyl) groups (**4.35c**).

Under the same conditions, the commercially available BOBPHOS ligand **4.11** provided full conversion, total chemoselectivity and a b/l ratio of 1.44 in Entry 10. These results therefore indicated that the phosphite moiety has little influence on the regioselectivity of the reaction while the steric hindrance at the phosphine fragment strongly affects the branched to linear ratio. Indeed, ligands bearing diphenyl- and dicyclohexyl-phosphine fragments provided similar regioselectivity than the reference BOBPHOS ligand **4.11** that contained a 2,5-diphenylphospholane unit while the introduction of a bulky fragment such as bis(*tert*-butyl) phosphine led to a drastic decrease in regioselectivity. Since isomerization was observed in some experiments, to investigate whether this process could have an influence on the regioselectivity of the overall reaction, it was decided to look at the hydroformylation of 2-octene and for this purpose, *cis* and *trans* 2- octene were used as substrate (Table 4.3).

Table 4.3. Optimization of the reaction conditions with ligand **4.25d**

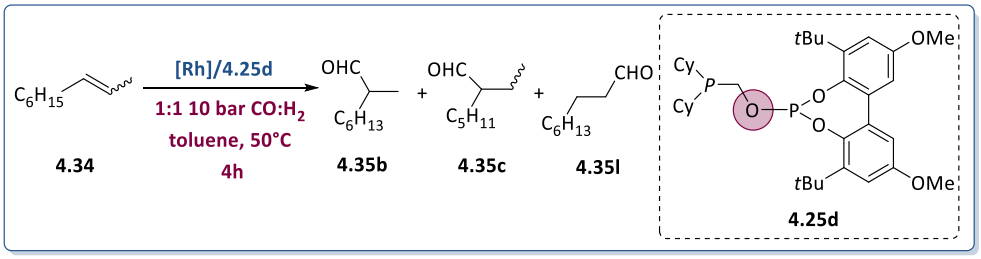

Entry [a]	substrate	4.35b/ 4.35c	(4.35b+4.35c)/4.35l	Conv %	Chemo %
1	1-octene	**1.44**	**>99**	>99	>99
2	cis-2-octene	**1.77**	**>99**	40	>99
3	*trans* 2-oct	**1.17**	**>99**	15	>99

Reaction conditions: [a] substrate (2 mmol) 50 °C, 10 bar, 1:1 $CO:H_2$, 1 mol% of $[Rh(acac)(CO)_2]$, 1.1 mol% of ligand for 4 hours in toluene. Conversion, chemoselectivity and regioselectivity determined by GC-FID and NMR using bicyclohexyl as internal standard.

Entry 1 (Table 4.3), shows the result obtained using 1-octene with ligand **4.25d.** Full conversion and a b/l ratio of 1.44 was obtained. When *cis* 2-octene was used as substrate under the same conditions (Entry 2), lower conversion was observed (40%) and no linear product was detected. The ratio between the branched 2-product (**4.35b**) to branched 3-product (**4.35c**) was 1.77. When trans 2-octene was tested as substrate (Entry 3), the conversion dropped dramatically (15%) and, similarly to the latter case, no linear aldehyde was formed. In this case, no clear preference in terms of regioselectivity between the two internal aldehydes (**4.35b** and **4.35c**) was observed with a ratio of 1.17. These results indicated that isomerization from 2-octene into 1-octene was not taking place under the studied conditions and that hydroformylation of 2-octene was taking place with a preference for the formation of 2-nonanal from *cis*-2-octene while from *trans*-2-octene, 2- and 3-nonanal were formed unselectively. Next, the possibility of performing a sort of "tandem" isomerization-hydroformylation process was tested to investigate whether the b/l ratio could be improved through this process (Scheme 4.12).

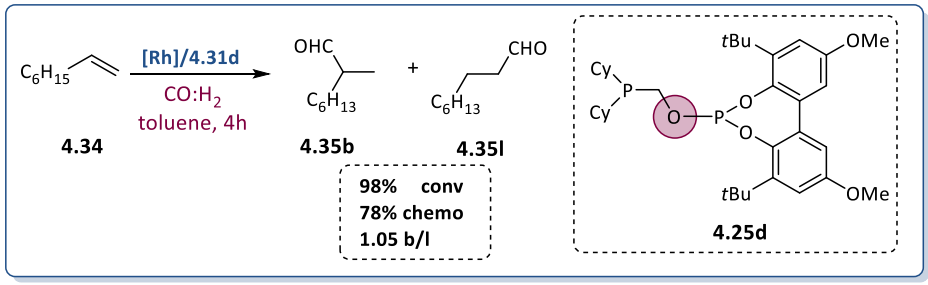

Scheme 4.12. Reaction conditions:[a] 1-octene **4.34** (2 mmol) 50 °C, 5 bar, 1:1 $CO:H_2$, 1 mol% of $[Rh(acac)(CO)_2]$, 1.1 mol% of ligand for 4 hours in toluene. Additional 4 hours at 50 °C, 10 bar, 1:1 $CO:H_2$, 1 mol% of $[Rh(acac)(CO)_2]$, 1.1 mol% of ligand for 4 hours. Conversion,

chemoselectivity and regioselectivity determined by GC-FID and NMR using bicyclohexyl as internal standard.

First, the conditions providing high level of isomerization of 1-octene were applied during 4h, after which the optimized hydroformylation conditions using ligand **4.25d** were applied. Therefore, the initial conditions selected were 50 °C, 1:4 CO/H_2, 5 total bar, using 1 mol% of $[Rh(acac)(CO)_2]$ pre-catalyst and 1.1 mol% of ligand during 4 hours. After this period, the reactor was depressurised and then recharged with 10 bar of 1:1 CO/H_2, and the reaction left stirring at 50 °C during 4 more hours. Analysis of the reaction mixture showed that 98% conversion of 1-octene was reached under these conditions. However, 23% of *trans*-2-octene remained and a branched to linear ratio of 1.05 was observed. Afterwards, the effect of the temperature in combination with the total syngas pressure was studied, employing ligand **4.25d**, the one that delivers the highest results in terms of regioselectivity (Table 4.2, Entry 4).

Table 4.4. Optimization of the reaction conditions with ligand **4.25d**

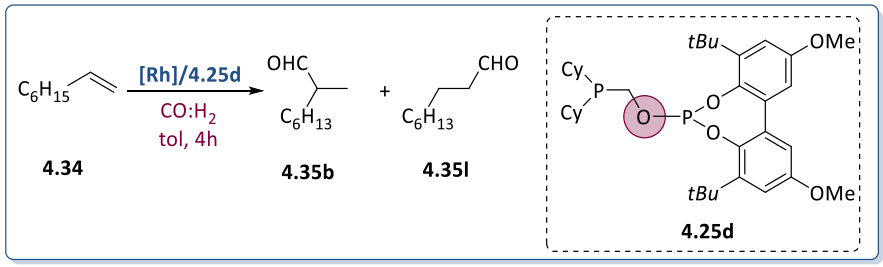

Entry [a]	CO:H_2 ratio	Bar	T °C	Conv%	Chemo%	b/l
1	1:4	10	50	>99	80	**1.54**
2	1:4	10	25	25	90	**1.02**
3	1:4	20	50	>99	>99	**1.44**
4	1:4	20	25	>99	25	**0.95**
5	1:1	10	50	>99	>99	**1.44**
6	1:1	10	25	20	>99	**1.70**

7	1:1	20	50	>99	>99	**0.81**
8	1:1	20	25	25	>99	**1.70**

Reaction conditions:[a] 1-octene **4.34** (2 mmol) 50 °C, 1 mol% of [Rh(acac)$(CO)_2$], 1.1 mol% of ligand for 4 hours in toluene. Conversion, chemoselectivity and regioselectivity determined by GC-FID and NMR using bicyclohexyl as internal standard.

The catalytic conditions selected were: 1 mol% of [Rh(acac)$(CO)_2$] pre-catalyst and 1.1 mol% of ligand for 4 hours (Table 4.4). When the hydroformylation process was carried out at 50 °C and 10 bar of 1:4 CO/H_2 (Entry 1), full conversion and 1.54 b/l ratio was observed. When the temperature was lowered to room temperature (Entry 2), a clear drop in both conversion and regioselectivity towards the branched aldehyde (b/l=1.02) was observed. In both cases, the use of low CO pressure (2 bar) resulted in a high percentage of isomerization (Entries 1 and 2, 80% and 90% chemoselectivity). A this point, the syngas pressure was increased (20 bar, Entries 3 and 4) while maintaining the same $CO:H_2$ ratio (1:4). As expected, under these conditions, full conversion was observed. The reaction performed at 50 °C (Entry 3) show similar b/l ratio of 1.44, compared with the results observed in Entry 1 (b/l=1.54). However, the combination of low temperature and high H_2 pressure (Entry 4, 15 bar) had a detrimental effect over the chemoselectivity, favouring the isomerization process. Next, variations in total pressure (10 and 20 bar) and temperature (25 °C and 50 °C) were performed under 1:1 $CO:H_2$ ratio. When 10 bar and 50 °C were used in the hydroformylation process, full conversion and 1.44 b/l was observed (Entry 5). Once again, lowering the temperature to 25 °C resulted into a severe drop in the conversion (20%), nonetheless the regioselectivity to the branched aldehyde was slightly higher (b/l=1.70, Entry 6). When the total pressure was then increased to 20 bar, the reaction carried out at 50 °C delivered a b/l ratio of 0.89 (Entry 7). Similarity to Entry 6, at lower temperature, a branched to linear ratio of 1.70 was observed, in combination with low conversion (Entry 8). Comparing these results, summarised in Table 4.5, at higher CO partial

pressure (1:1 vs 1:4), an increase of branched aldehyde percentage was noticed, but at the cost of lower conversion rate. In the meantime, low temperatures were beneficial in the production of branched aldehyde (Entries 6 and 8), in combination with 1:1 ratio of $CO:H_2$ pressure (Entries 6 and 8 vs Entries 2 and 4).

4.3.3 HP-NMR studies

In order to gain understanding into the reactivity of the Rh species involved during the catalysis, HP-NMR experiments were conducted under different reaction conditions. These studies were performed using 0.02 mmol of $[Rh(acac)(CO)_2]$ as precursor, 0.022 mmol of ligand, toluene-d_8 as solvent in a total volume of 0.4 ml. Systems bearing ligand **4.25d** was thus investigated using a 5 mm HP NMR tube and the reaction mixtures were analysed by ^{1}H, ^{31}P and ^{13}C NMR spectroscopy. These HP-NMR *in situ* experiments aimed at determining the coordination mode of the ligand in the hydroformylation resting state, namely the rhodium hydride dicarbonyl species.

4.3.3.1 Reactivity of $[Rh(acac)(CO)_2]$ in the presence of ligand 4.25d

First, a solution of the precursor $[Rh(acac)(CO)_2]$ **4.36** (0.02 mmol) and ligand **4.25d** (0.022 mmol) in toluene-d_8 (0.4 ml) was left one hour at room temperature prior to NMR analysis.

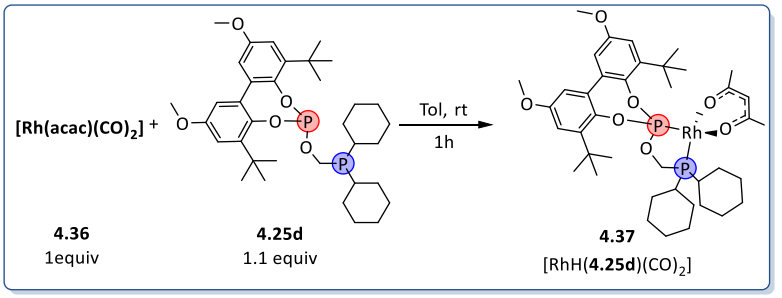

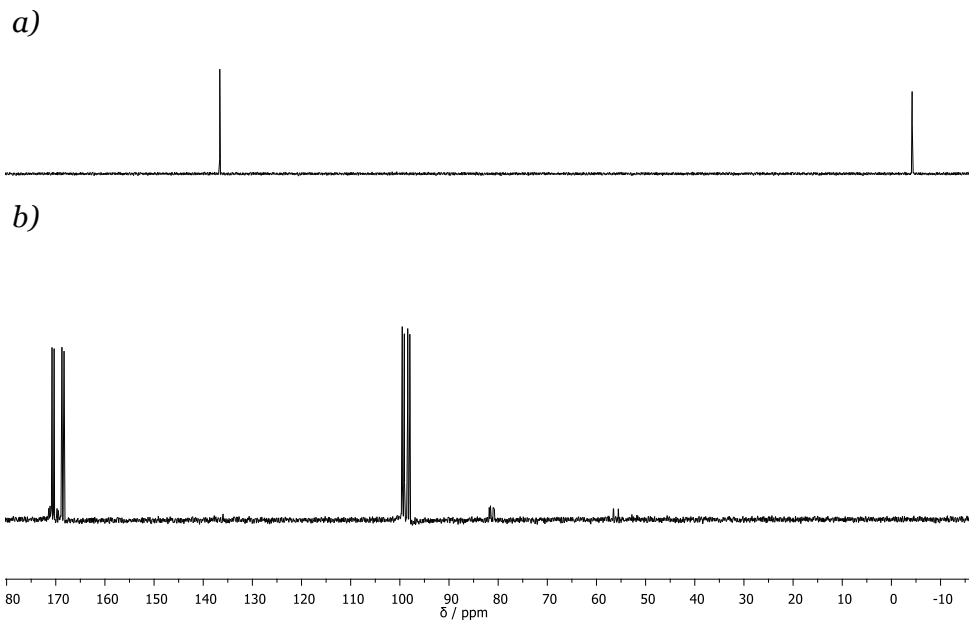

Scheme 4.13. Selected NMR signals for HP NMR analysis [Rh(acac)(CO)$_2$] **4.36** and ligand **4.25d**. a) $^{31}P\{^1H\}$ NMR (162 MHz, RT) ligand phosphine-phosphite **4.25d**. b) $^{31}P\{^1H\}$ NMR (162 MHz, RT) rhodium complex [Rh(**4.25d**)(acac)] **4.37**.

The $^{31}P\{^1H\}$ NMR spectrum of the non-coordinated phosphine-phosphite ligand **4.25d** displayed two singlet signals at 135.9 and -2.9 ppm (Scheme 4.13, a). When the precursor [Rh(acac)(CO)$_2$] was reacted with ligand **4.25d**, two new doublets of doublets were observed at 98.7 and 169.5 ppm (Scheme 4.13, b). The first signal exhibited a J_{P-P} coupling of 70 Hz and a J_{P-Rh} coupling of 180 Hz and was attributed to the phosphine fragment of the ligand coordinated to the Rh centre. The second signal exhibited a J_{P-P} coupling of 70 Hz and a J_{P-Rh} coupling of 362 Hz and was assigned to the coordinated phosphite fragment of the ligand. In agreement with literature values, these signals were attributed to the formation of a new Rh complex identified as the square planar complex [Rh(**4.25d**)(acac)] **4.37**.[7]

4.3.3.2 Reactivity of [Rh(acac)(CO)$_2$] in the presence of ligand 4.25d under H_2/CO pressure

At this point, to selectively form the rhodium hydride dicarbonyl complex **4.37**, 5 bar of total pressure (H_2:CO ratio of 3:1) were introduced in the HP NMR tube in the presence of the square planar complex [Rh(**4.25d**)(acac)] **4.37** and left shaking for 1 hour at 50°C. Signals corresponding to the rhodium hydride dicarbonyl complex [RhH(**4.25d**)(CO)$_2$)] **4.38** were readily detected (Scheme 4.14).

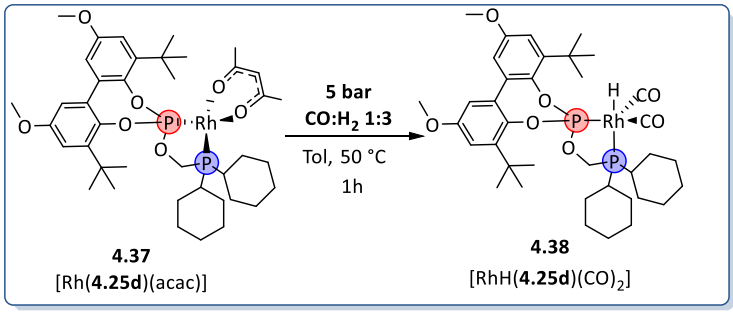

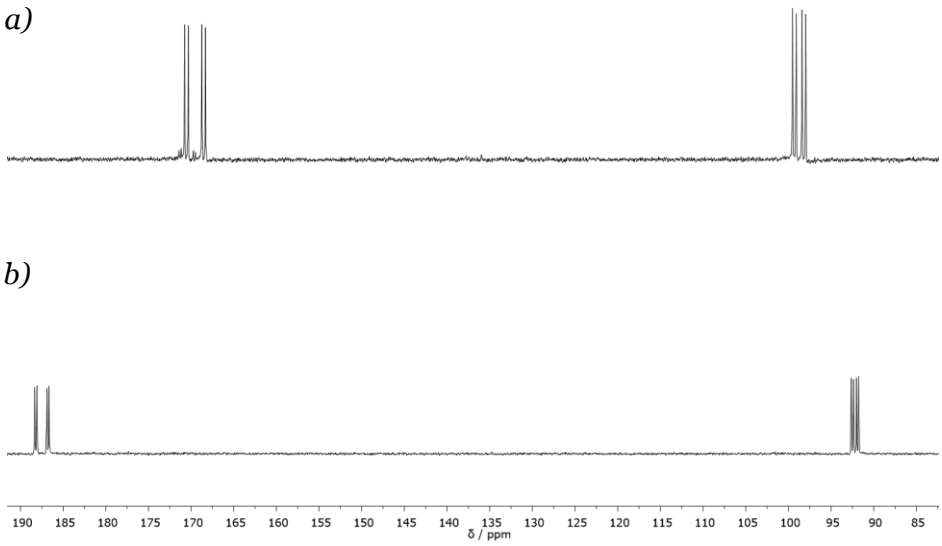

Scheme 4.14. Selected NMR signals for HP NMR analysis RhH(**4.25d**)(acac) **4.38**. a) $^{31}P\{^1H\}$ NMR (162 MHz, RT) rhodium complex [Rh(**4.25d**)(acac)]**4.37**. b) Rhodium hydride dicarbonyl complex [Rh(H)(**4.25d**)(CO)$_2$] **4.38**.

In the $^{31}P\{^{1}H\}$ NMR spectrum, two set of signals were detected: a doublet of doublets at 187.4 ppm and a second doublet of doublets at 92.2 ppm, with J_{P-Rh} coupling for the phosphite and phosphine of 230 and 95 Hz, respectively (Scheme 4.14, b). The magnitude of these couplings is consistent with a trigonal bipyramidal geometry of the complex where the phosphite moiety occupies an equatorial position and the phosphine moiety an axial site.[7]

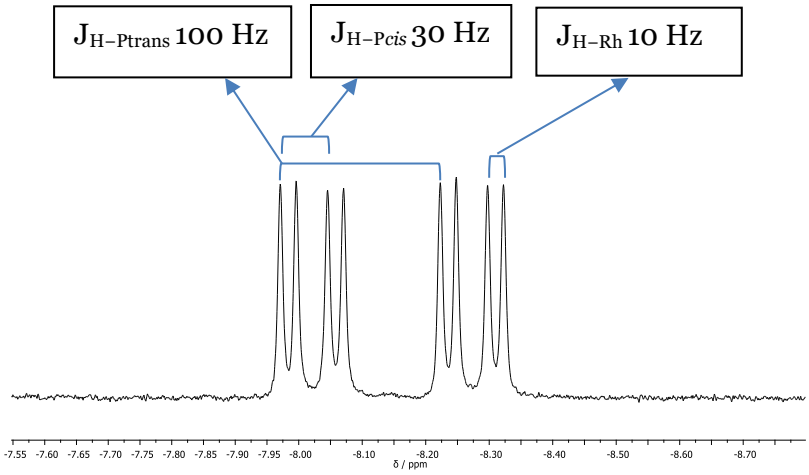

Figure 4.4: [RhH(**4.25d**)$(CO)_2$] structure in tol-d^8 (10 bar CO/H_2, 50 °C, 1h); (a) ^{1}H NMR (400 MHz, RT) of the hydride of the [RhH(**4.25d**)$(CO)_2$] **4.38**.

In the corresponding ^{1}H NMR spectrum (Figure 4.4), a doublet of doublet of doublet signal at δ −8.15 (ddd, $J_{H-Ptrans}$ 100 Hz, J_{H-Pcis} 30 Hz, J_{H-Rh} 10 Hz), was detected. The magnitude of the J_{H-P} couplings is indicative that the hydride ligand is in *cis* position to one phosphorus atom and in *trans* position to another phosphorus atom. These results are in agreement with those reported by Clarke and co-workers for the phosphine-phospholane BOBPHOS ligand **4.11** and therefore indicate that both ligands coordinate to Rh in the same manner.[7] Additionally, this was confirmed by the acquisition of selective $^{1}H\{^{31}P\}$ NMR spectra. This means that the J_{H-Pcis} of 30 Hz is due to a coupling with the phosphite moiety, while the $J_{H-Ptrans}$ of 100 Hz can be attributed to a coupling to the phosphine. This demonstrated the axial:equatorial

coordination mode of the ligand in these species, where the hydride is *trans* to the phosphine moiety.

Furthermore, terminal carbonyls coordinated to the rhodium centre were also detected by ^{13}C NMR spectroscopy as a multiplet at 195.2 ppm. In the ^{1}H-^{31}P HMBC spectrum, a correlation was evidenced between the hydride signal at −8.15 ppm and the corresponding phosphorus signals at 92.2 ppm and 187.4 ppm in $^{31}P\{^{1}H\}$ NMR spectrum. In this spectrum, the signal corresponding to the CH_2 bridge between the nitrogen and the phosphorus atoms was also identified as a doublet at 3.65 ppm in ^{1}H NMR spectrum. In view of these results, the reaction product was identified as [RhH(**4.25d**)$(CO)_2$] **4.38** and its molecular structure is displayed in Figure 4.5. The data obtained via 1D and 2D NMR spectroscopy experiments are summarised in Figure 4.9 and Table 4.7.

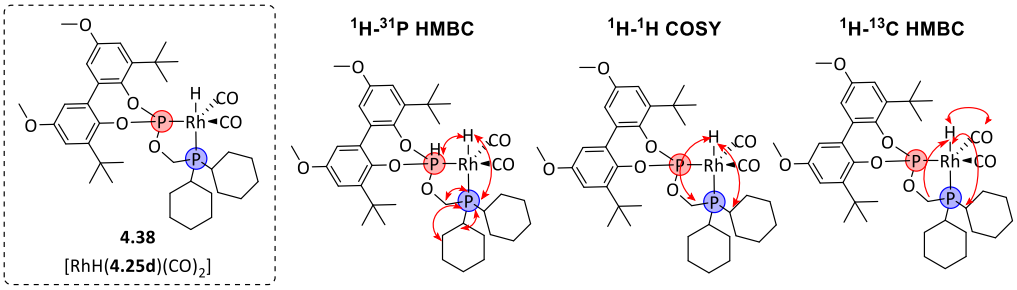

Figure 4.5. Correlations observed via 2D NMR experiments for the characterization of the [RhH(**4.25d**)$(CO)_2$] **4.38** complex.

δ ^{31}P ppm	δ ^{1}H ppm	δ ^{13}CO ppm
187.4 (dd, $J_{P\text{-}Rh}$=230 Hz, $J_{P\text{-}P}$=40 Hz) 92.2 (dd, $J_{P\text{-}R}$ =95 Hz, $J_{P\text{-}P}$ =40 Hz)	-8.15 (ddd, $J_{H-Ptrans}$ =100 Hz, J_{H-Pcis} =30 Hz, J_{H-Rh} =10 Hz)	195.17 ppm (m)

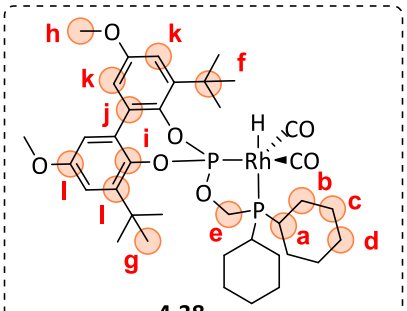

4.38

[RhH(**4.25d**)$(CO)_2$]

δ ^{1}H ppm	δ ^{13}C ppm	Assignment
1.35-1.05 (m, C<u>H</u>$_2$, C<u>H</u>) 1.79- 1.55 (m, C<u>H</u>$_2$, C<u>H</u>)	26.4 (s) 27.2 (d, $J_{C\text{-}P}$ = 10.2 Hz) 29.4 (d, $J_{C\text{-}P}$ = 9.3 Hz)	**d** **a, b, c**
1.53 (s, C<u>H</u>$_3$)	31.3 – 32.6 (m)	**g**
	35.8 (m)	**f**
3.35 (m, C<u>H</u>$_3$)	55.6 (m)	**h**
3.60 (d, $J_{P\text{-}H}$ = 18 Hz, C<u>H</u>$_2$)	61.6 (m)	**e**
6.65 (d, $J_{H\text{-}H}$ = 3.1 Hz, C<u>H</u>) 7.11 (d, $J_{H\text{-}H}$ = 3.1 Hz, C<u>H</u>)	113.3 (m) 114.7 (m)	**k**
	133.5 (m) 143.2 (m) 157.0-155.5 (m)	**j** **i** **l**

Table 4.7. Correlations observed via 2D NMR experiments for the characterization of the [RhH(**4.25d**)$(CO)_2$] complex.

It was therefore concluded that under these conditions, the phosphine-phosphite ligand **4.25d** provides the hydride dicarbonyl rhodium intermediate [RhH(**4.25d**)$(CO)_2$] **4.38** with an equatorial:axial structure.

4.4. Conclusions

From the study described in this chapter, the following conclusions can be drawn:

I. The development of a protocol for the synthesis of phosphine-phosphite **4.25a-f** and phosphine-phosphoramidite **4.27a-c** ligands has been achieved.

II. The attempts to synthesise the phosphine-phosphoramidite **4.30** ligand show that the selection of the substituents at the phosphorus and nitrogen atoms is critical for the stability of reaction intermediates.

III. The ligands **4.25a-f** and **4.27a-c** were tested in the rhodium catalysed hydroformylation of 1-octene under the optimized conditions: 50 °C and 10 bar of 1:1 CO/H_2 using 1 mol% of $[Rh(acac)(CO)_2]$ pre-catalyst and 1.1 mol% of ligand for 4 hours (Table 4.2).

IV. The phosphite moiety has little influence on the regioselectivity, while the steric hindrance of the phosphine fragment strongly affects the branched to linear ratio.

V. The ligands bearing diphenyl- and dicyclohexyl phosphine fragments (**4.25b**, **4.25c** and **4.25d**) provided similar regioselectivity than the reference BOBPHOS ligand **4.11** under these conditions. The introduction of a bulky fragment such as bis(*t*Bu)phosphine (**4.27f**) led to a drastic decrease in regioselectivity.

VI. High CO partial pressure (Table 4.4, 1:1 vs 1:4) favours the formation of the branched aldehyde (b/l=1.70), but at the cost of the conversion (25%). Low temperatures were beneficial to the production of branched aldehyde (Table 4.4, Entries 6 and 8), but in combination with 1:1 ratio of $CO:H_2$ pressure (Table 4.4, Entries 6 and 8 vs Entries 2 and 4).

VII. The rhodium hydride dicarbonyl species [RhH(**4.25d**)$(CO)_2$] **4.38** has been detected and fully characterised by NMR and an equatorial:axial coordination mode was demonstrated for this ligand, with the phosphine moiety in *trans* position to the hydride.

4.5 Experimental Part

4.5.1 General information

All the reactions were carried out using Schlenk-line inert atmosphere techniques or glovebox techniques. Anhydrous solvents were collected from the system Braun MB SPS-800. Commercially available reagents and solvents were purchased at the highest commercial quality from Sigma-Aldrich, Fluka, Alfa Aesar, Fluorochem, Strem and were used as received, without further purification, unless otherwise stated. ^{1}H, $^{13}C\{^{1}H\}$ and $^{31}P\{^{1}H\}$ NMR spectra were recorded using a Varian Mercury VX 400 (400, 100.6, and 161.97 MHz respectively). Chemical shift values (δ) are reported in ppm relative to TMS (^{1}H and $^{13}C\{^{1}H\}$) or H_3PO_4 ($^{31}P\{^{1}H\}$), and coupling constants are reported in Hertz. The following abbreviations are used to indicate the multiplicity: s, singlet; d, doublet; t, triplet; q, quartet; m, multiplet; bs, broad signal. High-resolution mass spectra (HRMS) were recorded on an Agilent Time-of-Flight 6210 using ESI-TOF (electrospray ionization-time of flight). Samples were introduced to the mass spectrometer ion source by direct injection using a syringe pump and were externally calibrated using sodium formate. The instrument was operating in the positive ion mode. Reactions were monitored by TLC carried out on 0.25 mm E. Merck silica gel 60 F_{254} glass or aluminium plates. Developed TLC plates were visualized under a short-wave UV lamp (254 nm) and by heating plates that were dipped in potassium permanganate. Flash column chromatography was carried out using forced flow of the indicated solvent on Merck silica gel 60 (230-400 mesh). The Rh-catalysed hydroformylation reaction were set up in a 7 tube

autoclave from HEL Inc. and single tube autoclave from HEL Inc and were stirred with a teflon-coated magnetic stir bar.

4.5.2 General procedure for hydroformylation of 1-octene reaction

A 10 mL glassware reactor tube was charged with 1-octene (2 mmol), dicarbonyl(acetylacetonato)rhodium(I) (1 mol%) in toluene (3.75 mL) and ligand (1.1 mmol%), the autoclave was closed in the glove-box. The reaction tube was placed in the reactor which was pressurized at the desired pressure, heated to 50 °C and left stirring at 900 rpm. The reaction was stopped after 24 hours by cooling the reactor in an ice bath for 20 minutes followed by venting of the system. After completion of the reaction, the crude mixture was analysed by GC-MS, GC-FID and ^{1}H NMR and the results compared to those previously reported in literature.

4.5.3 Synthesis of phosphine-phosphite ligand 4.25a-f

General Procedure A: Synthesis of phosphine-phosphite (4.25a-f)

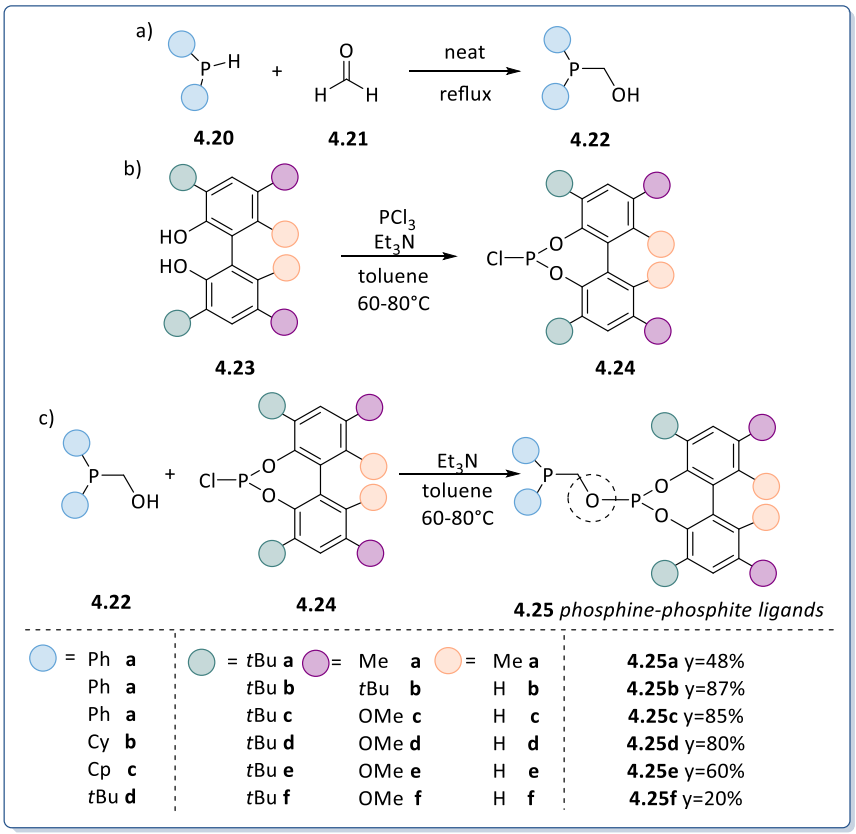

Scheme 4.15. Synthesis of phosphine-phosphite ligands **4.25a-f.**

The reaction (step a) was carried out in an oven dried, argon purged, Schlenk fitted with an argon inlet and a septum and following a modified literature procedure.[18,19] A neat mixture of phosphine **4.20** (10 mmol) and paraformaldehyde **4.21** (10 mmol) was stirred and heated to 110 °C from 30 minutes to 1 hour, until the paraformaldehyde was completely converted, highlighted by the appearance of a clear solution. The liquid was then allowed to cool to room temperature to afford the desired compound **4.22** in quantitative yield. The diol **4.23** (2.5 mmol) was placed in an oven dried,

argon purged, Schlenk tube and dissolved in 10 mL of toluene. NEt_3 (7.45 mmol) was added and the resulting solution was cooled in an ice bath (step b). PCl_3 (3.1 mmol) was added dropwise to the reaction mixture which was then removed from the ice bath and were heated to 80°C while stirring.[22] The suspension was filtered *via* a filtrating plate under an inert atmosphere, and the filtrate was evaporated using a Schlenk line and dried under vacuum to remove any residual PCl_3 and give the product **4.24** as a white solid which was used in the next step without further purification. To a Schlenk flask containing a solution of from chlorophosphite **4.24** the previous step in toluene (8.5 mL) and NEt_3 (1.2 equiv.) was added a solution of **4.22** (1.2 equiv.) in toluene (10 mL). The reaction mixture (step c) was then allowed to stir at room temperature overnight. The resulting suspension was filtered through silica gel (previously dried overnight in an oven) under an inert atmosphere, using toluene to compact (10 mL), and wash (40 mL) the SiO_2 after filtration. The resulting solution was evaporated *in vacuo* to afford a white foamy solid.

Synthesis of (hydroxymethyl)diphenyl phosphine 4.22a

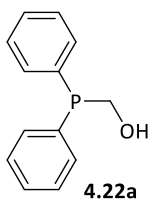

4.22a

General procedure A was followed employing diphenyl phosphine (10 mmol) and paraformaldehyde (10 mmol). Compound **4.22a** was obtained as a clear liquid. Yield of **4.22a**: 2.46 g (100%); **^{1}H NMR** (400 MHz, Tol-d_8): δ 7.46–7.37 (m, 5H), 7.13–7.02 (m, 5H), 4.15 (d, J_{P-H}= 8.3 Hz, 2H), 1.36 (bs). **^{31}P{^{1}H} NMR** (162 MHz, Tol-d_8): δ –10.5 ppm. **^{13}C NMR** (101 MHz, $CDCl_3$): δ 138.5 (d, J_{P-C} = 13.0 Hz), 133.2 (d, J_{P-C} = 18.2 Hz), 128.4 (dd, J_{P-C} = 9.3, 5.9 Hz), 59.0 (dd, J_{P-C} = 9.2, 5.2 Hz). These signals are in agreement with those reported in the literature.[23]

Synthesis of (hydroxymethyl)dicyclohexyl phosphine 4.22b

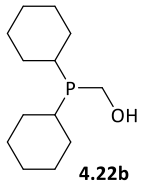

4.22b

General procedure A was followed employing dicyclohexyl phosphine (10 mmol) and paraformaldehyde (10 mmol). Compound **4.22b** was obtained as a clear liquid. Yield of **4.22b**: 2.28 g (100%); **^{1}H NMR** (400 MHz, $CDCl_3$): δ 4.01 (d, J_{H-P} = 6.5 Hz, 4H), 2.91 (bs, 1H), 1.99 – 1.52 (m, 11 H), 1.49 – 0.97 (m, 11 H). **^{31}P{^{1} H} NMR** (162 MHz, $CDCl_3$): δ -1.27.

Synthesis of (hydroxymethyl)dicyclopenthy phosphine 4.22c

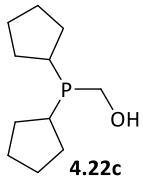

4.22c

General procedure A (Step a) was followed employing dicyclohexyl phosphine (10 mmol) and paraformaldehyde (10 mmol). Compound **4.22c** was obtained as clear liquid. Yield of **4.22c**: 2.28 g (100%); **^{1}H NMR** (400 MHz, $CDCl_3$): δ 4.01 (d, J_{P-H}= 6.4 Hz, 2H), 2.20-1.40 (m, 18H); **^{31}P{^{1}H} NMR** (162 MHz, $CDCl_3$): δ 1.85.

Synthesis of (hydroxymethyl)di*tert*-butyl phosphine 4.22d

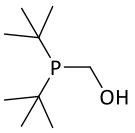

4.22d

General procedure A (Step a) was followed employing dicyclohexyl phosphine (10 mmol) and paraformaldehyde (10 mmol). Compound **4.22d** was obtained as clear liquid. Yield of **4.22d**: 2.28 g (100%); **^{1}H NMR** (400 MHz, $CDCl_3$): δ 4.10 (d, J_{P-H}= 7.0 Hz, 2H), 0.98 (s, 18H), **^{31}P{^{1}H} NMR** (162 MHz, $CDCl_3$): δ 20.3 ppm . These signals are in agreement with those reported in the literature.[24]

Synthesis of (3,3',5,5'-tetra-tert-butyl-1,1'-biphenyl-2,2'-diyl)-phosphorochloridite 4.24a

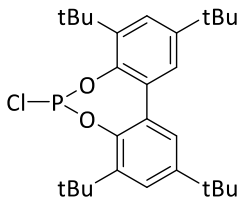

4.24a

General procedure A (Step b) was followed employing 3,3',5,5'-tetra-tert-butyl-[1,1'-biphenyl]-2,2'-diol (2 mmol) and PCl_3 (2.5 mmol). Yield of **4.24a**: 945 mg (95%); **^{1}H NMR** (400 MHz, $CDCl_3$): 7.50 (d, J_{P-H}= 2.5 Hz, 2H), 7.21 (d, J_{P-H}= 2.5 Hz, 2H), 1.51 (s, 18H), 1.39 (s, 18H). **^{31}P{^{1}H} NMR** (162 MHz, $CDCl_3$): δ 171 ppm (s). **^{13}C NMR** (101 MHz, $CDCl_3$): δ 31.5 (s), 31.5 (s), 34.8 (s), 35.6 (s), 124.9 (s), 126.8 (s), 132.7 (d, J_{C-P} = 4.2 Hz), 140.5 (d, J_{C-P} = 2.2 Hz), 145.6 (d, J_{C-P} = 6.2 Hz). These signals are in agreement with those reported in the literature.[25]

Synthesis of 4,8-di-tert-butyl-6-chloro-1,2,10,11-tetramethyldibenzo[d,f][1,3,2]dioxaphosphepine 4.24b

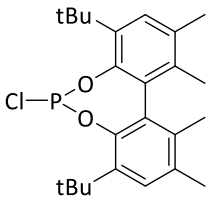

4.24b

General procedure A (Step b) was followed employing 3,3'-di-tert-butyl-5,5',6,6'-tetramethyl-[1,1'-biphenyl]-2,2'-diol (2.5 mmol) and PCl_3 (2.5 mmol). The liquid was allowed to cool to room temperature. Yield of **4.24b**: 839 mg (95%); **^{1}H NMR** (400 MHz, $CDCl_3$): δ 7.33 (s. 1H), 7.32 (s, 1H), 2.39 (s, 6H), 1.99 (s, 3H), 1.93 (s, 3H), 1.56 (s, 18H). **^{31}P{^{1}H} NMR** (162 MHz, $CDCl_3$): δ 164.3 (s). **^{13}C NMR** (101 MHz, $CDCl_3$): δ 16.6 (s), 16.9 (s), 20.1 (s), 31.2 (s), 32.3 (d, J_{C-P} = 5.0 Hz), 34.7 (s), 35.1 (s),128.3 (s), 129.0 (s), 130.4 (d, J_{C-P} = 2.8 Hz), 131.9 (d, J_{C-P} = 5.7 Hz), 132.9 (s), 133.9 (s), 137.6 (d, J_{C-P} = 1.8 Hz), 138.5 (d, J_{C-P} = 3.5 Hz), 143.9 (d, J_{C-P} = 5.7 Hz), 145.5 (s). These signals are in agreement with those reported in the literature.[26]

Synthesis of 4,8-di-tert-butyl-6-chloro-2,10-dimethoxydibenzo[d,f][1,3,2]dioxaphosphepine 4.24d

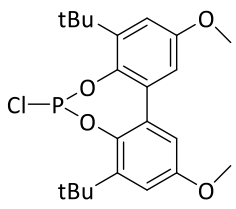

4.24d

General procedure A (Step b) was followed employing 3,3'-di-tert-butyl-5,5'-dimethoxy-[1,1'-biphenyl]-2,2'-diol (10 mmol) and PCl_3 (2.5 mmol). The liquid was allowed to cool to room temperature. Yield of **4.24d**: 840 mg (95%): **^{1}H NMR** (400 MHz, $CDCl_3$): δ 7.02 (d, J_{H-H}= 3.09 Hz, 2H), 6.74 (d, J_{H-H}= 3.09 Hz, 2H), 3.82 (s, 6H), 1.45 (s, 18H). **^{31}P{^{1}H} NMR** (162 MHz, $CDCl_3$): δ 172.30 (s) ppm. **ESI-HRMS:** Calculated for $C_{22}H_{28}O_4ClP$. Exact: (M: 422.1414, M+: 422.1408); Experimental: (M+H: 422.1407). These signals are in agreement with those reported in the literature.[26]

Synthesis of phosphine-phosphite 4.25a

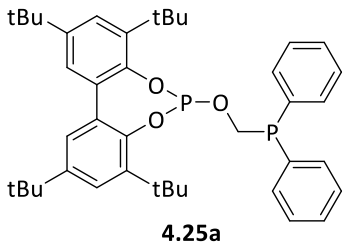

4.25a

General procedure A (Step c) was followed employing (3,3',5,5'-tetra-tert-butyl-1,1'-biphenyl-2,2'-diyl)-phosphorochloridite **4.24a** (1 mmol) and (hydroxymethyl)diphenyl phosphine **4.22a** (1 mmol). Purification of the crude material by column chromatography on silica gel in toluene with 5% Et_3N. Yield of **4.25a**: 313 mg (48%); **^{1}H NMR** (400 MHz, $CDCl_3$): 1.33 (s, 18H), 1.42 (s, 18H), 4.43 (t, J_{P-H} = 5.7 Hz, 2H), 7.15 (d, J_{H-H} = 2.5 Hz, 2H), 7.27–7.38 (m, 10H), 7.43 (d, J_{H-H} = 2.5 Hz, 2H). **^{31}P{^{1}H} NMR** (162 MHz, $CDCl_3$): δ 15.5 (s), 135.6 (s). **^{13}C NMR** (101 MHz, $CDCl_3$): δ 31.3 (s), 31.8 (s), 35.1 (s), 35.8 (s), 64.4 (d, J_{C-P} = 13 Hz), 124.8 (s), 126.8 (s), 128.8 (d, J_{C-P}=7 Hz), 129.3 (s), 132.9 (s), 133.4 (d, J_{C-P}=18 Hz), 136.0 (d, J_{C-P}=12 Hz), 140.3 (s), 146.5 (d, J_{C-P}=5 Hz), 147.3 (s); **ESI-HRMS:** Calculated for $C_{41}H_{53}O_3P_2$. Exact (M+: 655.3451), Experimental: (M+: 654.3392). These signals are in agreement with those reported in the literature.[27]

Synthesis of phosphine-phosphite 4.25b

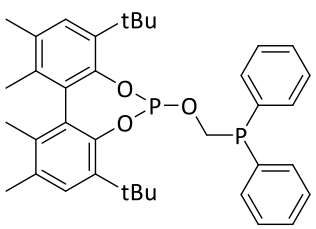

4.25b

General procedure A (Step c) was followed employing 4,8-di-tert-butyl-6-chloro-1,2,10,11-tetramethyldibenzo[d,f][1,3,2]dioxaphosphepine **4.24b** (1 mmol) and (hydroxymethyl)diphenyl phosphine **4.22a** (1 mmol). The liquid was allowed to cool to room temperature. Purification of the crude material by column chromatography on silica gel in toluene with 5% Et_3N. Yield of **4.25b**: 520 mg (87%); **^{1}H NMR** (400 MHz, $CDCl_3$): δ 1.32 (s, 9H), 1.42 (s, 9H), 2.96 (s, 3H), 1.84 (s, 3H), 2.22 (s, 3H), 2.24 (s, 3H), 3.70 (ddd, J_{P-H} = 4.1, 7.0 Hz, J_{H-H} = 12.8 Hz, 1H), 4.69 (ddd, J_{P-H} = 5.0, 7.4 Hz, J_{H-H} = 12.8 Hz, 1H), 7.08 (s, 1H), 7.14 (s, 1H), 7.27–7.43 (m, 10H). **^{31}P{^{1}H} NMR** (162 MHz, $CDCl_3$): δ 14.0 (s), 125.4 (s). **^{13}C NMR** (101 MHz, $CDCl_3$): δ 16.6 (s), 16.8 (s), 20.5 (s), 20.6 (s), 31.1 (s), 31.5 (d, J_{C-P}=5 Hz), 34.7 (s), 63.3 (dd, J_{C-P}=15, 3 Hz), 127.9 (s), 128.3 (s), 128.4 (s), 128.5 (s), 128.5 (s), 128.5 (s), 128.7 (s), 129.1 (s), 130.9 (d, J_{C-P}=2 Hz), 131.7 (d, J_{C-P}=5 Hz), 131.8 (s), 132.5 (s), 132.8 (s), 133.0 (s), 133.7 (s), 133.8 (s), 134.6 (s), 135.1 (s), 135.6 (d, J_{C-P}=11 Hz), 136.1 (d, J_{C-P}=11 Hz), 136.9 (s), 138.3 (s), 145.7 (d, J_{C-P}=3 Hz), 145.9 (d, J_{C-P}=3 Hz). **ESI-HRMS:** Calculated for $C_{37}H_{44}O_3P_2$. Exact: (M+: 598.2755); Experimental: (M+: 598.2766). These signals are in agreement with those reported in the literature.[27]

Synthesis of phosphine-phosphite 4.25c

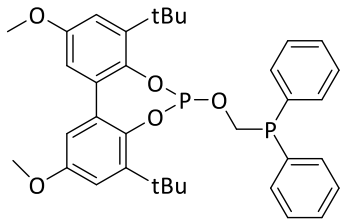

4.25c

General procedure A (Step c) was followed employing 4,8-di-tert-butyl-6-chloro-2,10-dimethoxydibenzo[d,f][1,3,2]dioxaphosphepine **4.24c** (1 mmol) and (hydroxymethyl)diphenyl phosphine **4.22a** (1 mmol). Purification of the crude material by column chromatography on silica gel in toluene with 5% Et_3N. Yield of **4.25c**: 511 mg (85%); **^{1}H NMR** (400 MHz, $CDCl_3$): δ 7.35 – 7.30 (m, 6H), 7.26 – 7.20 (m, 4H), 6.88 (d, J_{H-H}=3.1 Hz, 2H), 6.61 (d, J_{H-H}= 3.1 Hz, 2H), 4.40 (t, J_{P-H}=5.9 Hz, 2H), 3.75 – 3.71 (m, 6H), 1.31 (s, 18H). **^{31}P{^{1}H} NMR** (162 MHz, $CDCl_3$): δ –10.5 ppm. **^{13}C NMR** (101 MHz, $CDCl_3$): δ 138.5 (d, J_{C-P}=13.0 Hz), 133.2 (d, J_{C-P}=18.2 Hz), 128.4 (dd, J_{C-P}=9.3, 5.9 Hz), 58.9 (dd, J_{C-P}=9.2, 5.2 Hz). These signals are in agreement with those reported in the literature.[27]

Synthesis of phosphine-phosphite 4.25d

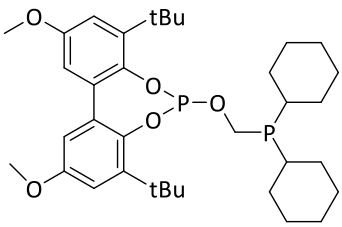

4.25d

General procedure A (Step c) was followed employing 4,8-di-tert-butyl-6-chloro-2,10-dimethoxydibenzo[d,f][1,3,2]dioxaphosphepine **4.24c** (1 mmol) and (hydroxymethyl)dicyclohexyl phosphine **4.22b** (1 mmol). Purification of the crude material by column chromatography on silica gel in toluene with 5% Et_3N. Yield of **4.25d**: 491 mg (80%); **^{1}H NMR** (400 MHz, $CDCl_3$): δ 6.97 (d, J_{H-H}=3.1 Hz, 2H), 6.69 (d, J_{H-H}=3.1 Hz, 2H), 4.09 (t, J_{P-H}=5.2 Hz, 2H), 3.81 (s, 6H), 1.71 (m, 11H), 1.47 (s, 18H), 1.27 – 1.11 (m, 11H). **^{31}P{^{1}H} NMR** (162 MHz, $CDCl_3$): δ 135.93 (s), -2.91 (s). **^{13}C NMR** (101 MHz, $CDCl_3$): δ 155.5 (s), 142.5 (d, J_{C-P} = 5.8 Hz), 142.2 (s), 133.5 (d, J_{C-P}= 3.5 Hz), 114.3 (s), 112.77 (s), 60.3 (d, J_{C-P} = 23 Hz), 55.5 (s), 35.3 (s), 31.3 (d, J_{C-P} = 11.2 Hz), 30.9 (d, J_{C-P} = 2.5 Hz), 30.0 (d, J_{C-P} = 13.7 Hz), 29.4 (d, J_{C-P} = 9.3 Hz), 27.2 (d, J_{C-P} = 10.2 Hz), 26.4 (s). **ESI-**

HRMS: Calculated for $C_{35}H_{52}O_5P_2$. Exact: (M: 614.3290, M+H: 615.3363); Experimental: (M+H: 615.3370).

Synthesis of phosphine-phosphite 4.25e

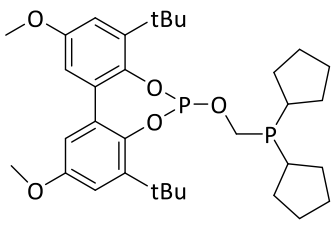

4.25e

General procedure A (Step c) was followed employing 4,8-di-tert-butyl-6-chloro-2,10-dimethoxydibenzo[d,f][1,3,2]dioxaphosphepine **4.24c** (1 mmol) and (hydroxymethyl)dicyclopentyl phosphine **4.22d** (1 mmol). Purification of the crude material by column chromatography on silica gel in toluene with 5% Et_3N. Yield of **4.25a**: 351 mg (60%); **^{1}H NMR** (400 MHz, $CDCl_3$). δ 6.97 (d, J_{H-H}= 3.1 Hz, 2H), 6.69 (d, J_{H-H}= 3.1 Hz, 2H), 4.09 (t, J_{P-H}= 5.2 Hz, 2H), 3.81 (s, 6H), 1.71 (m, 9H), 1.47 (s, 18H), 1.27 – 1.11 (m, 9H). **^{31}P{^{1}H} NMR** (162 MHz, $CDCl_3$): δ 133.61 (s), -5.23 (s). **^{13}C NMR** (101 MHz, $CDCl_3$): δ 155.5 (s), 142.5 (d, J_{C-P} = 5.8 Hz), 142.2 (s), 133.5 (d, J_{C-P}=3.5 Hz), 114.3 (d, J_{C-P}=156.9 Hz), 112.7 (s), 60.4 (d, J_{C-P}=22 Hz), 55.5 (s), 35.3 (s), 31.3 (d, J_{C-P}=11.2 Hz), 30.9 (d, J_{C-P}=2.5 Hz), 30.0 (d, J_{C-P}=13.7 Hz), 27.1 (d, J_{C-P}=10.2 Hz), 26.3 (s). **ESI-HRMS:** Calculated for $C_{33}H_{48}O_5P_3$. Exact: (M: 586.2977, M+H: 587.3057); Experimental: (M+H: 587.305).

Synthesis of phosphine-phosphite 4.25f

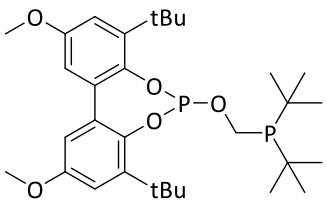

4.25f

General procedure A (Step c) was followed employing 4,8-di-tert-butyl-6-chloro-2,10-dimethoxydibenzo[d,f][1,3,2]dioxaphosphepine **4.24c** (1 mmol) and (hydroxymethyl)ditert-butyl phosphine **4.22c** (1 mmol). Purification of the crude material by column chromatography on silica gel in toluene with 5% Et_3N. Yield of **4.25f**: 116 mg (20%); **^{1}H NMR** (400 MHz, $CDCl_3$): δ 7.14 – 7.06 (m, 2H), 6.69 (d, J_{H-H}= 3.1 Hz, 2H), 3.39 (s, 6H), 2.97 (m, 2H), 1.55 (s, 18H), 0.99 (d, J_{P-H}=10.9 Hz, 18H). **^{31}P{^{1}H} NMR** (162 MHz, $CDCl_3$): δ 145.98 (s), 18.91 (s). **^{13}C NMR** (101 MHz, $CDCl_3$): δ 155.9

(s), 153.5 (s), 146.2 (s), 142.7 (s), 114.6 (s), 113.1 (s), 66.2 (J_{C-P}=23 Hz), 55.9 (s), 35.7 (s), 31.2 (d, J_{C-P} = 5.6 Hz), 30.3 (s), 30.2 (s), 29.8 (s). **ESI-HRMS:** Calculated for $C_{31}H_{48}O_5P_3$. Exact: (M: 562.2977, M+H: 563.3057); Experimental: (M+H: 563.3067).

4.5.4 Synthesis of bidentate phosphine-phosphoramidite ligand 4.27a-c

General Procedure B: Synthesis of phosphine-phosphoramidite (4.27a-f)

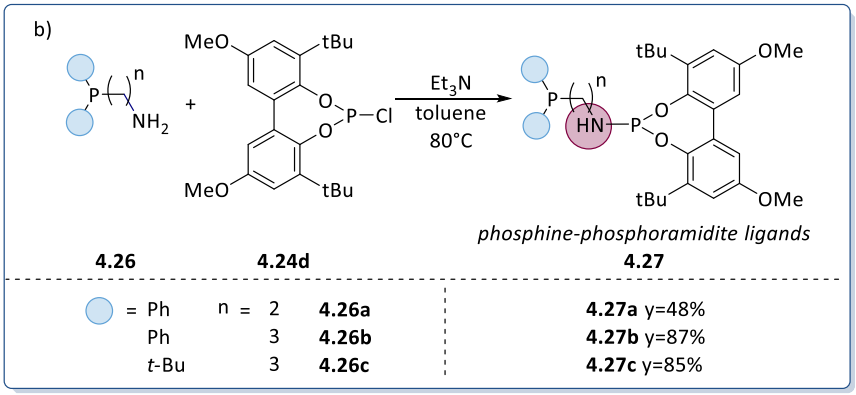

Scheme 4.16. Synthesis of phosphine-phosphoramidite ligands **4.27a-c.**

To a Schlenk flask containing a solution of 4,8-di-tert-butyl-6-chloro-2,10-dimethoxydibenzo [d,f] [1,3,2] dioxaphosphepine **4.24d** (1.1 mmol) in toluene (8.5 mL) and NEt_3 (1.2 equiv.) was added a solution of commercial aminophosphine **4.26** (1 equiv.) in toluene (10 mL). The reaction mixture was then allowed to stir at 80 °C overnight. The resulting suspension was filtered through silica gel (previously dried overnight in an oven) under an inert atmosphere, using toluene to compact (10 mL), and wash (40 mL) the SiO_2 after filtration. The resulting solution was evaporated *in vacuo* to afford a white foamy solid.

Synthesis of phosphine-phosphoramidite 4.27a

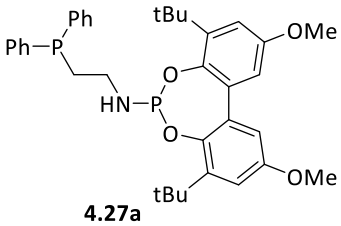

4.27a

General procedure B was followed. Purification of the crude material by column chromatography on silica gel in toluene with 5% Et_3N. Yield of **4.27a**: 491 mg (48%); **^{1}H NMR** (400 MHz, $CDCl_3$): δ 7.37 – 7.30 (m, 10H), 6.93 (d , J_{H-H} = 3.1 Hz, 2H), 6.61 (d, J_{H-H} = 3.1 Hz, 2H), 3.77 (s, 6H), 2.85 (m, 2H), 2.14 (m, 2H), 1.43 (s, 18H). **^{31}P{^{1}H} NMR** (162 MHz, $CDCl_3$): δ 146.63 (s), -21.63 (s). **^{13}C NMR** (101 MHz, $CDCl_3$): δ 155.3 (s), 143.3 (s), 142.4 (s), 137.9 (d, J_{C-P}=12.1 Hz), 133.8 (d, J_{C-P}=3.3 Hz), 132.9 (s), 128.5 (d, J_{C-P} = 6.6 Hz), 114.4 (s), 112.6 (s), 55.7 (s), 35.4 (s), 22.8 (s), 14.3 (s). **ESI-HRMS:** Calculated for $C_{36}H_{43}NO_4P_2$. Exact: (M: 615,2667M+H: 616.2740); Experimental: (M+H: 616.2737).

Synthesis of phosphine-phosphoramidite 4.27b

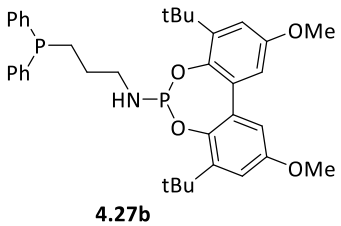

4.27b

General procedure B was followed. Purification of the crude material by column chromatography on silica gel in toluene with 5% Et_3N. Yield of **4.27b**: 491 mg (87%); **^{1}H NMR** (400 MHz, $CDCl_3$): δ 7.36 – 7.17 (m, 10H), 6.87 (d, J_{H-H} = 3.1 Hz, 2H), 6.61 (d, J_{H-H}= 3.1 Hz, 2H), 3.73 (s, 6H), 2.89 – 2.79 (m, 2H), 1.97 – 1.88 (m, 2H), .34 (s, 18H), 0.81 (m, 2H). **^{31}P{^{1}H} NMR** (162 MHz, $CDCl_3$): δ 147.41 (s), -16.19 (s). **^{13}C NMR** (101 MHz, $CDCl_3$): δ 154.2 (s), 141.4 (s), 137.4 (s), 132.8 (d, *J* = 3.2 Hz), 131.7 (d, J_{C-P}=18.3 Hz), 127.5 (d, J_{C-P}=7.3 Hz), 127.4 (d, J_{C-P}=6.6 Hz), 113.1 (s), 111.4 (s), 54.5 (s), 34.3 (s), 29.9 (d, *J* = 2.7 Hz), 21.6 (s), 13.1 (s). **ESI-HRMS:** Calculated for $C_{37}H_{45}NO_4P_2$. Exact: (M: 629,2824, M+H: 630.2897); Experimental: (M+H: 630.2888).

Synthesis of phosphine-phosphoramidite 4.27c

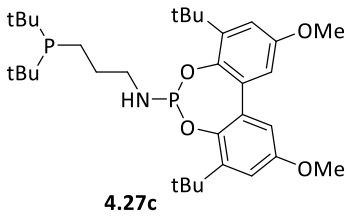

4.27c

General procedure B was followed. Purification of the crude material by column chromatography on silica gel in toluene with 5% Et_3N. Yield of **4.27c**: 491 mg (85%); **^{1}H NMR** (400 MHz, $CDCl_3$): δ 6.88 (d, J_{H-H}= 3.1 Hz, 2H), 6.60 (d, J_{H-H}= 3.1 Hz, 2H), 3.73 (s, 6H), 2.83 (m, 2H), 1.39 (s, 18H), 1.30 (m, 2H), 1.07 (m, 2H), 0.96 (d, J = 11.2 Hz, 18H). **^{31}P{^{1}H} NMR** (162 MHz, $CDCl_3$): δ 145.2 (s), 19.9 (s). **^{13}C NMR** (101 MHz, $CDCl_3$): δ 154.11 (s), 142.18 (d, J_{C-P}=5.0 Hz), 141.28 (d, J_{C-P}= 1.2 Hz), 113.1 (s), 111.5 (s), 54.5 (s), 34.3 (s), 30.6 (s), 29.9 – 29.85 (m), 28.5 (s, J_{C-P}=13.2 Hz), 28.4 (s), 21.6 (s), 13.1 (s). **ESI-HRMS:** Calculated for $C_{33}H_{53}NO_4P_2$. Exact: (M: 589,345, M+H: 590.3523); Experimental: (M+H: 590.3527).

4.5.5 Synthesis of bidentate phosphine-phosphoramidite ligand 4.39a-c

General Procedure C: Synthesis of aminophosphine fragment (4.37a-e)

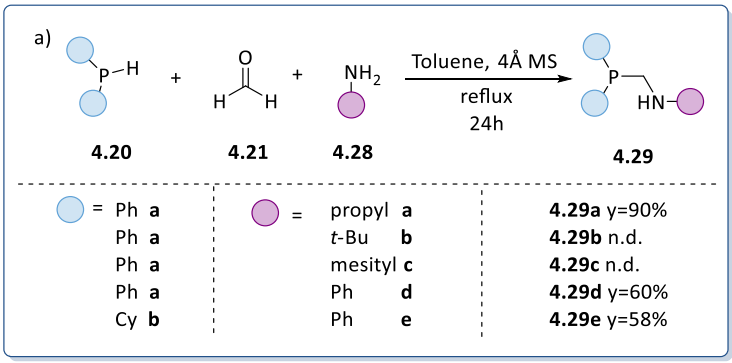

Scheme 4.17. Synthesis of aminophosphine fragments **4.37a-d.**

All reactions were routinely performed under argon or nitrogen by using standard Schlenk and glove-box techniques following a modified reported procedure.[28] The reaction was carried out in an oven dried, argon purged,

Schlenk fitted with an argon inlet, where phosphine **4.20** (5.92 mmol) was added to a mixture of desired amine **4.28** (5.92 mmol) and paraformaldehyde **4.21** (5.92 mmol) in toluene (30 mL) at reflux under nitrogen, with 4A MS, and stirred for 24 hours. The resulting suspension was filtered through silica gel (previously dried overnight in an oven) under an inert atmosphere, using toluene to compact (10 mL), and wash (40 mL) the SiO_2 after filtration. The resulting solution was evaporated *in vacuo* to afford a clear liquid.

Synthesis of aminophosphine fragment 4.29a

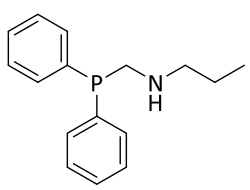

4.29a

General procedure C was followed employing phosphine **4.20a** (1 mmol), propylamine **4.28a** (1 mmol) and paraformaldehyde **4.21** (1 mmol). Yield of **3.29a**: 231 mg (90%); **^{1}H NMR** (400 MHz, $CDCl_3$): δ δ 7.28 – 7.20 (m, 4H), 7.12-7.09 (m, 6H), 3.40 (d, J_{P-H}= 3.0 Hz, 1H), 2.69 – 2.53 (m, 1H), 1.32 – 1.17 (m, 1H), 0.58 (t, J_{H-H}= 7.3 Hz, 1H). **^{31}P{^{1}H} NMR** (162 MHz, $CDCl_3$): δ - 19.56 (s). **^{13}C NMR** (101 MHz, $CDCl_3$): δ 138.3 (d, J_{C-P}=13.0 Hz), 133.4 – 129.3 (m), 128.4 – 128.1 (m), 58.8 (dd, J_{C-P}= 9.2, 5.1 Hz), 58.3 (t, J_{C-P}= 9.1 Hz), 19.7 (s), 11.6 (s).

Synthesis of aminophosphine fragment 4.29d

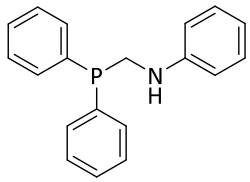

4.29d

General procedure C was followed employing phosphine **4.20a** (1 mmol), aniline **4.28d** (1 mmol) and paraformaldehyde **4.21** (1 mmol). Yield of **4.29d**: 174 mg (60%); **^{1}H NMR** (400 MHz, $CDCl_3$): δ 3.11 (bs), 3.36 (d, J_{P-H}= 4 Hz), 6.16 (d, J_{P-H}= 8 Hz), 6.49 (d, J_{P-H}= 8 Hz), 6.84 (m), 7.14 (m). **^{31}P{^{1}H} NMR** (162 MHz, $CDCl_3$): δ -19.14 (s). **^{13}C NMR** (101 MHz, $CDCl_3$): δ 148.6 (d, J_{P-C}= 6 Hz), 137.4 (d, J_{P-C}= 14 Hz), 133.2 (d, J_{P-C}= 18 Hz), 129.5 (s), 128.9 (d, J_{P-C}= 7.5 Hz), 128.8 (s, J_{P-C}= 6.5 Hz), 118.1

(s), 113.5 (s), 44.1 (d, J_{P-C}= 11 Hz). Experimental: (M+H: 496.2325). These signals are in agreement with those reported in the literature.[29]

Synthesis of aminophosphine fragment 4.29e

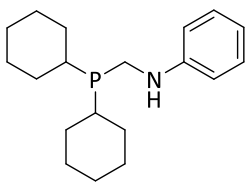

4.29d

General procedure C was followed employing phosphine **4.20b** (1 mmol), aniline **4.28d** (1 mmol) and paraformaldehyde **4.22** (1 mmol). Yield of **4.29e**: 175 mg (58%); **^{1}H NMR** (400 MHz, $CDCl_3$): δ 1.27 (10H, m, CH_2), 1.68 (4H, m, CH_2, CH), 1.77 (8H, m, CH_2), 3.19 (2H, d, J_{P-H} = 5 Hz, CH2), 6.63 (2H, d, J_{H-H} = 7.5 Hz, CH), 6.69 (1H, t, J_{H-H} = 7.5 Hz, CH), 7.18 (2H, t, J_{H-H} = 7.5 Hz, CH). **^{31}P{^{1}H} NMR** (162 MHz, $CDCl_3$): δ -1.92 (s). **^{13}C NMR** (101 MHz, $CDCl_3$): δ 26.4 (s), 27.0 (d, J_{C-P} = 2.5 Hz), 27.2 (d, J_{C-P} = 7.0 Hz), 29.0 (d, J_{C-P} = 7.0 Hz), 30.2 (d, J_{C-P} = 14.5 Hz), 32.6 (d, J_{C-P} = 11.0 Hz), 38.1 (d, J_{C-P} = 13.0 Hz), 112.6 (s,), 117.2 (s), 129.1 (s), 148.9 (d, J_{C-P} = 9.5 Hz). These signals are in agreement with those reported in the literature.[21]

4.5.6 In situ HP-NMR experiments

In a typical experiment, a sapphire tube (Ø = 5 mm) was filled under nitrogen atmosphere with a solution of the rhodium precursor $Rh(acac)(CO)_2$ and the ligand **2.17** in a ratio Rh/L = 1:1.1 in a total volume of 0.4 mL. The HP-NMR tube was purged CO, pressurized to the appropriate pressure of H_2/CO, heated if required, and left shaking. After that, the solution was analysed by NMR spectroscopy.

4.6 References

[1] P. W. N. M. Van Leeuwen, C. Claver and Editors, *Rhodium Catalyzed Hydroformylation.*, Kluwer, **2000**.

[2] a) N. Sakai, S. Mano, K. Nozaki and H Takaya, J. *Am. Chem. Soc.,* **1993**, *115*, 7033-7034. b) N. Sakai, K. Nozaki and H Takaya, *J. Chem. Soc. Chem. Commun.*, **1994**, 395-396. c) T. Higashijima,N. Sakai, K. Nozaki and H. Takaya, *Tetrahedron Lett.,* **1994**, *35*, 2023-2026. d) T. Horiuchi, T. Ohta, K. Nozaki and H. Takaya, *Chem. Commun.*, **1996**, 155-156. e) T. Horiuchi, T. Ohta, E. Shirakawa, K. Nozaki and H. Takaya, *J. Org. Chem.*, **1997**, *62*, 4285-4292.

[3] R. Tanaka, K. Nakano and K. Nozaki, *J. Org. Chem.*, **2007**, *72*, 8671-8676.

[4] K. Nakano,R. Tanaka and K. Nozaki, *Helv. Chim. Acta***, 2006**, *89*, 1681-1686.

[5] Z. Xiaowei, C. Bonan, Y. Shichao and Z. Xumu, *Angew. Chem. Int. Ed.,* **2010**, *49*, 4047-4050.

[6] K. Nozaki, H. Takaya and T. Hiyama, *Top. Catal.*, **1997**, *4*, 175-185.

[7] G. M. Noonan, J. A. Fuentes, C. J. Cobley and M. L. Clarke, *Angew. Chem. Int. Ed.*, **2012**, *51*, 2477-2480.

[8] V. F. Slagt, M. Roeder, P. C. J. Kamer, P. W. N. M. Van Leeuwen and J. N. H. Reek, *J. Am. Chem. Soc.,* **2004**, *126*, 4056-4057.

[9] A. Phanopoulos and K. Nozaki, *ACS Catal.*, **2018**, *8*, 5799-5809.

[10] D. W. Norman, J. N. H. Reek, T. Renee and M.-L. Besset, *US Patent*, **2014**, US 8710275 B2.

[11] X. Wang, S. S. Nurttila, W. I. Dzik, R. Becker, J. Rodgers and J. N. H. Reek, *Chem. Eur. J.,* **2017**, *23*, 14769-14777.

[12] R. Pittaway, J. A. Fuentes and M. L. Clarke, *Org. Lett.,* **2017**, *19,* 2845–2848.

[13] R. C. How, P. Dingwall, R. T. Hembre, J. A. Ponasik, G. S. Tolleson and M. L. Clarke, *Mol. Catal.,* **2017**, *434*, 116-122.

[14] P. Dingwall, J. Fuentes, L. Crawford, A. M. Z. Slawin, M. Bühl and M. L. Clarke, *J. Am. Chem. Soc.,* **2017**, *139*, 15921-15932.

[15] L. Iu, J. A. Fuentes, M. E. Janka, K. J. Fontenot and M. L. Clarke, *Angew. Chem. Int. Ed.*, **2019**, *58*, 2120-2124.

[16] L. Iu, M. Clarke, K. J. Fontenot and M. E. Janka, *World Patent*, **2019**, WO 2019108502 A1.

[17] L. Iu, M. Clarke and M. E. Janka, *US Patent*, **2019**, US 10183961 B1.

[18] F. Kuhl; S. Blaurock, J. Sieler and E. Hey-Hawkins, *Polyhedron*,**2001**, *20*, 2171-2177.

[19] a) J. Holz, M. Quirmbach, A. Borner, *Synthesis,* **1997**, 983-1006; b) J. Velder, T. Robert, I. Weidner, J.-M. Neudorfl, J. Lex and H.-G. Schmalz, *Adv. Synth. Catal.* **2008**, *350*, 1309-1315.

[20] J-F. Zhang, W.-F. Fu, X. Gan, J.-H.Chen, *Dalton Trans*., **2008**, 3093-3100.

[21] E. Payet, A. Audrey Auffrant, X.F. Le Goff and P. Le Floch, *J. Organomet. Chem.,* **2010**, *695*, 1499-1506.

[22] G. J. H. Buisman, P. C. J. Kamer and P. W. N. M. van Leeuwen, *Tetrahedron: Asymmetry,* **1993**, *4*, 1625-1634.

[23] O. Kuhl, S. Blaurock , J. Sieler and E. Hey-Hawkins, *Polyhedron,* **2001**, *17*, 2171-2177.

[24] D. A. Clarke, P. W. Miller, N. J. Long, and A. J. P. White, *Dalton Trans*., **2007**, 4556-4564.

[25] J. Coetzee, R. E. Graham, A. M. Z. Slawina and D. J. Cole-Hamilton,*Org. Biomol. Chem*., **2012**, *10*, 3677-3688.

[26] B. Zhang, H. Jiao, D. Michalik, S. Kloß, L. M. Deter, D. Selent, A. Spannenberg, R. Franke and A. Börner, *ACS Catal.* **2016**, *6*, 7554-7565.

[27] P. Kleman, M. Vaquero, I. Arribas, A. Suarez, E. Alvarez and A. Pizzano, *Tetrahedron Asymmetry*, **2014**, *25*, 744-749.

[28] A. L. Balch, M. M. Olmstead and S. P. Rowley, *Inorg. Chim. Acta*, **1990**, *168*, 255-264.

[29] K.-H. Wong, M. C.-W. Chan and C.-M. Che, *Chem. Eur. J.,* **1999**, *5*, 10, 2845-2849.

Rhodium and Palladium Catalysed Unusual Regioselective Hydroformylation and Rhodium Catalysed Reductive Carbonylation

Benedetta Palucci

Chapter V

Rhodium catalysed hydroformylation of styrene for the production of linear aldehyde

Rhodium and Palladium Catalysed Unusual Regioselective Hydroformylation and Rhodium Catalysed Reductive Carbonylation

Benedetta Palucci

5.1 Introduction

5.1.1 Rh-catalysed hydroformylation of styrene

Although short olefins such as ethylene, propene and butenes are the main substrates in industrial Rh-catalysed hydroformylation, the transformation of styrene into the corresponding aldehydes has been extensively studied as a model for the hydroformylation of vinyl arenes. The branched aldehydes, produced in the vinyl arenes hydroformylation, are intermediates in the synthesis of pharmaceuticals and fine chemicals. For this reason styrene was particularly studied in asymmetric hydroformylation.[1,2] For styrene, the formation of the branched product is favoured by electronic reasons. The mechanism of the rhodium catalysed hydroformylation of styrene has been studied and the accepted catalytic cycle is displayed in Scheme 5.1.[3]

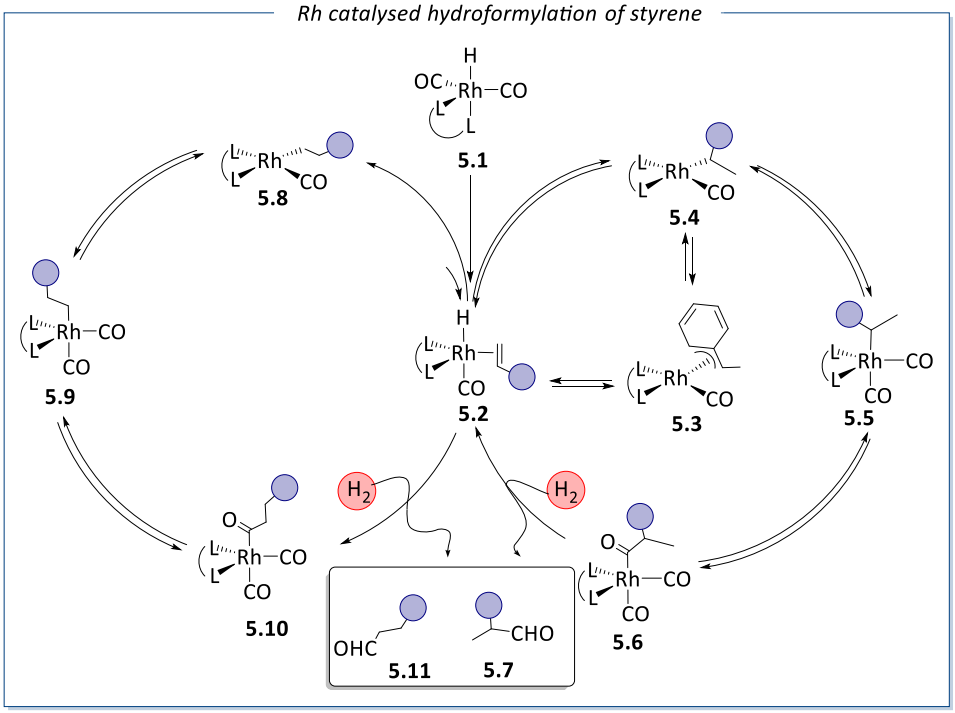

Scheme 5.1. Proposed mechanism for the rhodium catalysed hydroformylation of styrene.

In this mechanism, the formation of the rhodium alkyl intermediates **5.5** and **5.9** from the rhodium hydride species **5.2** is the key step controlling the regioselectivity. Lazzaroni and co-workers showed that in this reaction, the kinetic product is the branched aldehyde **5.7** and is therefore favored when the reaction is conducted at low temperature.[3] The formation of this product is favored by the formation of the stable Rh(η^3-allyl) species **5.3**, which is in equilibrium with the branched Rh-alkyl species **5.4** that is at the origin of the production of the branched aldehyde. The presence of these species tends to shift the equilibrium towards the catalytic cycle affording the branched product.[1] In these studies, the effect of the temperature was shown to affect the regioselectivity of the overall process and isotopic labeling experiments demonstrated that the formation of both linear and branched Rh-alkyl species is irreversible at low temperature but becomes reversible at high temperature.[3] Brown and Kent reported that the coordination mode of the phosphine ligands could also influence the regioselectivity of the reaction: the steric hindrance provided by the ee:ee (equatorial:equatorial) coordination favors the formation of the linear aldehyde while the eq:ax (equatorial:axial) coordination of the ligand favors the formation of the branched product.[4] There are only a few examples in the literature concerning the selective formation of the linear aldehyde in the Rh-catalysed hydroformylation of styrene.[5,6,7,8] The most relevant systems providing the regioselective linear hydroformylation of styrene are those presenting a large natural bite angle, such as **5.13** and **5.14** (Figure 5.2), and those presenting an atropoisomeric backbone such as **5.15** and **5.16**.

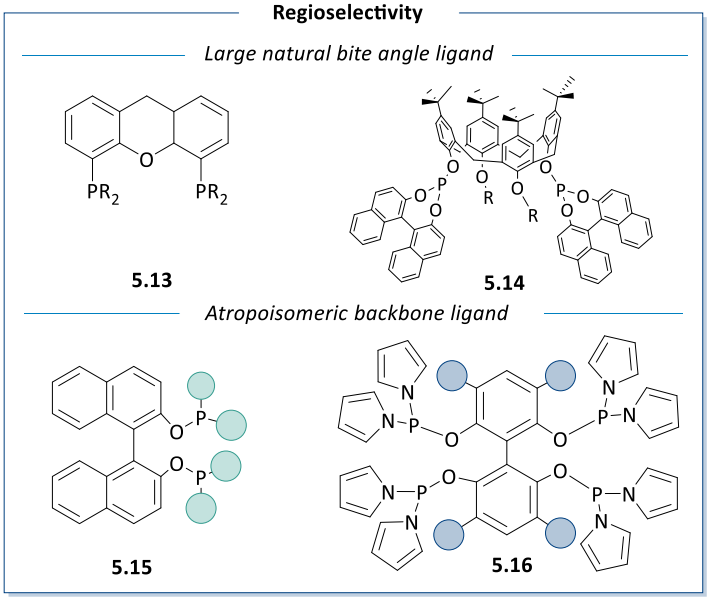

Figure 5.2. Ligands reported to provide high linear regioselectivity in the Rh-catalysed hydroformylation of styrene.

Specifically, in the following sections, we will describe the most relevant systems providing the regioselective linear hydroformylation of styrene, presenting an atropoisomeric backbone.

5.1.2 Rh-catalysed hydroformylation of styrene: atropoisomeric backbone ligand

The recent ligands providing high linear selectivity in the Rh-catalysed hydroformylation of styrene containing an atropoisomeric backbone are based on either bis(hydroxy)phenol or binaphthol structures. The results reported for these ligands will be described in the following sections.

5.1.2.1 Tetraphosphorus binol-based ligands

One family of ligands able to effectively promote the formation of the linear aldehyde from styrene is based on a bis(hydroxy)phenol scaffold containing

four phosphorus atoms (Ligand 5.16, Scheme 5.3) that was developed by Zhang and co-workers.[8,9]

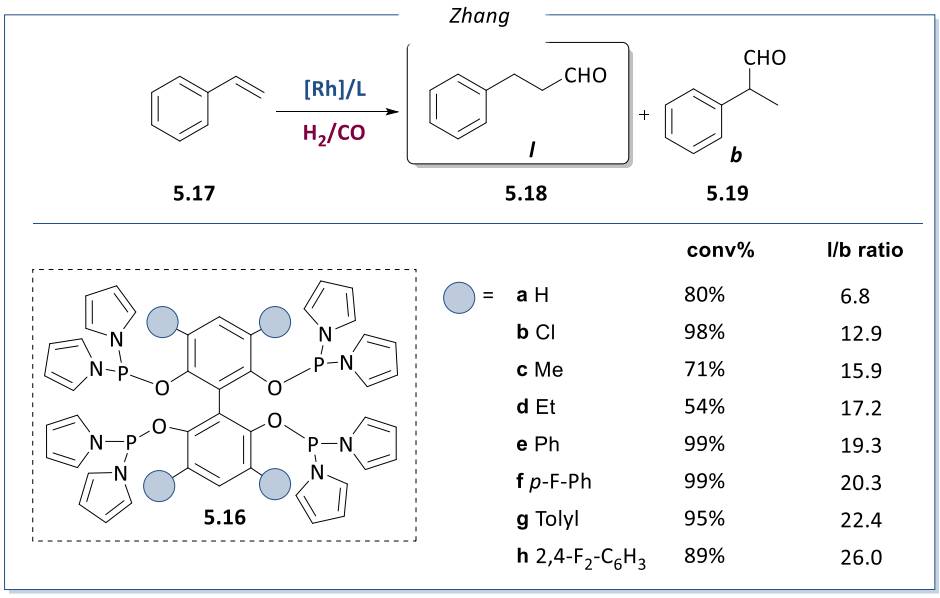

Scheme 5.3. Styrene hydroformylation with tetraphosphorus derivatives reported by Zhang.

Using these ligands, the hydroformylation of styrene **5.17** was carried out at 80 °C and 10 bar of 1:1 CO/H_2 using a 1.0 mM solution of rhodium pre-catalyst and 3 equivalents of ligand. These results clearly indicated that an increase in steric bulk in 3,3'-5,5' positions of the biphenyl moiety favour the regioselectivity of the reaction towards the linear aldehyde while the electronic properties of the ligand mainly affect the catalytic activity. Indeed, the use of ligand **5.16b** bearing a chloride substituent increased the linear to branched ratio from 6.8 to 12.9 when compared to the unsubstituted ligand. Similar regioselectivity was obtained using the alkyl substituted ligands **5.16c** and **5.16d** although in these latter cases, the conversion dropped significantly. Further increase in steric hindrance (and 120 °C instead of 80 °C) of the ligands by introduction of aryl substituents provided l/b ratios up to 26. The difference observed between the catalytic performance of **5.16g**

and **5.16h** was attributed to an electronic effect since similar steric hindrance is expected for both ligands. They concluded that for two ligands exhibiting similar steric hindrance, the presence of electron withdrawing groups like in **5.16h** favours the formation of the linear aldehyde. To explain these excellent results, the authors postulated that the high steric hindrance at the ortho position could inhibit the formation of the η^3-benzylic rhodium coordination that favours the formation of the branched aldehyde, and therefore results in a higher linear regioselectivity. To better understand these results, the Hammett constants for *para* substituent on phenyl group of ligands **5.16a** to **5.16h** were analysed. The Hammett equation, which explains the influence of the aromatic substituents can be simply expressed using two different kinetic constants; one for the formation of linear aldehyde **5.18** and one for the branched aldehyde **5.19**. Their results clearly showed that an electron-withdrawing group had a positive effect on the linear selectivity. The highest linear selectivity was afforded by ligand **5.16h** (Scheme 5.3, l/b ratio of 26), which bears two strong electron-withdrawing CF_3- groups on the phenyl ring (Hammet constant $\sigma_p = 0.4$).

5.1.2.2 Bidentate binaphthol based ligand

The second family of atropoisomeric ligands that provided high selectivity to the linear aldehyde is constituted by binaphthol based ligands, which had been previously applied in several other catalytic reactions.[10,11] In 2013, Vogt et al. compared the catalytic performance of a series of rhodium catalysts bearing various bidentate ligands: four binaphthol based ligands (**5.15a-d**, Scheme 5.4), one tetraphosphorus ligand (**5.16a**) and one Xantphos derivative (**5.20**).[12]

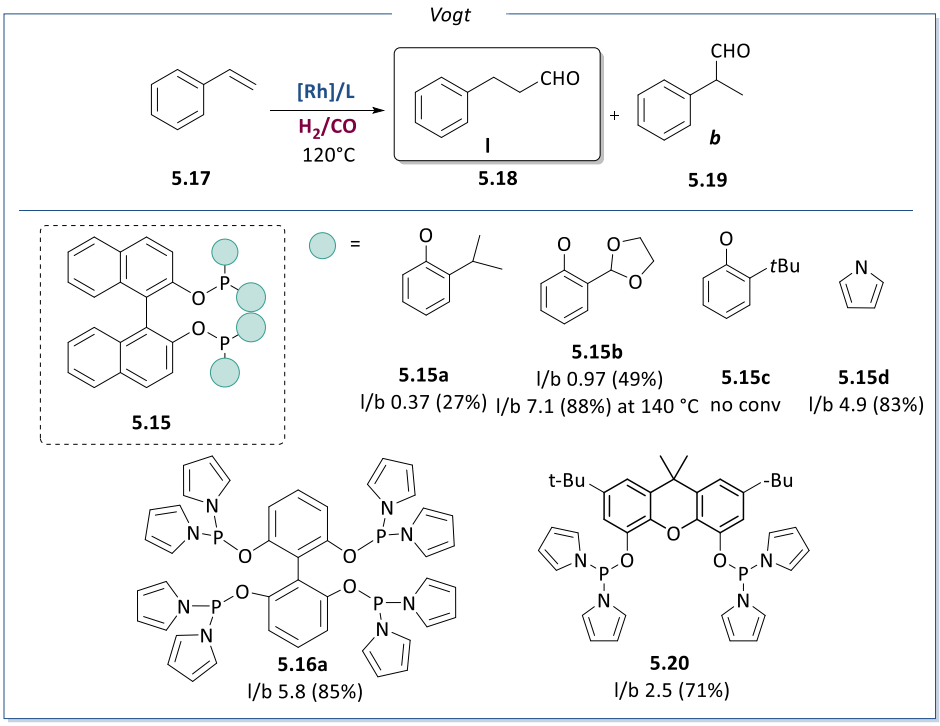

Scheme 5.4. Rh-catalysed hydroformylation of styrene using binaphthol derivatives and phosphorodiamidite based ligands.

The binaphthol based ligands **5.15a**, **5.15b** and **5.15d** showed good activity, while **5.15c** did not provide any conversion. The absence of activity in the latter case was attributed to the high steric hindrance induced by the *tert*-butyl groups in the ortho position of the phenoxy moiety on the ligand. When the reaction was performed with ligand **5.15b** at 140 °C, an increase in linear to branched ratio up to 7.1 was observed, although a higher amount of the hydrogenation product was also detected. The highest regioselectivities at 80 °C were obtained with the pyrrole substituted ligands **5.15d**, **5.16a** and **5.20**, indicating that ligands with more pronounced π-accepting properties favour the linear product under these conditions. In 2013, Zheng and co-workers compared a series of ligands based on various types of backbones.[13] Eight different ligand backbones were tested under the same conditions and the

ligands that contain the pyrrole moiety showed better performance in terms of regioselectivity for the linear aldehyde (Scheme 1.12).

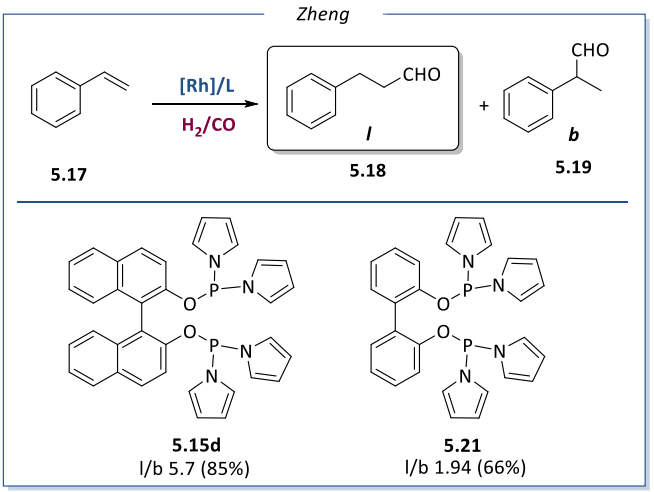

Scheme 5.5. Comparison of the results reported by Zheng on the Rh-catalysed hydroformylation of styrene using binaphthol and BINOL-based ligands.

The binaphthol based ligand **5.15d** provided the highest regioselectivity with 85% of linear aldehyde. Interestingly, the ligand **5.21**, which presents structural properties related to those of **5.15d**, provided much lower selectivity to the linear aldehyde under the same conditions, indicating that the atropoisomeric backbone is key to reach high selectivity in this reaction.

5.2 Objectives

The main objective of this chapter is the development of a novel family of bis(dipyrrolyl-phosphorodiamidite) and bis(dipyrazolyl-phosphorodiamidite) ligands which could provide the formation of the linear aldehyde in the rhodium catalysed hydroformylation of styrene.

The specific objectives of this chapter are:

- The synthesis of bis(dipyrrolyl-phosphorodiamidite) ligands using commercially available diols and amines.

- The synthesis of bis(dipyrazolyl-phosphorodiamidite) ligands using commercially available pyrazole and its commercial derivatives.
- The study of the effect of commercial ligands on the rhodium catalysed styrene hydroformylation reaction outcome.
- The study of the effect of rhodium to ligand ratio and temperature control on the reaction outcome.
- The study of the effect of the rhodium loading, the pressure and the temperature on the reaction outcome.
- The study of the effect of the rhodium catalysts containing newly synthesised ligands, in the selective production of the linear aldehyde in the hydroformylation of styrene.

5.3 Results and discussion

Inspired by the ligand structure described by Vogt and co-workers, we proposed some modification over the backbone structure, in order to get insight into the regioselective formation of the linear aldehyde from styrene.[12]

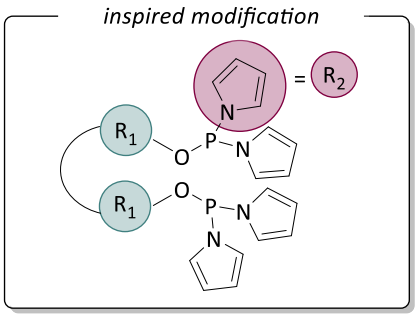

Figure 5.6. Inspired modification over the structure of ligand **5.15**, reported by Vogt.

As depicted in figure **5.6**, we envisioned to modify the scaffold of ligand **5.15** through two approaches: first, on the phosphite backbone R_1, next, one the nitrogen-heterocycle R_2.

5.3.1 Synthesis of bis(dipyrrolyl-phosphorodiamidite) ligands

The synthesis of the novel ligand bearing bis(dipyrrolyl) moieties was proposed as a two-step synthesis as depicted in Scheme 5.6, based on reported literature procedure.[14,18]

- In the first step, pyrrole **5.22** reacts with PCl_3 and Et_3N in THF at -40 °C and then at room temperature overnight, as previously reported in the literature.[14] The corresponding phosphochloridite intermediate **5.23** was obtained in 96% yield after distillation under inert atmosphere.
- In the second step, the intermediate **5.23** was reacted with several diols and diamines **5.24** to afford the corresponding compounds **5.25**.[12]

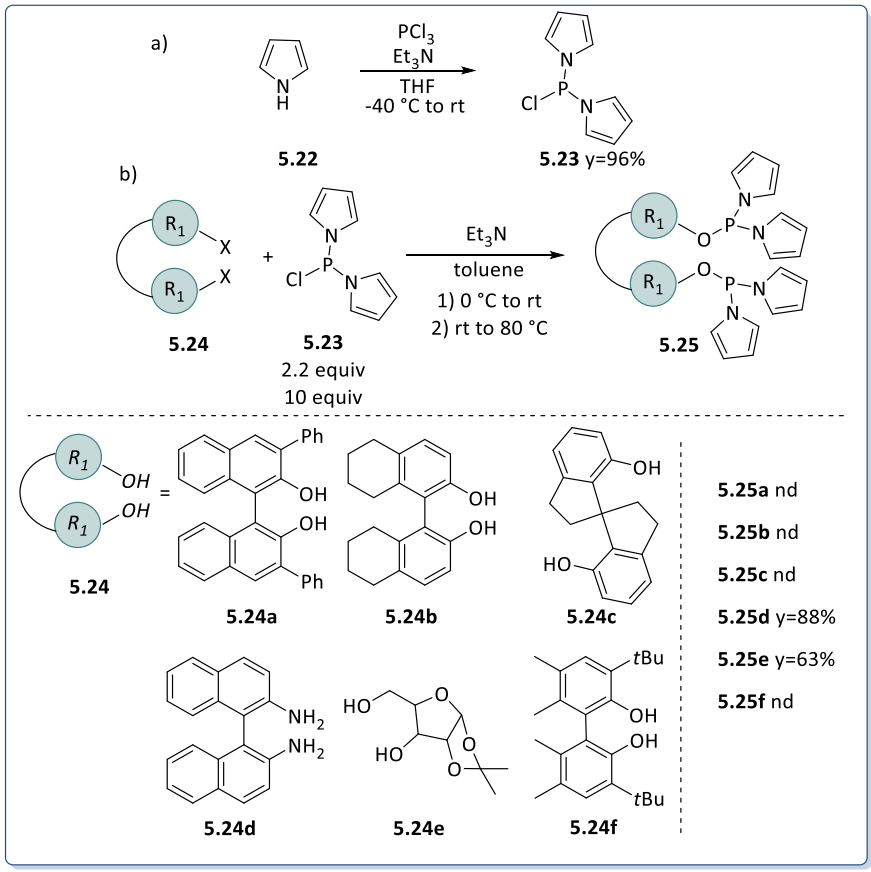

Scheme 5.6. Synthesis of binaphthol-based ligands with pyrrole substituents

When employing 2 equivalents of **5.23** in combination with diol **5.24a**, monitoring the reaction *via* ^{31}P $\{^{1}H\}$ NMR, no formation of the desired product was observed. To this end, 10 equivalents of **5.23** were employed to enhance the formation of the bis dipyrrolyl ligand with diol **5.24a**, but no product formation was observed. As a last attempt, the reaction mixture was further heated up to 80 °C. However, the (dipyrrolyl-phosphorodiamidite) ligand **5.25a** was once more not detected. Similar behaviour was observed when **5.24b** and **5.24c** were used as starting diols. When 2.2 equivalents of the commercial BINAM **5.24d** were employed, the formation of a product was observed *via* ^{31}P $\{^{1}H\}$ NMR, where a signal at 113 ppm was detected. Complete NMR and ESI mass spectrometry characterization suggested that

the product formed was the bis dipyrrolyl-phosphorodiamidite ligand **5.25d** in 88% yield. Using the commercial isopropylidene-*α*-*D*-xylofuranose **5.24e**, a new peak at 114 ppm was observed *via* $^{31}P\{^{1}H\}$ NMR, which was ascribed to the expected bis dipyrrolyl-phosphorodiamidite ligand **5.25e**. The reaction crude was purified by filtration under inert atmosphere and over neutral alumina, delivering the compound **5.25e** in 63% yield. NMR analysis confirmed the purity of this ligand. When 2.5 equivalents of the commercial biphenol **5.24f** were employed, the formation of a new product was observed by $^{31}P\{^{1}H\}$ NMR where a new peak 125 ppm was detected.

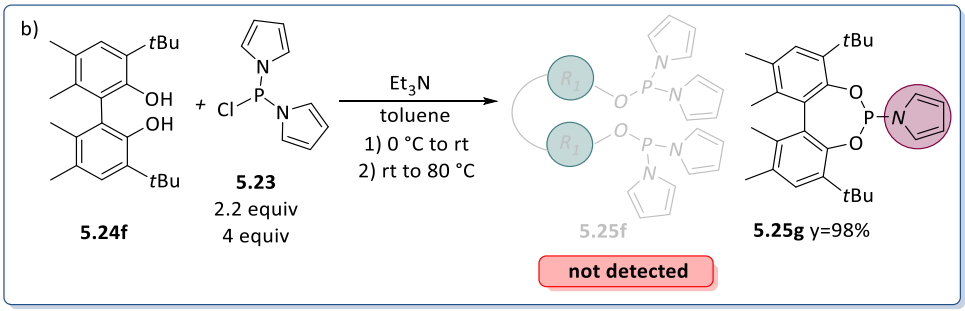

Scheme 5.7. Synthesis of binaphthol-based ligands with pyrrole substituents

However, complete NMR and ESI mass spectrometry characterization suggested that the product formed was phosphoramidite ligand **5.25g**. In order to shift the selectivity towards ligand **5.25f**, 4 equivalents of **5.23** were employed during the synthesis. Though, the sole formation of **5.25g** was again observed in 98% yield (Scheme 5.7). Nonetheless, with this new family of ligands in hand, we investigated their activity and selectivity in the hydroformylation of styrene in combination with $Rh(acac)(CO)_2$ as metal precursor.

5.3.2 Synthesis of bis (dipyrazolyl-phosphorodiamidite) ligands

In order to achieve the second type of modification, namely the introduction of various nitrogen-based heterocycles within the scaffold of **5.15** in Figure

5.6, 2,5-dimethylpyrrole **5.26** was first employed. In this case, we envisioned a two-step procedure where the nitrogen-based heterocycle was first reacted with PCl_3 to afford the corresponding phosphochloridite that was subsequently converted into the desired bis-phosphorodiamidite. For this purpose, in the specific case of the synthesis of the bis (2,5-dimethylpyrrole) phosphochloridite **5.28**, several conditions have been screened, as described in scheme 5.8.[14,15]

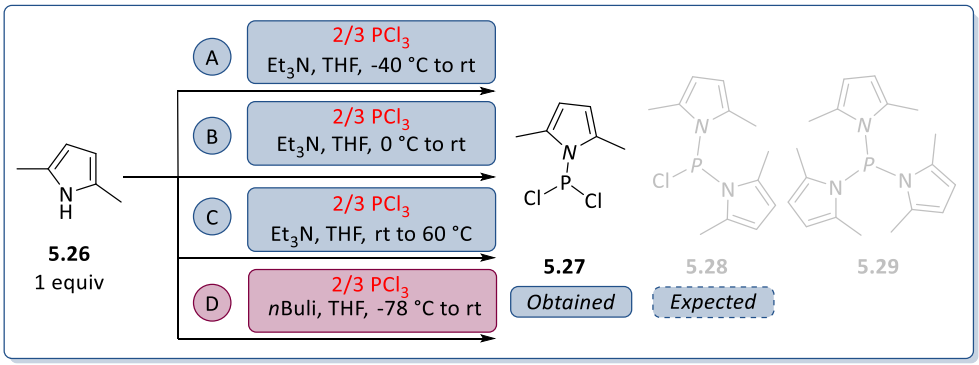

Scheme 5.8. Attempts for the synthesis of the phosphochloridite intermediate

First, the commercial di-methyl pyrrole **5.26** was reacted with PCl_3, in the presence of Et_3N as base. The addition of PCl_3 was performed at -40 °C (**A**), 0 °C (**B**) and room temperature (**C**) and the mixture was left stirring overnight at room temperature (**A** and **B**) or at 50 °C (**C**). However, in all the cases, product **5.27** derived from the reaction of only one pyrrole unit, was obtained. To increase the nucleophilicity of the amine, the use of *n*-BuLi was also probed (**D**). However, also in this case, the selective formation of product **5.27** was observed.

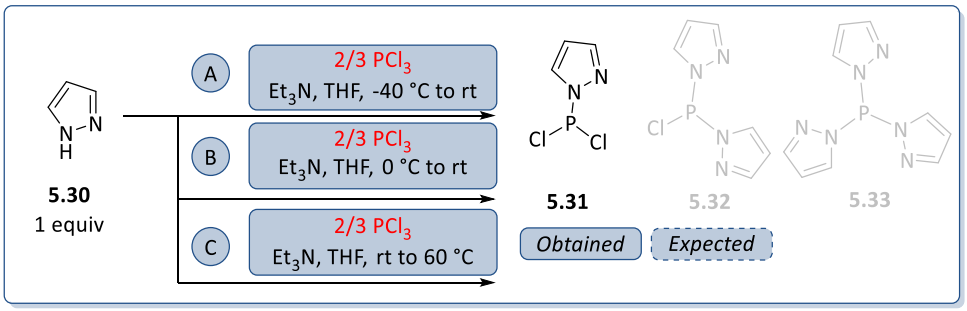

Scheme 5.9. Attempts for the synthesis of the phosphochloridite intermediate

The same approach was then applied with the pyrazole **5.30** to promote the formation of derivative **5.32** (Scheme 5.9). The addition of PCl_3 was performed at - 40 °C (**A**), 0 °C (**B**) and room temperature (**C**) and the mixture was left stirring overnight at room temperature (**A** and **B**) or at 50 °C (**C**). Also in this case, the sole formation of compound **5.31** was observed.

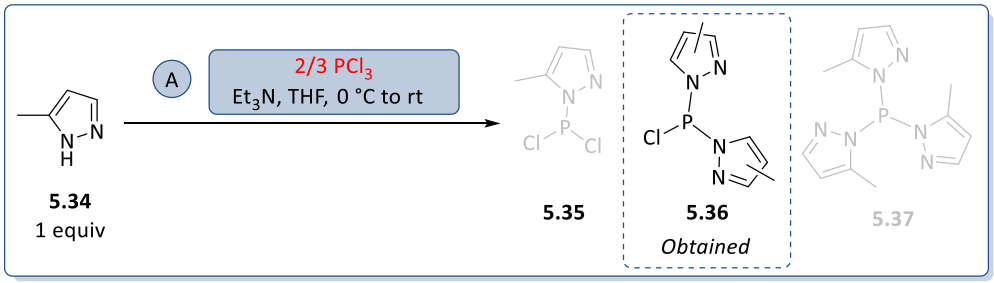

Scheme 5.10. Synthesis of phosphochloridite intermediate

On the other hand, when methyl-pyrazole **5.34** was employed as reagent, added at 0 °C, the reaction smoothly proceeded overnight, with 90% yield (Scheme 5.10). Compound **5.36** was obtained through filtration under inert atmosphere.

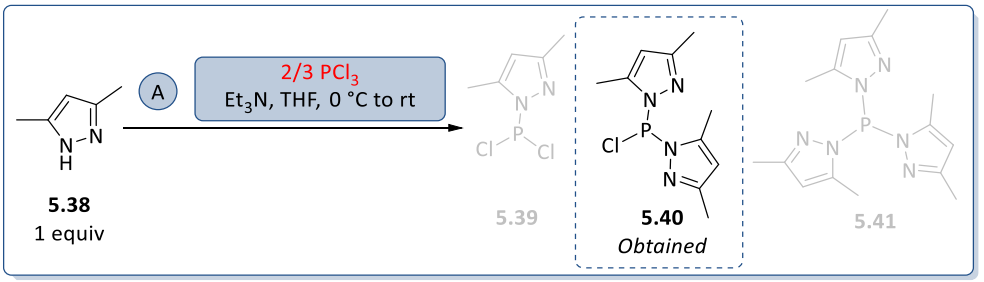

Scheme 5.11. Synthesis of phosphochloridite intermediate

Similarly to methyl pyrazole **5.34**, the reaction proceeded smoothly when dimethyl pyrazole **5.38** is added at 0 °C, with 80% yield (Scheme 5.11). The compound **5.40** was obtained through filtration under inert atmosphere.

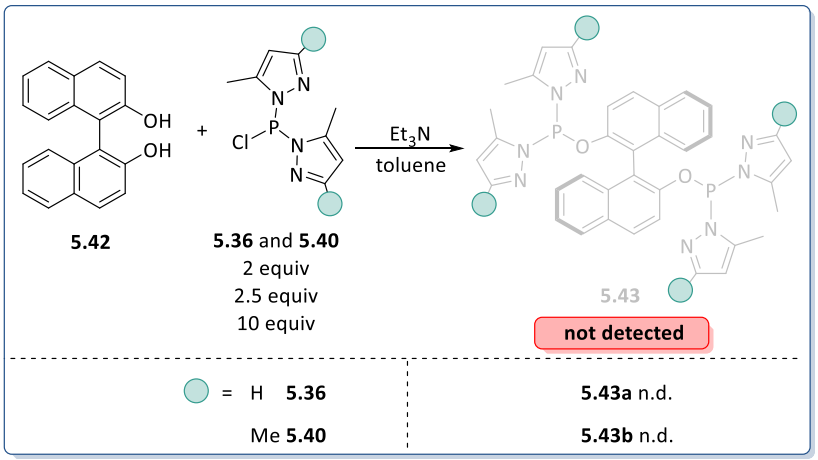

Scheme 5.12. Attempts for the synthesis of binaphthol-based ligands with pyrazole substituents

At this point, the commercial binaphthol **5.42** was reacted in THF at room temperature in the presence of Et_3N with either 2, 2.5 or 5 equivalents of the previously synthesised compounds **5.36** or **5.40**. In all the cases, monitoring *via* $^{31}P\{^1H\}$ NMR, several peaks were detected, suggesting that the reaction is probably not selective towards the formation of **5.43**. Additionally, attempts in the purification of the resulting crude did not afford the expected product. In order to gain further insight about the reaction, it was decided to monitor the reaction *via* $^{31}P\{^1H\}$ NMR.

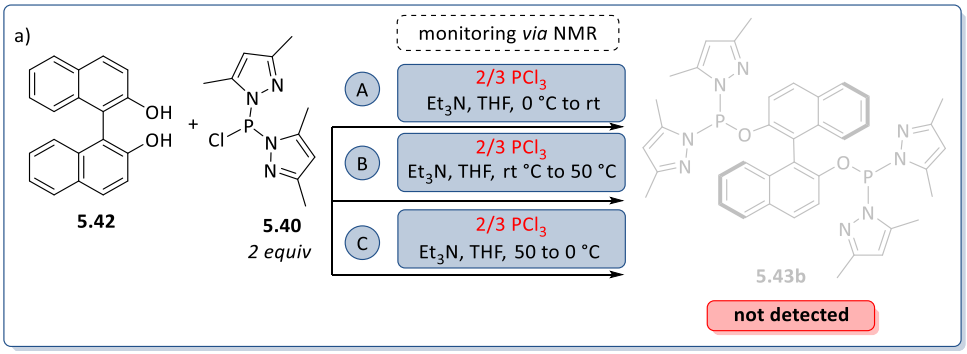

Scheme 5.13. Attempts for the synthesis of binaphthol-based ligands with pyrazole substituents

Upon addition of diol **5.42** on dimethyl pyrazole **5.40**, the appearance of several peaks between 140 and 150 ppm by ^{31}P $\{^{1}H\}$ NMR was observed. Subsequently, upon heating the reaction at 50 °C for 3 hours, the number of peaks in that region increased. The same situation was observed also while keeping the reaction at 50 °C overnight or after cooling down the reaction at 0 °C for 1 hour, pointing toward a detrimental effect of the temperature in this reaction. An explanation of what was observed during the reaction is that, after the addition of **5.42** to intermediate **5.40**, HCl is released. The latter could promote a protonation of the product **5.43b**, which could explain the presence of the several peaks observed in the range of 140-150 ppm by ^{31}P $\{^{1}H\}$ NMR when running the reaction at 50 °C. On the other hand, when running the reaction at a lower temperature (0 °C), the protonation of **5.43b** is less favoured, delivering a cleaner reaction. It was concluded that the proposed modification (Figure 5.6) over the pyrrole moiety within ligand **5.15** was detrimental in the synthesis of the desired ligand.

5.3.3 Optimization of Rh-catalysed hydroformylation of styrene

In order to evaluate and compare the efficiency of the ligands previously synthetized, it was decided to test them in the hydroformylation of styrene with the aim of obtaining the linear aldehyde. First, commercially available

ligands were employed to carefully optimize the reaction conditions based on previous reports by Van Leeuwen.[7] Subsequently, with the optimized conditions in hand, the newly synthetised ligands have been tested.

5.3.3.1 Xantphos ligand

To explore the influence of the reaction conditions in the catalytic regime, different parameters were varied and the initial experiments were performed using Xantphos **5.47** as ligand, following the catalytic conditions reported by Van Leeuwen and co-workers.[7] The styrene hydroformylation process was carried out at 120 °C and 10 bar of 1:1 CO/H_2 using a 0.5 mM solution in toluene of rhodium pre-catalyst $Rh(acac)(CO)_2$ and 10 equivalents of ligand **5.47**.

Table 5.1. Rh-catalysed hydroformylation of styrene using Xantphos **5.47** as ligand[a]

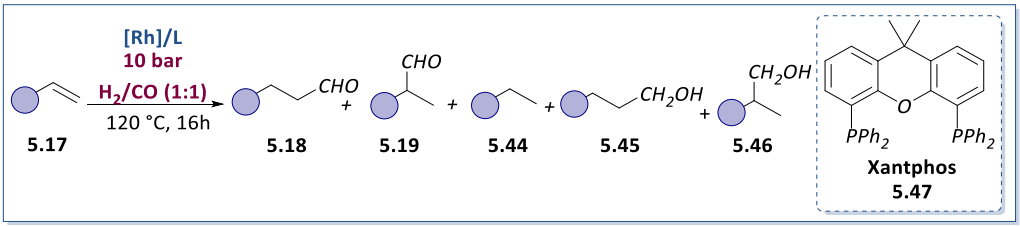

Entry [a]	Conv (%)	5.18 (%)	5.19 (%)	5.44 (%)	5.45 (%)	5.46 (%)	l/b (5.18/5.19)
1	69	48	26	2	16	7	**1.80**
2[b]	>99	38	28	2	20	11	**1.40**
3[b,c]	90	37	22	32	6	3	**1.70**
4[b,d]	>99	54	35	3	5	3	**1.50**
5[b,e]	>99	41	31	3	16	10	**1.30**

Reaction conditions:[a] styrene **5.17** (7.51 mmol), $Rh(acac)(CO)_2$ 0.057 mol%, 10 mol% ligand **5.47**, toluene (1.7 ml), 10 bar $CO:H_2$ (1:1), 120°C for 16 hours. Conversion, chemoselectivity and regioselectivity determined by GC-FID and NMR using bicyclohexyl as internal standard. [b] styrene 5.17 (1.55 mmol). [c] no ligand employed. [d] $[Rh(COD)(\mu Cl)]_2$ as Rh precursor. [e] DCM as solvent.

The reaction was carried out using Rh:L:Substrate=1:10:1764, based on 7.51 mmol of styrene (Entry 1, Table 5.1). Under these conditions, at the end of the reaction, it was observed that the total pressure in the autoclave had decreased to 2 bar and the substrate was not fully converted into the corresponding aldehydes (69% conversion). The linear to branched ratio obtained was 1.8, which was higher than that described by Van Leeuwen (1.45). These observations were attributed to the low pressure in the reactor due to the consumption of the syngas under these conditions, which decreased the reaction rate and favoured the formation of the linear product. Furthermore, the presence of the branched and linear alcohol (**5.45** and **5.46**) as reaction products (23% in total) was also detected. Later, the reaction was performed using the same Rh:L:Substrate ratio, but the overall amounts of reagents were scaled down using 1.55 mmol of styrene (Entry 2, Table 5.1). The conversion increased up to >99%, the linear to branched ratio observed was 1.4 as the one proposed by Van Leeuwen, but the amount of alcohol as reaction by-product increased up to a total of 31%. The formation of this by-product has been already observed in Rh-catalysed hydroformylation processes, involving the use of a biphasic system[16] (water and toluene) or Xantphos supported on silica.[17] In order to investigate the origin of the formation of alcohols, various parameters were varied. The catalytic reaction was performed without ligand (Entry 3, Table 5.1), using $[Rh(COD)(\mu Cl)]_2$ as a rhodium precursor (Entry 4, Table 5.1), and using DCM as solvent (Entry 5, Table 5.1). However, in all these experiments, the presence of the alcohols as by-product of the reaction was detected. In view of these results, a series of other commercially available ligands was tested for the styrene hydroformylation process.

5.3.3.2 Ligand screening

Commercially available ligands with large natural bite angle were tested in the rhodium catalysed hydroformylation of styrene under the conditions

reported by van Leeuwen and co-workers for Xantphos **5.47** (Table 5.2, Entries 1-6).[7] The styrene hydroformylation process was carried out at 120 °C and 10 bar of 1:1 CO/H_2 using a 0.5 mM solution in toluene of rhodium pre-catalyst $Rh(acac)(CO)_2$ and 10 equivalents of ligand.

Table 5.2. Rh-catalysed hydroformylation of styrene using commercial ligands[a]

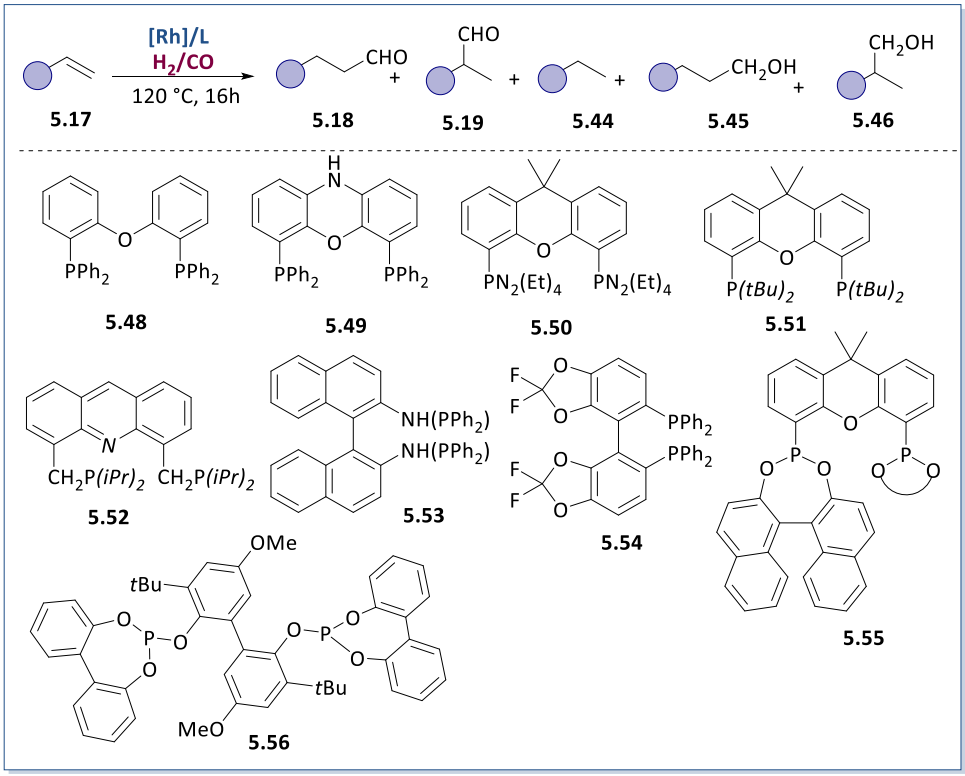

Entry[a]	L	Conv (%)[a]	5.18 (%)	5.19 (%)	5.44 (%)	5.45 (%)	5.46 (%)	l/b
1	**5.48**	>99	41	49	3	3	4	**0.80**
2	**5.49**	>99	39	26	3	21	11	**1.50**
3	**5.55**	83	54	34	6	5	1	**1.50**
4	**5.50**	57	29	41	4	16	10	**0.70**
5	**5.51**	82	49	43	4	1	3	**0.60**
6	**5.52**	10	35	60	5	-	-	**0.60**
7	**5.53**	97	52	34	7	4	2	**1.52**
8[b]	**5.54**	62	31	65	4	-	-	**0.50**

9	**5.54**	84	30	67	1	0.5	2	**0.44**
10	**5.56**	>99	62	31	7	-	-	**2.0**

Reaction conditions:[a] styrene **5.17** (1.55 mmol), $Rh(acac)(CO)_2$ 0.057 mol%, 10 mol% ligand, toluene (1.7 ml), 10 bar $CO:H_2$ (1:1), 120°C for 16 hours. Conversion, chemoselectivity and regioselectivity determined by GC-FID and NMR using bicyclohexyl as internal standard. [b] 2.0 mol% ligand **5.54,** DCM as solvent.

Under these conditions, using ligands DPEphos **5.48** and the related *N*-Xantphos **5.49**, the conversion was quantitative. The DPEphos **5.48** provided a low linear to branched ratio (0.8) together with only 7% of alcohol as subproduct. In contrast, the *N*-Xantphos **5.49** ligand provided l/b= 1.5 together with 30% of alcohol. This latter value was in agreement with the results previously reported by Van Leeuwen.[7] Ligand **5.55**, provided a linear to branched ratio of 1.6 and 83% of conversion (Entry 3). Using ligands **5.50, 5.51** and **5.52** (Entries 4, 5 and 6, Table 5.2), lower conversions of the starting material were obtained with low selectivities to the linear product (l/b= 0.7, 1, and 0.6, respectively). All the experiments show the presence of the alcohols as by-products of the reaction, except for ligand **5.52** (Entry 6, Table 5.2). Ligands with an atropoisomeric backbone were then tested (Entries 7- 10). When BINAM **5.53** was tested (Entry 7, Table 5.2), high conversion (97%) was obtained, together with a linear to branched ratio of *ca*. 1.5. The Difluorophos **5.54** was tested in DCM and toluene as solvents (Entries 8 and 9, Table 5.2). In both cases, the linear to branched ratio was very low (0.5). In toluene, the amount of alcohols formed was 2.5% in total while in DCM, no formation of the alcohol was observed. When the BiphePhos ligand **5.56** was used (Entry 10, Table 5.2), total styrene conversion and no formation of the alcohol was observed. Furthermore, the highest linear to branched ratio observed in this ligand screening (l/b= 2) was obtained.

5.3.3.3 Rhodium to substrate ratio effect

In order to observe the influence of the loading of the catalyst, the rhodium loading was varied from 0.057 mol% to 0.00057 mol%, but keeping the same rhodium to ligand ratio (Rh:L 1:10) using ligand BiphePhos **5.56** (Table 5.3).

Table 5.3. Rh loading optimization in the Rh-catalysed hydroformylation of styrene using ligand **5.56**[a]

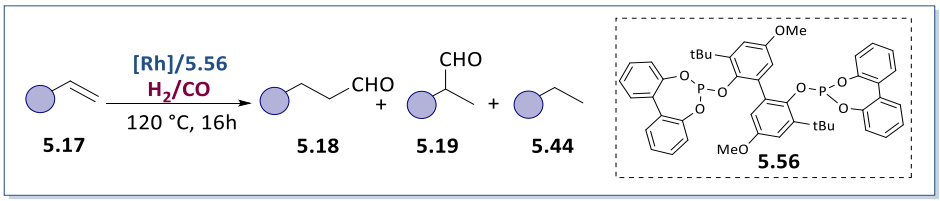

Entry [a]	Rh loading (mol%)	Conv (%)[a]	Chemo (%)	l/b
1	**0.057**	>99	96	**1.70**
2	**0.029**	>99	96	**1.80**
3	**0.0145**	>99	96	**1.60**
4	**0.0057**	90	95	**1.50**
5	**0.00145**	30	87	**1.23**
6	**0.00057**	25	84	**1.40**

Reaction conditions:[a] styrene **5.17** (1.55 mmol), $Rh(acac)(CO)_2$ as rhodium precursor, 10 mol% ligand **5.47**, toluene (1.7 ml), 10 bar $CO:H_2$ (1:1), 120°C for 16 hours, temperature measured by termocouple in the oil bath. Conversion, chemoselectivity and regioselectivity determined by GC-FID and NMR using bicyclohexyl as internal standard.

Surprisingly, when the rhodium loading was lowered four times (to 0.0145 mol%), both conversions and l/b remained unchanged (Entries 1-3, Table 5.3). At lower loadings, the conversion was observed to decrease from 99% to 25% at 0.00057 mol% of rhodium (Entry 6, Table 5.3). In all the cases, no relevant variation in regioselectivity was observed. Next, the effect of the Rh/L ratio at a rhodium loading of 0.0057 mol% was explored and the results are summarised in Table 5.4.

Table 5.4. Rh/L ratio optimization in the Rh-catalysed hydroformylation of styrene using ligand **5.56**[a]

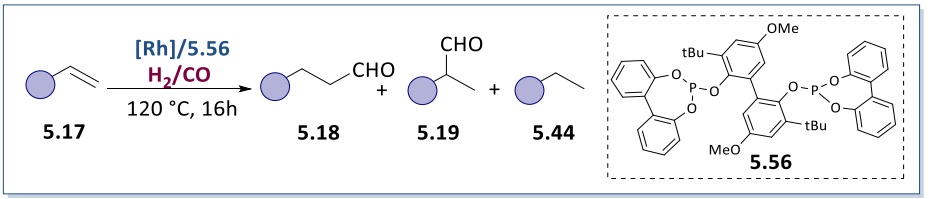

Entry[a]	Rh/L ratio	Conv (%)[a]	Chemo (%)	l/b
1	**1:2**	68	96	**1.40**
2	**1:4**	70	92	**1.30**
3	**1:8**	85	94	**1.30**
4	**1:10**	90	95	**1.50**
5	**1:20**	95	96	**1.40**
6	**1:40**	>99	99	**1.50**

Reaction conditions:[a] styrene **5.17** (1.55 mmol), Rh(acac)$(CO)_2$ 0.0057 mol%, toluene (1.7 ml), 10 bar CO:H_2 (1:1), 120°C for 16 hours, temperature measured by termocouple in the oil bath. Conversion, chemoselectivity and regioselectivity determined by GC-FID and NMR using bicyclohexyl as internal standard.

The rhodium to ligand ratio was increased from 1:2 to 1:40 while the others reaction conditions remained constant. In this series of experiments, a constant increase in conversion from 68 to >99% was observed when the rhodium to ligand ratio was increased from 1:2 to 1:40. In contrast, the regioselectivity of the reaction remained quite unaltered in all experiments. These results therefore clearly indicated that the metal to ligand ratio affect the activity but not the regioselectivity.

5.3.3.4 Pressure effect

Next, the effect of the total syngas pressure was investigated at 120 °C and using the BiphePhos ligand **5.56** (Table 5.5). Pressures of 5, 10 and 15 bars were probed using Rh/L ratios of 1:8 (Entries 1-3) and 1:10 (Entries 4-6).

Table 5.5. Pressure optimization in the Rh-catalysed hydroformylation of styrene ligand **5.56**[a]

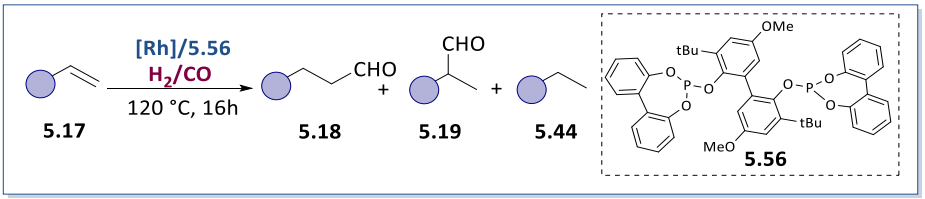

Entry	Rh/L ratio	P_{total} (bar)	Conv (%)[a]	Chemo (%)	l/b
1	**1:8**	**15**	96	95	**1.2**
2	**1:8**	**10**	85	94	**1.3**
3	**1:8**	**5**	94	96	**2.2**
4	**1:10**	**15**	96	93	**1.2**
5	**1:10**	**10**	90	95	**1.6**
6	**1:10**	**5**	96	94	**2.4**

Reaction conditions:[a] styrene **5.17** (1.55 mmol), $Rh(acac)(CO)_2$ 0.0057 mol%, toluene (1.7 ml), $CO:H_2$ (1:1), 120°C for 16 hours, temperature measured by termocouple in the oil bath. Conversion, chemoselectivity and regioselectivity determined by GC-FID and NMR using bicyclohexyl as internal standard.

The optimization process was completed maintaining the same amount of rhodium precursor (Rh 0.0057 mol %), with two different rhodium to ligand ratios (1:8 and 1:10), and varying the pressure from 5 to 15 bar. When the syngas pressure was lowered, no relevant differences in terms of conversions were observed, while an increase in the selectivity to the linear aldehyde from 1.2 to 2.2 l/b was detected. Overall, these experiments showed that, under these reaction conditions, the regioselectivity is not affected by the rhodium to ligand ratio.

5.3.3.5 Temperature effect

Subsequently, the role of the temperature on the regioselectivity of this hydroformylation process was assessed. These experiments were performed using the same amount of rhodium precursor (Rh 0.0057 mol %) and two

different rhodium to ligand ratio (1:8 and 1:10) under a total pressure of 5 bar. The temperature was varied from 90 to 150 °C (Table 5.6).

Table 5.6. temperature optimization in the Rh-catalysed hydroformylation of styrene using ligand **5.56**[a]

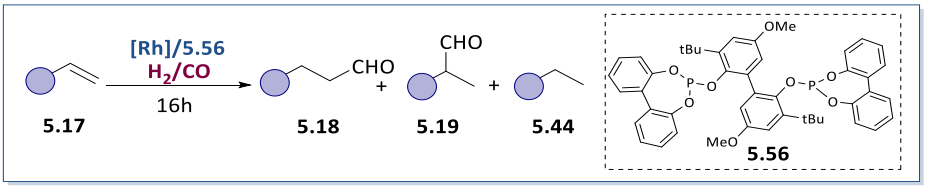

Entry	Rh/L ratio	T °C	Conv (%)[a]	Chemo (%)	l/b
1	**1:8**	**90**	78	93	**1.6**
2	**1:8**	**120**	94	95	**2.2**
3	**1:8**	**150**	>99	89	**3.1**
4	**1:10**	**90**	80	96	**1.5**
5	**1:10**	**120**	96	94	**2.4**
6	**1:10**	**150**	>99	89	**3.0**

Reaction conditions:[a] styrene **5.17** (1.55 mmol), $Rh(acac)(CO)_2$ 0.0057 mol%, toluene (1.7 ml), 5 bar $CO:H_2$ (1:1), 120°C for 16 hours, temperature measured by termocouple in the oil bath. Conversion, chemoselectivity and regioselectivity determined by GC-FID and NMR using bicyclohexyl as internal standard.

When the temperature was lowered down to 90 °C, the conversion dropped to 78% and the selectivity to the linear aldehyde decreased from 67 to 58% (Entries 1-4). When the temperature was increased up to 150 °C, no relevant difference in terms of conversion was observed, however the linear to branched ratio increased up to 3.1, although the chemoselectivity dropped: the formation of by-products coming from the hydrogenation of the aldehydes became more prominent. These results are in agreement with the results observed in the first part of the optimization (Section 5.4.1). After this extensive optimization screening, the best conditions, using the Biphephos ligand **5.56**, are the one depicted in Entry 3: using 1:8 Rh/L ratio, a $[Rh(acac)(CO)_2]$ loading of 0.0057 mol% and with a total syngas pressure of

5 bar on a 1:1 ratio. Under this set of conditions, the product was obtained with a linear to branched ratio of 3.1.

5.3.3.6 Optimization using ligand 5.15d

In view of the excellent results reported by Vogt in the rhodium hydroformylation of styrene with ligand **5.15d**, it was decided to evaluate the influence of crucial parameters, such as temperature, rhodium to ligand ratio, total and partial CO:H_2 pressure (Table 5.7).[12]

Table 5.7. Optimization in the Rh-catalysed hydroformylation of styrene using ligand **5.15d**[a]

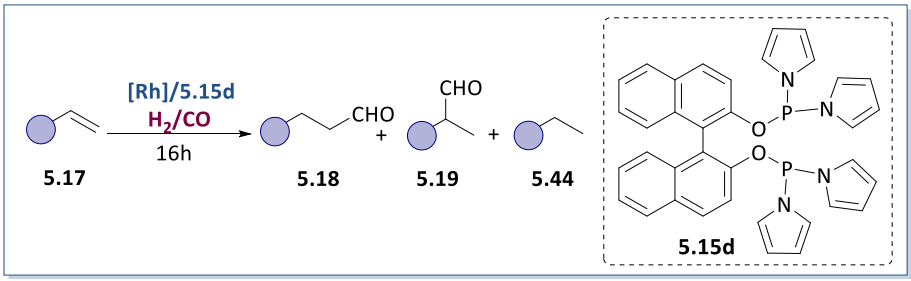

Entry[a]	T(°C)	L/Rh	P_{total}	$P_{partial}$ CO/H_2	Conv(%)	Chem(%)	l/b
1	80	5	10	1:1	99	99	**4.9**
2	120	10	5	1:1	88	96	**6.1**
3	120	5	5	1:1	88	95	**5.9**
4	120	10	10	1:1	95	97	**5.5**
5	120	5	10	1:1	98	97	**5.3**
6	120	10	5	1:4	86	74	**7.3**
7	120	5	5	1:4	94	64	**7.1**
8	100	10	5	1:4	76	78	**9.5**
9	100	5	5	1:4	59	66	**9.1**
10	80	10	5	1:4	55	88	**11.4**
11	80	5	5	1:4	45	69	**12.2**
12	60	10	5	1:4	12	94	**8.3**
13	60	5	5	1:4	55	89	**13.5**
14	40	5	5	1:4	18	95	**6.3**

15	40	2	5	1:4	34	92	**7.0**
16	**60**	**2**	**5**	**1:4**	**57**	**81**	**15.0**

Reaction conditions:[a] styrene **5.17** (1.55 mmol), $Rh(acac)(CO)_2$ 0.0057 mol%, toluene (1.7 ml), 16 hours. Conversion, chemoselectivity and regioselectivity determined by GC-FID and NMR using bicyclohexyl as internal standard.

Initially, the binaphthol based ligand **5.15d** (Scheme 5.5) was synthesised using the reported procedure.[12] The results highlighted in Entry 1 show the same results in terms of activity and selectivity, compared to the ones reported by Vogt. Next, various parameters such as ligand to rhodium ratio, total syngas pressure and $CO:H_2$ ratio were analysed, at 120 °C (Entries 2-7). It was therefore concluded that lower amount of CO pressure (1:4 $CO:H_2$) in combination with 5 bar, has a beneficial effect in the linear to branched ratio (l/b= 7.3, Table 5.7, Entry 6). Once established the $CO:H_2$ ratio and the total syngas pressure, the effect of the temperature was analysed. Lowering the temperature from 120 °C to 40 °C has a crucial effect over the regioselectivity of the process. The highest value of linear aldehyde was obtained at 60 °C, with a linear to branched ratio of 13.5 (Table 5.7, Entry 13). In the end, lowering the rhodium to ligand ratio to 1:2 (Table 5.7, Entry 16), provided much higher selectivity and a l/b ratio=15 (93% linear aldehyde) was obtained, but with low conversion (57%). After having established a new set of conditions that affords the linear aldehyde with high selectivity, it was decided to screen the ligands synthesised in section 5.3.1.

5.3.3.7 Hydroformylation experiments using ligand 5.25d, 5.25e and 5.25g

Albeit having found a set of catalytic conditions for the selective linear aldehyde formation with ligand **5.15d** (Table 5.7, Entry 16), for the screening of ligands **5.25d, 5.25e** and phosphoramidite **5.25g**, the effect of crucial parameters such as temperature, $CO:H_2$ ratio, total syngas pressure and rhodium to ligand ratio (Table 5.8) was studied.

Table 5.8. Optimization of the Rh-catalysed hydroformylation of styrene using ligand **5.24g, 5.24e** and **5.24d**[a]

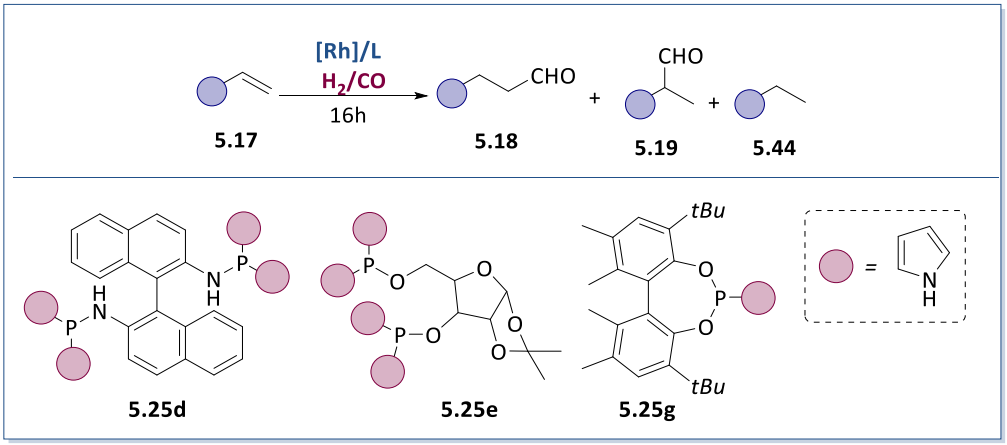

E	L	T(°C)	L/Rh	P_{total}	$P_{partial}$ CO/H_2	Conv(%)	Chem(%)	l/b
1	**5.15d**	80	5	10	1:1	99	99	**4.9**
2	**5.25d**	80	5	10	1:1	30	99	**1.0**
3	**5.25e**	80	5	10	1:1	70	99	**1.0**
4	**5.25g**	80	5	10	1:1	65	99	**1.3**
5	**5.15d**	120	10	10	1:1	95	97	**5.5**
6	**5.25d**	120	10	10	1:1	10	95	**1.2**
7	**5.25e**	120	10	10	1:1	65	89	**2.0**
8	**5.25g**	120	10	10	1:1	45	94	**1.5**
9	**5.15d**	60	2	5	1:4	57	81	**15.0**
10	**5.25d**	60	2	5	1:4	5	85	**1.0**
11	**5.25e**	60	2	5	1:4	-	-	**-**
12	**5.25g**	60	2	5	1:4	7	96	**1.4**

Reaction conditions: [a]Conversion, chemoselectivity and regioselectivity determined by GC-MS. Rh(acac)(CO)2 (Styrene/Rh = 17544, 0.0057 % mol), Styrene (1.55 mmol), toluene (1.7 mL), 16 h.

The first set of conditions selected were: $Rh(acac)(CO)_2$ (Rh 0.0057 % mol), L/Rh =2, styrene (1.55 mmol), P_{tot}=5 bar, $CO:H_2$ 1:1, 16 h, at 80 °C. Under

these conditions the ligand **5.25d**, containing the BINAM backbone, was used (Entry 2). In this case, 30% of conversion and l/b ratio of 1.0 was observed. Next, the rhodium system with the ligand containing the isopropylidene-*α*-*D*-xylofuranose backbone **5.25e** was tested but provided 70% of conversion and 1 of l/b ratio (Entry 3). When **5.25g** was used as ligand, under the described catalytic conditions, slightly higher value of linear to branched ratio was observed (l/b=1.3, Entry 4), with 65% of conversion. Therefore it is shown that under this set of conditions, the reference ligand **5.15d** deliver the highest linear to branched ratio (Entry 1, 4.9= l/b). The second set of selected catalytic conditions are the one described in Table 5.7, Entry 4, namely 120 °C and 10 bar of 1:1 CO/H_2 using 0.0057 mol% of $[Rh(acac)(CO)_2]$ pre-catalyst and 10 Rh:L ratio for 16 hours. The use of ligand **5.15d** provided the product with 95% conversion and a l/b ratio of 5.5 (Entry 5). When the catalytic system contains ligand **5.25d** low conversion (10%) and l/b ratio of 1.2 was observed (Entry 6). Ligand **5.25e** and **5.25g**, provided respectively a l/b ratio of 2 and 1.5 (Entries 7 and 8), with slightly higher conversion (65% and 45%). In the end, the last set of selected catalytic conditions were: 60 °C and 5 bar of 1:4 CO/H_2 using 0.0057 mol% of $[Rh(acac)(CO)_2]$ pre-catalyst and 2 Rh:L ratio for 16 hours (Entry 16, Table 5.7). When the ligand is **5.15d** the system provided the product with 57% conversion and a l/b ratio of 15 (Entry 9). When ligand **5.25d** was used, both the conversion and the linear to branched ratio dropped to 5% of conversion and l/b = 1.0 (Entry 10). Next, the rhodium system with the ligand containing the isopropylidene-*α*-*D*-xylofuranose backbone **5.25e** was tested but provided less than 1% of conversion (Entry 11). When ligand **5.25g** was employed, only 7% of conversion and 1.4 of linear to branched selectivity was observed. The comparison between the ligands screened under the same conditions shows a clear trend: the use of ligand **5.15d** provides higher linear selectivity and higher conversion in the in the Rh catalysed hydroformylation of styrene.

5.4 Conclusions

From the study described in this chapter, the following conclusions can be extracted:

I. The synthesis of unreported bis(dipyrrolyl-phosphorodiamidite) ligands **5.25d** and **5.25e**, and (pyrrolyl-phosphoramidite) **5.25g** was achieved *via* a two-step procedure.

II. The optimization of the catalytic reaction was performed initially using Xantphos **5.47** as ligand, under the following conditions: 120 °C ,10 bar of 1:1 CO/H_2, 0.5 mM solution of toluene, $Rh(acac)(CO)_2$ as pre-catalyst and 10 equivalents of ligand **5.47**. Alcohols as by-products were detected at the end of the process.

III. The screening of the commercially available ligands **5.48-56** in the rhodium catalysed hydroformylation of styrene shows that using the BiphePhos ligand **5.56** (Table 5.1, Entry 10) the Rh catalytic system delivers total styrene conversion and no formation of the alcohol as by-product. Furthermore, the highest linear to branched ratio was observed in this screening (l/b= 2) employing ligand **5.56**.

IV. The rhodium loading did not affect the selectivity of the process, but only the activity of hydroformylation of styrene. Similarly, the metal to ligand ratio affected the activity but not the regioselectivity.

V. When the ligand **5.15**, reported by Vogt, was employed in a brief optimization process, it was concluded that a low amount of CO pressure (1:4 of $CO:H_2$), in combination with 5 bar of total pressure, has a beneficial effect in the linear to branched ratio. Low temperature has a crucial effect over the regioselectivity of the process. The highest value of linear aldehyde was obtained at 60 °C, with a linear to branched ratio of 15 (Table 5.7, Entry 16).

VI. The newly synthesised ligands **5.25d**, **5.25e**, **5.25g** did not provide similar results in term of activity and selectivity compared to ligand **5.15**, that shows higher linear selectivity in the hydroformylation of styrene, and higher conversion.

5.5 Experimental Part

5.5.1 General considerations

All the reactions were carried out using Schlenk-line inert atmosphere techniques or glovebox techniques. Anhydrous solvents were collected from the system Braun MB SPS-800. Commercially available reagents and solvents were purchased at the highest commercial quality from Sigma-Aldrich, Fluka, Alfa Aesar, Fluorochem, Strem and were used as received, without further purification, unless otherwise stated. ^{1}H, $^{13}C\{^{1}H\}$ and $^{31}P\{^{1}H\}$ NMR spectra were recorded using a Varian Mercury VX 400 (400, 100.6, and 161.97 MHz respectively). Chemical shift values (δ) are reported in ppm relative to TMS (^{1}H and $^{13}C\{^{1}H\}$) or H_3PO_4 ($^{31}P\{^{1}H\}$), and coupling constants are reported in Hertz. The following abbreviations are used to indicate the multiplicity: s, singlet; d, doublet; t, triplet; q, quartet; m, multiplet; bs, broad signal. High-resolution mass spectra (HRMS) were recorded on an Agilent Time-of-Flight 6210 using ESI-TOF (electrospray ionization-time of flight). Samples were introduced to the mass spectrometer ion source by direct injection using a syringe pump and were externally calibrated using sodium formate. The instrument was operating in the positive ion mode. Reactions were monitored by TLC carried out on 0.25 mm E. Merck silica gel 60 F_{254} glass or aluminium plates. Developed TLC plates were visualized under a short-wave UV lamp (254 nm) and by heating plates that were dipped in potassium permanganate. Flash column chromatography was carried out using forced flow of the indicated solvent on Merck silica gel 60 (230-400 mesh).

The Rh-catalysed hydroformylation reaction were set up in a 7 tube autoclave from HEL Inc. and single tube autoclave from HEL Inc and were stirred with a teflon-coated magnetic stir bar.

5.5.2 General procedure for hydroformylation of styrene reaction

A 10 mL glassware reactor tube was charged with styrene **5.17** (2 mmol), Dicarbonyl(acetylacetonato)rhodium(I) (1 mol%) in toluene (3.75 mL) and ligand (1.1 mmol%), the autoclave was closed in the glove-box. The reaction tube was placed in the reactor which was pressurized at the desired pressure, heated to 50°C and left stirring at 900 rpm. The reaction was stopped after 24 h by cooling the reactor in an ice bath for 20 min followed by venting of the system. After completion of the reaction, the crude mixture was analysed by GC-MS, GC-FID and ^{1}HNMR and the results compared to those previously reported in literature.

5.5.3 Synthesis of bis (dipyrrolyl-phosphorodiamidite) ligands

Synthesis of 5.23

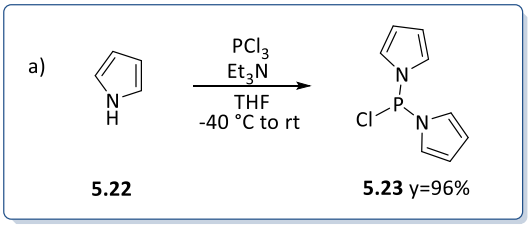

Scheme 5.14: Synthesis of chloro-pyrrolyl intermediates

The reaction was carried out in an oven dried, argon purged, Schlenk fitted with an argon inlet and a septum and following a literature procedure.[14] A solution of triethylamine (5.1 g; 50.4 mmol) and pyrrole **5.22** (2.9 g; 43.6 mmol) in THF (25 mL) was added to a cooled (–40 °C) and stirred solution of PCl_3 (3.0 g; 21.8 mmol) in THF (10 mL). The reaction mixture was warmed

to rt overnight and the triethylamine salts were filtered over a neutral alumina pad (4 cm). The solvent was removed in vacuum and the coloured liquid residue was distilled to yield the pure product **5.23** as a colourless liquid. Yield of **5.23**: 11 g (96%); **^{1}H NMR** (400 MHz, $CDCl_3$): δ 7.08-7.12 (m, 4H), 6.39-6.42 (m, 4H). **^{31}P{^{1}H} NMR** (162 MHz, $CDCl_3$): δ 104.3 (s). **^{13}C NMR** (101 MHz, $CDCl_3$): δ 113.9 (d, J_{P-C}= 5 Hz), 122.7 (d, J_{P-C} = 17 Hz). These signals are in agreement with those reported in the literature. [18]

Synthesis of 5.40

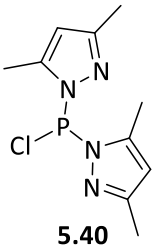

5.40

The reaction was carried out in an oven dried, argon purged, Schlenk fitted with an argon inlet and a septum and following a literature procedure.[14] A solution of triethylamine (2.9 mmol) and dimethyl pyrazole **5.38** (2.5 mmol) in THF (2.5 mL) was added to a cooled (0 °C) and stirred solution of PCl_3 (1 mmol) in THF (2 mL). The reaction mixture was warmed to rt overnight and the triethylamine salts were filtered over a neutral alumina pad (4 cm). The solvent was removed in vacuum to afford product **5.40** as a colourless liquid. Yield of **5.40**: 111 mg (43%); **^{1}H NMR** (400 MHz, $CDCl_3$): δ 6.95 (s, 2H), 2.46 (s, 12H). **^{31}P{^{1}H} NMR** (162 MHz, $CDCl_3$): δ 107.3 (s). **^{13}C NMR** (101 MHz, $CDCl_3$): δ 144.6 (d, J_{P-C}= 5 Hz), 106.0 (d, J_{P-C} = 17 Hz) 11.0 (s).

General procedure A:

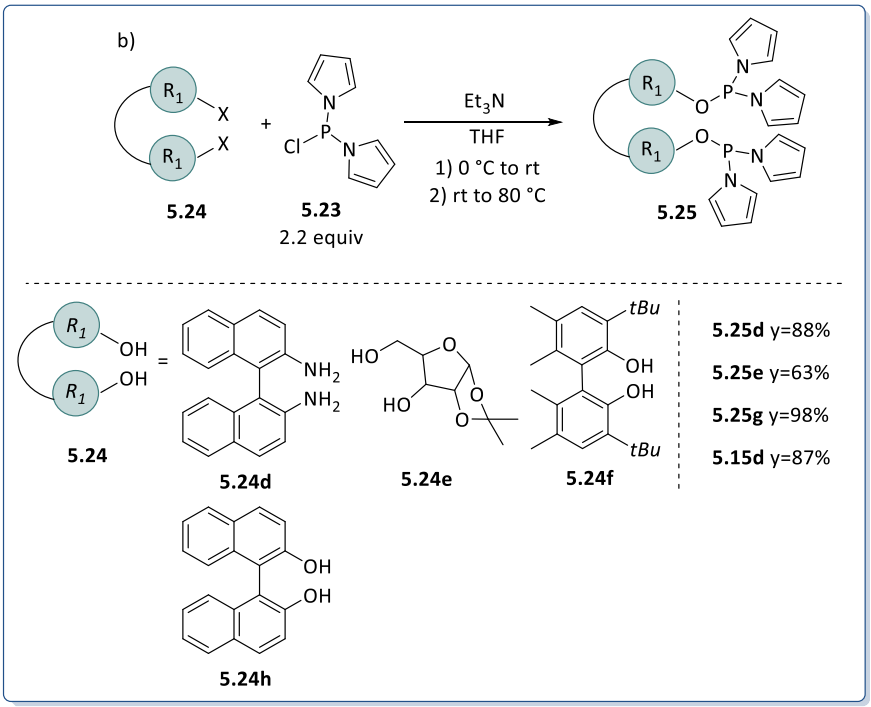

Scheme 5.15: Synthesis of bis (dipyrrolyl-phosphorodiamidite) ligands

In an oven dried, argon purged, Schlenk tube, phosphochloridite **5.23** (2.2 mmol) and Et_3N (4.4 mmol) are dissolved in dry THF (0.35 M) and cooled at 0°C. To this mixture, a solution of compound **5.24** (1 mmol) in dry THF (0.35 M) was added. The reaction mixture was stirred overnight at 25°C. The salts were filtered over a short path of basic alumina (4 cm) and all volatiles were evaporated. A white solid was obtained after recrystallization from EtOAc/hexane.

Synthesis of 5.25d

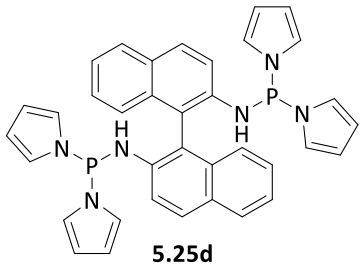

5.25d

General procedure A was followed employing **5.23** (2.2 mmol) and **5.24d** (1 mmol). Purification of the crude material by column chromatography on silica gel in toluene with 5% Et_3N. Yield of **5.25d**: 535 mg (88%); **^{1}H NMR** (400 MHz, $CDCl_3$): δ 7.89 (dd, J_{H-H}=26.0, 8.5 Hz, 4H), 7.64 (dd, J_{H-H}=8.9, 2.7 Hz, 2H), 7.40 – 7.31 (m, 2H), 7.30 – 7.22 (m, 2H), 7.06 (d, J_{H-H}=8.4 Hz, 2H), 6.49 – 6.37 (m, 8H), 6.23 – 6.04 (m, 8H), 5.02 (d, J_{P-H} = 5.0 Hz, 2H). **^{31}P{^{1}H} NMR** (162 MHz, $CDCl_3$): δ 76.70 (s). **^{13}C NMR** (101 MHz, $CDCl_3$): δ 139.2 (d, J_{P-C}=19.2 Hz), 133.1 (s), 130.7 (s), 129.8 (s), 128.5 (s), 127.8 (s), 124.3 (d, J_{P-C}= 22.3 Hz), 121.3 (dd, J_{P-C}=14.0, 10.0 Hz), 117.2 (s), 117.0 (s), 116.5 (d, J_{P-C}=4.8 Hz), 112.6 (d, J_{P-C}=4.0 Hz), 112.3 (d, J_{P-C}= 3.8 Hz). **ESI-HRMS:** Calculated for $C_{36}H_{30}N_6P_2$. Exact: (M: 608.2007, M+H: 609.2080); Experimental: (M+H: 609.2087).

Synthesis of 5.25e

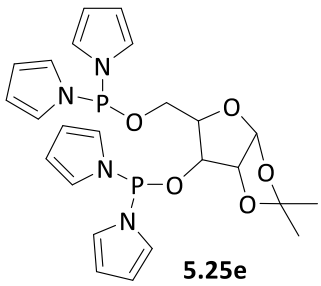

5.25e

General procedure A was followed employing **5.23** (2.2 mmol) and **5.25e** (1 mmol). Purification of the crude material by column chromatography on silica gel in toluene with 5% Et_3N. Yield of **5.25e**: 325 mg (63%);**^{1}H NMR** (400 MHz, $CDCl_3$): δ 6.96 – 6.77 (m, 8H), 6.46 – 6.23 (m, 8H), 6.09 (d, J_{H-H}= 3.7 Hz, 1H), 4.70 (d, J_{H-H}= 3.7 Hz, 1H), 4.50 (s, 1H), 4.39 – 4.15 (m, 1H), 4.11 – 3.86 (m, 2H), 1.45 (s, 3H), 1.34 (s, 3H). **^{31}P{^{1}H} NMR** (162 MHz, $CDCl_3$): δ 114.44 (s), 113.55 (s). **^{13}C NMR** (101 MHz, $CDCl_3$): δ 122.9 (d, J_{P-C}= 14.3 Hz), 121.5 (t, J_{P-C}= 15.2 Hz), 119.8 (d, J_{P-C}= 6.5 Hz), 113.2 (d, J_{P-C}= 4.8 Hz), 113.0 (s), 112.8 (s), 112.7 (s), 112.3 (s), 105.1 (s), 84.6 (d, J_{P-C}= 2.9 Hz), 73.4 (d, J_{P-C}= 5.1 Hz), 72.1 (d, J_{P-}

$_{C}$= 3.9 Hz), 58.6 (d, J_{P-C}= 3.7 Hz). **ESI-HRMS:** Calculated for $C_{24}H_{28}N_4O_5P_2$. Exact: (M: 514.1536, M+H: 515.1608); Experimental: (M+H: 515.1612).

Synthesis of 5.25g

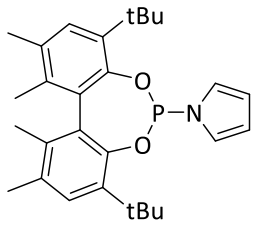

5.25g

General procedure A was followed employing **5.23** (2.2 mmol) and **5.24f** (1 mmol). Purification of the crude material by column chromatography on silica gel in toluene with 5% Et_3N. Yield of **5.25g**: 441 mg (98%);**^{1}H NMR** (400 MHz, $CDCl_3$): δ 7.20 (s, 1H), 7.07 (s, 1H), 6.59 (s, 2H), 6.16 – 6.13 (m, 2H), 2.30 (d, J= 6.7 Hz, 6H), 1.93 (s, 3H), 1.83 (s, 3H), 1.43 (s, 9H), 1.00 (s, 9H). **^{31}P{^{1}H} NMR** (162 MHz, $CDCl_3$): δ 125.5 (s). **^{13}C NMR** (101 MHz, $CDCl_3$): δ 145.6 (s), 144.4 (d, J_{P-C}= 5.3 Hz), 138.1 (d, J_{P-C}= 3.2 Hz), 137.4 (s), 135.1 (s), 134.1 (s), 133.0 (s), 132.1 (s), 131.9 (d, J_{P-C}= 5.1 Hz), 130.5 (d, J_{P-C}= 2.9 Hz), 128.3 (s), 128.0 (s), 121.5 (d, J_{P-C}= 18.3 Hz), 34.6 (d, J_{P-C}= 10.8 Hz), 31.3 (d, J_{P-C}= 5.0 Hz), 30.3 (s), 20.4 (s), 16.7 (s), 16.4 (s). **ESI-HRMS:** Calculated for $C_{28}H_{36}NO_2P$. Exact: (M: 449.2484, M+H: 450.2556); Experimental: (M+H: 450.2561).

Synthesis of 5.15

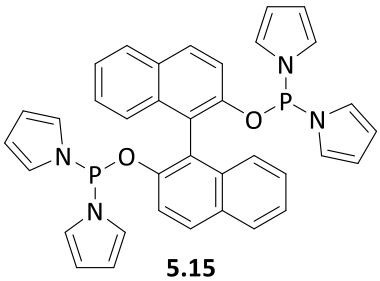

5.15

General procedure A was followed employing **5.23** (2.2 mmol) and **5.24h** (1 mmol). Purification of the crude material by column chromatography on silica gel in toluene with 5% Et_3N. Yield of **5.15d**: 530 mg (87%);. Yield of 4.15: 3 g (4.9 mmol, 47%). **^{1}H NMR** (400 MHz, $CDCl_3$): δ 7.91 (d, J=8.0 Hz, 4H), 7.45 (t, J=8.0 Hz, 2H), 7.33 (t, J=8.0 Hz, 2H), 7.24 (d, J=8.8 Hz, 2H), 7.17 (d, J=8.8 Hz, 2H), 6.50 (dt, J=8.8 Hz, J=2.0 Hz, 8H), 6.17 (t, J=2.0 Hz, 4H), 6.11 (t, J=2.4 Hz, 4H). **^{31}P{^{1}H} NMR** (162 MHz, $CDCl_3$): δ 109.05 (s). **^{13}C NMR** (101 MHz, $CDCl_3$): δ 149.2, 133.7, 130.9, 130.5, 128.2, 127.2, 125.9, 125.3,

122.5, 121.2, 119.2, 112.1. These signals are in agreement with those reported in the literature.[12]

5.6 References

[1] P. W. N. M. Van Leeuwen, C. Claver and Editors, *Rhodium Catalyzed Hydroformylation. [In: Catal. Met. Complexes,* **2000***; 22]*, Kluwer, **2000**.

[2] a) M. Dieguez, O. Pamies, A. Ruiz, S. Castillon and C. Claver, *Chem. Eur. J.*, **2001**, *7*, 3086-3094 b) T. P. Clark, C. R. Landis, S. L. Freed, J. Klosin and K. A. Abboud, *J. Am. Chem. Soc.,* **2005**, *127*, 5040-5042 c) A. T. Axtell, C. J. Cobley, J. Klosin, G. T. Whiteker, A. Zanotti-Gerosa, K. A. Abboud, *Angew. Chem., Int. Ed.*, **2005**, *44*, 5834-5838.

[3] R. Lazzaroni, A. Raffaelli, R. Settambolo, S. Bertozzi and G. Vitulli, *J. Mol. Catal.,* **1989**, *50*, 1-9.

[4] J. M. Brown and A. G. Kent, *J. Chem. Soc., Perkin Trans.*, **1987**, *2*, 1597-1607.

[5] M. Kranenburg, Y. E. M. van der Burgt, P. C. J. Kamer, P. W. N. M. van Leeuwen, K. Goubitz and J. Fraanje, *Organometallics*, **1995**, *14*, 3081-3089.

[6] L. A. van der Veen, M. D. K. Boele, F. R. Bregman, P. C. J. Kamer, P. W. N. M. van Leeuwen, K. Goubitz, J. Fraanje, H. Schenk and C. Bo, *J. Am. Chem. Soc.*, **1998**, *120*, 11616-11626.

[7] L. A. van der Veen, P. H. Keeven, G. C. Schoemaker, J. N. H. Reek, P. C. J. Kamer, P. W. N. M. van Leeuwen, M. Lutz and A. L. Spek, *Organometallics*, **2000**, *19*, 872-883.

[8] S. Yu, Y. M. Chie, Z. H. Guan, Y. Zou, W. Li and X. Zhang, *Org. Lett.*, **2009**, *11*, 241-244.

[9] Cai, C., Yu, S., Cao, B. and Zhang, X. *Chem. Eur. J.*, **2012**, *18*, 9992-9998.

[10] Y. Chen, S. Yekta and A. K. Yudin, *Chem. Rev.*, **2003**, *103*, 3155-3212.

[11] P. C. J. Kamer and P. W. N. M. van Leeuwen, *Phosphorus(III) Ligands in Homogeneous Catalysis: Design and Synthesis*, John Wiley & Sons, Ltd, Chichester, **2012**.

[12] E. Boymans, M. Janssen, C. Müller, M. Lutz and D. Vogt, *Dalton Trans.*, **2013**, *42*, 137-142.

[13] C.-Y. Zheng, M. Mo, H.-r. Liang, X.-l. Zheng, H.-y. Fu, M.-l. Yuan, R.-x. Li and H. Chen, *Appl. Organomet. Chem.*, **2013**, *27*, 474-478.

[14] B. Hamers, E. Kosciusko-Morizet, C. Müller and D. Vogt, *ChemCatChem* **2009**, 1, 103 – 106

[15] N. Kuhn, and K. Jendral 1991). Tetramethylpyrrolyl-Phosphane/ Tetramethylpyrrolyl Phosphanes, *Zeitschrift für Naturforschung B*, **1990**, 46 (3), 280-284.

[16] O. Diebolt, C. Muller, D. Vogt, *Catal. Sci. Technol.*, **2012**, *2,* 773-777.

[17] P. W. N. M. van Leeuwen, A. J. Sandee, J. N. H. Reek, P. C. J. Kamer, *J. Molec. Catal.*, **2002**, *182*, 107-123.

[18] K. G. Moloy, J. L. Petersen, *J. Am. Chem. Soc.*, **1995**, *117*, 7696-7710.

Rhodium and Palladium Catalysed Unusual Regioselective Hydroformylation and Rhodium Catalysed Reductive Carbonylation

Benedetta Palucci

Chapter VI

Formaldehyde as syngas surrogates for palladium catalysed hydroformylation

Rhodium and Palladium Catalysed Unusual Regioselective Hydroformylation and Rhodium Catalysed Reductive Carbonylation

Benedetta Palucci

6.1 Introduction

6.1.1 Alternative syngas surrogates

The functionalisation of substrates using CO as the carbonyl source is of paramount importance for the industrial manufacture of bulk and fine chemicals.[1] For hydroformylation, the most common CO / H_2 source until now has been the synthesis gas (syngas). The synthesis gas is a mixture of CO and H_2 that can be derived from almost every carbon source, such as natural gas, naphtha or coal.[2] However, the toxicity of CO requires significant safety protocols and the use of surrogates could serve as a convenient approach for the synthesis of carbonyl derivatives avoiding the need to use gaseous CO. In 2004, Morimoto, Kakiuchi[3] and Beller[4] summarized several developments in the carbonylation area without the use of gaseous CO including some hydroformylation examples. Scheme 6.1 summarises different ways to obtain this mixture, in which the different oxidation state that the carbon atom possesses is the main difference.

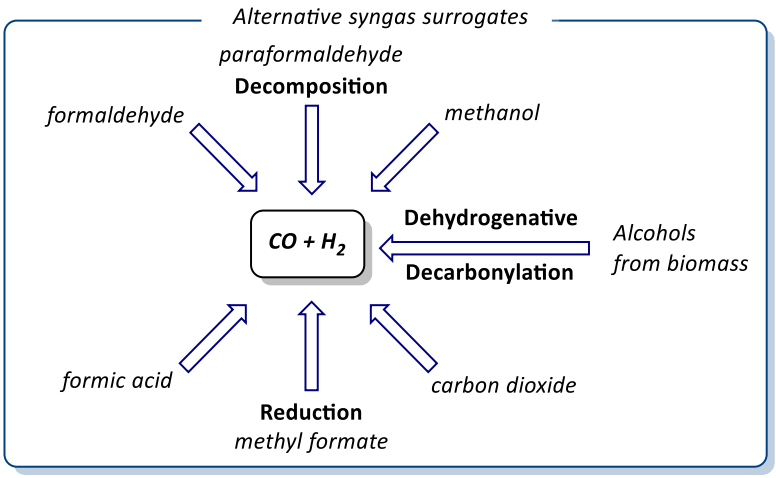

Scheme 6.1. Syngas surrogates.

Typically, industrial hydroformylation processes are performed at medium or high pressure (20–100 bar) of syngas at temperatures between 100–140 °C

in the presence of rhodium as the metal catalyst. Despite the significant industrial interest in hydroformylation reactions, little work has been performed with catalysts based on other metals, except cobalt that was initially used. Palladium-catalysed hydroformylation has been studied for 1-octene by Beller *et al.* using syngas as CO and H_2 source. By using dppp (1,3-bis(diphenylphosphino)propane) as ligand, and under 40 bar of pressure, they reported a 95% of conversion and a chemoselectivity towards the aldehyde of a 13% with a l:b ratio of 6:4.[5] As indicated in Scheme 6.1, formaldehyde is a possible syngas surrogate that could be utilized in the hydroformylation of olefins.[6,7] Indeed, it has been used as CO and H_2 source for the hydroformylation of olefins using various metals such as rhodium[8,9,10,11] or ruthenium[12] but there is no information about palladium catalysed hydroformylation using formaldehyde as syngas surrogate. Formaldehyde can be found in different forms, and the most common ones are as an aqueous solution and in the solid state (as a polymer). Formalin (or formol) is the name for the commercial solution that contains *ca.* 37% weight of formaldehyde in water, while paraformaldehyde (PFA) is a solid polymer with an average degree of polymerization of 8-100 units.[13] By dry heating, PFA can depolymerize to formaldehyde and then subsequently, CO and H_2 are released.[14]

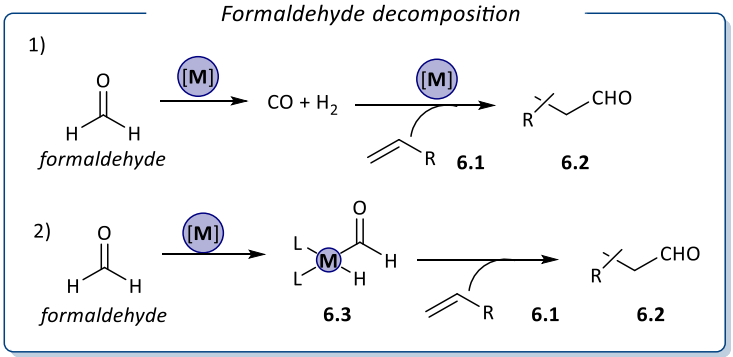

Scheme 6.2. Possible pathways for the hydroformylation of alkenes using formaldehyde.

There are two possible pathways to obtain the aldehyde product in the hydroformylation process using formaldehyde (Scheme 6.2). The first one is by decomposition into CO and H_2, which generally depends strongly on reactant concentration,[15] and the temperature.[16] In this case, the classical hydroformylation mechanism operates.

On the other hand, the oxidative addition of formaldehyde to a metal centre to form a metal hydride formyl unit **6.3** was also proposed.[17] In this case, the formyl and the hydride groups can be transferred to the olefin into the coordination sphere of the transient metal-formyl complex, providing the aldehyde product. Baricelli et al reported experimental results and theoretical DFT-calculations that allowed them to propose a catalytic cycle, in which the insertion of the olefin into the rhodium formyl species **6.3** (generated by oxidative addition of formaldehyde) was considered to be the rate determining step.[17]

6.1.2 Palladium catalyst for hydroformylation process

In contrast to rhodium catalysis, palladium has not played a significant role in the area of hydroformylation of olefins [18] since catalysts based on this metal originally targeted the formation of alternating polyketones from olefins with carbon monoxide,[19] or esters/carboxylic acids in the presence of methanol or water as nucleophiles.[20] Although the palladium catalysed hydroformylation was first discovered by Shell in 1986,[21] very little is known. To have an idea about the mechanism, it is necessary to understand the background of other carbonylation reactions with palladium-based catalysts, such as methoxycarbonylation of olefins or copolymerization.[19,20,22,23,24,25,26] The mechanism of the palladium catalysed hydroformylation has been investigated by Drent and Budzelaar[27] where upon hydrogenolysis of the palladium acyl bond, an aldehyde is released. But because of the high hydrogenation activity of palladium complexes, the aldehydes can be quickly converted into the corresponding alcohols. There is also a competition

between hydroacylation and copolymerization owing to the possible insertion of a second olefin (Scheme 6.3).[13]

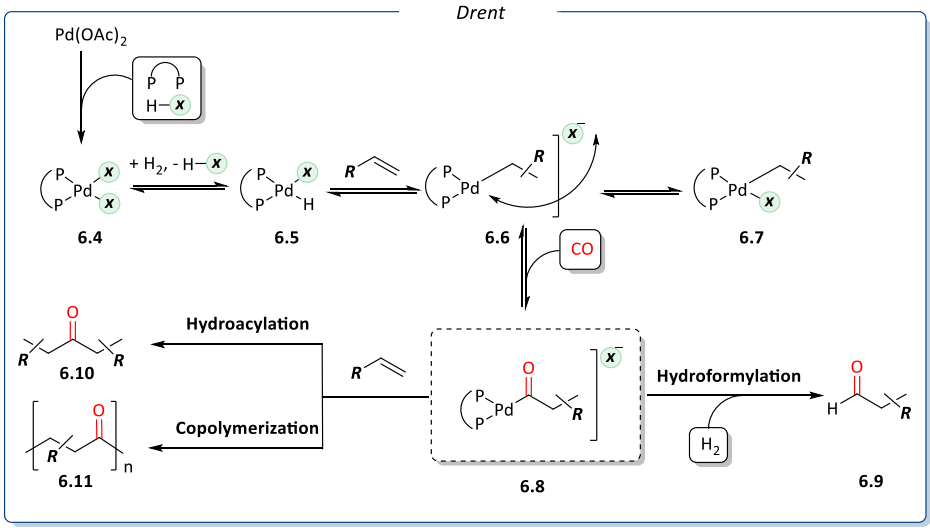

Scheme 6.3. Mechanism of the palladium catalysed hydroformylation and alternative reaction routes proposed by Drent and co-workers.

In 2016, the group of Shi reported that employing formic acid and acetic anhydride as syngas surrogates, excellent regioselectivity toward the linear product could be achieved for a range of alkene substrate (Scheme 6.4).[28] In this study, the nature of the ligand and solvent, as well as the presence of additives, were key parameters to obtain high selectivity.

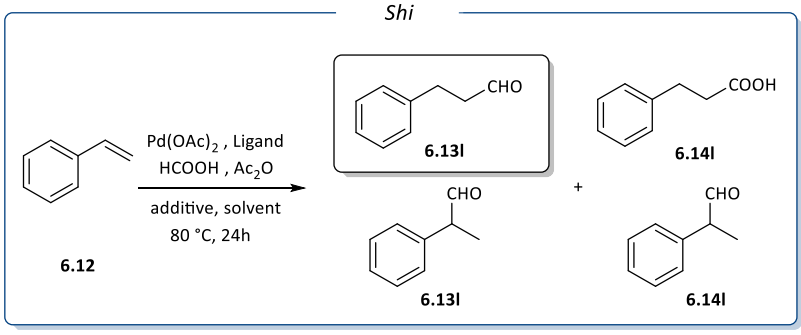

Scheme 6.4. Palladium catalysed hydroformylation of styrene reported by Shi.

It should be noted that formic acid had previously been used as hydrogen source in rhodium hydroformylation processes but the addition of CO gas was

required.[29,30] In the work of Shi, CO was generated *in situ* from the formic acid and the acetic anhydride. The authors proposed the catalytic cycle displayed in Scheme 6.5.

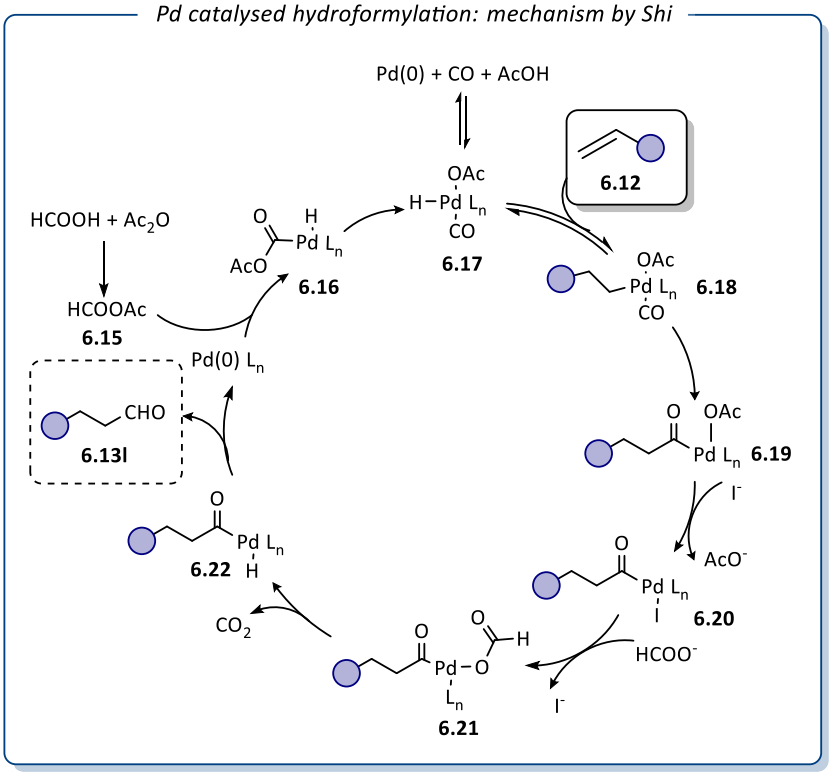

Scheme 6.5. Palladium hydroformylation mechanism reported by Shi and co-workers.

Palladium (0) complex may be oxidatively inserted into HCOOAc **6.15** to give palladium hydride complex **6.16,** which would rearrange to complex **6.17**. The olefin would be hydropalladated by **6.17** to generate alkylpalladium complex **6.18**, which would undergo migratory insertion to give acylpalladium complex **6.19.** The acetate group of **6.19** would subsequently be replaced by the iodide to give Pd–I complex **6.20**, which would react with formic acid to form complex **6.21**. The palladium hydride complex **6.22** would be formed from complex **6.21** via release of CO_2. Reductive elimination of **6.22** would then lead to aldehyde **6.13l** and regenerate the Pd(0) catalyst.

This study evidenced that high selectivity can be achieved in the transformation of styrene (**6.12**) into 3-phenyl propanal **6.13l** without syngas using a palladium catalyst.

6.2 Objectives

The main objective of this chapter is the development of a palladium based catalytic system for the linear hydroformylation of styrene using formaldehyde as syngas surrogate.

The specific objectives of this chapter are:

- The study of the effect and the optimization of the reaction parameters such as the addition of acid, nature of the ligand and palladium precursors, temperature, formaldehyde source, on the outcome of the palladium catalysed hydroformylation of styrene **6.12**.
- To perform mechanistic studies by evaluating deuterium-incorporation and kinetic isotopic effect (KIE) related with rate determining step using formaldehyde-d_2 D_2O.
- To perform mechanistic studies by NMR techniques and propose a potential mechanism for the hydroformylation reaction catalysed by palladium employing formaldehyde as syngas surrogate.

6.3 Results and discussion

6.3.1 Optimization of the reaction conditions: initial screening

First, the reaction was performed under the conditions optimized by Shi and co-workers, but using formaldehyde as syngas source.[28] Thus $Pd(OAc)_2$ and 1,3-bis(diphenylphosphino)propane (dppp) were used as catalytic system and styrene **6.12** was used as model substrate, dichloroethane (DCE) as solvent,

acetic anhydride and tetrabutylammonium iodide as additives, respectively at 80 °C (Table 6.1).[28]

Table 6.1. Pd-catalysed hydroformylation of styrene using formaldehyde as syngas surrogate: Initial optimization[a]

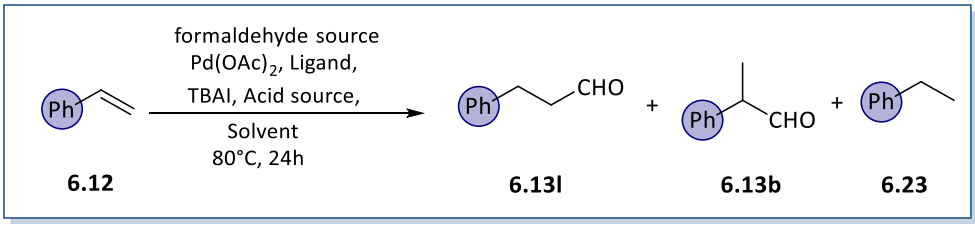

Entry	Formaldehyde source (Equiv.)	Solvent	Additive (Equiv.)	Conv (%)	Chemo (%)	l/b
1	PFA (3.9)	DCE	Ac_2O 3	-	-	-
2[b]	Formalin (3.9)	DCE	Ac_2O 3	42	67	>99
3	Formalin (5)	DCE	Ac_2O 3	54	76	>99
4	Formalin (5)	Toluene	Ac_2O 3	54	78	>99
5	Formalin (5)	Toluene	AcOH 6	51	60	>99
6[c]	Formalin (5)	Toluene	AcOH 6	63	88	>99

Reaction conditions:[a] Styrene (0.5 mmol, 58.1 uL), $Pd(OAc)_2$ (0.025 mmol, 5.6 mg), dppp (0.050 mmol, 21.0 mg), Bu4NI (0.013 mmol, 4.6 mg), solvent (1.5 mL), 24 h, 900 r.p.m.; Conversion, chemoselectivity and regioselectivity determined by GC-MS using bicyclohexyl as internal standard; Chemoselectivity towards aldehydes **6.13**.[b] Formalin is formaldehyde, 37% in aq. soln., ACS, 36.5-38.0%, stab. with 10-15% methanol. [c] reaction performed at 95°C.

The use of paraformaldehyde (Table 6.1, Entry 1) did not deliver the hydroformylated product **6.13l**. However, switching to formalin (formaldehyde, 37% in aq. Solution, Entry 2) provided moderate results in terms of conversion and chemoselectivity since the hydrogenation product **6.23** was also observed, but excellent regioselectivity (>99) was achieved. Increasing the equivalents of formalin to 5 (Table 6.1, Entry 3) resulted in a slight increase of the conversion (54%). This reaction could also be carried

out in a non-chlorinated solvent such as toluene (Table 6.1, Entry 4) without affecting the yield and regioselectivity. It was thought that, employing an aqueous solution such as formalin, acetic anhydride was readily converted into acetic acid, and thus the use of acetic acid in place of acetic anhydride was tested (Table 6.1, Entry 5) but this proved to promote the formation of the corresponding carboxylic acid in 20% yield. Nonetheless, when the reaction temperature was increased up to 95 °C (Table 6.1, Entry 6), higher conversion and higher selectivity towards the aldehyde **6.13l** were observed. It is important to mention that under the depicted conditions, the regioselectivity was always total to the linear aldehyde **6.13l** (>99%). In view of the results obtained by switching from acetic anhydride to acetic acid, it was decided to test the activity of several other acids.

6.3.2 Effect of the additive

Beller *et al.* described experiments for the Pd-hydroformylation of 1-octene using various $CO:H_2$ and acids such as trifluoroacetic acid (TFA), trifluoromethane sulfonic acid (TfOH) and *para*-toluene sulfonic acid (*p*-TsOH), obtaining the linear aldehyde as the main product without the presence of by-products. [31] Therefore, these acids were tested at various concentrations to determine which was the most appropriate in this process (Table 6.2). When 20 mol% of TFA were used, 94% conversion was obtained with a 60% selectivity towards the aldehyde, and 2% of the new by-product **6.24** was detected (Table 6.2, Entry 1). When the amount of TFA was lowered to 15 mol% to styrene, the conversion decreased to 81% although the selectivity to **6.13l** increased to 77% (Table 6.2, Entry 2).

Table 6.2. Pd-catalysed hydroformylation of styrene using formaldehyde as syngas surrogate: Effect of TFA, TfOH and *p*-TsOH[a]

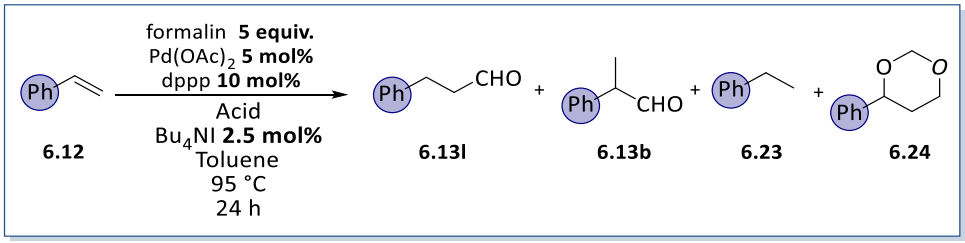

Entry	Acid	Acid mol% (b)	Conv (%)	6.24 (%)	6.13 (%)	l/b
1	TFA	20	94	2	60	>99
2	TFA	15	97	-	62	>99
3	TFA	5	24	-	8	>99
4	TFA	2.5	7	-	14	>99
5	TFA	1	4	-	6	>99
6	TfOH	20	42	11	34	>99
7	TfOH	15	81	-	51	>99
8	TfOH	5	30	-	17	>99
9	TfOH	2.5	6	-	0	>99
10	TfOH	1	1	-	0	>99
11	*p*-TsOH	20	63	66	5	>99
12	*p*-TsOH	15	70	-	51	>99
13	*p*-TsOH	5	38	-	21	>99
14	*p*-TsOH	2.5	15	-	13	>99
15	*p*-TsOH	1	7	-	8	>99

Reaction conditions:[a] Styrene (0.5 mmol, 58.1 uL), Formalin (2.5 mmol, 195 µL), $Pd(OAc)_2$ (0.025 mmol, 5.6 mg), dppp (0.050 mmol, 21.0 mg), Bu4NI (0.013 mmol, 4.6 mg), toluene (1.5 mL), 24 h, 900 r.p.m.; Conversion, chemoselectivity and regioselectivity determined by GC-MS using bicyclohexyl as internal standard; Chemoselectivity towards aldehydes **6.13**. [b] mol % referred to Styrene.

By further decreasing the loading of TFA, the conversion kept lowering while the chemoselectivity towards **6.23** rise. Under these reaction conditions, compound **6.24** was not detected (Table 6.2, Entries 3, 4 and 5). In case of TfOH, when 20 mol% were used, a conversion of 42% was observed, and various products were detected, namely the linear aldehyde **6.13l** (34%), ethylbenzene **6.23** (55%) and 4-phenyl-1, 3-dioxane **6.24** (11%). When the acid concentration was lower, the conversion decreased, as well as the selectivity towards the aldehyde (Table 6.2, Entries 7, 8 and 9). In all the cases where TfOH was used, ethylbenzene **6.23** was the main product obtained, while **6.24** was barely detected. When the reaction was carried out with a 20 mol% of *p*-TsOH, the conversion was 63% with a selectivity of 66% for the compound **6.24**. Under these conditions, only 5% of the aldehyde were obtained (Table 6.2, Entry 11). An increase in conversion (70%) was achieved using 15 mol% of acid with 51% selectivity towards aldehyde **6.13l** (Table 6.2, Entry 12). With lower acid loading, lower conversions were obtained, with higher selectivity towards the hydrogenated product **6.23** (in Table 6.2, Entries 13, 14 and 15). In some of these reactions, 4-phenyl-1, 3-dioxane (**6.24**) was obtained (Table 6.2, Entries 1, 6, 11). The electrophilic addition of an aldehyde to an alkene followed by capture of a nucleophile is known as the Prins reaction.[32] In the presence of water, protic acids and formaldehyde, a 1,3-diol is formed, and if an excess of formaldehyde is added, the resulting product is a dioxane. The reaction between styrene and formalin using TfOH as catalyst was previously reported and produces the dioxane derivative **6.24** as the main product (Scheme 6.6).[33]

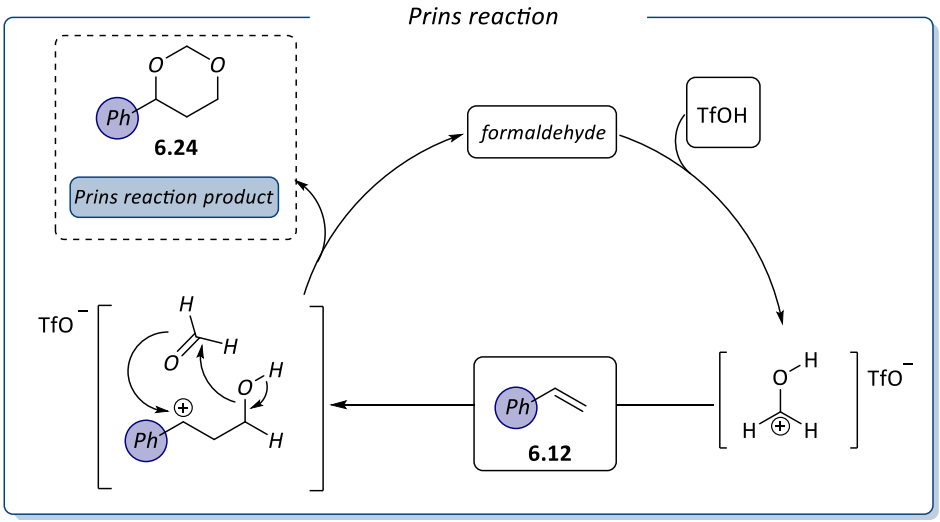

Scheme 6.6. Mechanism proposed by Prins for the formation of **6.24** from styrene and formaldehyde in acidic medium.

In all the cases, low concentrations of acid favoured the formation of ethylbenzene **6.23**. By increasing the amount of acid, the selectivity was shifted towards the linear aldehyde **6.13l**. However, at high acid concentration of TfOH and *p*-TsOH, the formation of the dioxane product **6.24** was observed, being the major reaction product in the case of *p*-TsOH (Table 6.2, Entry 11). Therefore, the amount and strength of the acid both affected the chemoselectivity of the hydroformylation process. In view of these results, the use of 15 mol% of TFA as acid co-catalyst seemed the most suitable since it provided the highest conversion and selectivity to **6.13l** of the series. Next, a series of ionic additives was tested in the reaction to evaluate the role of the cationic and anionic moieties of these compounds. For this purpose, tetrabutylammonium bromide (TBAB), tetramethylammonium bromide (TMAB), potassium iodide (KI) were tested.

Table 6.3. Pd-catalysed hydroformylation of styrene using formaldehyde as syngas surrogate: Effect of additives[a]

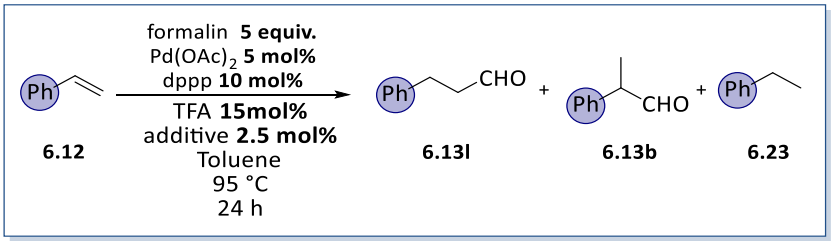

Entry	Additive	Conv (%)	6.13 (%)	l/b
1	TBAI	97	62	>99
2	TBAB	0	-	-
3	TMAB	0	-	-
4	KI	0	-	-
5	-	0	-	-

Reaction conditions:[a] Styrene (0.5 mmol, 58.1 uL), formalin (2.5 mmol, 197 uL), $Pd(OAc)_2$ (0.025 mmol, 5.6 mg), ligand (0.050 mmol), TFA (0.075 mmol, 5.8 uL), additive (0.013 mmol), toluene (1.5 mL), 95°C, 24 h, 900 r.p.m.; Conversion, chemoselectivity and regioselectivity determined by GC-MS using bicyclohexyl as internal standard; Chemoselectivity towards aldehydes **6.13**.

Under the conditions described in Table 6.2, no conversion of the substrate was observed when these additives were used (Table 6.3, Entry 2-4), nor in the absence of additive (Entry 5). These results highlighted the crucial role of both the cationic and the anionic moieties of the TBAI (Tetra-n-butylammonium iodide) additive for the outcome of the reaction.

6.3.3 Effect of the ligand

In most homogeneous catalytic reactions, the steric and electronic properties of the ligands have a great influence on the activity and selectivity of the corresponding catalysts. For this reason, bidentate ligands with different bite angle were tested. The results are displayed in Table 6.4.

Table 6.4. Pd-catalysed hydroformylation of styrene using formaldehyde as syngas surrogate: Ligand effect[a]

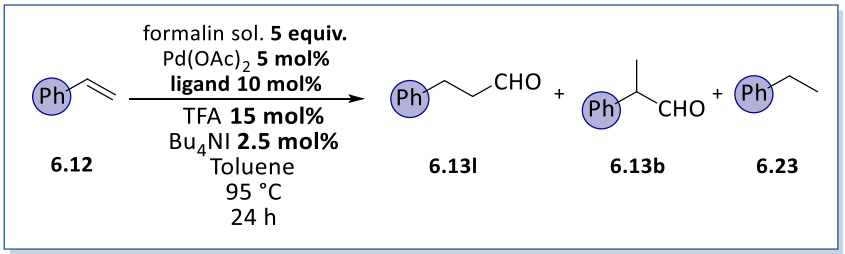

Entry	Ligand	Conv (%)	Chemo (%)	l/b
1	-	0	-	-
2	dppp	97	62	>99
3	dppb	6	0	-
4	d^{t}bpx	0	-	-
5[b]	d^{t}bpx	9	-	-
6	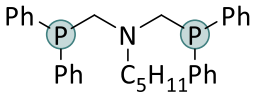 **6.25**	10	0	-
7	Xantphos	0	-	-
8	PPh_3	0	-	-

Reaction conditions:[a] Styrene (0.5 mmol, 58.1 uL), formalin (2.5 mmol, 197 uL), $Pd(OAc)_2$ (0.025 mmol, 5.6 mg), ligand (0.050 mmol), TFA (0.075 mmol, 5.8 uL), Bu_4NI (0.013 mmol, 4.6 mg), toluene (1.5 mL), 95°C, 24 h, 900 r.p.m.; Conversion, chemoselectivity and regioselectivity determined by GC-MS using bicyclohexyl as internal standard; Chemoselectivity towards aldehydes **6.13**. [a] 20% mol of d^{t}bpx ligand.

Strikingly, among all the other systems tested in this screening, dppp/Pd (Table 6.4, Entry 2), was the only one that provided activity and selectivity toward the hydroformylation product. Low conversions with full selectivity to hydrogenation product **6.23** were measured using Pd-catalyst system with ligands dppb and ligand **6.26** (Table 6.4, Entries 3 and 6), whereas the systems with Xantphos or d^{t}bpx as ligands were inactive (Table 6.4, Entries 4

and 7). Using the monodentate PPh_3, no activity was observed (Table 6.4, Entry 8). It was thought that the low activity could be related with the poor coordination of the ligand to the metal catalyst under these conditions. However, when the reaction was carried out using 20% mol of d^{t}bpx ligand, as reported by Beller,[34] an increase in conversion was observed (Table 6.4, Entries 4 vs 5), but with total chemoselectivity to the hydrogenation product. This behaviour was explained because the formation of Pd/dtppx complex was favoured at high L/Pd ratios, and the formed complex displayed mainly hydrogenation activity probably due to the fast decomposition of the HCHO into CO and H_2. We therefore hypothesized that the Pd/dppp forms a really stable catalytic system able to perform the activation of formaldehyde to form the Pd-hydrido-formyl species (Pd(H)(CHO)) and that with this ligand, this intermediate is stable enough to react with the substrate before its transformation into the Pd-dihydride species responsible for the hydrogenation activity. It is worth to mention that the process did not proceed in absence of ligand (Table 6.4, Entry 1).

6.3.4 Effect of the Pd precursor

Several palladium precursors were tested and the results obtained are summarized in Table 6.5. Using $Pd(OAc)_2$, $Pd(acac)_2$ and $Pd(TFA)_2$, as palladium (II) source, the conversions were similar (97%-98%) (Table 6.5, Entries 2, 3 and 4). The chemoselectivity was slightly higher when $Pd(OAc)_2$ is used with a 62% towards the aldehyde **6.13l** (vs 52% for $Pd(acac)_2$ and $Pd(TFA)_2$). Entry 4 summarises the result of using $Pd(TFA)_2$ in the absence of acid to check whether the only presence of the trifluoroacetate counteranion was enough to carry out the hydroformylation. However, only a 9% of conversion was achieved with a 44% of **6.13l** obtained. There was no conversion using $PdCl_2$, probably due to its low solubility (Table 6.4, Entry 6). Using $Pd(dba)_2$ as Pd (0) source (Table 6.5, entries 7 and 8) low activity was obtained. One explanation could be that under these conditions, the Pd(0)

precursor rapidly decomposed into Pd black, as observed in the sample at the end of the reaction.

Table 6.5. Pd-catalysed hydroformylation of styrene: Effect of Pd precursor[a]

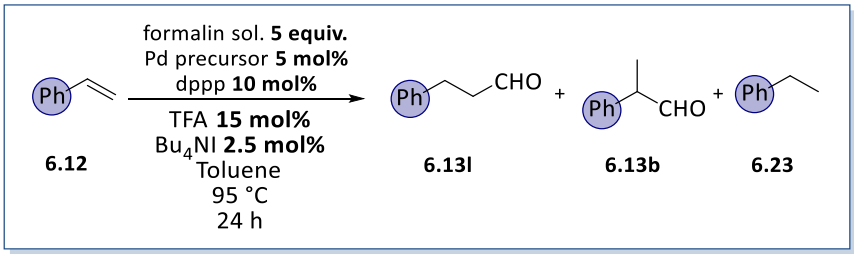

Entry	Pd precursor	Conv (%)	Chemo (%)	l/b
1	-	-	-	-
2	$Pd(OAc)_2$	97	62	>99
3	$Pd(acac)_2$	97	52	>99
4	$Pd(TFA)_2$	98	52	>99
5[b]	$Pd(TFA)_2$	9	44	>99
6	$PdCl_2$	-	-	-
7	$Pd(dba)_2$	16	43	>99
8[b]	$Pd(dba)_2$	-	-	-
9	$[Pd(Allyl)(COD)]BF_4$	77	12	>99

Reaction conditions: [a] Styrene (0.5 mmol, 58.1 uL), formalin (2.5 mmol, 197 uL of solution at 37%), Pd precursor (0.025 mmol), dppp (0.050 mmol, 21 mg), TFA (0.075 mmol, 5.8 uL), Bu_4NI (0.013 mmol, 4.6 mg), toluene (1.5 mL), 95°C, 24 h, 900 r.p.m.; Conversion, chemoselectivity and regioselectivity determined by GC-MS using bicyclohexyl as internal standard; Chemoselectivity towards aldehydes **6.13**. [b] Without TFA.

Employing a source of cationic Pd(II) provided 77% conversion of styrene **6.12** but with only 12% of chemoselectivity (Table 6.5, Entry 9). As a conclusion, Pd(II) cationic and Pd(II) neutral precursors provided better catalytic results concerning the conversion of styrene. However, the chemoselectivity remained higher using $Pd(OAc)_2$, where 77% of aldehyde

product was obtained. This can be explained because the pH in each reaction is affected by the metal precursor. Pd(II) cationic has BF_4^- as counter-ion, that contains the weak conjugated base of the tetrafluoroboric acid (HBF_4), whereas Pd(II) neutral has ^-OAc, a strong conjugated base that can establish an equilibrium with the acid co-catalyst (TFA). Next, the effect of the temperature was studied.

6.3.5 Effect of the temperature

Three different temperatures were tested: 65, 95 and 125 °C. The results obtained are listed in Table 6.6.

Table 6.6. Pd-catalysed hydroformylation of styrene: Effect of the temperature[a]

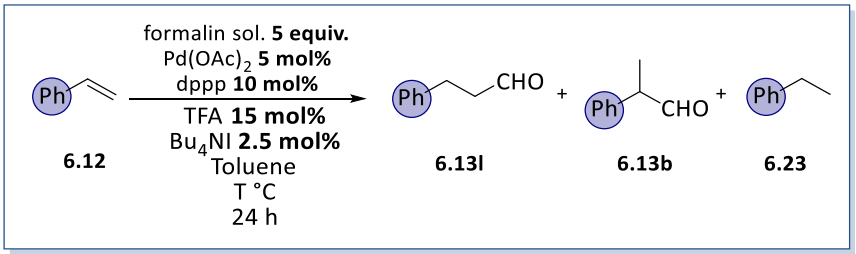

Entry	T (°C)	Conv (%)[b]	Chemo (%)[b]	l/b
1	65	25	72	42
2	95	97	62	>99
3	125	83	0	-

Reaction conditions:[a] Styrene (0.5 mmol, 58.1 uL), formalin (2.5 mmol, 197 uL of solution at 37%), Pd precursor (0.025 mmol), dppp (0.050 mmol, 21 mg), TFA (0.075 mmol, 5.8 uL), Bu_4NI (0.013 mmol, 4.6 mg), toluene (1.5 mL), 95°C, 24 h, 900 r.p.m.; Conversion, chemoselectivity towards aldehydes, and regioselectivity determined by GC-MS using bicyclohexyl as internal standard; Chemoselectivity towards aldehydes **6.13**.

At 65 °C (Table 6.6, Entry 1), only 25% of styrene was converted, with low linear aldehyde selectivity (42%), but higher chemoselectivity was obtained, with 72% of aldehyde **6.13l** product. In contrast, at 95 °C (Table 6.6, Entry 3

vs Entry 1), higher conversion was achieved, with 96% of styrene converted, but with lower chemoselectivity (62%). At higher temperatures (Table 6.6, Entry 3), side-reactions (hydrogenation and other products) dominated the reaction outcome and hydroformylation products were not detected. It was therefore concluded that at high temperature the active catalytic species "Pd-(H)CHO" rapidly decarbonylates to give the corresponding $Pd(H)_2$ and CO, resulting in high hydrogenation activity.

6.3.6 Effect of the formaldehyde source

Finally, the effect of the formaldehyde source was evaluated (Table 6.7).

Table 6.7. Pd-catalysed hydroformylation of styrene: Effect of formaldehyde source[a]

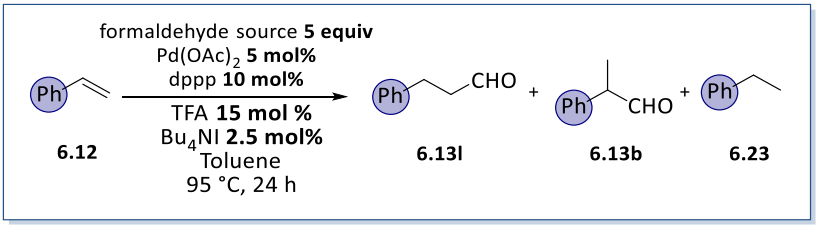

Entry	Formaldehyde source	Conv (%)	Chemo (%)	l/b
1	Formalin[b]	96	62	>99
2	PFA	12	35	>99
3	PFA + H_2O	95	61	>99
4	PFA + H_2O + MeOH	95	56	>99

Reaction conditions:[a] Styrene (0.5 mmol, 58.1 uL), formaldehyde (2.5 mmol), $Pd(OAc)_2$ (0.025 mmol, 5.6 mg), dppp (0.050 mmol, 21.0 mg), TFA (0.075 mmol, 5.8 uL), Bu_4NI (0.013 mmol, 4.6 mg), toluene (1.5 mL), 95°C, 24 h, 900 r.p.m.; Conversion, chemoselectivity and regioselectivity determined by GC-MS using bicyclohexyl as internal standard; [b] Formalin is formaldehyde, 37% in aq. soln., ACS, 36.5-38.0%, stab. with 10-15% methanol.

The reactions were carried out following the optimized reaction conditions up to this point (Table 6.6, Entry 2) employing formalin, paraformaldehyde, paraformaldehyde with water, and paraformaldehyde with water and

methanol. The results are displayed in Table 6.7. Using only PFA (Table 6.7, Entry 2) low catalytic activity was observed, obtaining 12% of conversion. However, the addition of water provided a large increase in activity and selectivity, providing similar results that when formalin was used. Overall, two sources of formaldehyde have been found suitable for the hydroformylation of styrene into the linear aldehyde: formalin and a solution of PFA in water.

6.3.7 Mechanism investigation: syngas and CO

To get insights into the mechanism of the reaction, experiments were carried out using syngas instead of formaldehyde under the optimized conditions (Table 6.7, Entry 2). The effect of the addition of CO alone to the reaction mixture was also examined. First, we performed the reaction using directly syngas instead of formalin (CO/H_2= 1, P_{total}= 2 bar) in toluene, but under these conditions, no conversion was observed. Higher syngas pressures were not tested since the reaction was usually performed in a Schlenk tube, and as such, it was estimated that the maximum pressure that could be produced in situ from decomposition of formaldehyde would be ca. 1.5-2 bar. Next, the effect of additional CO on the selectivity of this reaction was investigated (Scheme 6.7).

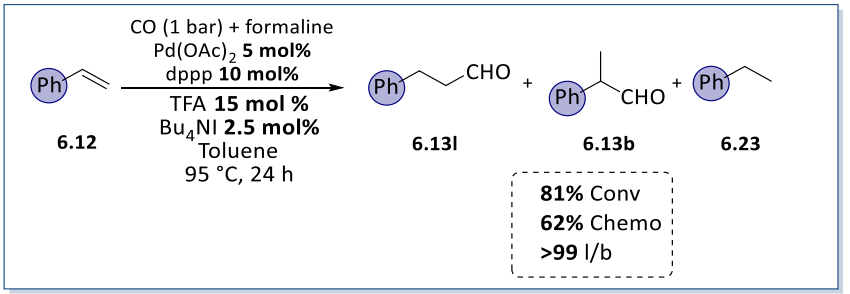

Scheme 6.7. Pd-catalysed hydroformylation of styrene. Effect of the addition of CO

The reaction using the formalin solution as syngas surrogate was repeated under the optimised conditions (Table 6.7, Entry 1) but under an additional

pressure of 1 bar of CO. It was observed that the addition of CO slightly lowered the conversion but did not affect the chemo- nor the regioselectivity of the reaction (Scheme 6.7).This result suggests that, under the optimized conditions, paraformaldehyde is not acting as a simple precursor to generate *in situ* CO and H_2, thus suggesting a reaction mechanism where oxidative addition of formaldehyde at Rh takes place to form a Rh hydride formyl intermediate (Scheme 6.2, 2).

6.3.8 Reaction monitoring

The reaction was monitored over time using the conditions described in Table 6.7, Entry 1.

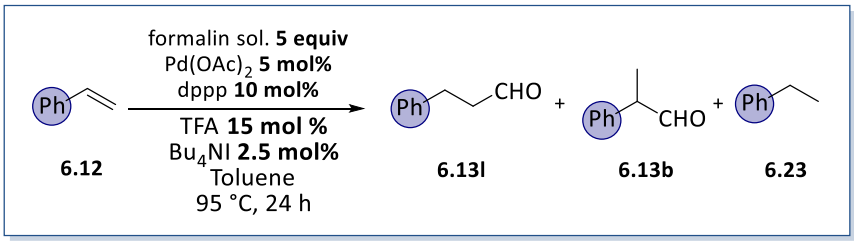

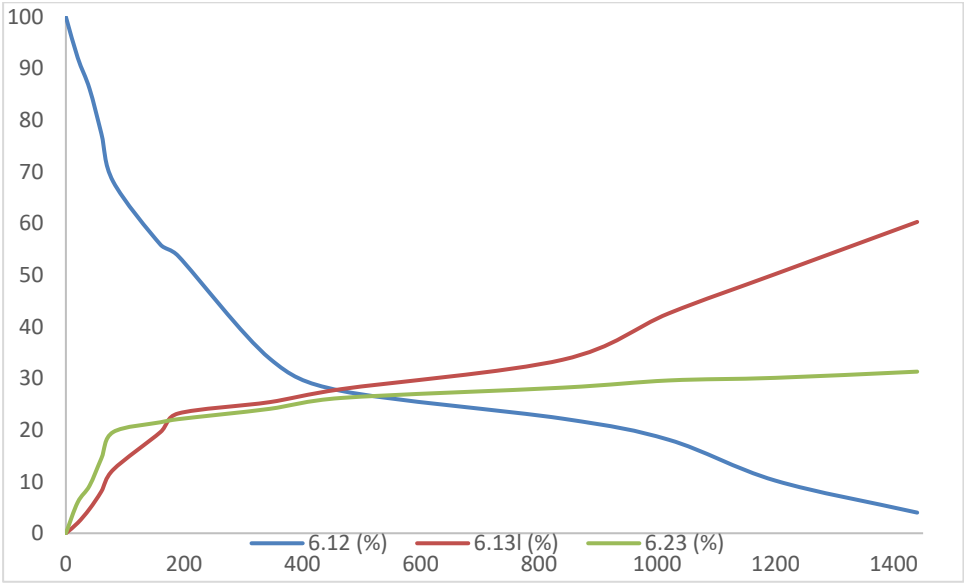

Scheme 6.8. Evolution of the Pd-catalysed hydroformylation through time.

At the beginning of the reaction (t < 200 minutes), the rate of formation of **6.23** was higher than that of **6.13l**. However, at longer reaction times, the process leading to the production of the aldehyde becomes faster than that of the hydrogenation product. After 1200 minutes, the product distribution of **6.13l** and **6.23** was the same and after 1440 minutes of reaction (90% conversion), 60% of linear aldehyde **6.13l** and a 30% of hydrogenated **6.23** was obtained. These results clearly indicate that under these conditions, the formation of the hydrogenation product is favoured at the beginning of the reaction while towards the end, the aldehyde formation is favoured.

6.3.9 Deuterium labelling experiments

To get insights into the mechanism of the reaction, an isotopic labelling experiment was performed. Two different systems, one composed by PFA solution in D_2O (98 atom % D) and a second one composed by PFA-d_2 with H_2O were evaluated (Scheme 6.9). In the first system, high degree (89% on the vinyl fragment) of deuteration was observed on the starting material **6.12**. As a consequence, also the alkylic part of the hydrogenation product **6.23** as well as the alkyl and aldehydic hydrogens within the hydroformylation product **6.13l** are completely deuterated (Scheme 6.9, a, 94% and 92% respectively).

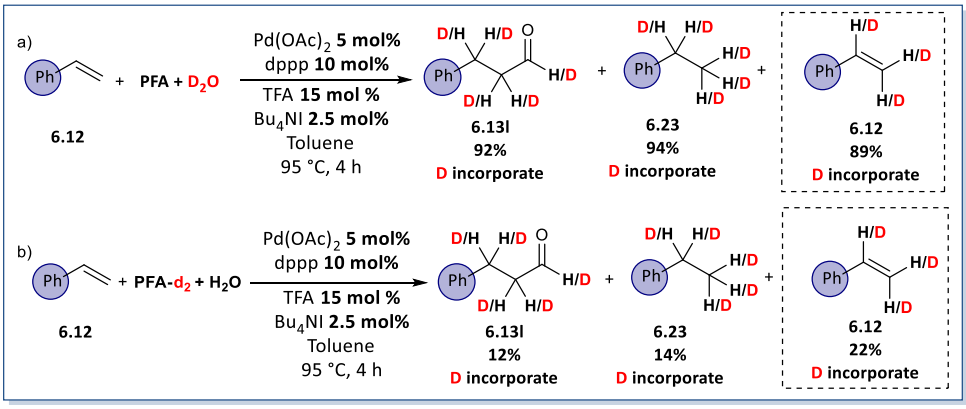

Scheme 6.9. Pd-catalysed hydroformylation of styrene using PFA solution in D_2O (a) and PFA-d_2 with H_2O (b).

On the other hand, when employing PFA-d_2 with H_2O, low deuterium incorporation was observed in the starting material **6.12**, the hydrogenation product **6.23** and the hydroformylation product **6.13l** (Scheme 6.9, b). Both the formation of the deuterated ethylbenzene **6.23** and of the incorporation of deuterium in the starting material **6.12**, cannot be explained through the interaction with the Pd-(H)(CHO) species. We envision that there are different catalytically active Pd species in the reaction media: Pd-H, Pd-$(H)_2$ and Pd-(H)(CHO). Indeed, on the basis of the H-D exchange, we propose Pd-D to be responsible of pre-deuteration of the styrene **6.12** by an insertion/β-elimination equilibrium. This species was formed by initial generation of Pd-H that undergoes H/D exchange from the D_2O. Pd-$(H)_2$ is responsible of the hydrogenation activity, while Pd-(H)(CHO) is responsible of the hydroformylation activity.

6.3.10 Kinetic studies

We also performed experiments in order to detect the magnitude of a possible kinetic isotope effect (KIE). To this end, we employed, similarly to the deuterium labelling experiments, two different systems: PFA solution in D_2O (98 atom % D) and PFA-d_2 with H_2O (Scheme 6.10, a vs b). In the first case, thus employing PFA in D_2O, a relatively low KIE was detected (KIE =1.6, Scheme 6.11, a). However, when employing the second system, namely PFA-d_2 with H_2O, a KIE of 5.3 was detected (Scheme 6.10, b). We envision that the formation of Pd-(H)(CHO), responsible for the production of **6.13l**, is influenced by the isotopic substitution during the oxidative addition step on the formaldehyde, thus originating the difference in the rate of formation of the deuterated and non-deuterated products. For the hydrogenated product **6.23**, employing PFA-d_2 with H_2O, a KIE of 1.1 was detected, while in the system PFA in D_2O an inverse KIE of 0.7 was detected. Inverse primary KIEs have been observed in the studies of reductive eliminations of many other alkyl/aryl hydride transition metal complexes (mostly iridium, rhodium and

tungsten). In analogy to these cases, the observed inverse KIE could arise from an equilibrium, prior to the formation of product **6.23**, involving the Pd alkyl hydride complex and D_2O.

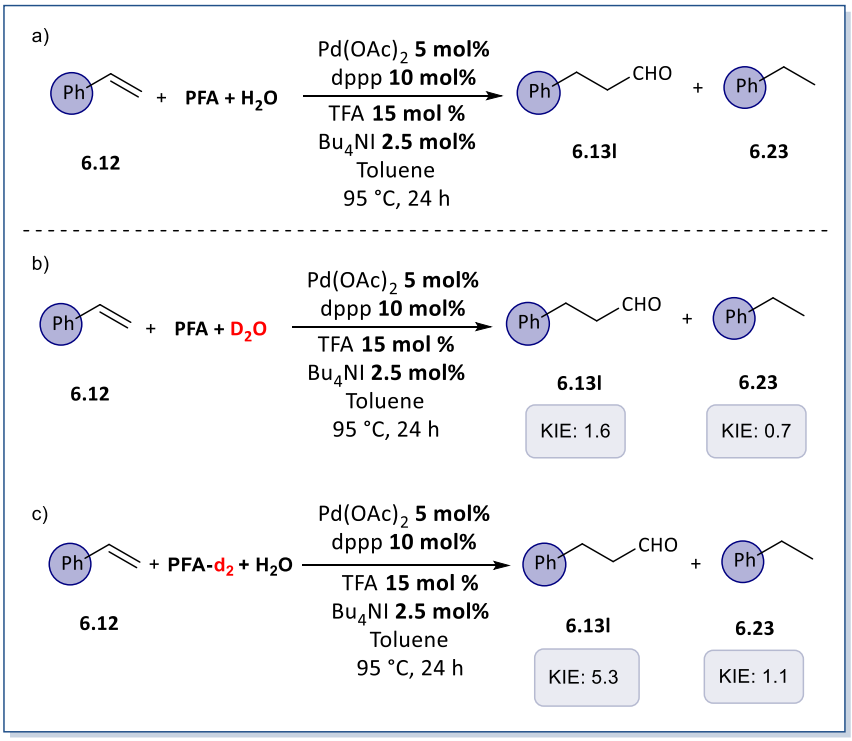

Scheme 6.10. Pd-catalysed hydroformylation of styrene using PFA solution in D_2O and PFA-d_2 with H_2O.

6.3.11 NMR studies

Additionally, NMR studies on the model reaction using the optimized conditions (Table 6.7, Entry 1,) were performed. The reaction was performed stepwise in toluene-d_8 and monitored by ^1H and ^{31}P NMR. In the $^{31}P\{^1H\}$ NMR spectrum of the free dppp, one singlet at -17 ppm was detected, in agreement with previous reports (Figure 6.1, a).[35] When 1.5 equivalent of TFA was added, no change in the spectrum was detected, indicating that the phosphine was not protonated under these conditions (Figure 6.1, b). The solution was then heated to 95 °C but no changes were observed.

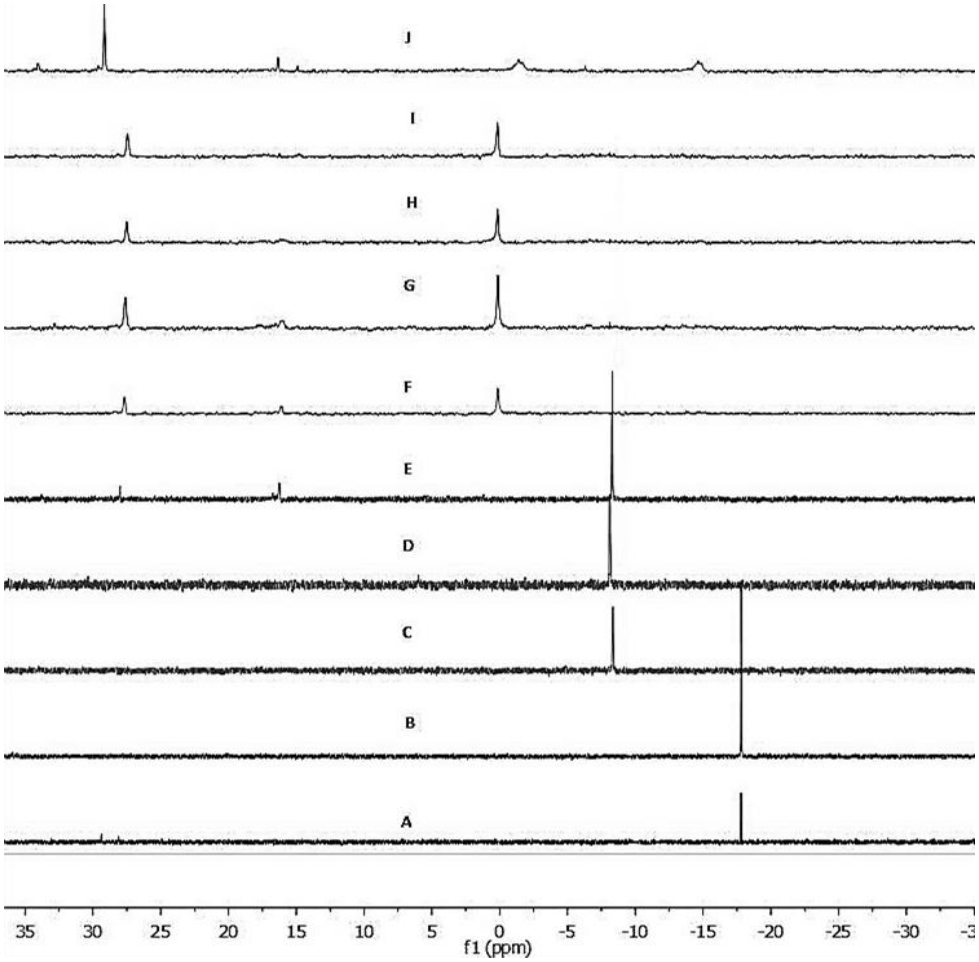

Figure 6.1. $^{31}P\{^{1}H\}$ NMR spectra obtained from the monitoring of the reaction. A) dppp in Toluene at rt. B) dppp, TFA in Toluene at rt. C) dppp, TFA and TBAI in toluene at rt. D) dppp, Tfa, TBAI and $Pd(OAc)_2$ in toluene at rt. e-j) dppp, Tfa, TBAI and $Pd(OAc)_2$ in toluene at 90°C and monitored over 90 minutes.

When the additive NBu_4I was added to the sample (L/additive= 10/2.5), a new singlet appeared at -8 ppm while the resonance for free dppp was not observed anymore (Figure 6.1, c). It is not easy to find a clear explanation on why the chemical shift changed by the addition of the salt. The mixture was heated during 9 hours at 90 °C but no changes were detected. Upon addition of $Pd(OAc)_2$ at room temperature, no changes were observed, indicating that no reaction had occurred under these conditions (Figure 6.1, d). The formalin

aqueous solution was then added into the NMR tube (100 equivalents of formaldehyde per Pd) at 25 °C. In the corresponding $^{31}P\{^{1}H\}$ NMR spectrum, the main peak was still detected at -8 ppm, and the appearance of two small signals at 16 and 28 ppm were also observed (Figure 6.2,c-e). Based on literature reports, these latter signals were attributed to $Pd(dppp)(OAc)_2$ and dppp oxide.[35] Increasing the temperature 50 °C, the peak centred at -8 ppm lowered in intensity while the one at 28 ppm raised (Figure 6.1, e-i). The signal at 16 ppm also first increased in intensity upon warming but after 40 minutes at 90 °C, the signal intensity started to lower and could not be detected after 90 minutes. After 40 minutes at 90 °C, a new signal at 0 ppm was observed and grew over time. This is ascribable to a Pd(0) complex bearing dppp as ligand.[13] At this point, the tube was cooled to room temperature. The signal corresponding to dppp oxide was at this point the main peak, while small resonances corresponding to $Pd(dppp)(OAc)_2$, $[Pd^{0}(dppp)L_n]$ and free dppp were also detected. A $^{13}C\{^{1}H\}$ spectrum was also recorded at this point. A singlet was detected at 184 ppm and assigned to free CO. Next, the catalytic reaction was studied in the presence of styrene (Figure 6.1). At the start of the reaction, the main signals were again those at -8 ppm, 16 ppm and 28 ppm. Upon heating, the peak at 0 ppm appeared again, this time with a bigger intensity. In this experiment, a new peak at 1 ppm that grows in parallel to the peak at 0 ppm was detected.

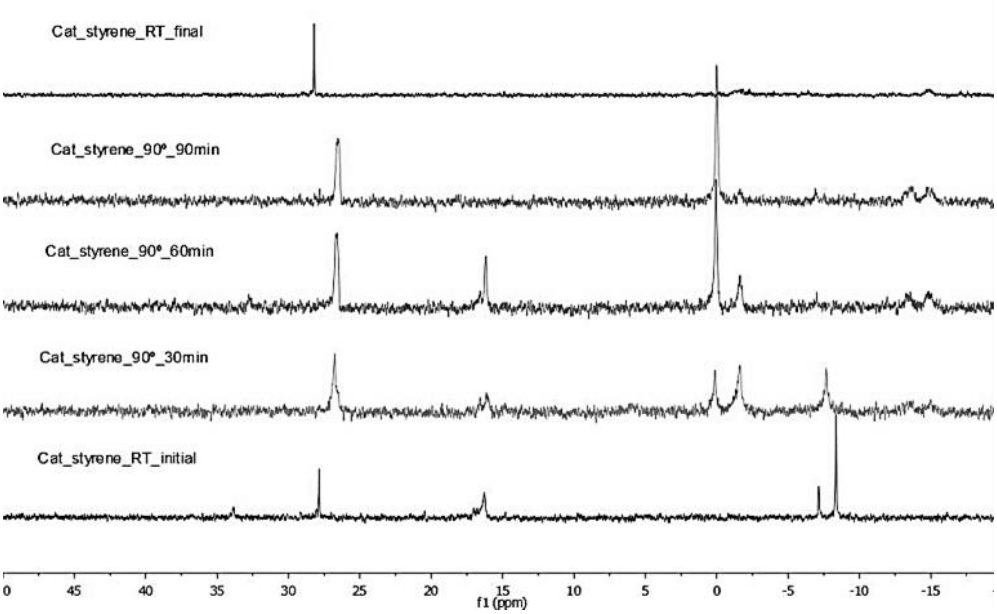

Figure 6.2. $^{31}P\{^{1}H\}$ NMR studies for the catalytic reaction using styrene.

This signal was not observed during the studies in the absence of styrene **6.12**. Due to its chemical shift next to 0 ppm, it was associated to another Pd(0) species, which could contain styrene such as [Pd(dppp)(**6.12**)] **6.26**.

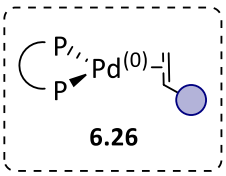

Figure 6.3. [Pd(dppp)(**6.12**)] **6.26**.

Both signals for Pd(0) species were observed to decrease in intensity over time at 90 °C and when the tube was cooled down to room temperature, the signal corresponding to dppp oxide was observed to be the main signal ^{1}H NMR studies for the catalytic reaction using styrene revealed the presence of a triplet at 9.90 ppm corresponding to the 3-phenylpropanal (**6.13l**), confirming that the hydroformylation reaction under these conditions had taken place.

6.3.12 Proposed mechanism

From the results described in the previous sections, the following mechanism for the Pd-catalysed hydroformylation of styrene using formaldehyde as syngas surrogate is proposed. First, the acid additive reacts with $Pd(OAc)_2$ to form the hydride palladium complex **6.27**. This intermediate can directly engage styrene **6.12** in an insertion/β-elimination equilibrium, as suggested by the deuteration of the starting material described in section 6.3.9. Alternatively, reduction of the Pd(II) precursor **6.27** forms a Pd(0) species **6.28** that can either react with styrene **6.12** to form **6.26**, as detected by NMR, or oxidatively add on formaldehyde to produce a Pd(II)-hydride(formyl) complex **6.29**.

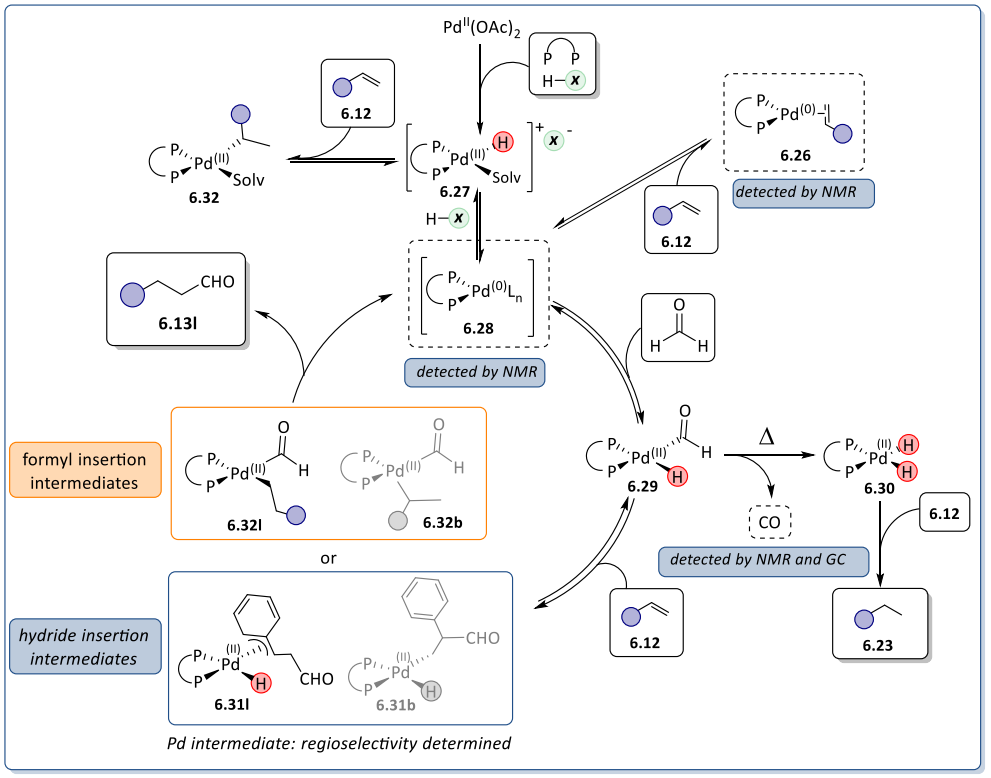

Scheme 6.11. Proposed mechanism of palladium catalysed hydorfomylation of styrene

The latter, can undergo a decarbonylation pathway (detected by NMR) to form a Pd(II)-dihydride species **6.30** that can act as a catalyst for the hydrogenation of styrene **6.12** to form **6.23**. On the other hand, Pd-hydride(formyl) complex **6.29** could productively react with styrene **6.12** through insertion into either the Pd-hydride or the Pd-formyl bonds to form intermediates Pd(II)(H)(acyl) **6.30** or Pd(II)(alkyl)(formyl) **6.31**, respectively. The insertion of styrene into a Pd-H bond has been reported in several catalytic processes such as methoxycarbonylation of alkenes [36] and the insertion of styrene into a Pd-acyl bond was reported in the Pd-catalysed CO/styrene copolymerization.[37] In previous studies on methoxy- and hydroxycarbonylation of styrene, the use of bidentate ligands mainly provided the linear products, indicating the insertion of styrene into a (P-P)Pd-H species undergoes preferentially towards the formation of linear Pd-alkyl intermediates. However, some branched product was always observed (typically, 15-20%).[20] Here, however, the total selectivity towards the linear aldehyde could indicate that the mechanism does not involve the styrene insertion into the Pd-H and hence that the insertion of styrene selectively takes place into the Pd-formyl group prior to reductive elimination to form the linear aldehyde product and regenerate the Pd(0) starting complex. There is currently no report on the preferred insertion of styrene into a Pd-formyl group and DFT calculations will be performed in the near future to clarify this possibility.

6.4 Conclusions

From the study described in this chapter, the following conclusions can be extracted:

I. The screening of various parameter led to a set of optimized conditions of the palladium catalysed hydroformylation of styrene

using $Pd(OAc)_2$ (5 mol%), dppp (10 mol%), TFA (15 mol %), TBAI (2.5 mol %) and formaline (2 mmol) in toluene (1 mL).

II. Under the optimized conditions, the system afforded the best result at 95 °C: 97% conversion, 62% chemoselectivity and l/b ratio >99 towards the linear aldehyde **6.13l**.

III. Deuterium labelling studies suggest that there are various Pd species in the reaction media that are catalytically active: Pd-H, $Pd-(H)_2$ and Pd-(H)(CHO). These experiments indicated that the insertion of styrene into Pd-H/D is reversible under these reaction conditions.

IV. Kinetic isotope effect studies suggest that the relative rate of the formation of Pd-(H)(CHO) and Pd-(D)(CDO) is influenced by the isotopic substitution during the oxidative addition step on the formaldehyde.

V. NMR investigation of the palladium catalytic system highlighted the formation of intermediates **6.26** and **6.28**.

VI. Based on the results obtained, a mechanism has been proposed.

6.5 Experimental Part

6.5.1 General information

All the reactions were carried out using Schlenk-line inert atmosphere techniques or glovebox techniques. Anhydrous solvents were collected from the system Braun MB SPS-800. Commercially available reagents and solvents were purchased at the highest commercial quality from Sigma-Aldrich, Fluka, Alfa Aesar, Fluorochem, Strem and were used as received, without further purification, unless otherwise stated. ^{1}H, $^{13}C\{^{1}H\}$ and $^{31}P\{^{1}H\}$ NMR spectra were recorded using a Varian Mercury VX 400 (400, 100.6, and 161.97 MHz respectively). Chemical shift values (δ) are reported in ppm relative to TMS (^{1}H and $^{13}C\{^{1}H\}$) or H_3PO_4 ($^{31}P\{^{1}H\}$), and coupling constants are reported in Hertz. The following abbreviations are used to indicate the multiplicity: s,

singlet; d, doublet; t, triplet; q, quartet; m, multiplet; bs, broad signal. High-resolution mass spectra (HRMS) were recorded on an Agilent Time-of-Flight 6210 using ESI-TOF (electrospray ionization-time of flight). Samples were introduced to the mass spectrometer ion source by direct injection using a syringe pump and were externally calibrated using sodium formate. The instrument was operating in the positive ion mode. Reactions were monitored by TLC carried out on 0.25 mm E. Merck silica gel 60 F_{254} glass or aluminium plates. Developed TLC plates were visualized under a short-wave UV lamp (254 nm) and by heating plates that were dipped in potassium permanganate.

6.6 References

[1] P. Gautam and B. M. Bhanage, *Catal. Sci. Technol.*, **2015**, *5*, 4663–4702.

[2] L. J. C. Jens Rostrup-Nielsen, *Concepts in Syngas Manufacture*, Imperial College Press, London, **2011**.

[3] T. Morimoto and K. Kakiuchi, *Angew. Chem.*, **2004**, *43*, 5580-5588.

[4] L. Wu, Liu, Q., Jackstell, R., and Beller, M., *Angew. Chem.*, **2014**, *53*, 6310-6320.

[5] R. P. Jennerjahn, I.; Jackstell, R., Franke, R.; Wiese, K.D.; Beller, M., *Chem. Eur. J.*, **2009**, *15*, 6383-6388.

[6] a) J. A. P. Fuentes, R.; Clarke, M, *Chem. Eur. J.*, **2015**, *21*, 10645-10649.

[7] G. M. Makado, T; Sugimoto, Y; Tsutsumi, K; Kagawa, N; Kakiuchi, K;, *Adv. Synth. Catal.*, **2010**, *352*, 299-304.

[8] A. S. C. Chan, W. E. Carroll and D. E. Willis, *J. Mol. Cat.*, **1983**, *19*, 377-391.

[9] H. Ren and W. D. Wulff, *Org. Lett.*, **2012**, *15*, 242-245.

[10] M. Uhlemann, S. Doerfelt and A. Börner, *Tetrahedron Lett.*, **2013**, *54*, 2209-2211.

[11] H. S. Ahn, S. H. Han, S. J. Uhm, W. K. Seok, H. N. Lee and G. A. Korneeva, *J. Mol. Cat.,* **1999**, *144*, 295-306.

[12] G. Jemier, E. M. Nahmed and S.Libs-Konrath, *J. Mol. Cat.*, **1991**, *64*, 337-347.

[13] A. F. R. Börner, *Hydroformylation: Fundamentals, Processes and Applications in Organic Synthesis*, **2016**.

[14] M. Yates, T,E; Dresser, M, *J. Catal.*, **1973**, *30*, 260-275.

[15] E. Irdam and J. Kiefer, *Int. J. Chem. Kinet.*, **1993**, *25*, 285-303.

[16] K. Saito, T. Kakumoto, Y. Nakanishi and A. Imamura, *J. Phys. Chem.*, **1985**, *89*, 3109-3113.

[17] M. Rosales, H. Pérez, F. Arrieta, R. Izquierdo, C. Morationos and P. J. Baricelli, *J. Mol. Cat. A: Chemical,* **2016**, *421*, 122-130.

[18] J. Pospech, Fleischer, I., Franke, R., Buchholz, S., and Beller, M., *Angew. Chem.*, **2013**, *52*, 2852-2872.

[19] B. H. M. Drent E., *Chem. Rev.*, **1996**, *96*, 663-681.

[20] I. del Río, C. Claver and P. W. N. M. van Leeuwen, *Eur. J. Inorg. Chem*, **2001**, 2719-2738.

[21] Patent D. E., 220767, **1986**.

[22] K.H. Dotz, *Organotransition Metal Chemistry: Application of organic Synthesis*, Pergamon, Oxford, UK, **1982**.

[23] R. E. R. Van Asselt, E. E. C. G. Gielens, K. Vrieze and C. J. Elsevier, *J. Am. Chem. Soc.*, **1994**, *116*, 977–985.

[24] B. A. Markies, D. Kruis, M. H. P. Rietveld, K. A. N. Verkerk, J. Boersma, H. Kooijman, M. T. Lakin, A. L. Spek and G. Vankoten, *J. Am. Chem. Soc.*, **1995**, *117*, 5263-5274.

[25] G.P.C.M. Dekker, K. Vrieze, P.W.N.M. Van Leeuwen and C.F. Roobeek, *J. Organomet. Chem.*, **1992**, *430*, 357-372.

[26] M.P. Maitlis, *The Organic Chemistry of Palladium*, Academic Press, London, UK, **1971**.

[27] E. Drent and P. H. M. Budzelaar, *J. Organomet. Chem.*, **2000**, 593-594, 211-225.

[28] W. Ren, J. Chang, J. Dai, Y. Shi, J. Li, Y. Shi , *J. Am. Chem. Soc.*, **2016**, 14864-14867.

[29] A. A. Somasunderam, *J. Mol. Catal.* , **1994**, *92*, 35-40.

[30] B. El Ali, G. Vasapollo, H. Alper, *J. Mol. Catal. A. Chem.*, **1996**, *112*, 195-201.

[31] R. P. Jennerjahn, I. Piras, R.cJackstell, R. Franke, K. D. Wiese and M. Beller, *Chem. Eur. J.* **2009**, *15*, 6383-6388.

[32] H. J. Prins., *Chem. Week.*, **1919**, *16*, 51-56.

[33] F. T. Y. Du, *Catal. Commun.* **2007**, *8*, 2012-2016.

[34] Q. Liu, K. Yuan, B. Arockiam, R. Franke, H. Doucet, R. Jackstell, M. Beller, *Angew. Chem. Int. Ed.*, **2015**, *54,* 4493-4497.

[35] C. Amatore, A. Jutand and A. Thuilliez, *Organometallics*, **2001**, *20,* 3241-3249.

[36] Q. Liu, K. Yuan, B. Arockiam, R. Franke, H. Doucet, R. Jackstell and M. Beller, *Angew. Chem. Int. Ed.*, **2015***, 54,* 4493-4497.

[37] M. Sperrle, A. Aeby, G. Consiglio, and A. Pfaltz, *Helv. Chem. Act.,* **1996**, *79*, 5, 1387-1392.

Chapter VII

Rhodium catalysed reductive carbonylation of cinnamyl acetate

Rhodium and Palladium Catalysed Unusual Regioselective Hydroformylation and Rhodium Catalysed Reductive Carbonylation

Benedetta Palucci

7.1 Introduction

7.1.1 Reductive carbonylation

The reductive carbonylation is a reaction where terminal aldehydes are produced. Many procedures, for the production of aldehyde (Scheme 7.1), are known as named reactions, like the Gattermann-Koch, Gattermann, Reimer-Tiemann, Duff, Vilsmeier-Haack, Nef, Zincke, McFadyen-Stevens, Meyers and also the Stephen aldehyde synthesis.[1] Nonetheless, the hydroformylation is the most widely industrial process to produce aliphatic aldehydes.[2,3,4,5]

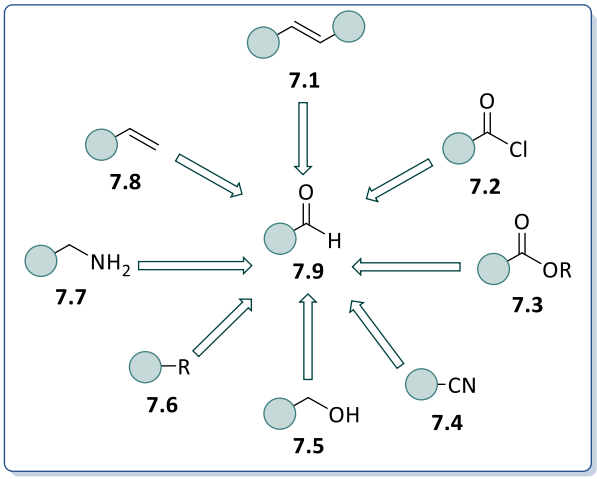

Scheme 7.1. procedures for the aldehyde productions

Reductive carbonylation procedures catalysed by transition metals offer a straightforward method for the preparation of aryl aldehydes. Specifically, starting from the corresponding aryl-X (X = I, Br, Cl, OTf, etc.), in the presence of the catalyst and syngas, aromatic aldehydes can be easily prepared (Scheme 7.2). Like alkoxycarbonylation, aminocarbonylation, and hydroxycarbonylation, the palladium-catalysed reductive carbonylation reaction was originally discovered by Schoenberg and Heck in 1974.[6] In the presence of catalytic amounts of $[PdX_2(PPh_3)_2]$ (1 mol%) under 80–100 bar

of syngas and at 80–150 °C, aryl and vinyl bromides or iodides were converted into the corresponding aldehydes in good yields.

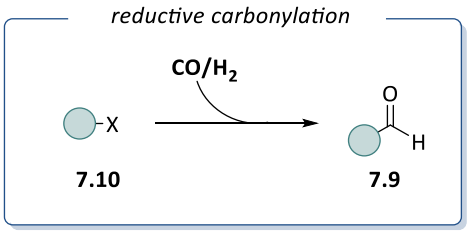

Scheme 7.2. reductive carbonylation

One decade later, this pioneering work was improved by Baillargeon and Stille,[7] using metal hydrides such as tributyltin hydride (Bu_3SnH), as reducing agents in the reductive carbonylation reaction. Because of the toxicity and waste generation of tin hydrides, these were substituted by the corresponding organosilanes.[8] Moreover, the use of readily available and cheap formate salts represents an economically attractive alternative to syngas for performing palladium-catalysed reductive carbonylation.[9] Due to the industrial importance of this protocol, the mechanism of the reductive carbonylation of aryl bromides with synthesis gas has been investigated.[10] A simplified mechanism has been detailed in Scheme 7.3. For the reductive carbonylation to proceeded, dissociation of a ligand from PdL_2 **7.11** to generate the active PdL species **7.12** is required. This active intermediate engages aryl halides **7.10** in an oxidative addition step, generating intermediate **7.13**. The insertion of CO generates acyl palladium intermediate **7.14**, that after hydrogenolysis, delivers the target aldehyde **7.9**. The ensuing palladium complex **7.15** is restored by the base and ligand dissociation.

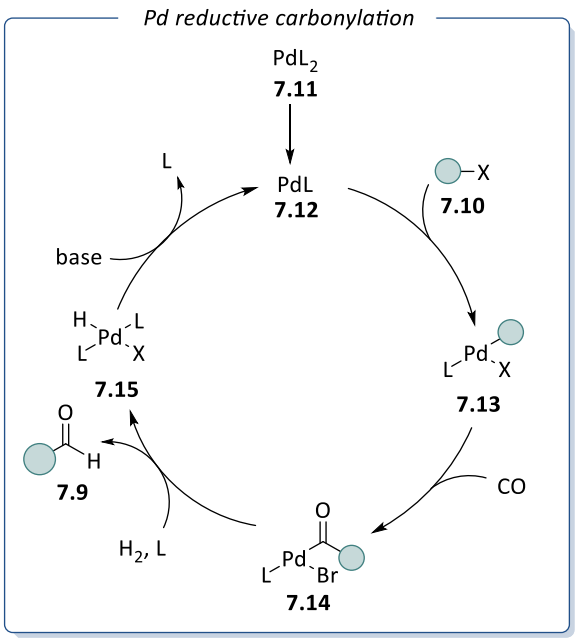

Scheme 7.3. Mechanism of reductive carbonylation

Reductive carbonylation reactions offer an interesting pathway for the synthesis of aromatic aldehydes, starting from the easily available corresponding halides. Overall the selective aldehydes are selectively produced in good yields. In view of these results, IFF began their investigation into the rhodium catalysed reductive carbonylation process, thus enabling the unprecedented use of allyl acetates as substrate.[11]

7.2 Objectives

The main objective of this chapter is the development of an unprecedent process called rhodium catalysed reductive carbonylation of cinnamyl acetate for the production of the corresponding aldehyde, and the investigation of the catalytic mechanism.

The specific objectives of this chapter are:

- The study of the effect of the ligand in the reductive carbonylation process.
- The study of the reactivity towards CO, and H_2/CO pressure of the rhodium precursors $RhH(CO)(PPh_3)_3$ in the presence of cinnamyl acetate **7.16b**, using HP NMR spectroscopy.
- The study of the reactivity towards CO, and H_2/CO pressure of the rhodium precursor $Rh(acac)(CO)_2$ /**7.21** in the presence of cinnamyl acetate **7.16b**, using HP NMR spectroscopy.

7.3 Results and discussion

7.3.1 Optimization of the reaction conditions

The reaction was performed under the catalytic conditions reported by a previous study carried out in the IFF laboratory. The reaction was performed under 13 bar of 1:1 CO/H_2 using $RhH(CO)(PPh_3)_3$ (0.1 mol%) as catalyst, and cinnamyl acetate **7.16b** as substrate in toluene (1.5 mL) for 6 hours at 120°C. It is noteworthy that these conditions are not identical to the original ones since the substrate tested in IFF contained an iso-propyl substituent (**7.16a**) at the *para* position of the aryl ring.

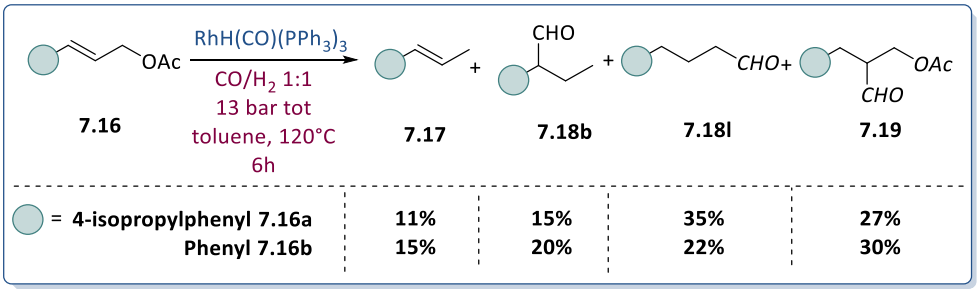

Scheme 7.4. Reductive carbonylation of allyl acetate

Scheme 7.4 shows the results obtained at IFF with substrate **7.16a**, where the conversion is at 85%. The product arising from the isomerization of the double bond after extrusion of the acetate group (**7.17**) was detected (11% in

the reaction crude). The branched (**7.18b**) and the linear (**7.18l**) aldehydes were obtained in 11% and 35% GC-yield, respectively, whereas the product **7.19**, due to the direct hydroformylation of the double bond, was also obtained (21%). When the reaction was tested in our laboratory with substrate **7.16b**, the conversion is slightly higher (92%), but the by-products **7.17** and **7.19** were present in slightly higher amounts (15% and 30% respectively).

Next, the study of the effect of the ligand in the reductive carbonylation process was performed (Table 7.1). The reactions were performed at 13 bar of 1:1 CO:H_2 using $RhH(CO)(PPh_3)_3$ (0.1 mol%) for 6 hours at 120 °C, as described in Table 7.1. In Entry 2, $Rh(acac)(CO)_2$ was used as Rh precursor with three equivalents of PPh_3 **7.22**, but only 4% of conversion of the starting material was observed. When two equivalents of PPh_3 **7.22** were used (Entry 3), 99% of conversion was observed, but the major product is **7.19**, with only 15% of aldehydes **7.18b** and **7.18l** formed. In Entry 4, two equivalents of $P(OPh)_3$ **7.23** with $Rh(acac)(CO)_2$ shows 91% of conversion, where the major product is the methyl styrene **7.17**. Commercial dppb **7.24** in Entry 5 delivers 3% of the desired aldehyde, over a 17% of conversion of the starting material. Next, BINAP **7.25** in Entry 6 was tested, and affords 43% of conversion, where the major product is the methyl styrene **7.17**. The use of the bidentate phosphine-phosphite ligand **7.21**, whose synthesis has been first carried out in our laboratories and described in Chapter IV, shows 87 % conversion, with 57 % of the desired aldehydes (Entry 7). Similarly, the use of commercially available BOBPHOS **7.26** (Entry 8) afforded the aldehydes **7.18b** and **7.18l** in slightly higher percentage (68%), along with the formation of **7.19**.

In conclusion, the screening of the ligands highlighted how the Rh-system bearing a bidentate phosphine-phosphite (**7.21**) or phosphine-phospholane (BOBPHOS **7.26**) structures, delivers the highest percentage of aldehyde under these reductive carbonylation conditions.

Table 7.1. Screening of the ligand of reductive carbonylation

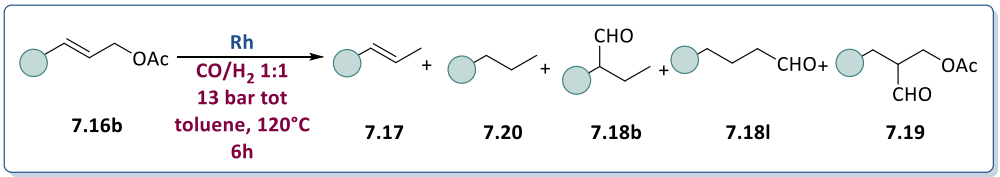

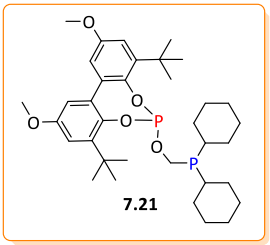

Entry[a]	Rh precursor	L	7.17	7.20	7.18 (b+l)	7.19
1	$RhH(CO)(PPh_3)_3$	-	15	-	42	30
2	$Rh(acac)(CO)_2$	$(PPh_3)_2$ **7.22**	-	-	4	-
3	$Rh(acac)(CO)_2$	$(PPh_3)_3$ **7.22**	-	-	15	74
4	$Rh(acac)(CO)_2$	$[P(OPh)_3]_2$ **7.23**	52	10	32	-
5	$Rh(acac)(CO)_2$	Dppb **7.24**	11	7	5	-
6	$Rh(acac)(CO)_2$	BINAP **7.25**	22	2	10	9
7	$Rh(acac)(CO)_2$	**7.21**	30	-	57	-
8	$Rh(acac)(CO)_2$	BOBPHOS **7.26**	25	-	68	5

Reaction conditions:[a] cinnamyl acetate **7.16b** (2.06 mmol), Rh precatalyst (0.1 mol%), ligand (1.1 mol%), 13 bar 1:1 $CO:H_2$, 120°C for 6 hours. Conversion, chemoselectivity and regioselectivity determined by GC-FID and NMR using bicyclohexyl as internal standard.

7.3.2 Mechanism investigation: HP-NMR studies

7.3.2.1 Mechanism insight using $RhH(CO)(PPh_3)_2$

In order to gain understanding about the species present during the catalysis, systematic study of HP-NMR experiments was conducted under different

reaction conditions. The reactivity of $RhH(CO)(PPh_3)_2$ **7.27** with cinnamyl acetate **7.16b** was studied by mixing them at room temperature inside a 5 mm HP-NMR tube and then the solution was analysed by $^{31}P\{^1H\}$ NMR, ^1H and ^{13}C NMR spectroscopy.

Reactivity of $RhH(CO)(PPh_3)_2$ in the presence of cinnamyl acetate 7.16b

First, a solution of the precursor $RhH(CO)(PPh_3)_2$ **7.27** (0.01 mmol) and cinnamyl acetate **7.16b** (0.01 mmol) in toluene-d^8 (0.4 ml) was analysed by NMR at room temperature (time zero).

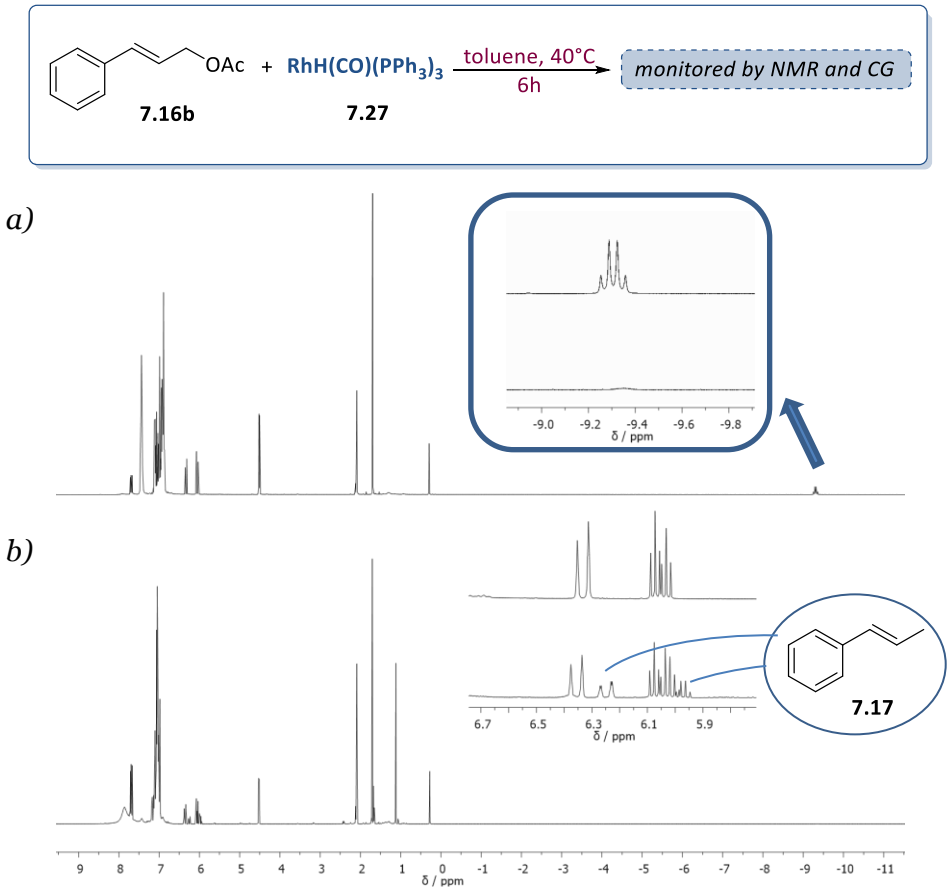

Scheme 7.5. Selected NMR signals for the stoichiometric reaction between $RhH(CO)(PPh_3)_3$ **7.27** and cinnamyl acetate **7.16b**. (a) ^1H NMR spectra (400 MHz, 0 °C), $RhH(CO)(PPh_3)_3$ **7.27** and cinnamyl acetate **7.16b** at time zero; (b) ^1H NMR spectra (400 MHz, RT), $RhH(CO)(PPh_3)_3$ **7.27** and cinnamyl acetate **7.16b** after 6 h at 40°C.

Subsequently the same mixture was heated at 40 °C for 6 hours, cooled to 25 °C and analysed by NMR. The reaction was monitored by both ^{1}H and ^{31}P NMR. The ^{1}H NMR spectrum recorded at time zero (Scheme 7.5, a), shows the expected characteristic signals recorded at 0 °C , as a quartet at -9.31 ppm with a J_{P-H} of 14 Hz of the $RhH(CO)(PPh_3)_3$ **7.27** according to the reported data,[12,13] and the signals corresponding to the substrate **7.16b** [δ 6.65 (d, J_{H-H} = 15.9 Hz, 1H), 6.29 (dt, J_{H-H} = 15.9, 6.5 Hz, 1H), 4.73 (dd, J_{H-H} = 6.5, 1.3 Hz, 2H), 2.10 (s, 3H)]. After heating at 40 °C for 6 hours, three new signals were readily detected in the ^{1}H NMR spectrum: a doublet of doublets at 6.25 ppm with a (J_{H-H}= 15.7 Hz and 1.8 Hz), a multiplet located at 6.02 ppm and a doublet of doublets at 1.88 ppm (dd, J_{H-H} = 6.5, 1.6 Hz). This new set of signals are diagnostic of the formation of β-methyl styrene, as confirmed by both 1D and 2D NMR spectroscopy experiments and from the analysis of the commercial original sample. Additionally, a new singlet at 1.12 ppm in ^{1}H NMR spectrum was detected. Bidimensional ^{1}H-^{13}C NMR experiments (HSQC and HMBC) revealed that the protons corresponding to the latter signal are directly bonded to a carbon at 23.3 ppm and close to a carbon from a carbonyl group at 175.0 ppm (Figure 7.1 and 7.2). This signal was therefore attributed to a new acetate moiety.

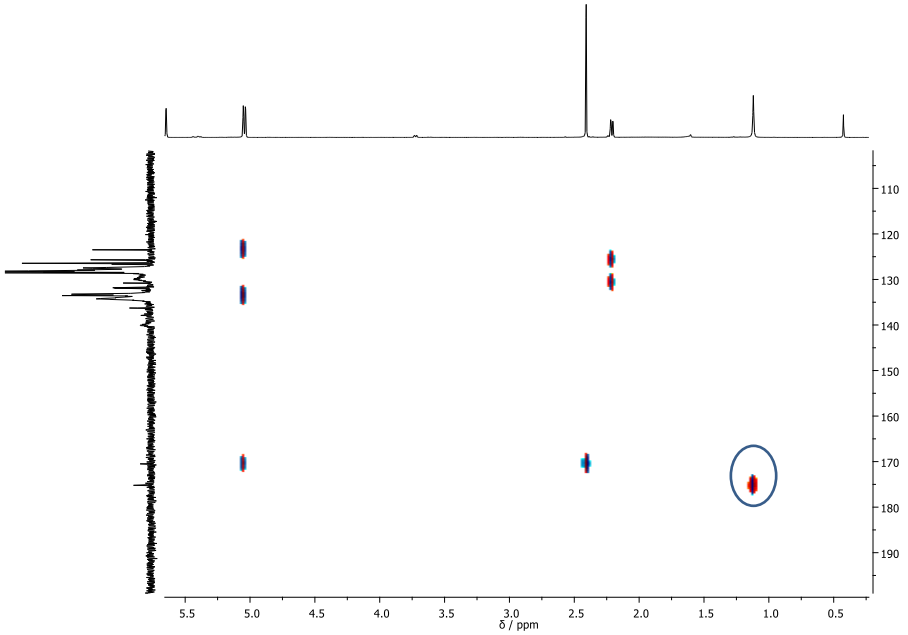

Figure 7.1. ^{1}H- ^{13}C HMBC NMR spectra (101 MHz, RT), Stoichiometric reaction between $RhH(CO)(PPh_3)_3$ **7.27** and cinnamyl acetate **7.16b.**

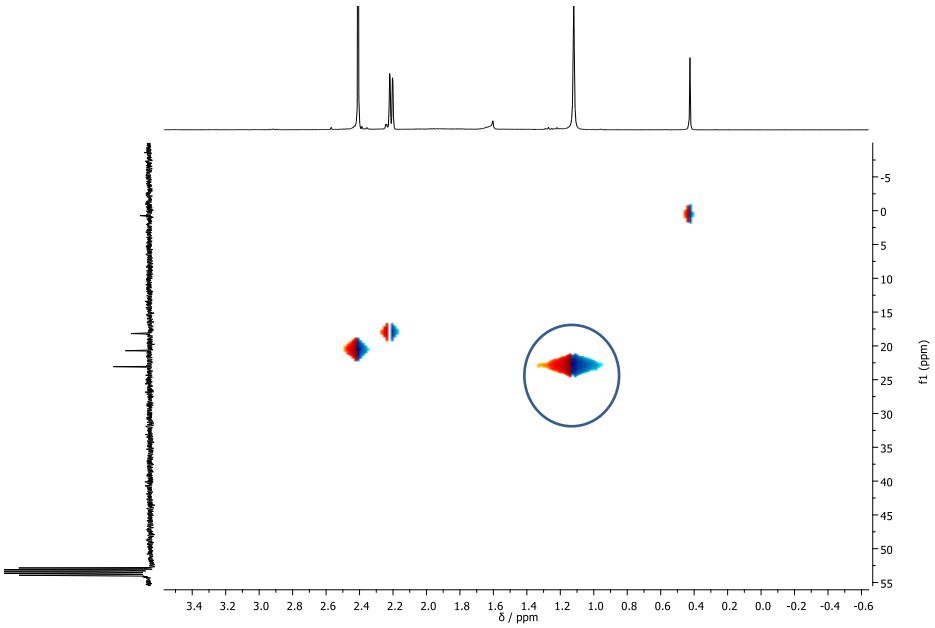

Figure 7.2. ^{1}H -^{31}P HSQC NMR spectra (101 MHz, RT), Stoichiometric reaction between $RhH(CO)(PPh_3)_3$ **7.27** and cinnamyl acetate **7.16b**

After having heated the NMR tube at 40 °C for 6 hours, the hydride signal corresponding to $RhH(CO)(PPh_3)_3$ **7.27** could not be detected anymore, thus indicating that these species had reacted to form the aforementioned β-methyl styrene **7.17**. The $^{31}P\{^1H\}$ NMR spectrum (Figure 7.3, a) acquired at time zero, revealed a doublet at 40 ppm with a J_{P-Rh} of 154 Hz corresponding to the starting Rh hydride complex **7.27**. A signal at 24.1 ppm was also detected and corresponded to an impurity already present in the commercial rhodium precursor. The $^{31}P\{^1H\}$ NMR spectrum acquired after 3 hours at 40 °C (Figure 7.3, b), shows the formations of a new doublet at 31.7 ppm with a J_{P-Rh} of 137 Hz, indicating the formation of a new Rh-phosphine species under these conditions.

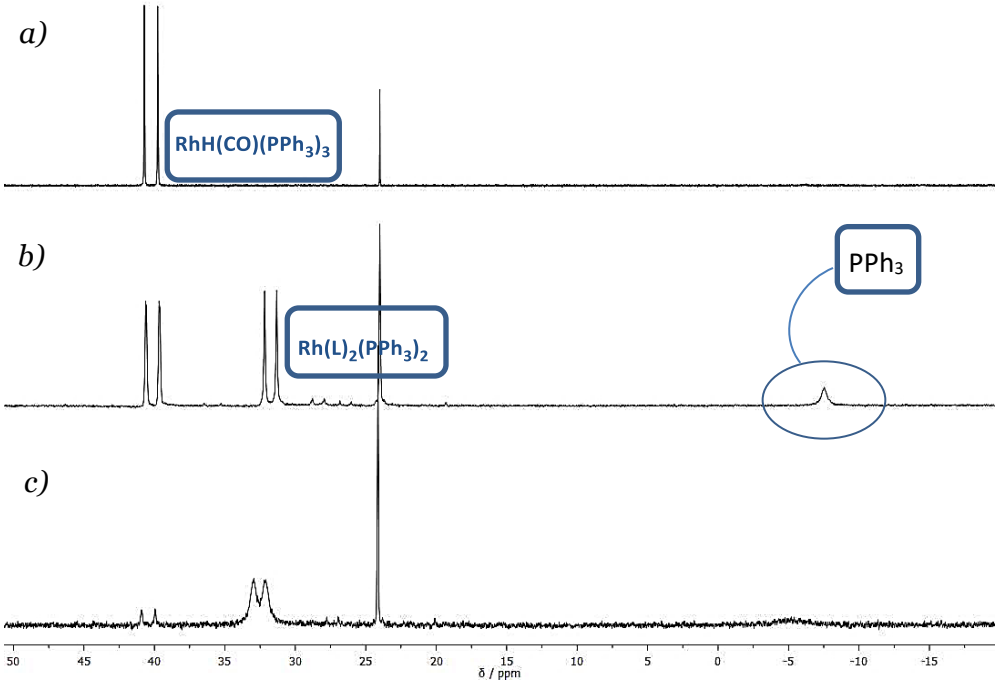

Figure 7.3. Selected ^{31}P NMR signals for the stoichiometric reaction between $RhH(CO)(PPh_3)_3$ **7.27** and cinnamyl acetate **7.16b**. (a) $^{31}P\{^1H\}$ NMR (162 MHz, 0 °C) $RhH(CO)(PPh_3)_3$ **7.27** and cinnamyl acetate **7.16b** at time zero; (b) $^{31}P\{^1H\}$ NMR (162 MHz, RT) $RhH(CO)(PPh_3)_3$ **7.27** and cinnamyl acetate **7.16b** after 3 hours at 40°C; (c) $^{31}P\{^1H\}$ NMR (162 MHz, RT) $RhH(CO)(PPh_3)_3$ **7.27** and cinnamyl acetate **7.16b**, 6 hours at 40°C.

At -7.72 ppm, the peak of the free phosphine was also detected. The $^{31}P\{^{1}H\}$ NMR spectrum acquired after 6 hours at 40°C (Figure 7.3, c), revealed the almost complete consumption of the starting species in favour of the species corresponding to the signal at 31.7 ppm.

These results thus indicated the transformation of the Rh hydride precursor **7.27** into a new Rh species containing 1 or 2 phosphine ligands that does not contain any hydride. It is important to mention that the formation of this species appeared concomitantly to the formation of β-methyl styrene **7.17**.

Based on these experiments, it can be concluded that the stoichiometric reaction between the rhodium precursor **7.27** and **7.16b** provides β-methyl styrene **7.17** as the main organic product and a new Rh species containing 2 equivalent phosphine ligands and no hydride. A possible mechanism is proposed in Scheme 7.6.

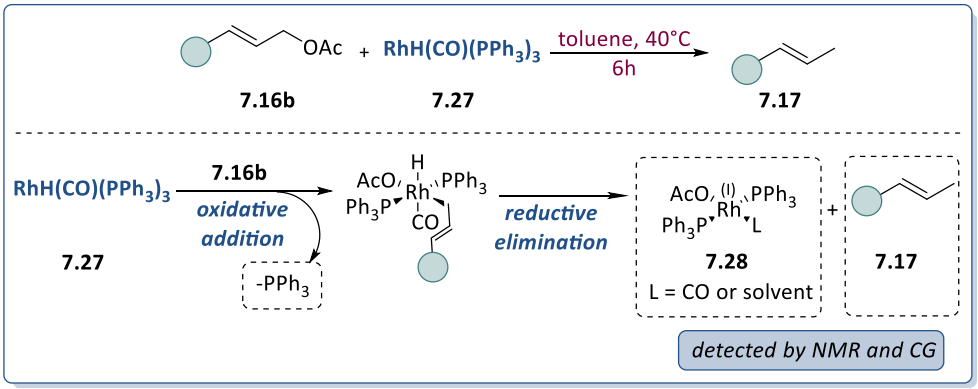

Scheme 7.6. Stoichiometric reaction for reductive carbonylation

The formation of the β-methyl styrene **7.17** suggests the involvement of an oxidative addition and a reductive elimination step. When the β-methyl styrene **7.17** is produced a new rhodium species **7.28** is also formed in the reaction mixture, probably containing an acetate, bonded to the Rh center. It is worth to mention that, when β-methyl styrene **7.17** was employed as substrate under the same hydroformylation conditions described in Table 7.1 Entry 1, no conversion towards the corresponding aldehydes was observed.

Subsequently, HP NMR experiments were carried out in the presence of CO pressure.

Reactivity of $RhH(CO)(PPh_3)_3$ in the presence of cinnamyl acetate 7.16b under CO pressure

First, a HP NMR tube was charged with a solution of substrate **7.16b** (0.01 mmol) and $RhH(CO)(PPh_3)_3$ (0.01 mmol) **7.27** in deuterated DCM (0.4 mL) and 7 bar of CO at room temperature. The reaction was then monitored by multinuclear NMR techniques at various temperatures.

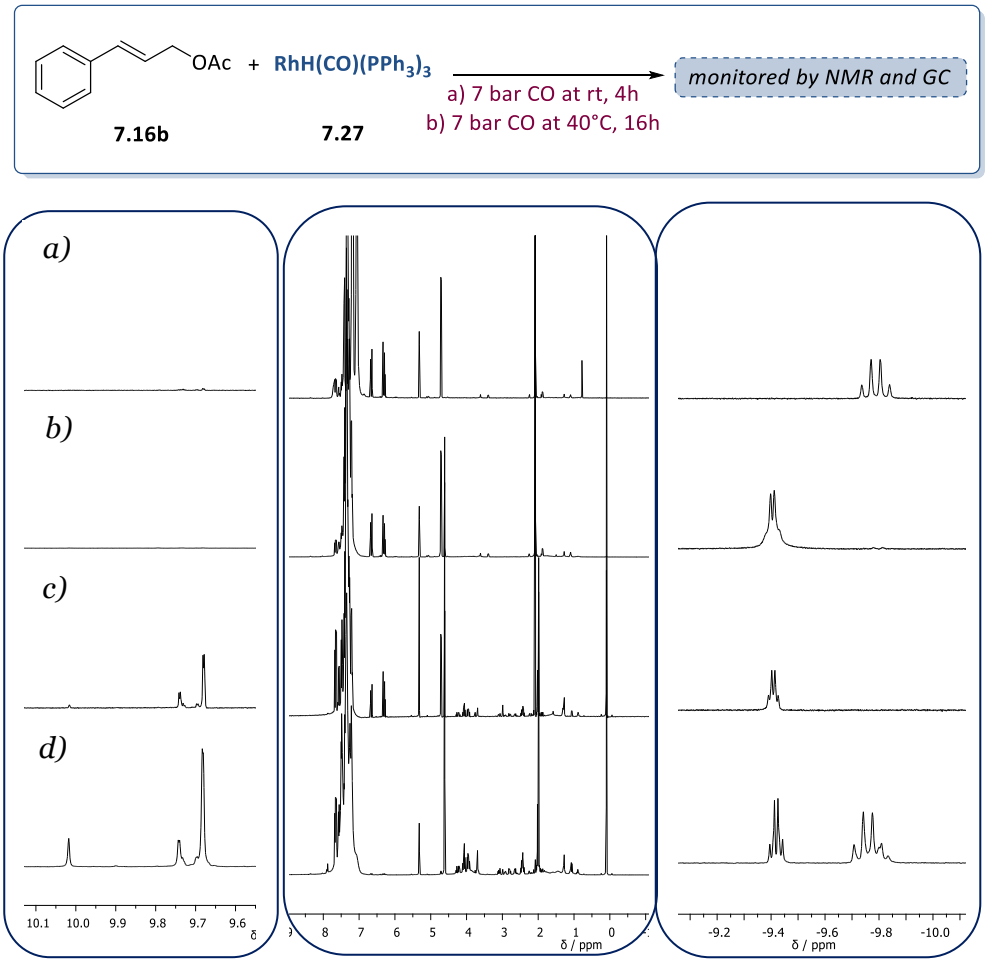

Scheme 7.7. Selected NMR signals for HP NMR analysis $RhH(CO)(PPh_3)_3$ **7.27** and cinnamyl acetate **7.16b**. (a) ^1H NMR spectra (400 MHz, -40 °C) $RhH(CO)(PPh_3)_3$ **7.27** and cinnamyl

acetate **7.16b** at time zero; (b) ^{1}H NMR spectra (400 MHz, -60 °C) $RhH(CO)(PPh_3)_3$ **7.27** and cinnamyl acetate **7.16b** with 7 bar CO, time zero; (c) ^{1}H NMR spectra (400 MHz, RT) $RhH(CO)(PPh_3)_3$ **7.27** and cinnamyl acetate **7.16b** 56 h at RT; (d) ^{1}H NMR spectra (400 MHz, -40 °C) $RhH(CO)(PPh_3)_3$ **7.27** and cinnamyl acetate **7.16b** with 7 bar CO at 40 °C for 16 h.

When the sample containing $RhH(CO)(PPh_3)_3$ **7.27** and the cinnamyl acetate **7.16b** was placed under 7 bar of CO and acquired at -60 °C, a change in the NMR spectra was observed (Scheme 7.7, spectra a vs b). A new singlet at 4.6 ppm was observed, and a new hydride signal was detected at -9.41 ppm as a quartet (J_{Rh-H}= J_{P-H}= 5 Hz). The same sample, left for 56 hours at room temperature, was acquired at 25 °C, revealing the formation of new signals in the aldehyde region (Scheme 7.7, c). Moreover, to probe the potential reversibility of the reaction, the CO pressure was released from the NMR tube. Subsequent acquisition displayed no changes, indicating that this process was irreversible. The tube was then charged with 7 bar of CO and left at 40 °C for 16 hours (Scheme 7.7, d). Acquisition at -40 °C revealed two quartet signals in the hydride region, one centred at -9.41 ppm (J_{Rh-H}= J_{P-H}= 5 Hz) and the other at -9.75 ppm (J_{Rh-H}= J_{P-H}= 14 Hz). The $^{31}P\{^{1}H\}$ spectra (Figure 7.4) displayed important changes as well. Once the NMR tube was charged with 7 bar of CO, the signal of the starting complex was not detected and a new doublet at 32.2 ppm with a J_{P-Rh} of 132 Hz was observed (Figure 7.4, a vs b). Moreover, a broad doublet was detected at 20.3 ppm together with a broad signal at -8.8 ppm attributed to uncoordinated triphenylphosphine. These results indicated that a new Rh-hydride species was formed under these conditions. The presence of free PPh_3 indicated that at least one of the phosphine ligands of the starting complex could have been substituted by CO.

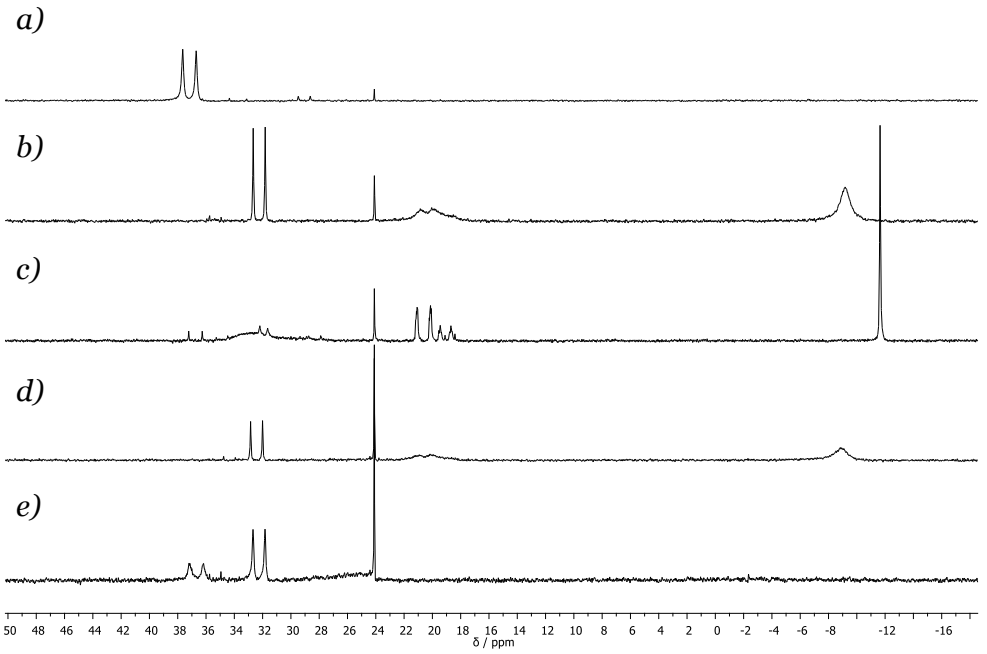

Figure 7.4. Selected NMR signals for HP NMR analysis $RhH(CO)(PPh_3)_3$ **7.27** and cinnamyl acetate **7.16b**. (a) $^{31}P\{^1H\}$ NMR (162 MHz, -40 °C) $RhH(CO)(PPh_3)_3$ **7.27** and cinnamyl acetate **7.11b** at time zero; (b) $^{31}P\{^1H\}$ NMR (162 MHz, RT) $RhH(CO)(PPh_3)_3$ **7.27** and cinnamyl acetate **7.11b** with 7 bar CO; (c) $^{31}P\{^1H\}$ NMR (162 MHz, -65 °C) $RhH(CO)(PPh_3)_3$ **7.27** and cinnamyl acetate **7.11b** with 7 bar CO; (d) $^{31}P\{^1H\}$ NMR (162 MHz, rt) $RhH(CO)(PPh_3)_3$ **7.27** and cinnamyl acetate **7.16b** after 52 hours at RT; (e) $^{31}P\{^1H\}$ NMR (162 MHz, rt) $RhH(CO)(PPh_3)_3$ **7.27** and cinnamyl acetate **7.16b** 7 bar CO at 40 °C for 16 hours.

HMBC ^1H-^{31}P showed a correlation between the new hydride signal and the ^{31}P resonance at 32.2 ppm. The formation of two isomers of $RhH(PPh_3)_2(CO)_2$ is proposed in scheme 7.8.

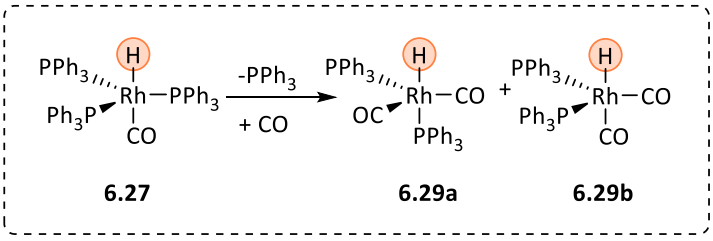

Scheme 7.8. Proposed rhodium species observed by NMR

NMR acquisitions performed at lower temperature (-65 °C, Figure 7.4, c) demonstrated how this broad signal could be resolved into two doublet of multiplets, centered at 20.63 ppm (J_{P-Rh}=154 Hz) and at 19.10 ppm (J_{P-Rh} = 124.17 Hz). These signals could be due to bridged rhodium species, in equilibrium in solution due to the presence of external CO pressure, such as the one proposed by Wilkinson $[Rh(CO)_2(PPh_3)_2]_2$.[13] When the sample was left 52 hours at room temperature, three signals were detected in the aldehyde region of the ^1H spectrum (Scheme 7.7, d), indicating the formation of hydroformylation products under these conditions. These signals were attributed to **7.18b, 7.18l** and **7.19** (Figure 7.5) based on their multiplicity and confirmed by GC-MS analyses.

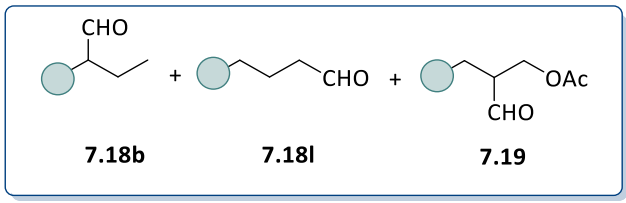

Figure 7.5. Aldehydes produced **7.18b, 7.18l** and **7.19**.

This result was unexpected due to the absence of exogenous H_2. Careful analysis of the spectrum revealed the appearance of a ^1H signal at ca. 4.5 ppm during the reaction (Scheme 7.7, d), suggesting that H_2 is somehow produced under these conditions and could result from the reaction between two Rh-H intermediates. The very same behaviour was observed by Wilkinson, H_2 is formed through a rapid equilibrium between two $RhH(CO)_2(PPh_3)_2$ species under CO pressure.[13] The formation of the aldehyde products could therefore be explained by the reductive hydroformylation of the substrate or by an intermolecular reaction between a Rh-H and Rh-acyl species formed after reaction of the Rh-H with the substrate followed by carbonylation. In the hydride region of the spectrum, (Scheme 7.7, d) one new quartet was detected at -9.75 ppm (J_{Rh-H}= J_{P-H}= 14 Hz). At the same time in the ^{31}P NMR, a new doublet at 40.23 ppm was detected with a J_{P-Rh} of 154 Hz, indicating the formation of a new Rh-P species. Moreover, the signal corresponding to the

free PPh_3 completely disappeared, suggesting the formation of a rhodium hydride containing 3 equivalent of PPh_3. This set of signal, detected by both ^1H and ^{31}P NMR, suggests that the starting complex **7.27** has been restored. One possible explanation is proposed in Scheme 7.9. A rapid equilibrium occurs between the Rh species depicted, the presence of external CO pressure tends to displace the PPh_3 from the initial Rh complex **7.27**, to form the $RhH(PPh_3)_2(CO)_2$ **7.29a** and **7.29b**. The last step is favored since carbon monoxide helps the extrusion of molecular H_2 from the two Rh-H species. The intramolecular reaction between the two rhodium hydride species delivers the proposed dimer (**7.29 c**). The generation of molecular hydrogen pushes the equilibrium back to the starting complex **7.27**, as detected by this set of NMR experiment.

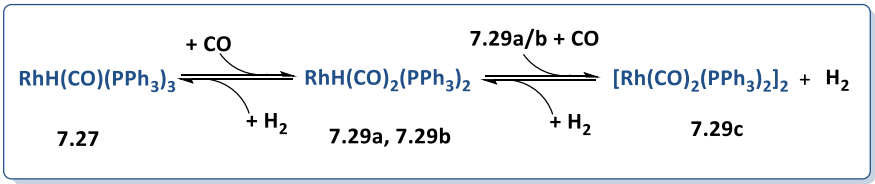

Scheme 7.9. Equilibrium between rhodium species under CO and H_2 pressure

Based on the results obtained, a potential mechanism is proposed (see Scheme 7.10). First, extrusion of the phosphine from **7.27** produces the active catalyst **7.30**. Oxidative addition onto **7.16b** produces the Rh allyl intermediate **7.31** that can undergo reductive elimination to form **7.17,** in the absence of CO. Under CO pressure, migratory insertion can produce the branched **7.32b** or linear intermediates **7.32l** that could undergo two different pathways: 1) extrusion of acetic acid to deliver the square planar acyl rhodium complexes **7.33b** and **7.33l**, that under CO/H_2 pressure deliver the desired aldehydes **7.18b** and **7.18l**.

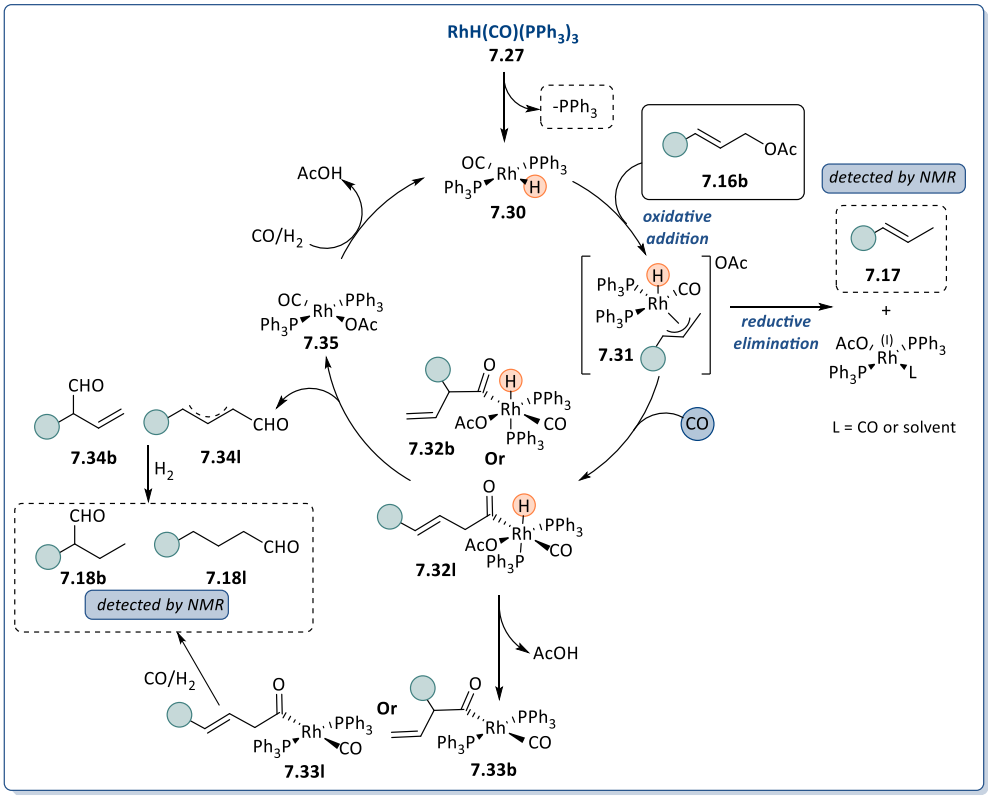

Scheme 7.10. Proposed mechanism for the reductive rhodium carbonylation

Alternatively, 2) the extrusion of unsaturated aldehydes **7.34b** and **7.34l**, form the rhodium species **7.35** that, through treatment with syngas, regeneratea the initial hydride species **7.30**. The unsaturated aldehydes (**7.34b** and **7.34l**) later can undergo hydrogenation to produce the desired products **7.18b** and **7.18l**. The aldehyde **7.19** (Figure 7.5), observed as product of the catalysis produced under the conditions described in Table 7.1 Entry 1, is not produced within this catalytic cycle, but in a classical hydroformylation pathway.

7.3.2.2 Mechanism insight using [Rh(acac)(CO)$_2$] with ligand 7.21

In order to gain understanding about the species present during the catalysis, systematic HP-NMR experiments were conducted under different reaction

conditions. The reactivity of [Rh(acac)(CO)$_2$] **7.18** with cinnamyl acetate **7.11b**, both in stoichiometric and catalytic ratios, was studied by mixing them at room temperature inside a 5 mm HP-NMR tube and then the solution was analysed by ^{1}H, ^{31}P and ^{13}C NMR spectroscopy.

Reactivity of [Rh(acac)(CO)$_2$] in the presence of ligand 7.21

First, a solution of the precursor [Rh(acac)(CO)$_2$] **7.25** (0.01 mmol) and ligand **7.21** (0.01 mmol) in toluene-d$_8$ (0.4 ml) was left one hour at room temperature prior to NMR analysis.

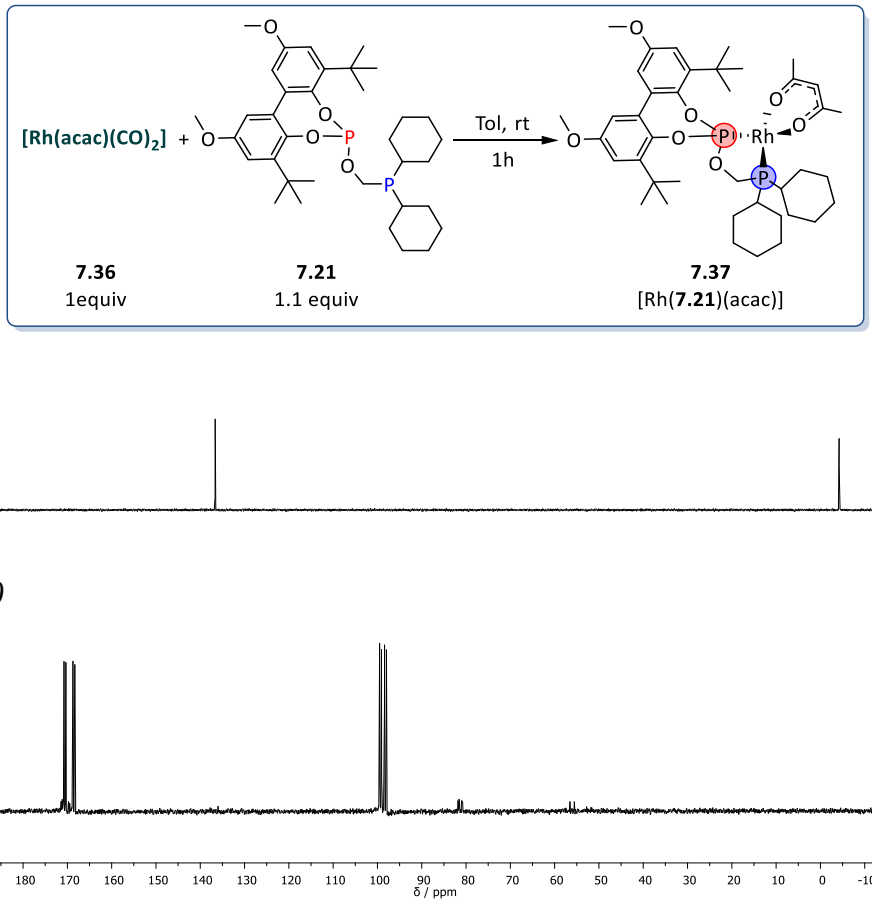

Scheme 7.11. Selected NMR signals for HP NMR analysis [Rh(acac)(CO)$_2$] **7.36** and ligand **7.21**; a) ^{31}P{^{1}H} NMR (162 MHz, RT) ligand phosphine-phosphite **7.21**. b) ^{31}P{^{1}H} NMR (162 MHz, RT) rhodium complex [Rh(**7.21**)(acac)] **7.37**.

The non-coordinated phosphine-phosphite ligand **7.21** displays, in the $^{31}P\{^{1}H\}$ NMR spectrum, two singlet signals at 135.93 ppm and -2.91 (Scheme 7.11, a). When the precursor [Rh(acac)$(CO)_2$] was mixed with ligand **7.21**, as expected, two doublets of doublets were observed in the $^{31}P\{^{1}H\}$ NMR spectrum at 98.7 ppm and 169.5 ppm (Scheme 7.11, b). This indicated the formation of a new Rh complex identified as the square planar complex [Rh(**7.21**)(acac)] **7.37**. The first signal exhibited a J_{P-P} coupling of 70 Hz and a J_{P-Rh} coupling of 180 Hz and was attributed to the phosphine fragment of the ligand coordinated to Rh. The second signal exhibited a J_{P-P} coupling of 70 Hz and a J_{P-Rh} coupling of 362 Hz and was assigned to the coordinated phosphite fragment of the ligand. These data agree with similar complexes previously described in the literature for other chelate ligands.[14]

Reactivity of [Rh(acac)$(CO)_2$] in the presence of ligand 7.21 under H_2/CO pressure

Next, to selectively form the rhodium hydride dicarbonyl complex, 5 bar of total pressure in a H_2:CO ratio of 3:1 were introduced in the HP NMR tube in the presence of the square planar complex [Rh(**7.21**)(acac)] **7.37**, left stirring for 1 hour at 50°C. The signals corresponding to the rhodium hydride dicarbonyl complex were readily detected (Figure 7.6).

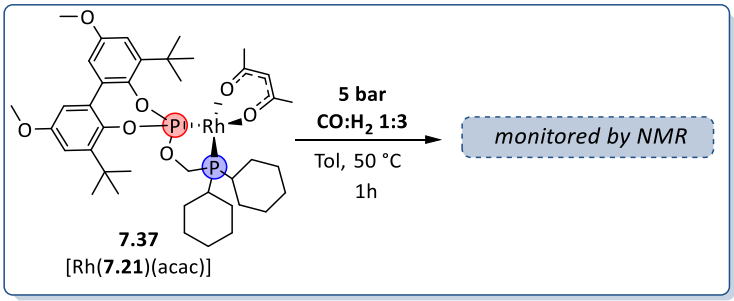

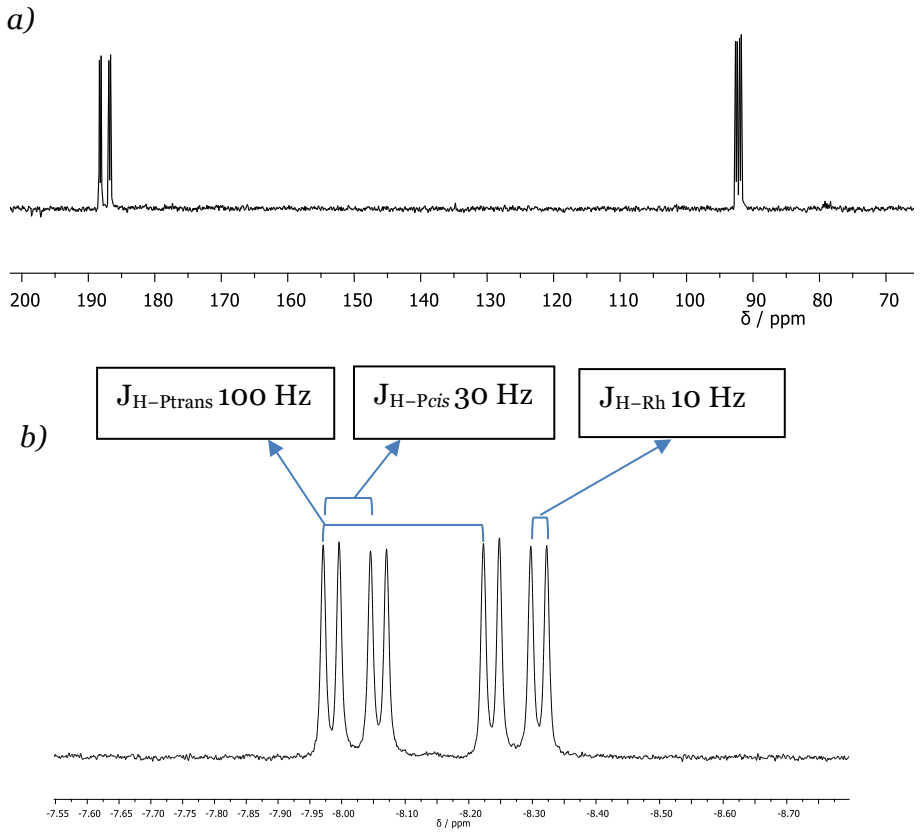

Figure 7.6. Selected NMR signals for HP NMR analysis RhH(**7.21**)(acac) **7.37** 5 bar of CO:H_2 1:3, 1h at 50°C. a) $^{31}P\{^1H\}$ NMR (162 MHz, RT), [Rh(H)(**7.21**)$(CO)_2$] **7.38**.b) ^1H NMR (400 MHz, RT), [Rh(H)(**7.21**)$(CO)_2$] **7.38**.

In the $^{31}P\{^1H\}$ NMR spectrum, two sets of signals were detected: a doublet of doublet at 187.4 ppm and a second doublet of doublet at 92.2 ppm, with J_{P-Rh} couplings for the phosphite and phosphine of 230 and 95 Hz, respectively (Figure 7.6, a). The magnitude of these couplings is consistent with a trigonal bipyramidal geometry of the complex where the phosphite moiety occupies an equatorial position and the phosphine moiety an axial site.[14] In the corresponding ^1H NMR spectrum (Figure 7.6, b), a doublet of doublet of doublet signal at δ –8.15 (ddd, $J_{H-Ptrans}$ =100 Hz, J_{H-Pcis} =30 Hz, J_{H-Rh} =10 Hz), was detected. The magnitude of the J_{H-P} couplings is indicative that the

hydride ligand is in *cis* position to one phosphorus atom and in *trans* position to another phosphorus atom. These results are in agreement with those reported by Clarke for the phosphine-phosphite BOBPHOS ligand and therefore indicate that both ligands coordinate to Rh in the same manner.[14] In addition, this was confirmed by the acquisition of selective $^{1}H\{^{31}P\}$ NMR spectra. The J_{H-P} *cis* 30 Hz correspond to the phosphite moiety and the J_{H-P} trans 100 Hz correspond to the phosphine part. This thus demonstrated the axial:equatorial coordination mode of the ligand in these species, with the hydride *trans* to the phosphine moiety, as depicted in Figure 7.7.

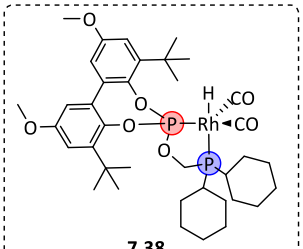

7.38

[RhH(**7.21**)$(CO)_2$]

Figure 7.7. RhH[(**7.21**)$(CO)_2$] **7.38**.

Furthermore, terminal carbonyls coordinated to rhodium were also detected by ^{13}C NMR spectroscopy as a multiplet at 195.167 ppm. ^{1}H-^{31}P Heteronuclear Multiple Bond Correlation (HMBC) exhibited correlation between the hydride signal at −8.15 ppm in ^{1}H NMR spectrum, and the corresponding phosphorus signals at 92.2 ppm and 187.4 ppm in $^{31}P\{^{1}H\}$ NMR spectrum. The CH_2 bridge between nitrogen and phosphorus atoms exhibited a correlation between the hydride signal at −8.15 ppm in $^{31}P\{^{1}H\}$ NMR spectrum with a doublet corresponding of the two equivalent proton at 3.65 ppm in ^{1}H NMR spectrum. Three signals at 1.76, 1.60 and 1.22 ppm in the ^{1}H NMR spectrum, part of the cyclohexyl structure of the ligand, have a correlation between the doublet at 92.2 ppm in $^{31}P\{^{1}H\}$ NMR spectrum and the hydride signal at -8.15 ppm. In view of these results, the reaction product was identified as [RhH(**7.21**)$(CO)_2$] **7.38** and its molecular structure is displayed in Figure 7.7.

Reactivity of [Rh(H)(7.21)(CO)$_2$] in the presence of cinnamyl acetate 7.16b with 7 bar of CO

Once the formation of the Rh hydride **7.38** was completed, the HP NMR tube was degassed, and charged inside the glovebox with 1 equivalent of cinnamyl acetate **7.16b**. The tube was then charged with 7 bar of CO and monitored by NMR over time (Scheme 7.12).

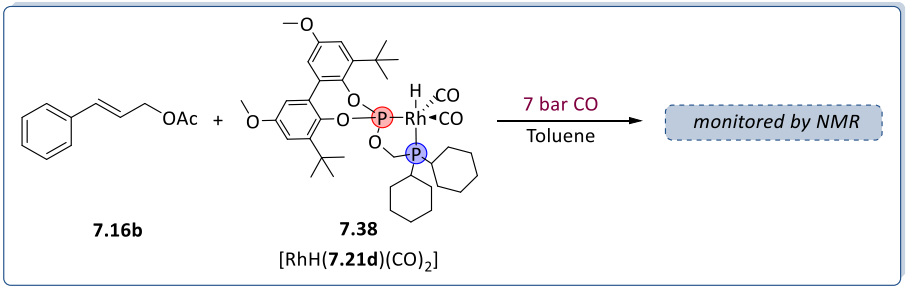

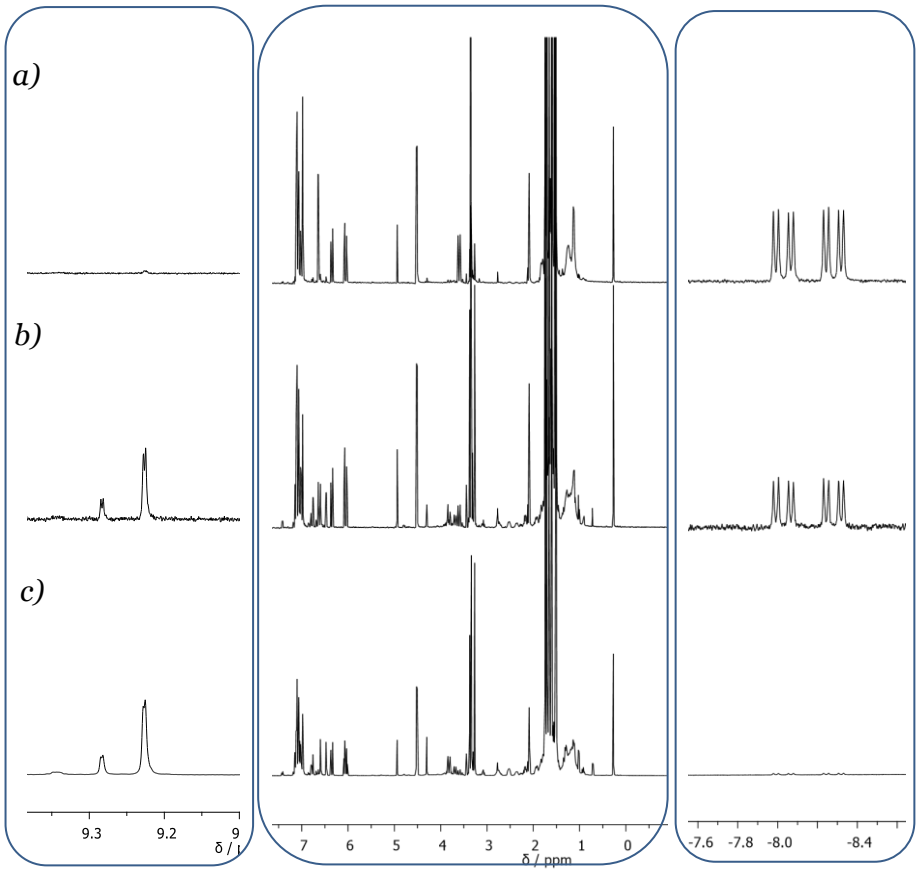

Scheme 7.12. Selected NMR signals for the stoichiometric reaction between [RhH(**7.21**)$(CO)_2$] **7.38** and cinnamyl acetate **7.16b**. (a) ^{1}H NMR spectra (400 MHz, rt), [RhH(**7.21**)$(CO)_2$] **7.38** and cinnamyl acetate **7.16b**, 7 bar of CO at time zero; (b) ^{1}H NMR spectra (400 MHz, rt), [RhH(**7.21**)$(CO)_2$] **7.38** and cinnamyl acetate **7.16b**, 7 bar of CO after 24 h at rt plus 4 at 50°C. (c) ^{1}H NMR spectra (400 MHz, rt), [RhH(**7.21**)$(CO)_2$] **7.38** and cinnamyl acetate **7.16b,** 7 bar of CO after 5 days at rt.

When the sample containing rhodium hydride dicarbonyl complex [RhH(**7.16**)$(CO)_2$] **7.38** and cinnamyl acetate **7.16b** was placed under 7 bar of CO at room temperature for 24 hours, only slight changes were observed by ^{1}H NMR, so it was decided to heat the tube at 50°C for 4 additional hours (Scheme 7.12, spectra a vs. b). When the sample was heated, two doublets were detected in the aldehyde region of the ^{1}H spectrum, indicating that

formylation reaction had taken place. One of these signals at 9.34 ppm was attributed to the aldehyde **7.18b,** (Figure 7.9) based on multiplicity, confirmed by GC-MS analysis and by ^{1}H-^{13}C Heteronuclear Multiple Bond Correlation (HMBC) and 2D ^{1}H COSY.

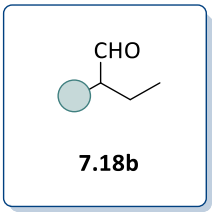

Figure 7.9. Aldehyde produced **7.13b.**

A comparison between the crude of the reaction under catalytic conditions and the spectrum acquired after 5 days (Scheme 7.12, c), further suggests that, under stoichiometric conditions, the aldehyde **7.18b** is formed (Figure 7.9). This result indicates that intermolecular reaction between Rh-H and Rh-acyl species could have taken place. Moreover, the second aldehydic signal detected by ^{1}H NMR might be due to the related structure, proposed in Figure 7.10.

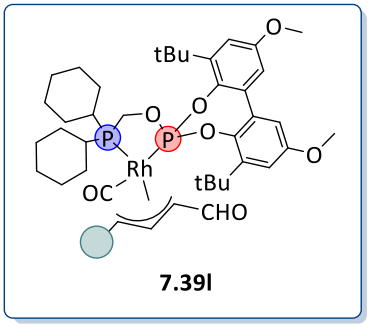

Figure 7.10. Rh allyl **7.39l**.

The aldehydic signal of **7.39l** appears as a doublet at 9.24 ppm, with J_{H-H} of 1.1 Hz. The aldehyde signal couples to two doublet signals at 6.6 and 6.40 ppm and a triplet at 3.08 ppm, detected by the 2D ^{1}H COSY. The two doublets shows a J_{H-H} of 3 Hz, while the triplet at 3.08 ppm exhibited a J_{H-H} of 7.3 Hz. ^{1}H-^{13}C HSQC exhibited correlation between the doublet at 9.22 ppm in the ^{1}H NMR spectrum, and the corresponding carbon signals at 198.0 ppm in the ^{13}C

NMR spectrum. ^{1}H-^{13}C HMBC exhibited correlation between the triplet at 3.08 ppm in ^{1}H NMR spectrum, and the corresponding carbon signals at 29.6, 36.4, 62.2, 129.3, 136.1, 197.9 ppm in ^{13}C NMR spectrum. The carbon at 29.6 ppm appear as a triplet (t, J_{Rh-C}=14 Hz) and the one at 36.4 ppm appears as a doublet (d, J_{Rh-C}=6 Hz) and the one at 62.2 ppm as a singlet. This is in agreement with similar rhodium allyl system reported in literature with bidentate ligand.[15] Furthermore, from the ^{1}H-^{31}P HMBC spectrum, the triplet at 3.08 in ^{1}H NMR spectrum has a correlation with a doublet of doublets centred at 74.23 ppm in the $^{31}P\{^{1}H\}$ NMR spectrum, (Figure 7.11, F), that exhibits a J_{P-P} of 72.5 and J_{Rh-P} of 47.0 Hz. From the ^{31}P-^{1}H HMBC spectrum the doublet of doublets in the $^{31}P\{^{1}H\}$ NMR spectrum shows correlation with a doublet at 3.65 ppm and 1.56 ppm in the ^{1}H NMR. The doublet at 3.65 ppm is due to the CH_2 bridge between the phosphine and phosphite part of the ligand **7.21**, while the signal at 1.56 ppm is corresponding to a proton of the cyclohexyl ligand scaffold. This doublet of doublets (Figure 7.11, G) in the $^{31}P\{^{1}H\}$ NMR spectrum, has the same intensity of a doublet of doublets in the phosphite region at 177.13 ppm (F) (dd, J_{P-P}=255.1, J_{Rh-P}=47.0 Hz). These correlations corroborate the hypothesis of the species **7.39l** (Figure 7.10). Moreover, in the ^{1}H NMR spectrum recorded at time zero, the hydride signal corresponding to [RhH(**7.21**)$(CO)_2$] was observed at −8.15 ppm. After 5 days at room temperature (Scheme 7.11, a vs c), no hydride was detected, thus suggesting the consumption of this species. Based on these experiments, the stoichiometric reaction between the [RhH(**7.21**)$(CO)_2$] and **7.16b**, under 7 bar of CO, provides branched aldehyde **7.19b** as organic product and no β-methylstyrene **7.17** was detected.

During this experiment, the corresponding $^{31}P\{^{1}H\}$ spectra displayed important changes (Figure 7.11). The $^{31}P\{^{1}H\}$ NMR spectrum acquired at time zero revealed the two doublet of doublets corresponding to the starting Rh hydride complex **7.38** (Figure 7.11,a) A and B.

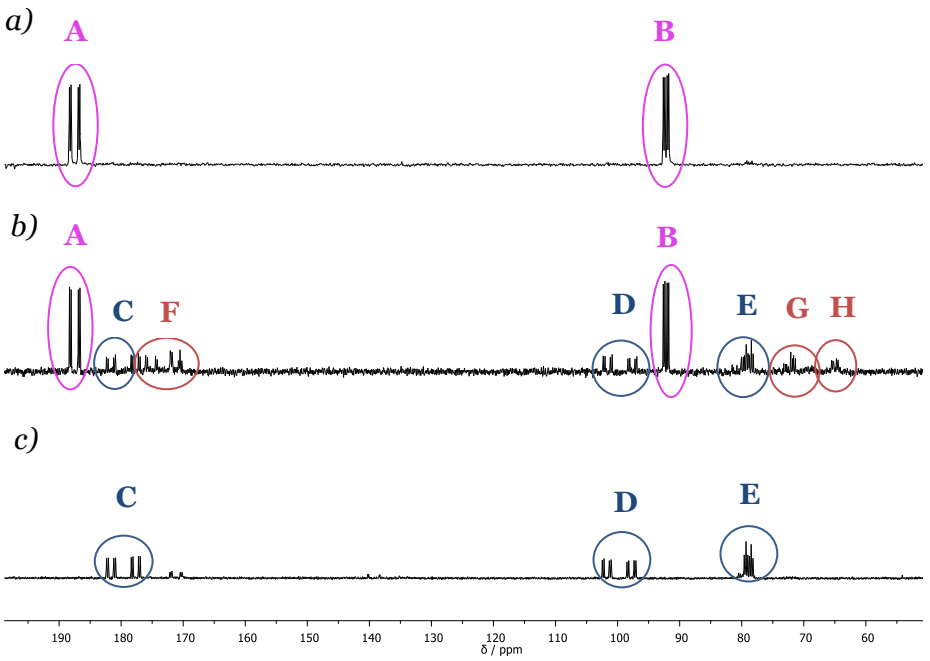

Figure 7.11. Selected NMR signals for the stoichiometric reaction [RhH(**7.21**)$(CO)_2$] **7.38** and cinnamyl acetate **7.16b**. (a) $^{31}P\{^1H\}$ NMR (162 MHz, rt), [RhH(**7.21**)$(CO)_2$] **7.38** and cinnamyl acetate **7.16b**, 7 bar of CO at time zero; (b) $^{31}P\{^1H\}$ NMR (162 MHz, rt), [RhH(**7.21**)$(CO)_2$] **7.38** and cinnamyl acetate **7.16b**, 7 bar of CO after 24 h plus 4 at 50°C. (c) $^{31}P\{^1H\}$ NMR (162 MHz, rt), [RhH(**7.21**)$(CO)_2$] **7.38** and cinnamyl acetate **7.16b,** 7 bar of CO after 5 days.

After heating the sample at 50 °C, the consumption of the starting species was observed and various ^{31}P signals at ca. 180, 100 and 80 ppm (Figure 7.11, b and c) were detected. This indicated the transformation of the Rh hydride precursor into new Rh species. It is noteworthy that in Figure 7.11 the signals A and B, two doublets of doublets, C, D and one doublet of triplet E (181, 177, 102 and 98 ppm) can be observed. These signals (C,D and E) already observed while preparing complex [RhH(**7.21**)$(CO)_2$] **7.38** in highly concentrated solutions (Figure 7.12, a), do not contain hydride ligands since no characteristic signals were detected by ^1H NMR. Four sets of signals, F, G and H indicated the transformation of the Rh hydride precursor into a new Rh species involving the substrate **7.16b**.

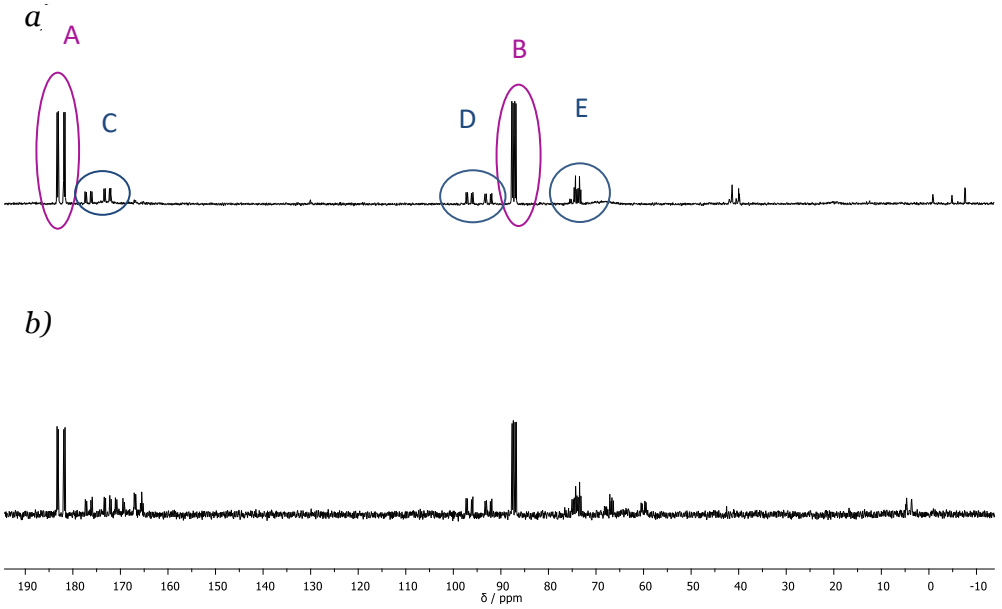

Figure 7.12. Selected NMR signals . (a) $^{31}P\{^{1}H\}$ NMR (162 MHz, rt) [RhH(**7.21**)$(CO)_2$] **7.38** (b) $^{31}P\{^{1}H\}$ NMR (162 MHz, rt), [RhH(**7.21**)$(CO)_2$] **7.38** and cinnamyl acetate **7.16b**, 7 bar of CO after 24 h plus 4 at 50°C.

The signals G and F disappear after 5 days under 7 bar of CO (Figure 7.11, spectra c), and this suggests that the proposed Rh allyl species **7.39l** releases the unsaturated aldehyde **7.40l** as detected by ^{1}H NMR (Figure 7.13) and GC.

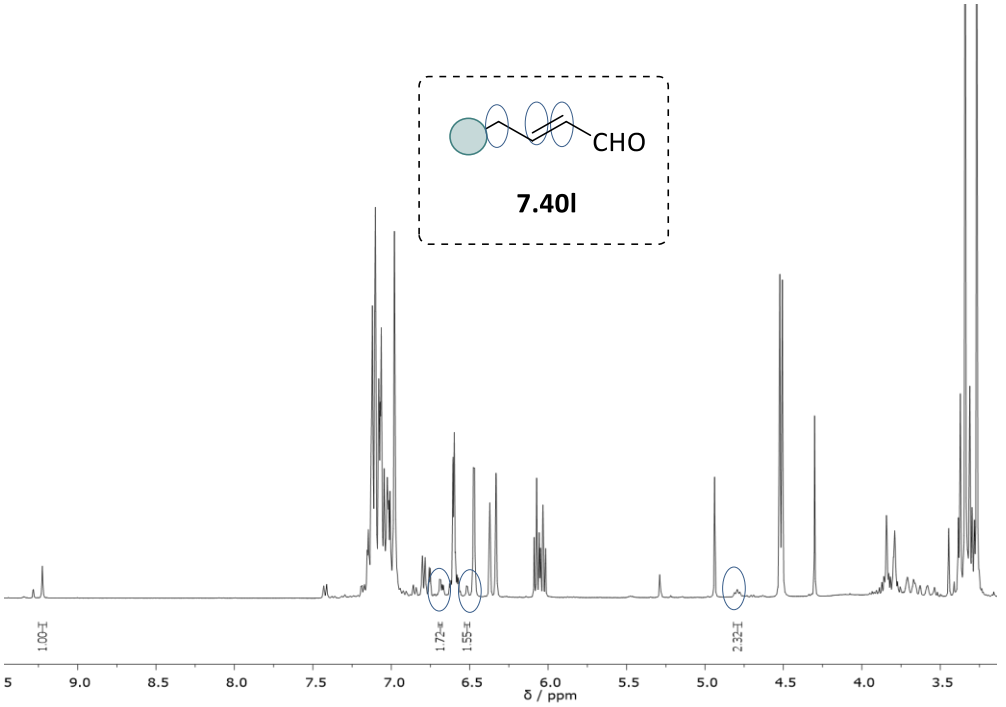

Figure 7.13. ^{1}H NMR spectra (400 MHz, rt), RhH(**7.21**)$(CO)_2$ **7.38** and cinnamyl acetate **7.16b,** 7 bar of CO after 5 days. aldehyde produced **7.40l.**

The aldehyde **7.40l** detected by ^{1}H NMR shows two doublets, at 6.51 and 6.68 ppm, and a triplet at 4.79 ppm (Figure 7.10). Based on these experiments, it can be concluded that the stoichiometric reaction between the RhH(**7.21**)$(CO)_2$ **7.38** and **7.16b** under 7 bar of CO, provides the branched aldehyde **7.18b** and the unsaturated aldehyde **7.40l** as the main organic products. An intermediate rhodium allyl species (**7.39l**) was detected. In order to gain more information a catalytic HP NMR test was performed and monitored by NMR.

Reactivity of catalytic amount of Rh(H)(7.21)$(CO)_2$] in the presence of cinnamyl acetate 7.16b

Then, it was decided to investigate the system under the catalytic conditions, using 40 mol% of the precursor [Rh(acac)$(CO)_2$] **7.36** (0.02 mmol), ligand **7.21** (0.022 mmol) and cinnamyl acetate **7.16b** (0.05 mmol) at room

temperature in a total volume of toluene-d_8 of 0.4 mL, the HP NMR tube was then charged with 13 bar of $CO:H_2$ in a ratio 1:1.

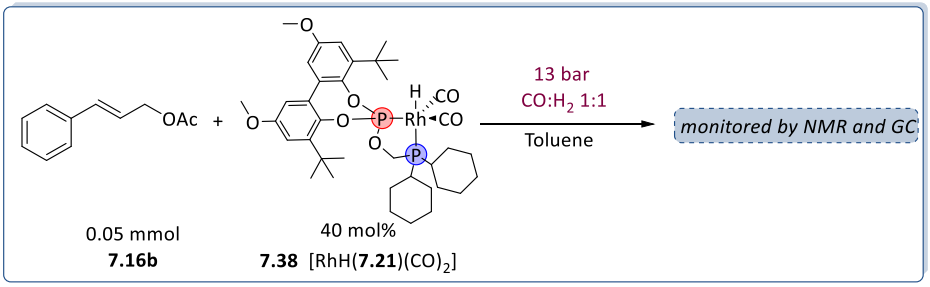

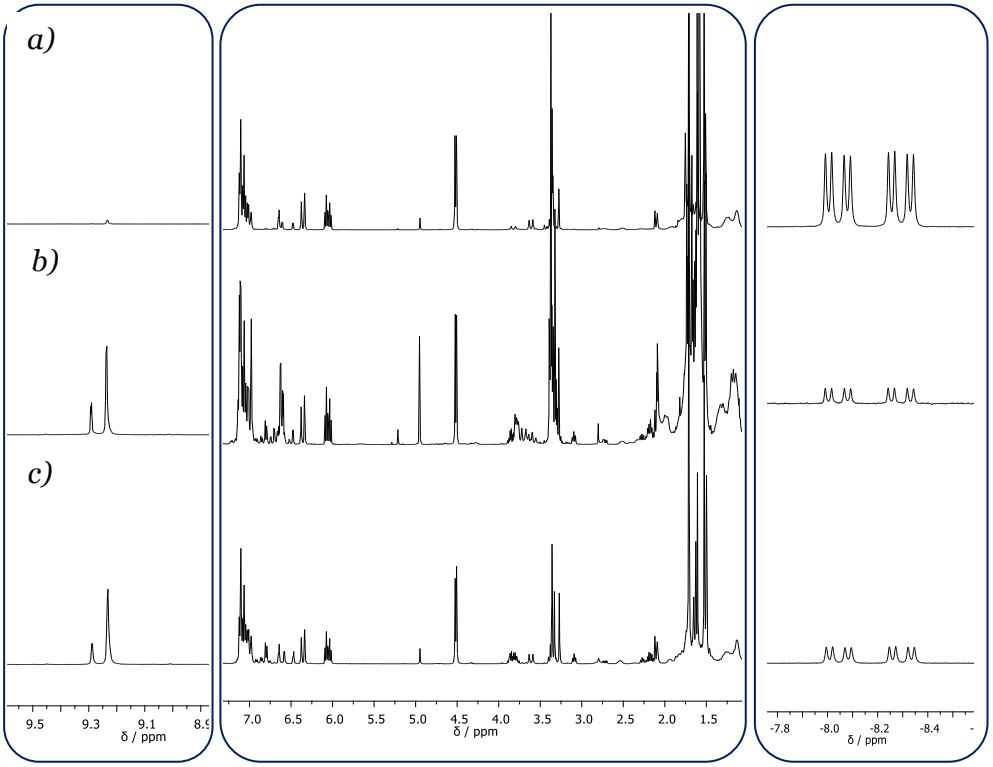

Scheme 7.13. Selected NMR signals for the catalytic reaction for [RhH(**7.21**)$(CO)_2$] **7.38** and cinnamyl acetate **7.16b**. (a) ^{1}H NMR spectra (400 MHz, rt), [RhH(**7.21**)$(CO)_2$] **7.38** and cinnamyl acetate **7.16b**, 13 bar of $CO:H_2$ at time zero; (b) ^{1}H NMR spectra (400 MHz, rt), [RhH(**7.21**)$(CO)_2$] **7.38** and cinnamyl acetate **7.16b**, 13 bar of $CO:H_2$ 1 hour at 60 °C. (c) ^{1}H NMR spectra (400 MHz, rt), [RhH(**7.21**)$(CO)_2$] **7.38** and cinnamyl acetate **7.16b,** 13 bar of $CO:H_2$ acquired after 16h at room temperature.

When the sample containing the rhodium hydride dicarbonyl complex [RhH(**7.21**)$(CO)_2$] **7.38** and cinnamyl acetate **7.16b** was placed under 13 bar of 1:1 ratio of $CO:H_2$, few changes were observed by ^1H NMR. On the other hand, when the HP NMR tube was heated up at 60 °C (Scheme 7.13, b), two doublets were detected in the aldehyde region of the ^1H spectrum, indicating that formylation reaction had taken place. In this case, we could observe a similar behaviour compared to the previously described stoichiometric experiment under 7 bar of CO. Indeed, also in this case, we observed a signal at 9.34 ppm, ascribable to the branched aldehyde **7.18b,** (Figure 7.5) based on the multiplicity and confirmed by GC-MS analysis. The second aldehydic signal shows the same correlation that was observed under stoichiometric conditions, and it was therefore attributed to the Rh allyl complex **7.39l** (Figure 7.14).

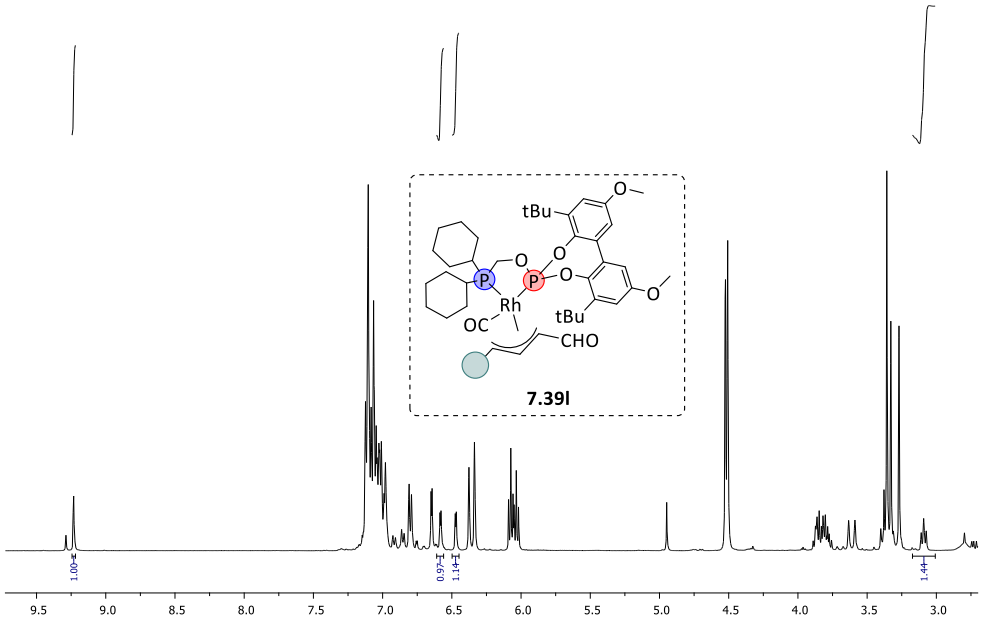

Figure 7.14. ^1H NMR spectra (400 MHz, RT), RhH(**7.21**)$(CO)_2$] **7.38** and cinnamyl acetate **7.16b,** 13 bar of $CO:H_2$ after 16h at room temperature.

From the $^{31}P\{^{1}H\}$ NMR, the starting species was evidenced and various signals at ca. 180, 100 and 80 ppm (Figure 7.15, a and b) were detected. These species, already observed while preparing complex [RhH(**7.21**)$(CO)_2$] in highly concentrated solutions (Figure 7.15, a), do not contain hydride ligands since no characteristic signals were detected by ^{1}H NMR. When the tube was heated up to 60 °C (Figure 7.15, b), two set of signal F and G indicated the transformation of the Rh hydride precursor into a new Rh species involving the substrate **7.16b.**

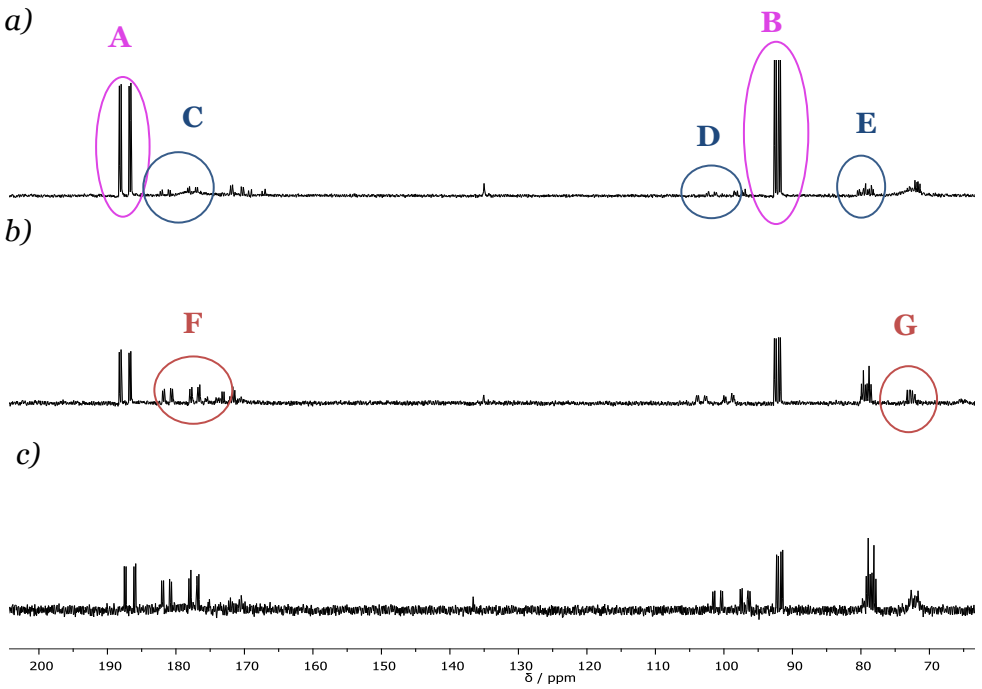

Figure 7.15. Selected NMR signals for the catalytic reaction for [RhH(**7.21**)$(CO)_2$] **7.38** and cinnamyl acetate **7.16b**. (a) $^{31}P\{^{1}H\}$ NMR (162 MHz, rt), [RhH(**7.21**)$(CO)_2$] **7.38** and cinnamyl acetate **7.16b,** 13 bar of CO:H_2 at time zero; (b) $^{31}P\{^{1}H\}$ NMR (162 MHz, rt), [RhH(**7.21**)$(CO)_2$] and cinnamyl acetate **7.16b,** 13 bar of CO:H_2 acquired after one hour at 60°C. (c) $^{31}P\{^{1}H\}$ NMR (162 MHz, rt), [RhH(**7.21**)$(CO)_2$] **7.38** and cinnamyl acetate **7.16b,** 13 bar of CO:H_2 acquired after 16h at room temperature.

The signals G and F almost completely disappear overnight under 13 bar of $CO:H_2$ (Figure 7.15, spectra c), as well as the signals corresponding to the starting complex [RhH(**7.21**)$(CO)_2$] **7.38**. Overall, this suggests that the Rh allyl species **7.39l** (Figure 7.14) releases the unsaturated aldehyde **7.40l** as detected by ^{1}H NMR in the previous paragraph (Figure 7.13). As a conclusion, in both the stoichiometric and catalytic experiments, two main organic species have been observed. The first one is the branched aldehyde **7.18b** (Figure 7.9), arising from the reductive carbonylation process, and the subsequent hydrogenation of the corresponding unsaturated aldehyde. On the other hand, the second one is the unsaturated linear aldehyde **7.40l** (Figure 7.13). This aldehyde is generated after the reductive carbonylation reaction. Both these species were confirmed by GC and NMR analyses. Our hypothesis to validate the formation of these species is the following: as the hydrogenation of terminal olefins is faster with respect to the internal ones, the branched aldehyde **7.18b** is selectively generated over linear aldehyde **7.18l**. As described in the stoichiometric HP NMR experiments performed in the absence of external H_2, the Rh allyl species **7.39l** is stable up to five days in the NMR tube. On the other hand, when external H_2 was employed under catalytic conditions, **7.39l** possess a shorter lifetime, as it is converted overnight to the linear unsaturated aldehyde **7.40l**. This is in agreement with the fact that the higher concentration of H_2, helps to liberate the linear unsaturated aldehyde **7.40l** from the Rh allyl complex **7.39l**. Under NMR time scale, the linear aldehyde **7.40l** produced contain a double bond, indicating that into the HP NMR tube the gas diffusion is slower than in the reactor vessel. According with these studies, a catalytic cycle is proposed for the catalytic system [Rh(acac)$(CO)_2$]/**7.21** (Scheme 7.14).

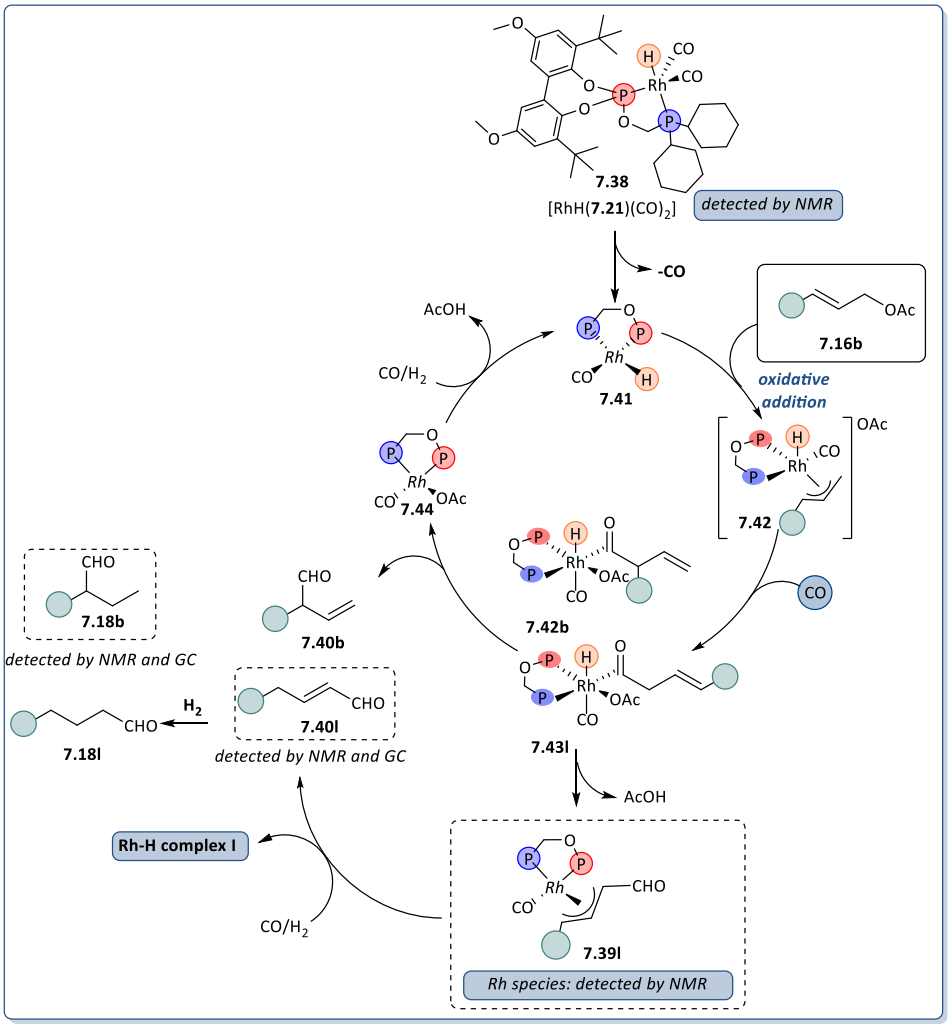

Scheme 7.14. Proposed mechanism for the reductive rhodium carbonylation with ligand **7.21.**

First, from the catalytic resting state **7.38** the extrusion of CO produces the active catalyst **7.41**. Oxidative addition on **7.16b** produces the Rh allyl intermediate **7.42**. Under CO pressure, migratory insertion can produce the branched or linear intermediates **7.34** that could undergo two different pathways: 1) extrusion of acetic acid to deliver the square planar Rh allyl species **7.39l**, that under CO/H_2 pressure deliver the unsaturated aldehydes **7.40l** and **7.40b,** restoring the Rh hydride starting complex **7.41**. 2) The

extrusion of unsaturated aldehydes (**7.40b** and **7.40l**) form the rhodium species **7.44** that, through treatment with syngas, regenerate the initial hydride species **7.41**. The unsaturated aldehydes (**7.40b** and **7.40l**) later can undergo hydrogenation to produce the desired products **7.18b** and **7.18l**.

7.4 Conclusions

From the study described in this chapter, the following conclusions can be extracted:

I. The development of a novel protocol for the production of the aldehyde have been achieved *via* a reductive carbonylation procedure, with cinnamyl acetate **7.16b** as substrate.
II. The optimized condition were: $RhH(CO)(PPh_3)_3$ (0.1 mol%), ligand **7.21** (0.11 mol%) at 13 bar of 1:1 $CO:H_2$ using for 6 hours at 120 °C, as described in Table 7.1. in Entry 7.
III. To the best of our knowledge this process constitutes the first reductive carbonylation process carried out using an allylic ester (cinnamyl acetate **7.16b**) to deliver the corresponding aldehyde.
IV. The reactivity of $RhH(CO)(PPh_3)_2$ **7.27** in the presence of cinnamyl acetate **7.16b** deliver provides β-methyl styrene **7.17** as the main organic product and a new Rh species containing 2 equivalent phosphine ligands and no hydride.
V. The reactivity of $RhH(CO)(PPh_3)_3$ **7.27** in the presence of cinnamyl acetate **7.16b** under CO pressure deliver the aldehydes **7.18b**, **7.18l** and **7.19** (Figure 7.5).
VI. The reactivity of $RhH(CO)(PPh_3)_3$ **7.27** in the presence of cinnamyl acetate **7.16b** under CO pressure produce two isomers $RhH(PPh_3)_2(CO)_2$ as proposed in scheme 7.8. [13]

VII. A new rhodium hydride species [RhH(**7.21**)$(CO)_2$] **7.38** was selectively form in **eq:ax** coordination mode and have been characterized.

VIII. The reactivity of [Rh(H)(**7.21**)$(CO)_2$] **7.38** in the presence of cinnamyl acetate **7.16b** with 7 bar of CO deliver the aldehyde **7.18b** and the unsaturated aldehyde **7.40l** as the main organic products.

IX. The reactivity of [Rh(H)(**7.21**)$(CO)_2$] **7.20** in the presence of cinnamyl acetate **7.11b** with 7 bar of CO forms intermediate novel rhodium allyl species (**7.39l**) that could be involved in the catalytic formation of aldehyde **7.18l**.

X. The reactivity of catalytic amount of Rh(H)(**7.21**)$(CO)_2$] **7.38** in the presence of cinnamyl acetate **7.16b,** under 13 bar of $CO:H_2$ pressure (1:1), deliver aldehyde **7.18b** and the unsaturated aldehyde **7.40l** as the main organic products.

XI. The system $RhH(CO)(PPh_3)_3$ **7.27** in the presence of cinnamyl acetate **7.16b** deliver the compounds **7.17**, **7.18a**, **7.18b** and **7.19**, as observed by the HP-NMR experiments. These results are agreement with the products obtained under the catalytic condition described in Table 7.1 (Entry 1).

7.5 Experimental part

7.5.1 General Information

All the reactions were carried out using Schlenk-line inert atmosphere techniques or glovebox techniques. Anhydrous solvents were collected from the system Braun MB SPS-800.

Commercially available reagents and solvents were purchased at the highest commercial quality from Sigma-Aldrich, Fluka, Alfa Aesar, Fluorochem, Strem and were used as received, without further purification, unless otherwise stated.

^{1}H, $^{13}C\{^{1}H\}$ and $^{31}P\{^{1}H\}$ NMR spectra were recorded using a Varian Mercury VX 400 (400, 100.6, and 161.97 MHz respectively). Chemical shift values (δ) are reported in ppm relative to TMS (^{1}H and $^{13}C\{^{1}H\}$) or H_3PO_4 ($^{31}P\{^{1}H\}$), and coupling constants are reported in Hertz. The following abbreviations are used to indicate the multiplicity: s, singlet; d, doublet; t, triplet; q, quartet; m, multiplet; bs, broad signal. High-resolution mass spectra (HRMS) were recorded on an Agilent Time-of-Flight 6210 using ESI-TOF (electrospray ionization-time of flight). Samples were introduced to the mass spectrometer ion source by direct injection using a syringe pump and were externally calibrated using sodium formate. The instrument was operating in the positive ion mode. Reactions were monitored by TLC carried out on 0.25 mm E. Merck silica gel 60 F_{254} glass or aluminum plates. Developed TLC plates were visualized under a short-wave UV lamp (254 nm) and by heating plates that were dipped in potassium permanganate. Flash column chromatography was carried out using forced flow of the indicated solvent on Merck silica gel 60 (230-400 mesh).

The Rh-catalysed hydroformylation reaction were set up in a 7 tube autoclave from HEL Inc. and single tube autoclave from HEL Inc and were stirred with a teflon-coated magnetic stir bar.

7.5.1 General procedure for reductive carbonylation of cinnamyl acetate 7.11b reaction

A 10 mL glassware reactor tube was charged with cinnamyl acetate **7.11b** (2.06 mmol), Rh precatalyst (1 mol%) in toluene (1.5 mL) and ligand (1.1 mmol%), the autoclave was closed in the glove-box. The reaction tube was placed in the reactor which was pressurized at the desired pressure, heated to 120°C and left stirring at 900 rpm. The reaction was stopped after 6 h by cooling the reactor in an ice bath for 20 min followed by venting of the system. After completion of the reaction, the crude mixture was analysed by GC-MS,

GC-FID and ^{1}HNMR and the results compared to those previously reported in literature.

7.5.2 *In situ* HP-NMR experiments

In a typical experiment, a sapphire tube (Ø = 5 mm) was filled under nitrogen atmosphere with a solution of the [Rh(acac)$(CO)_2$] **7.36**, and a solution of ligand **7.61** in a ratio Rh/L = 1:1.1 in a total volume of 0.4 mL. The HP-NMR tube was purged with CO, pressurized to the appropriate pressure of H_2/CO, heated if required, and left shaking. After that, the solution was analysed by NMR spectroscopy, and the solution was analysed by GC-MS after depressurizing if required. Next, to selectively form the rhodium hydride dicarbonyl complex, 5 bar of total pressure in a H_2:CO ratio of 3:1 were introduced in the HP NMR tube in the presence of the square planar complex [Rh(**7.21**)(acac)] **7.38**, left stirring for 1 hour at 50°C.

7.6 References

[1] a) L. N. Ferguson, *Chem. Rev.*, **1946**, *38*, 227-253. b) F. Aldabbagh, *Comp. Org. Funct. Group Transforma. II*. **2005,** *3*, 99.

[2] P.W.N.M. Van Leeuwen, P.C.J Kamer, J.N.H. Reek, P. Dierkes, *Chem. Rev.* **2000**, *100*, 2741-2770.

[3] R. Franke, D. Selent, A. Börner, *Chem. Rev.* **2012**, *112*, 5675-5732.

[4] M. Torrent, M. Solà, G. Frenking, *Chem. Rev.* **2000**, *100*, 439-494.

[5] a) B. Breit, *Top. Curr. Chem.*, **2007**, *297*, 139-172. b) C. Dwyer, H. Assumption, J. Coetzee, C. Crause, L. Damoense, M. Kirk, *Coord. Chem. Rev.*, **2004**, *248*, 653-669. c) L. Damoense, M. Datt, M. Green, C. Steenkamp,

Coord. Chem. Rev., **2004**, *248*, 2393-2407. d) P. C. J. Kamer, A. van Rooy, G.C. Schoemaker, van Leeuwen, P.W.N.M. *Coord. Chem. Rev.*, **2004**, *248*, 2409. e) R. Lazzaroni, R. Settambolo, G. Alagona, C. Gio, *Coord. Chem. Rev.* **2010**, *254*, 696. f) M. Haumann, A. Riisager, *Chem. Rev.*, **2008**, *108*, 1474. g) F. Hebrard, P. Kalck, *Chem. Rev.,* **2009**, *109*, 4272. h) A. Gual, C. Godard, S. Castillón, C. Claver, *Tetrahedron: Asymmetry*, **2010**, *21*, 1135-1146. i) H. Fernández-Pérez, P. Etayo, A. Panossian, A. Vidal-Ferran, *Chem. Rev.,* **2011***, 111*, 2119-2176.

[6] A. Schoenberg, R.F. Heck, *J. Am. Chem. Soc.*, **1974**, *96*, 7761-7764.

[7] a) V. P. Baillargeon, J. K. Stille, *J. Am. Chem. Soc.*, **1986**, *108*, 452-461. b) V. P. Baillargeon, J. K. Stille, *J. Am. Chem. Soc.,* **1983**, *105*, 7175-7176.

[8] a) H. Kotsuki, P. K. Datta, H. Suenaga, *Synthesis*. **1996**, 470-472. b) K. Kikukawa, T. Totoki, F. Wada, T. Matsuda, *J. Organomet. Chem.* **1984**, *270*, 283-287. c) I. Pri-Bar, O. Buchman, *J. Org. Chem.,* **1984***, 49*, 4009.

[9] A) T. Okano, N. Harada, J. Kiji, *Bull. Chem. Soc. Jpn.*, **1994**, *67*, 2329-2332. b) I. Pri-Bar, O. Buchman, *J. Org. Chem.*, **1988**, *53*, 624-626.

[10] A. G. Sergeev, A. Spannenberg, M. Beller, *J. Am. Chem. Soc.*, **2008**, *130*, 15549-15563.

[11] B. Amorelli, IFF International Flavors & Fragrances, **2020**, *manuscript in preparation.*

[12] S. S. Bath and L. Vaska, *J. Am. Chem. Soc.*, **1963**, *85*, 3500-3501.

[13] D. Evans, G. Yagupsky, G. Wilkinson, *J. Am. Chem. Soc.*, **1968**, 2660-2665.

[14] G. M. Noonan, J. A. Fuentes, C. J. Cobley and M. L. Clarke, *Angew. Chem. Int. Ed.*, **2012**, *51*, 2477-2480.

[15] R. J. Van Haaren, E. Zuidema, J. Fraanje, K. Goubitz, P. C. J. Kamer, P. W. N. M. van Leeuwen, G. P. F van Strijdonck, *Chimie 5*, **2002,** *5*, 431–440.

Rhodium and Palladium Catalysed Unusual Regioselective Hydroformylation and Rhodium Catalysed Reductive Carbonylation

Benedetta Palucci

Chapter VIII

General conclusions

Rhodium and Palladium Catalysed Unusual Regioselective Hydroformylation and Rhodium Catalysed Reductive Carbonylation

Benedetta Palucci

The conclusions arising from this study of rhodium and palladium catalysed regioselective hydroformylation as well as rhodium reductive carbonylation are summarized in the following sections. After a general introduction and justification of objectives, (Chapters I and II), the main conclusions are presented according the Thesis Chapters.

From the study of the rhodium catalysed hydroformylation of 1-hexene with bidentate phosphorus-nitrogen-centred ligands, described in Chapter III, the following conclusions were extracted:

I. The development of a protocol for the synthesis of new bidentate phosphorus-nitrogen-centred ligands **3.17a-k** was achieved *via* a two-step procedure.
II. The optimized conditions for the catalytic hydroformylation included the use of [Rh(acac)$(CO)_2$] (1 mol%) as rhodium precursor, 1.1 mol% of ligand **3.17a-k**, at 50 °C, 10 bar of total pressure with 1:4 CO/H_2 for 24 hours.
III. The screening of ligands **3.17a-k** in the rhodium catalysed hydroformylation of 1-hexene under the optimized conditions, indicated that an increase in steric hindrance at the nitrogen or at the phosphorus centres, severely affects the regioselectivity of the reaction in favour of the linear product.
IV. When compounds **3.17a-c**, that contain a *N*-*n*-alkyl fragment, are used as ligands, the branched to linear ratio increased up to 1.4 b/l.
V. When ligands **3.17i-k**, that contain a bulky phosphine fragment, are used in the hydroformylation process, a negative effect on the branched selectivity of the reaction (b/l=0.5, 0.6, 0.3) was observed.
VI. When ligands **3.17e-h**, containing large groups at the nitrogen atom are used, the formation of the linear aldehyde (b/l=0.5, 0.4) was observed.

VII. When ligand **3.17c** was employed under the optimized conditions, the system delivered the highest value of branched to linear ratio in hydroformylation of 1-hexene (b/l=1.4).

VIII. When [Rh(acac)$(CO)_2$]/**3.17c** was submitted to 10 bar (H_2/CO, 4:1) of syngas at 50 ˚C for 24 hours, the rhodium hydride dicarbonyl species [RhH(**3.17c**)$(CO)_2$] was characterised by NMR spectroscopy and revealed an eq:ax coordination mode. The same coordination mode was observed when ligand **3.17j** was used. Therefore, the coordination mode of these ligands cannot be hold responsible for the difference in performance in the Rh-catalysed hydroformylation of 1-hexene.

From the study of the rhodium catalysed hydroformylation of 1-octene with phosphine-phosphite and phosphine-phosphoramidite ligands described in Chapter IV, the following conclusions were extracted:

I. The development of a protocol for the synthesis of phosphine-phosphite **4.25a-f** and phosphine-phosphoramidite **4.27a-c** ligands was achieved.

II. The synthetised ligands **4.25a-f** and **4.27a-c** were tested in the rhodium catalysed hydroformylation of 1-octene under the previously optimized conditions: 50 ˚C and 10 bar of 1:1 CO/H_2 using 1 mol% of [Rh(acac)$(CO)_2$] as precursor and 1.1 mol% of ligand for 4 hours.

III. While the phosphite moiety revealed having little influence on the regioselectivity, the steric hindrance of the phosphine fragment strongly affected the branched to linear ratio.

IV. The ligands bearing diphenyl- and dicyclohexyl phosphine fragments (**4.25b**, **4.25c** and **4.25d**) provided similar regioselectivity than the reference BOBPHOS **4.11** ligand under the conditions used in this work. However, the introduction of a bulky fragment such as

bis(*t*Bu)phosphine (**4.27f**) led to a drastic decrease in the regioselectivity.

V. The higher CO partial pressure (1:1 vs 1:4), favored the branched aldehyde formation (b/l=1.70), but at the cost of the conversion (25%). Low temperatures were also beneficial to the production of branched aldehyde (60 °C vs 120 °C), when a 1:1 ratio of CO:H_2 pressure was used.

VI. The rhodium hydride dicarbonyl species [RhH(**4.25d**)$(CO)_2$] **4.38** has been detected and characterized through HP NMR techniques. In this species, the ligand presented an eq:ax coordination.

From the study of the rhodium catalysed hydroformylation of styrene for the production of linear aldehyde described in Chapter V, the following conclusions were extracted:

I. The synthesis of bis(dipyrrolyl-phosphorodiamidite) ligands **5.25d** and **5.25e**, and (pyrrolyl-phosphorodiamidite) **5.25g** was achieved *via* a two-step procedure.

II. The optimization of the conditions for the rhodium catalysed hydroformylation of styrene was performed initially using Xantphos **5.47** as ligand, under the following conditions: 120 °C ,10 bar of 1:1 CO/H_2, 0.5 mM solution of toluene, Rh(acac)$(CO)_2$ as precursor and 10 equivalents of ligand **5.47**. Alcohols were detected as by-products at the end of the process.

III. The screening of the commercially available ligands **5.48-56** in the rhodium catalysed hydroformylation of styrene shows that using the BiphePhos ligand **5.56**, the Rh catalytic system delivers total styrene conversion and no formation of the alcohol as by-product. Furthermore, the highest linear to branched ratio was observed in this screening (l/b= 2) employing ligand **5.56**.

IV. The rhodium loading did not affect the selectivity of the process. Similarly, the metal to ligand ratio affected the activity but not the regioselectivity of the reaction.

V. When the ligand **5.15**, reported by Vogt, was employed in a brief optimization process, it was concluded that the use of a low partial CO pressure (1:4 of CO:H_2) with 5 bar of total pressure had a beneficial effect in the linear to branched ratio. Low temperature has a crucial effect on the regioselectivity of the process. The highest value of linear aldehyde was obtained at 60 °C, with a linear to branched ratio of 15.

VI. The newly synthesised ligands **5.25d**, **5.25e**, **5.25g** provided lower conversion and linear selectivity in the hydroformylation of styrene, compared to ligand **5.15**.

From the study of the palladium catalysed hydroformylation with formaldehyde as syngas surrogate described in Chapter VI, the following conclusions were extracted:

I. The screening of various parameters led to a set of optimized conditions of the palladium catalysed hydroformylation of styrene using $Pd(OAc)_2$ (5 mol%), dppp (10 mol%), TFA (15 mol), TBAI (2.5 mol %) and formaline (2 mmol) in toluene (1 mL).

II. Under the optimized conditions, the best results were at 95 °C: 97% conversion, 62% chemoselectivity and l/b ratio >99 towards the linear aldehyde **6.13l**.

III. Deuterium labelling studies suggest that there are various Pd species in the reaction media that are catalytically active: Pd-H, $Pd(H)_2$ and Pd-(H)(CHO). These experiments indicated that the insertion of styrene into Pd-H/D is reversible under these reaction conditions.

IV. Kinetic isotope effect studies suggest that the relative rate of the formation of Pd-(H)(CHO) and Pd-(D)(CDO) is influenced by the

isotopic substitution during the oxidative addition step on the formaldehyde.

V. NMR investigation of the palladium catalytic system highlighted the formation of intermediates **6.26** and **6.28**.

From the study of rhodium catalysed reductive carbonylation of cinnamyl acetate described in Chapter VII, the following conclusions were extracted:

I. The development of a novel protocol for the production of the aldehyde 7.18b and 7.18l have been achieved *via* a reductive carbonylation procedure, with cinnamyl acetate **7.16b** as substrate.

II. The optimized condition were: $Rh(acac)(CO)_2$ (0.1 mol%), ligand **7.21** (0.11 mol%) at 13 bar of 1:1 $CO:H_2$ using for 6 hours at 120 °C, as described in Table 7.1. in Entry 7.

III. To the best of our knowledge, this process constitutes the first reductive carbonylation process carried out using an allylic ester (cinnamyl acetate **7.16b**) to deliver the corresponding aldehyde.

IV. The reactivity of $RhH(CO)(PPh_3)_2$ **7.27** in the presence of cinnamyl acetate **7.16b** deliver provides β-methyl styrene **7.17** as the main organic product and a new Rh species containing 2 equivalent phosphine ligands and no hydride.

V. The reactivity of $RhH(CO)(PPh_3)_3$ **7.27** in the presence of cinnamyl acetate **7.16b** under CO pressure deliver the aldehydes **7.18b**, **7.18l** and **7.19** (Figure 7.5).

VI. The reactivity of $RhH(CO)(PPh_3)_3$ **7.27** in the presence of cinnamyl acetate **7.16b** under CO pressure produce two isomers $RhH(PPh_3)_2(CO)_2$ as proposed in scheme 7.8.

VII. A new rhodium hydride species [RhH(**7.21**)$(CO)_2$)] **7.38** was selectively form and have been characterized, revealing an **eq:ax** coordination mode of this ligand.

VIII. The reactivity of [Rh(H)(**7.21**)$(CO)_2$] **7.38** in the presence of cinnamyl acetate **7.16b** with 7 bar of CO deliver the aldehyde **7.18b** and the unsaturated aldehyde **7.40l** as the main organic products.

IX. The reactivity of [Rh(H)(**7.21**)$(CO)_2$] **7.20** in the presence of cinnamyl acetate **7.11b** with 7 bar of CO forms intermediate novel rhodium allyl species (**7.39l**) that could be involved in the catalytic formation of aldehyde **7.18l**.

X. The reactivity of catalytic amount of Rh(H)(**7.21**)$(CO)_2$] **7.38** in the presence of cinnamyl acetate **7.16b,** under 13 bar of $CO:H_2$ pressure (1:1), deliver the aldehyde **7.18b** and the unsaturated aldehyde **7.40l** as the main organic products.

XI. During the HPNMR study, when the catalytic reaction was performed using the system $RhH(CO)(PPh_3)_3$ **7.27**, the compounds **7.17**, **7.18a**, **7.18b** and **7.19** were formed, in agreement with the results obtained using an autoclave.

Rhodium and Palladium Catalysed Unusual Regioselective Hydroformylation and Rhodium Catalysed Reductive Carbonylation

Benedetta Palucci

Rhodium and Palladium Catalysed Unusual Regioselective Hydroformylation and Rhodium Catalysed Reductive Carbonylation

Benedetta Palucci

Rhodium and Palladium Catalysed Unusual Regioselective Hydroformylation and Rhodium Catalysed Reductive Carbonylation

Benedetta Palucci

UNIVERSITAT
ROVIRA i VIRGILI